Universidad de **Valladolid**

FACULTAD DE CIENCIAS

DEPARTAMENTO DE FÍSICA DE LA MATERIA CONDENSADA, CRISTALOGRAFÍA Y MINERALOGÍA

TESIS DOCTORAL:

STIMULI-RESPONSIVE SYSTEMS BASED ON ELASTIN-LIKE RECOMBINAMERS FOR BIOMEDICAL APPLICATIONS

Presentada por Laura Martín Maroto para optar al grado de

Doctora por la **Universidad** de **Valladolid**

Dirigida por:

Dr. Matilde Alonso Rodrigo

Dr. José Carlos Rodríguez Cabello

AGRADECIMIENTOS

Llegando al final de mi tesis doctoral, me enfrento al capítulo más complicado, los *AGRADECIMIENTOS*, ya que no es fácil agradecer con palabras, a la gran cantidad de personas que han contribuido de una forma u otra a este trabajo. Sin vosotros hubiera sido imposible terminar este proyecto con éxito.

De forma muy especial, quiero dejar constancia de mi más sincero agradecimiento a mis directores de tesis, *Dra. Matilde Alonso Rodrigo* y *Dr. J. Carlos Rodríguez Cabello*, por su apoyo, confianza y sus sabios consejos, no sólo en el desarrollo de esta tesis sino también en mi formación, tanto a nivel científico como personal. Gracias de todo corazón.

Me gustaría agradecer también a *Javier Arias* su total disponibilidad e infinita paciencia, de no ser por su ayuda y sus palabras de ánimo hubiera desfallecido en gran cantidad de ocasiones. A mis "seniors" *Alessandra* (mi rubita), *Anita* y *Merche*, ha sido un placer compartir con vosotras este trabajo que ha forjado una gran amistad.

Mi gratitud, para mis compañeros de Bioforge, por haber compartido tanto los malos como los buenos momentos. A los que iniciaron mis pasos (*Susana, Artur, Javi*), a los que compartieron conmigo su tesis doctoral (*Menchu* y *María*) y a los recién llegados (*Guille, Isra, Alicia, Piña, Mohammed, Ito*) de los que me llevo grandes recuerdos. Me gustaría hacer una mención especial a *Rocío*, sin tu ayuda (incluso inconscientemente) no hubiera sido capaz de trabajar en este laboratorio de "locos", sinceramente, mil gracias.

Quiero dar las gracias a *Celia* y a *Marisa* por despertar en mí el "gusanillo" de la investigación y darme la oportunidad de descubrir cuánto me motiva.

Un agradecimiento particular, es para mis compañeros *Emilio*, *Girish*, *Rui*, *Mariana*, *Petra*… por su colaboración durante la realización y elaboración de numerosos proyectos comunes, que se han llevado a cabo durante todo este tiempo.

Por último, en el apartado personal, mi gratitud a mi familia, en especial, a mis padres (*Jesús y Feli*) por enseñarme que con esfuerzo y dedicación todo es posible y a mis hermanos (*Chuchi y Nano*) que todavía están intentado entender en qué consiste mi trabajo. También gracias, una y otra vez, a mis amigos, por su comprensión para sobrellevar mis ausencias (tanto físicas como mentales) cuando estaba dedicada a esta tarea.

A las personas que aunque no aparecen nombradas aquí han estado presentes durante la elaboración de este trabajo haciéndolo posible, gracias.

Y finalmente, a mi amor *David*, quien ha estado incondicionalmente a mi lado durante la última etapa, animándome en todo momento a continuar. Por creer en mí. Por compartir mi vida. Por hacerme feliz.

"Cuando quieres algo, todo el Universo conspira

para que realices tu sueño."

Paulo Coehlo (El alquimista)

TABLE OF CONTENTS

ABSTRACT

The challenges facing the biomaterials field have intensified during the last decade. Present research in the design of novel "smart" materials has been directed towards this field looking for materials that mimic biological tissues and cellular functionality through the experimentation with nanostructured systems. Nanobiotechnology provides the possibility of producing textured surfaces and materials in the nanoscale simulating natural environments. As example, tissue engineering and regenerative medicine require biomaterials that promote specific cellular responses generating substrates and scaffolds that influence cell adhesion, growth, and organization. Therefore, considerable effort has been focused to the development of new materials and fabrication techniques to generate novel substrates that exhibit some of the most important chemical, biological and physical characteristics of the extracellular matrix (ECM).

Genetic engineering techniques offer a straightforward route to design and biosynthesise protein polymers which provide a base that can incorporate structural and functional domains to construct an artificial ECM. The elastin-like recombinamers (ELRs) are based on the recurrence of certain short peptides that are present in the natural elastin and can be produced with extraordinary degree of complexity and control. They are made of pentameric repeat amino acid sequences VPGXG (*Val-Pro-Gly-Xaa-Gly*), where *Xaa* is any natural amino acid except *L*-proline. This family shows a wide set of interesting properties: extraordinary biocompatibility, excellent mechanical properties, stimuli-responsive nature and self-assembly behavior. They undergo a phase transition in response to changes in the temperature in aqueous

solutions. Below the so-called Inverse Transition Temperature (ITT) the uncrosslinked polymer chains are soluble in water; however, above the Transition Temperature (T_t) the polymer chains form nano- and microaggregates which segregate from the solution. The adequate mechanical properties and biocompatibility make them good candidates to incorporate short peptides having specific bioactivities, cell attachment REDV (*Arg-Glu-Asp-Val*), specific for endothelial cells, or the general RGD (*Arg-Gly-Asp*) domain for tissue engineering, cross-linking domains as VPGKG (*Val-Pro-Gly-Lys-Gly)* those contain γ-amino groups and others. ELRs are a kind of protein materials that exhibit certain properties that make them suitable for some of the applications were the research in polymer science nowadays is being more active, such as the use of block copolymers with tailored characteristics for nano(bio)technological applications. Amphiphilic elastin-like block corecombinamers (ELbcRs) comprise well-defined blocks of compositionally dissimilar monomers that have significantly different polarities and interaction affinities for aqueous solutions that are impossible to obtain by more conventional chemical techniques. The phase transition in response to changes in the temperature can be modulated conveniently through manipulation of the macromolecular architecture, i.e., length, composition, and sequence of the individual blocks. The identity and sequence of the individual block units within the polymer dictates the nature of the supramolecular assembly.

The work compiled here is part of a long term project focused on the development of new biomaterials showing increasing functionality for several biomedical applications ranging from bioactive hydrogels to nanoparticles with the aim of opening its promising field of applications. A general introduction is presented in Chapter 1 showing an extensive bibliographic revision concerning the promising versatility of ELRs.

The first objective of this thesis was to obtain hydrogels from multifunctional ELRs incorporating different cell binding peptides, RGD or REDV, obtained by chemical cross-linking with hexamethylene diisocyanate (HDI), a lysine-targeted cross-linker, with well-defined biological activity, appropriate mechanical properties and controlled topography for tissue engineering. Hydrogels are one of the most promising and versatile materials with enormous possibilities and potentials in the field of biomedical sciences. Among the materials used for regenerative applications, hydrogels are receiving increasing attention due to their ability to entrap large amount of water, good biocompatibility and mimicking tissue environment. Interestingly, hydrogels based on ELRs retain the thermo-responsiveness characteristics of the ELR family and a clear T_t can be studied in crosslinked hydrogels by calorimetric techniques. From this goal, we established two lines of research: Micropatterned and porous hydrogels.

The first research line presented in Chapter 2 was the combination of soft-lithographic methods (replica molding) with bioactive hydrogels, to obtain chemically cross-linked hydrogels with selected patterns of different features in terms of size and topography and biochemical specificity. These novel bioactive hydrogels showed smart behaviour in aqueous media which would provide functional substrates for studying cell behaviour mimicking biological systems for tissue engineering purposes. Several studies are being carried out to investigate cell attachment, growing and proliferation onto these scaffolds.

The second research line presented in Chapter 3 was to obtain hydrogels with a suitable space in which transplanted cells can growth and generate their own extracellular matrix. High porosity is required to offer sufficient space for tissue ingrowth and to improve the invasion of surrounding tissue. An appropriate pore size

and interconnecting pore network is also essential for vascularization and diffusion of nutrients. This study has developed a salt leaching/gas foaming technique for preparing biodegradable highly porous hydrogels as bioactive implants in cellular therapies. The results showed clear differences in the physical properties of the hydrogels with the variation of the weight ratio salt/polymer and the environmental temperature. The distribution of medium pore size was controlled by the salt particle size. The gas-forming process, by immersion in a citric acid solution after the cross-linking, facilitated the interconnectivity and the obtaining of a grooved surface, which is important to allow cell colonization. Cell viability assays *in vitro* with endothelial cells showed the success of the two main general objectives for its future application in tissue engineering: first to test the biocompatibility of the 3D-hydrogels and secondly to prove that the porous structure was suitable for the infiltration of cells through their surface and subsequent cell colonization.

The second objective of this thesis was to study the supramolecular self-assembly of amphiphilic ELbcRs for development of new nanotherapeutic platforms based in stimuli-responsive nano-objects and gels. The increasing need for drug-delivery systems that improve specificity and activity, whilst being biocompatible at the same time has led to the development of a wide variety of new materials. The bulk of this effort has been developed in polymeric systems because of their ability to form a range of different nanoparticulate structures, including micelles, nanospheres, nanocapsules or polymersomes. In this work, presented in the Chapter 4, amphiphilic elastin-like di- and triblock corecombinamers exhibit thermally triggered nanoscale self-assembly in aqueous neutral solution. The control over the molecular weight and the hydrophilic-to-hydrophobic ratio changing the arrangement and length of the hydrophilic block affords to different nano-objects as micelles or vesicles with several

sizes. The potential of ELbcRs to self-assemble in response to environmental changes as pH or temperature makes them very attractive for the construction of nano-devices for use as controlled delivery and stimuli-responsive systems or advanced nanobiotechnological applications.

The subsequent design and development of an amphiphilic tetrablock ELbcR showed in the last part of this work, Chapter 5, has allowed the obtaining of an *in situ* injectable gel performed by temperature-triggered reversible gelation under mild, physiological conditions. A major limitation of most scaffold materials used for tissue engineering is the need for surgical implantation. For many clinical uses, injectable hydrogels would be strongly preferred because could be formed into any desired shape at the site of the injury and would adhere to the tissue during gel formation minimizing the invasiveness of the procedure. In addition, they may incorporate various therapeutic agents (e.g., growth factors) and encapsulate cells, amongst others. Among approaches that involve solvent exchange, UV-irradiation, ionic cross-linkage and pH change, temperature-responsive hydrogels under physiological conditions have caused the interest of many investigators for biomedical applications. In this regard, we have obtained physically or self-assembly hydrogels with selected patterns combining replica molding with reversible thermo-gelling properties. This approach could be used to study cell behaviour on microstructured surfaces with the possibility of tuning the mechanical properties during the cell culture varying the temperature or could be also exploited in combined strategies of, for example, cell harvesting, in which, once cells has growth on the substrate and can be harvested from simply cooling the system below the gelation temperature. Regarding to the application as injectable gel, the incorporation of bioactive sequences has allowed its use in different studies to investigate cell

attachment, growing and proliferation onto these gels developing the outstanding potential of this novel family of ELRs for tissue regeneration.

In general, the work developed along this thesis intended to contribute to the evolution of the emerging applications of ELRs to the biomaterial field, some of them are summarize in the Chapter 6 as future perspectives. Starting with the knowledge of the required properties of “smart” biomaterials to obtain different hydrogels with specific functionalities and bioactivity; and ending with new stimuli-responsive nanoplatforms for nanobiotechnological applications.

RESUMEN

OBJETIVOS

1.- Esta tesis tiene como objetivo principal el desarrollo de sistemas multifuncionales con aplicación en el campo de la biomedicina y nanotecnología a partir de polímeros recombinantes tipo elastina diseñados por el GIR Bioforge. Para la obtención de dichos sistemas se pretende aprovechar características de gran interés en estos campos y que presentan estos biopolímeros, como su sensibilidad a diferentes estímulos como la temperatura y el pH, su elevada biocompatibilidad y la posibilidad de inclusión de diversas bioactividades en su cadena peptídica.

2.- Los primeros sistemas que se pretende obtener son nuevos sustratos para ingeniería de tejidos con características superiores a los descritos en la bibliografía tanto en relación a sus bioactividades y especificidad a distintos tejidos o líneas celulares como a sus propiedades mecánicas, porosidad o biodegradabilidad; de manera que simulen de forma precisa las características de las matrices extracelulares. Se pretenden obtener sistemas mediante entrecruzamiento químico de los recombinámeros de tipo elastina que contienen diferentes dominios bioactivos, tales como péptidos de adhesión celular o de reconocimiento de elastasas, así como dominios de entrecruzamiento.

3.- Se pretende también desarrollar soportes más avanzados como hidrogeles 3D porosos para su utilización como implantes biomédicos o substratos que presenten

topografías microestructuradas en superficie útiles en aplicaciones de confinamiento y guiado celular.

Para conseguir hidrogeles 3D eficaces debe ser posible obtenerlos con distribuciones variables de porosidad y tamaño de poro controlado. Además será necesario optimizar una técnica que nos permita obtener poros interconectados, para así conseguir una buena adhesión, proliferación y colonización celular.

Respecto a la consecución de superficies bioactivas para el guiado celular será necesario obtener hidrogeles que presenten diversas topografías del orden de micras mediante técnicas como micro impresión o litografía suave.

4.- Otro objetivo fundamental de esta tesis ha consistido en desarrollar nuevos sistemas nanoterapéuticos con aplicaciones en dosificación de fármacos y otras biomacromoléculas como hormonas, vitaminas o factores de crecimiento. Los nanosistemas desarrollados están basados en corecombinámeros de tipo elastina, que fueron diseñados previamente en el grupo, inspirándose en los polímeros sintéticos de bloque anfifílicos y en las propiedades de autoensamblado mostradas por los recombinámeros de tipo elastina.

Se pretende comprobar si los corecombinámeros en bloque anfifílicos pueden dar lugar, como resultado a la respuesta a un cambio en la temperatura en medio acuoso, a diferentes nano-objetos autoensamblados, como por ejemplo micelas o vesículas mediante interacciones no covalentes, hidrófobas y reversibles.

Determinar si la polaridad media, la masa molecular, la secuencia de aminoácidos, así como la manera en que los bloques están dispuestos a lo largo de la

molécula son factores que determinarán la temperatura de transición, la morfología y el tamaño de los nano-objetos.

5.- Por último y conociendo la capacidad de autoensamblado de los corecombinámeros en bloque de tipo elastina mediante termogelificación reversible, se pretende diseñar y obtener un hidrogel inyectable simple en condiciones fisiológicas que sirva como soporte o vehículo tanto celular como de diversos principios activos o agentes terapéuticos con aplicación en terapias locales mínimamente invasivas.

Con este objetivo se pretende estudiar el comportamiento de un corecombinámero tetrabloque de tipo elastina y optimizar los parámetros de gelificación (concentración, temperatura, viscosidad) en condiciones fisiológicas y caracterizar las propiedades mecánicas del hidrogel.

1. INTRODUCCIÓN

Los biomateriales son materiales especialmente utilizados en aplicaciones médicas, aunque su uso se ha extendido a aplicaciones biológicas y de diagnóstico en laboratorios clínicos. El concepto de "biomaterial" ha cambiado en la medida que a la ciencia de materiales se han incorporado los avances en biología molecular, ingeniería tisular, nanotecnología e ingeniería de superficies.[1] La ciencia de los biomateriales estudia las propiedades físicas y biológicas así como las aplicaciones de materiales (sintéticos o naturales) que van a estar en contacto con sistemas biológicos. El avance en las técnicas del diseño de biomateriales inteligentes ha direccionado la investigación en este campo hacia la búsqueda de materiales que bio-mimeticen la funcionalidad celular y tisular, mediante la experimentación con sistemas nanoestructurados. De este

modo, la nanotecnología provee la posibilidad de producir superficies estructuradas y materiales que en la nanoescala imitan el ambiente natural de las células y promueven ciertas funciones. La utilización de estos biomateriales en la ingeniería de tejidos tiene un gran potencial de aplicación para la medicina regenerativa.[2]

Más concretamente, la ciencia de biomateriales necesita obtener soportes más sofisticados con una actividad biológica y química bien definida, adecuadas propiedades mecánicas y con una topografía controlada. En ingeniería de tejidos, los sustratos deben proporcionar un espacio adecuado en el cual las células trasplantadas puedan crecer y generar su propia matriz extracelular (ECM).[3] *En vivo*, las células se relacionan con el ambiente que las rodea a través de señales extrínsecas e intrínsecas procedentes de interacciones célula-célula y célula-componentes de la matriz extracelular. Dicha matriz se compone de una variedad de proteínas y polisacáridos que son secretados localmente en una red organizada y estrechamente relacionada con la célula productora. Las variaciones en las cantidades relativas de los diferentes tipos de macromoléculas de la matriz y la manera en que se organizan dan lugar a una asombrosa diversidad de formas, cada una adaptada a los requisitos funcionales del tejido en particular. Todas estas señales determinan el comportamiento celular. Las proteínas tienen una función estructural además de bioactiva y las más abundantes son colágeno, elastina, fibronectina y laminina. Mediante el estudio de estas proteínas se han identificado distintas secuencias aminoacídicas con influencia decisiva en el comportamiento celular. Así, por ejemplo, la secuencia RGD[4] presente en la fibronectina está directamente relacionada con la adhesión celular mediada por integrinas. Además de la secuencia RGD, se encuentran otras secuencias proteicas con diferentes funciones (REDV,[5] YIGSR,[6] VGVAPG,[7] DDDEEKFLRRIGRFG,[8] etc.) que se están utilizando en la bioactivación de sustratos con el fin de promover específicamente la adhesión celular,

proliferación, bioabsorción programada y mediada por elastasas o biomineralización entre otras para crear sustratos óptimos para la ingeniería de tejidos. Para reproducir este diálogo natural entre la célula y el material, se está realizando un considerable esfuerzo en el desarrollo de nuevos materiales y nuevas técnicas de fabricación con el fin de generar nuevos sustratos que puedan imitar algunas de las características químicas, biológicas y físicas más importantes de la ECM.

Los hidrogeles constituyen unos de los biomateriales más prometedores y versátiles en el campo de las ciencias biomédicas.[9] Su amplia gama de propiedades facilita su uso en numerosas aplicaciones, en particular en los sectores médicos y farmacéuticos. Se utilizan por ejemplo, en lentes de contacto, recubrimientos médicos, matrices para la liberación de fármacos y andamios para la ingeniería de tejidos. Entre los materiales más utilizados para aplicaciones regenerativas, los hidrogeles están recibiendo una atención creciente debido a su capacidad para retener grandes cantidades de agua, su elevada biocompatibilidad y la posibilidad que ofrecen de imitar las condiciones de los tejidos naturales. Algunos ejemplos de estos materiales incluyen polímeros naturales como gelatina, quitosano, fibrina, colágeno o alginato, y también polímeros sintéticos como poliésteres, polialcoholes vinílicos o poliuretanos.[10, 11] Uno de los principales inconvenientes surgido del uso de hidrogeles para aplicaciones biomédicas es, por ejemplo, el asociado a su biodegradabilidad; reabsorción, tiempo de permanencia, reactividad, subproductos tóxicos, lo cual tendría por ejemplo, un efecto importante en procesos de liberación de fármacos. Esta consideración es crítica también en el diseño de hidrogeles para medicina regenerativa, puesto que existe un compromiso entre la necesidad de un andamio funcional y su degradación para generar un tejido emergente durante el proceso de curación. Este efecto ha sido estudiado examinando la

viabilidad celular de condrocitos en hidrogeles no degradables basados en polietilenglicol (PEG) para regeneración de cartílago.[12] Las células dentro del hidrogel permanecieron viables y uniformemente dispersas, pero debido a la naturaleza no degradable de estos materiales, el número de células tendió a disminuir significativamente con el tiempo.

Otro de los campos que está mostrando un alto interés es el desarrollo de nuevos sistemas terapéuticos basados en vehículos nanoparticulados, que podríamos denominar sistemas nanoterapéuticos. El objetivo es resolver algunas limitaciones de los sistemas convencionales de suministro de fármacos no específicos, tales como la biodistribución no controlada y su orientación a dianas específicas, la falta de solubilidad en agua, la baja biodisponibilidad por vía oral, y los bajos índices terapéuticos de los diversos agentes activos tales como fármacos, biomacromoléculas (factores de crecimiento, proteínas, hormonas…) o en terapias génicas de ADN o siRNA. Con este fin, diversas nanopartículas biodegradables han sido preparadas a partir de proteínas, polisacáridos y polímeros sintéticos biodegradables como el ácido poliláctico (PLA), policaprolactona (PCL) o derivados de polialquilcianoacrilatos (PAC) entre otros con aplicaciones de liberación de fármacos o en terapias génicas o vacunales.[13] Muchos de ellos requieren de la modificación de la superficie de las nanopartículas con polímeros hidrofílicos como el PEG o por ejemplo con biomoléculas que impidan su reconocimiento como partículas extrañas por parte del organismo, y así incrementa el tiempo de vida media en el sistema circulatorio.

Las principales variables a tener en cuenta en un sistema sencillo de liberación de un fármaco y para la selección del polímero serían respecto al fármaco, su solubilidad en agua, estabilidad, etc. y en consecuencia su potencialidad de ser encapsulado en el polímero; en cuanto a las nanopartículas, su tamaño, las características de su superficie

y funcionalidad, el grado de biodegradabilidad y biocompatibilidad; y por último el perfil de liberación del principio activo del sistema compuesto por nanopartícula-fármaco. Pero para obtener sistemas nanoterapéuticos realmente eficaces es necesario obtener nanoplataformas biocompatibles inteligentes que presenten propiedades intrínsecas de respuesta a diferentes estímulos (temperatura, luz, reconocimiento celular, etc.) que permitirán su orientación controlada a dianas específicas o su seguimiento en el interior del organismo.[14]

En la última década existe un tipo de biomateriales con gran potencial que está suscitando un creciente interés en éste área y más concretamente en los dos campos de trabajo arriba descritos y de interés para esta tesis. Las técnicas de ingeniería genética ofrecen una ruta sencilla para diseñar y biosintetizar polímeros proteicos con un grado incomparable de complejidad y control que permiten incorporar dominios estructurales y funcionales derivados de proteínas contenidas en la ECM e imposibles de obtener por métodos convencionales de síntesis química. Además y más concretamente, los "recombinámeros" tipo elastina ("elastin-like recombinamer" ELRs),[15] han suscitado un creciente interés debido a su excelente biocompatibilidad, bioactividad y a su naturaleza intrínseca "inteligente", como por ejemplo su comportamiento termosensible. Los ELRs están basados en secuencias repetidas de aminoácidos presentes en la elastina natural y pueden contener dominios multifuncionales en su estructura para de esta forma presentar propiedades adicionales, tales como una bioactividad específica o adecuadas propiedades mecánicas, para así conseguir imitar las de diferentes tejidos. El más representativo de estos "bloques aminoacídicos" es el pentapéptido (VPGVG) o sus permutaciones, así como una amplia variedad de recombinámeros que han sido biosintetizados con diferentes objetivos con la fórmula general (VPGXG), donde X

representa cualquier aminoácido natural excepto prolina. Estos biomateriales son producidos a partir de construcciones de ADN sintético como biopolímeros recombinantes monodispersos con un rendimiento medio de entre 200 y 300 mg/L de cultivo bacteriano y mediante un proceso biotecnológico. La fermentación realizada en *Escherichia coli* supone un proceso limpio, barato y fácilmente escalable, donde el coste y tiempo de producción no depende de la complejidad del material obtenido. Además, estos materiales proteicos son absolutamente susceptibles de fabricación en condiciones "GMP" (Good manufacture practise) y pueden producirse también en plantas transgénicas, levaduras o bacterias lácticas.[16]

Los ELRs en disolución acuosa presentan una transición de fase en respuesta a cambios en la temperatura. Se denomina transición inversa, viene definida por la temperatura a la que tiene lugar (T_t) y es específica para cada ELR. El recombinámero sufre una transición desde un estado disuelto a un estado insoluble, que conlleva una segregación de fases, al elevar su temperatura por encima de la T_t. Esta transición es completamente reversible y se produce mediante un proceso complejo que ocurre como consecuencia de una asociación hidrófoba del polímero en el que las cadenas pasan de un estado de desorden conformacional a una disposición más ordenada denominada *espiral β*. [15]

Los copolímeros anfifílicos en bloque contienen monómeros con composiciones distintas y que poseen polaridades sensiblemente diferentes en disoluciones acuosas.[17] Mediante técnicas recombinantes es posible también la síntesis de recombinámeros en bloque anfifílicos fusionando los genes que codifican los distintos bloques aminoacídicos individuales con una precisión muy superior a la alcanzable con tecnologías más convencionales. Estos recombinámeros en bloque ("elastin-like block corecombinamer" ELbcR),[18] no sólo conservan la transición de fase en respuesta a

cambios en la temperatura y en disolución acuosa, sino que ésta puede ser modulada convenientemente mediante la manipulación de su arquitectura macromolecular; modificando la longitud, la composición o la secuencia de los bloques individuales. Dicha posibilidad abre un importante campo de aplicación de estos biomateriales consistente en el diseño de sistemas autoensamblables con estructura, morfología y dimensiones variadas, pasando de nano-objetos, tales como micelas, vesículas o nanotubos a hidrogeles inteligentes. [17]

La gran versatilidad de estos recombinámeros inteligentes, ha favorecido en la última década la obtención de distintos sistemas a partir de recombinámeros de tipo elastina con funcionalidades crecientes y "a la carta" para distintas aplicaciones. En esta tesis se han recogido dos de las recopilaciones publicadas más importantes que he realizado sobre el estado del arte de estos biomateriales como una introducción en el capítulo 1 *(''Recombinamers'' as Advanced Materials for the Post-oil Age*) y una vista de perspectivas futuras en el capítulo 6 (*Emerging Applications of Multifunctional Elastin-like Recombinamers).* Los biomateriales que se han obtenido a partir de ELRs incluyen hidrogeles,[19,20] fibras,[21] superficies,[22,23] sistemas inyectables,[24,25] micropartículas,[26] nanopartículas,[27] etc. de aplicación biomédica y nanotecnológica, muchos de los cuales se tratan en este trabajo.

3. METODOLOGÍA

3.1. MATERIALES

3.1.1. Reactivos

Todos los reactivos empleados en este trabajo se enumeran en la siguiente Tabla 1.

Tabla 1. *Reactivos, medios, material de cultivos celulares utilizados y empresas proveedoras.*

REACTIVOS QUÍMICOS Y ABREVIATURA	**ORIGEN**		**REACTIVOS DE CULTIVO CELULAR Y ABREVIATURA**	**ORIGEN**
Aceite mineral	Sigma Aldrich		Accutase	Sigma Aldrich
Ácido cítrico	Sigma Aldrich		Cloruro de calcio ($CaCl_2$)	Sigma Aldrich
Ácido clorhídrico	Sigma Aldrich		DAPI	Invitrogen
Bicarbonato sódico ($NaHCO_3$)	Merck		Faloidina-Alexa-Fluor 488	Invitrogen
Cloruro de sodio (NaCl)	Sigma Aldrich		Glutaraldehido	Sigma Aldrich
Decalina	Sigma Aldrich		Medios de cultivo endotelial (EGM y EBM)	Lonza
Diisocianato de metileno (HDI)	Panreac		Paraformaldehído	Sigma Aldrich
Dimetilformamida (DMF)	Sigma Aldrich		Tampón fosfato salino (PBS)	Gibco
Dimetilsulfóxido (DMSO)	Sigma Aldrich		Tritón X-100	Sigma Aldrich
Elastómero de silicona (PDMS y agente de curado)	Dow Corning			
Etanol	Merck			
Hidróxido sódico	Sigma Aldrich			

Metanol Tolueno	Sigma Aldrich Sigma Aldrich			

Todas las soluciones empleadas se preparan utilizando agua tipo I (Millipore) y el pH se ajusta añadiendo pequeñas cantidades de HCl o NaOH 1M.

Las disoluciones acuosas que se utilizarán en técnicas de dispersión de luz se filtran a través de membranas de *polifluoruro de vinilideno* (PVDF, Whatman©) de tamaño de poro de 0,45 μm para asegurar la eliminación de cualquier residuo de polvo en la muestra.

La limpieza del material de vidrio (tubos porta muestras) es muy importante, ya que la presencia de residuos orgánicos, grasa o polvo modifican drásticamente los fenómenos observados en dispersión de luz. El procedimiento para el lavado del material de vidrio se inicia enjuagando abundantemente con agua corriente para eliminar restos de polvo, después se prosigue con un lavado en una mezcla jabón-agua de la marca Hellmanex® II, especial para lavado óptico en un baño de ultrasonidos durante 15 minutos. Para finalizar, se enjuaga de nuevo con agua tipo I y se deja secar colocando el material de vidrio en una estufa a 60°C durante 4h.

El resto de material de laboratorio (puntas de micropipeta, microtubos, tubos cónicos, etc.) se adquieren estériles o se esterilizan en autoclave (Autester E-75) a 121ºC y 1 atmósfera de sobrepresión durante 20 minutos.

3.1.2. Recombinámeros de tipo elastina utilizados

Todos los recombinámeros (ELRs and ELbcRs) utilizados han sido previamente sintetizados en nuestro laboratorio mediante tecnología de DNA recombinante, producidos en una fermentación de *Escherichia coli* y purificados mediante ciclos de segregación reversibles termodependientes. Tras la última solubilización se dializaron frente a agua de tipo I a 4 °C, posteriormente se liofilizaron y se conservaron a -20 °C.[18, 19, 20, 24, 27, 28]

Los recómbinameros que se han utilizado en este trabajo, la abreviatura, el peso molecular (M_W) y la secuencia de aminoácidos están resumidos en la siguiente tabla (Tabla 2).

Tabla 2. *Composición y peso molecular de los ELRs y ELbsRs utilizados.*

Abreviatura	**Composición de aminoácidos**	**PM (kDa)**
ELRs		
HRGD6	MGSSHHHHHHSSGLVPRGSHMESLLP{[(VPGIG)$_2$VPG**K**G(VPGIG)$_2$]$_2$ (AVTGRGDSPASS)[(VPGIG)$_2$VPG**K**G(VPGIG)$_2$]$_2$}$_6$	60.6
REDV10	MESLLP{(VPGIG)$_2$VPG**K**G(VPGIG)$_2$EEIQIGHIPREDVDYHLYP(VPGIG)$_2$VPG**K**G(VPGIG)$_2$(VGVAPG)$_3$}$_{10}$	83.1
ELbcRs		
E50A40	MESLLP[(VPGVG)$_2$(VPG**E**G)(VPGVG)$_2$]$_{10}$-(VP**A**VG)$_{40}$	38.5
E100A40	MESLLP[(VPGVG)$_2$(VPG**E**G)(VPGVG)$_2$]$_{20}$-(VP**A**VG)$_{40}$	59.3
E50A40E50	MESLLP[(VPGVG)$_2$(VPG**E**G)(VPGVG)$_2$]$_{10}$-(VP**A**VG)$_{40}$-[(VPGVG)$_2$(VPG**E**G)(VPGVG)$_2$]$_{10}$	59.3
(E50I60)$_2$	MESLLP{[(VPGVG)$_2$-(VPG**E**G)-(VPGVG)$_2$]$_{10}$-[VG**I**PG]$_{60}$}$_2$	92.9

3.1.2.1. Recombinámeros químicamente entrecruzables para la formación de hidrogeles bioactivos

Los recombinámeros (ELRs) HRGD6 y REDV10 se diseñaron con la intención de obtener un soporte multifuncional para ingeniería de tejidos, que incluyera las propiedades generales requeridas para un biomaterial (biocompatible y biodegradable) y que permitiera mimetizar al mismo tiempo las propiedades estructurales, mecánicas y funcionales de la matriz extracelular. En ellos, la unidad monomérica contiene tres bloques funcionales diferentes con el fin de lograr un equilibrio adecuado entre la bioactividad y las propiedades mecánicas (Figura 1).

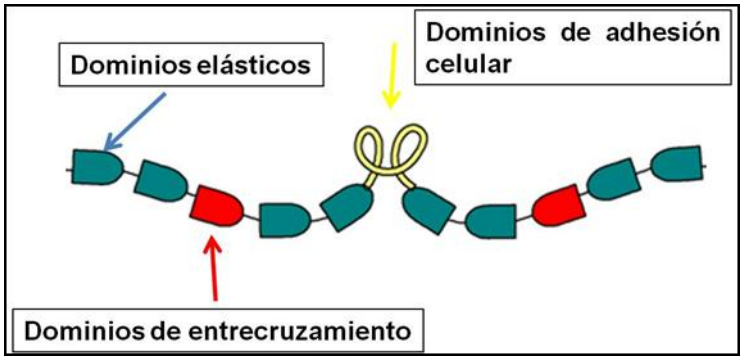

Figura 1. *Esquema general de la parte central del monómero de los ELRs.*

Así, en ambos monómeros está presente el pentapéptido $(VPGIG)_n$ en verde que confiere elasticidad, biocompatibilidad, y comportamiento termosensible. Algunos de los dominios elásticos han sido modificados sustituyendo la isoleucina (I) por lisina (K), representados en color rojo, con el propósito de incluir grupos funcionales que posibiliten reacciones de entrecruzamiento u otras modificaciones químicas. El bloque central del monómero, en amarillo, contiene bucles peptídicos encontrados en la proteína fibronectina que envuelven las secuencias de adhesión celular (RGD universal o REDV, específica para células endoteliales). En el caso del HRGD6 el monómero esta repetido 6 veces dando un peso molecular total de 60.6 kDa. Finalmente en el monómero del REDV10, se ha introducido una secuencia hexapéptidica $(VGVAPG)^{24}$,

repetida 3 veces y reconocida por elastasas, que una vez liberada por la acción proteolítica presenta propiedades bioactivas adicionales (modulación de la proliferación y migración entre otras). Este monómero se ha repetido 10 veces dando un peso molecular de 83.1 kDa.

3.1.2.2. Corecombinámeros: Dibloques, tribloques y tetrabloques para la formación de nano-objetos e hidrogeles

Estos corecombinámeros en bloque (ELbcRs) se diseñaron inspirándose en los polímeros sintéticos de bloque anfifílicos y en las propiedades de autoensamblado mostradas por los recombinámeros de tipo elastina. Los copolímeros en bloque anfifílicos pueden dar lugar, como resultado a la respuesta a un cambio en la temperatura en medio acuoso, a diferentes nano-objetos autoensamblados por interacciones no covalentes, hidrófobas y reversibles. El estudio de la polaridad media, la masa molecular, la secuencia de aminoácidos, así como la manera en que los bloques están dispuestos a lo largo de la molécula son los factores que determinarán la temperatura de transición, así como la morfología y el tamaño de los nano-objetos. Con el fin de obtener diferentes nano-objetos, se diseñaron los corecombinámeros (ELbcRs) E50A40, E100A40 y E50A40E50 de la Tabla 2 y representados en la Figura 2.[14]

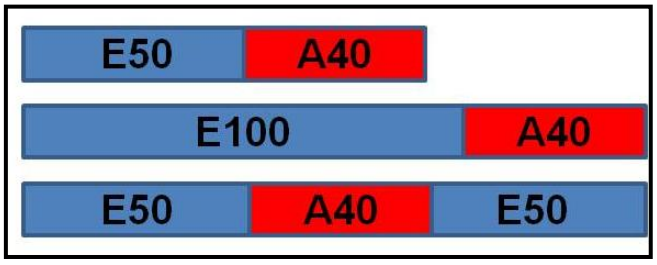

Figura 2. *Esquema de la arquitectura molecular de los corecombinameros E50A40, E100A40 y E50A40E50.*

En esta tesis se caracterizó la formación de dichos nano-objetos. Éstos recombinámeros son también anfifílicos en bloque previamente biosintetizados en el grupo. El primer bloque, denominado bloque E en azul y de composición $((VPGVG)_2$-(VPG**E**G)-$(VPGVG)_2)$, es sensible al pH y el segundo bloque (VP**A**VG) representado como A y en rojo, es termosensible pero no tiene respuesta al pH. Estos corecombinameros se diferencian entre sí en el número de pentapéptidos de cada bloque dando lugar a distintos pesos moleculares, o en la posición de los bloques. Es decir, el número de pentapéptidos para el bloque hidrófobo A (A40) es fijo, habiéndose variado el bloque hidrófilo E en la longitud (E100A40) y en el orden para obtener el tribloque (E50A40E50), manteniendo el peso molecular constante en los dos últimos casos y así poder comparar ambas variables en la formación de los nano-objetos.

Con la misma metodología se construyó un tetrabloque que en función de la concentración posibilitaría no sólo la formación de los nano-objetos sino también la obtención de un hidrogel inyectable para regeneración de tejidos (Figura 3).

Figura 3. *Esquema de la arquitectura molecular del* $(E50I60)_2$

El corecombinámero anfifílico $(E50I60)_2$[20] de la Tabla 2 y representado en la Figura 3 se diseñó con el fin de obtener un sistema autogelificable en condiciones fisiológicas para su aplicación como sistema inyectable en terapias celulares de regeneración de tejidos. Para ello, era necesario que el sistema fuera un líquido de baja viscosidad que permitiera su inyección a temperaturas inferiores a la temperatura corporal y que gelificara instantáneamente al ser introducido en el organismo de manera

que no difundiera consiguiendo de esta manera una terapia local. Su abreviatura se relaciona con las cantidades relativas de pentapéptidos de ambos bloques. El primer bloque E es el mismo descrito previamente en los dibloques y tribloques y el segundo bloque (VG**I**PG) identificado como I es termosensible.

3.2. MÉTODOS

3.2.1. Obtención de hidrogeles químicamente entrecruzados para ingeniería de tejidos

Para la obtención de hidrogeles entrecruzados covalentemente se ha seguido la reacción que se representa en el esquema de la Figura 4. Los recombinámeros utilizados en la reacción de entrecruzamiento han sido el HRGD6 y el REDV10 y la reacción se ha llevado a cabo con diisocianato de hexametileno (HDI) como agente entrecruzante.

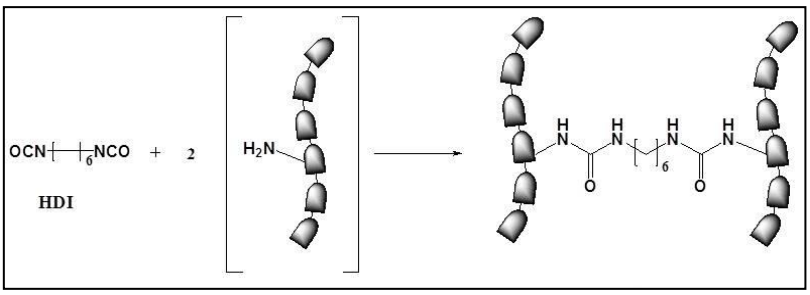

Figura 4*. Reacción de entrecruzamiento mediante diisocianato de metileno.*

3.2.1.1. Preparación de moldes microestructurados y obtención de hidrogeles microestructurados en superficie

El prepolímero de polidimetilsiloxano (PDMS) y el agente de curado, se mezclaron agitando vigorosamente en una relación en peso 10:1 y se desgasificó la mezcla durante 1 h en un desecador a vacío. Ésta se depositó sobre un máster de silicio

estampado con diversas topografías previamente diseñado en el laboratorio y elaborado en el Instituto de Microelectrónica de Barcelona (CNM-IMB). El PDMS se curó a 65°C durante 1 h, y las réplicas de PDMS se despegaron cuidadosamente de la oblea de silicio y se utilizaron sin tratamiento superficial adicional. Se han utilizado diferentes obleas de silicio que presentan surcos, pilares circulares y hendiduras hexagonales, circulares y cuadradas con distintas anchuras (*w*) e inter-distancias (*s*) entre ellos. En concreto, hendiduras hexagonales: *w* = 100 µm, *s* = 100 µm; hendiduras circulares y cuadradas: *w* = *s* = 40 µm, pilares circulares: *w* =5, 10 µm, *s* = 15, 10 µm y surcos: *w* = 15, 20 o 25 µm, *s* = 25, 50 o 100 y 255 µm respectivamente. La altura de las microestructuras fue de 15 µm para los pilares y las hendiduras y 9 µm para los pilares más pequeños.

La reacción de entrecruzamiento se llevó a cabo utilizando DMF como disolvente a una concentración de HRGD6 de 100 mg/mL. Por otro lado se preparó una disolución de HDI en DMF a 25 mg/mL. Ambas disoluciones se mantuvieron a 4° C. La mezcla ELR/HDI en una relación molar de 1:4 y 1:7 se depositó sobre las superficies microestructuradas de PDMS y se mantuvo a temperatura ambiente durante la noche. Una vez entrecruzados, los geles se despegaron cuidadosamente del molde para obtener distintas topografías en superficie.[15] Un esquema del proceso de formación de los moldes de PDMS y del proceso de réplica en los hidrogeles ("replica molding") está representado en la Figura 5.

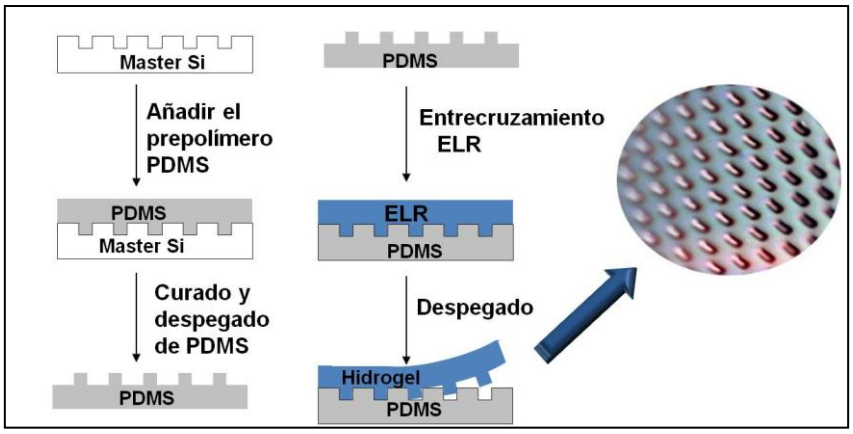

Figura 5. *Esquema del proceso de "replica molding".*

3.2.1.2. Obtención de hidrogeles porosos

El REDV10 liofilizado se disolvió a una concentración de 80 mg/mL en una mezcla de DMSO: DMF (80:20) siendo DMSO; dimetilsufóxido y DMF; dimetilformamida, para disminuir la temperatura de trabajo introduciendo DMF en la mezcla. Por otro lado, se preparó la disolución de HDI en DMF, manteniendo todas las disoluciones a -20° C para disminuir la velocidad de reacción. Posteriormente, los hidrogeles se obtuvieron mezclando las disoluciones de ELR y HDI en una relación molar 1:3 con vigorosa agitación en un vórtex dentro de una cámara frigorífica a 4° C. Finalmente, la mezcla se depositó rápidamente (la reacción se inicia inmediatamente) sobre un molde de teflón de 13.5 mm de diámetro y 2 mm de altura y se dejó reaccionar durante 3h a temperatura ambiente. Los hidrogeles se retiraron del molde y se dializaron en agua ultra pura durante 3 días para eliminar el disolvente y los reactivos en exceso.

Para obtener hidrogeles porosos, entrecruzados químicamente mediante la técnica de adición de sales, se añadió a la mezcla de reacción una relación en peso de sal / REDV10 de 10:1 o 20:1 y se agitó para homogeneizar la muestra en el molde de teflón. Las sales de NaCl o $NaHCO_3$ fueron tamizadas previamente para obtener dos distribuciones de tamaño con intervalos entre 180 y 250 μm y entre 250 y 425 μm.

Pasadas 3h, las muestras de hidrogel que incorporaban $NaHCO_3$ se extrajeron del molde y se sumergieron en una disolución 3 M de ácido cítrico durante 45 minutos en un baño de ultrasonidos para provocar la salida del gas. Finalmente, todas las matrices se lavaron a fondo mediante diálisis con agua ultra pura durante 3 días.[16] Un esquema del proceso de formación de los hidrogeles está representado en la Figura 6.

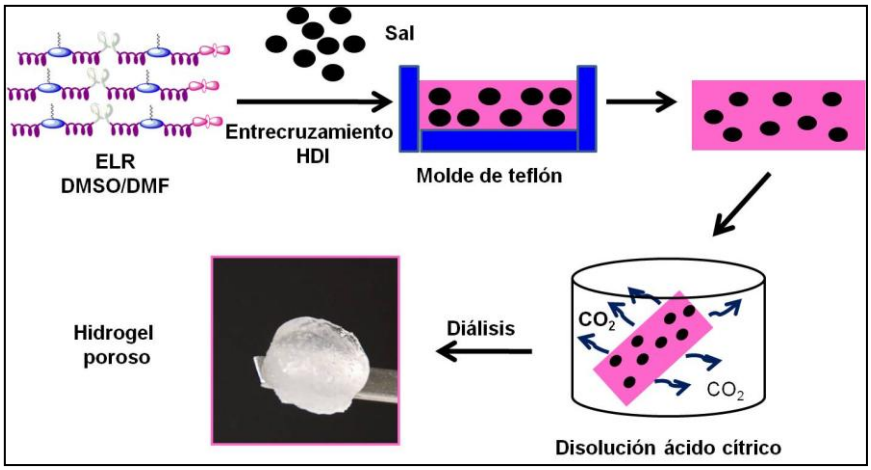

Figura 6. *Esquema de la formación de hidrogeles porosos*

3.2.2. Obtención de hidrogeles mediante autoensamblado y microestructurados en superficie para regeneración de tejidos

Los hidrogeles se obtuvieron depositando una disolución de $(E50I60)_2$ al 15,0% en peso en PBS sobre las réplicas microestructuradas de PDMS a 5° C y calentando a 37° C. La formación de los geles es inmediata una vez que la muestra alcanza la temperatura (inferior a 2 minutos) por lo que la manipulación de la muestra en disolución se debe hacer con todos los materiales previamente enfriados. Los hidrogeles se despegaron del molde y la topografía de la superficie se observó mediante microscopía óptica sin ningún tratamiento o manipulación adicional de los mismos.[20]

3.2.3. Cultivo celular

Los hidrogeles para los ensayos de cultivo celular se prepararon con una relación en peso de $NaHCO_3$: REDV10 (20/1) utilizando partículas de sal tamizadas de tamaño 180-250µm.[16] Se esterilizaron por exposición a rayos UV durante la noche y se almacenaron en etanol al 70%. Se lavaron con agua estéril, se liofilizaron, y se colocaron en una placa de cultivo de 24 pocillos. Las células humanas endoteliales procedentes del cordón umbilical (HUVECs) se cultivaron en medio EGM, que fue remplazado cada dos días, y se incubaron a 37° C en un 5% de CO_2. Una vez confluentes (3-5 pasajes) se incubaron con acutasa, se lavaron y se resuspendieron en EBM. Se sembraron 10000 células/cm^2 sobre los hidrogeles liofilizados sumergidos, y se incubaron a 37° C. Pasadas 48 h de la siembra de las células, los hidrogeles se lavaron con PBS para eliminar las células no adheridas. Las muestras se fijaron en una solución de paraformaldehído al 4% en PBS durante 10 min, se permeabilizaron con Triton 0,2% X-100, y se tiñeron con los reactivos fluorescentes (faloidina-Alexa Fluor488R y DAPI) para su observación por contraste de fases y microscopía de fluorescencia utilizando un microscopio Nikon Eclipse Ti invertido con aumentos de x10 x20 y x40.

Por otro lado, los hidrogeles sembrados con células para su análisis en microscopía electrónica de barrido fueron fijados en Palay (1% glutaraldehído y paraformaldehído en solución 0,1 N de cloruro de calcio) a pH 7,4 durante 2 horas a temperatura ambiente. Las muestras fueron progresivamente deshidratadas en soluciones de etanol/agua con un porcentaje creciente de etanol de 15, 30, 50, 70, 90, y, finalmente al 100% tres veces.

3.2.4. Técnicas experimentales en la caracterización de hidrogeles

3.2.4.1. Calorimetría diferencial de barrido

Para estudiar la transición inversa con la temperatura de los ELRs con los que se ha trabajado se utilizó calorimetría diferencial de barrido (DSC). Los experimentos se realizaron en un DSC Mettler Toledo 822e equipado con un controlador de temperatura refrigerado con nitrógeno líquido y calibrado con muestras patrón de indio, zinc y *n*-octano. Para el análisis de los ELRs, se depositó 20 µL de una disolución de concentración 50 mg/mL en agua ultrapura tipo I en un crisol de aluminio de 40 µL sellado herméticamente. El mismo volumen de agua se dispuso en el crisol de referencia. Para el análisis del hidrogel químicamente entrecruzado de tipo elastina, se colocaron 20 mg del hidrogel hidratado en el crisol de muestra. Para tener en cuenta la cantidad exacta de material en el hidrogel, la muestra se liofilizó y se pesó una vez terminado el experimento de DSC. Los experimentos consistentes en barridos de temperatura para ambos tipos de muestras incluían una etapa inicial isotérmica (5 min a 0° C) seguida de un programa de calentamiento a una velocidad constante de 5° C/ min desde 0 a 50° C.

El proceso reversible de segregación y redisolución experimentado por el ELbcR $(E50I60)_2$ correspondiente a la transición inversa fue monitorizado también por DSC. La disolución se preparó al 15.0 % en peso en PBS. Para el análisis se utilizaron 25 µL y el mismo volumen de PBS fue colocado como referencia. El procedimiento térmico que se utilizó fue el siguiente: una isoterma durante 5 min a -10° C, seguida de una rampa de calentamiento de -10 a 20° C. Posteriormente, la muestra se mantuvo a 20° C durante 1 min, y se realizó una rampa de enfriamiento hasta -10 ° C. Las rampas se llevaron a cabo a una velocidad de 1.0 °C/ min.

3.2.4.2. Análisis de porosidad y grado de hinchamiento

El cálculo de la porosidad de los hidrogeles hidratados se llevó a cabo mediante la ecuación 1:

$$porosity\ \% = \frac{W_1 - W_2}{d_{water}} \times \frac{100}{V} \quad (1)^{20}$$

donde W_1 y W_2 se corresponden con el peso del gel hidratado y liofilizado, respectivamente, d_{water} es la densidad del agua pura, y V ($\Pi r^2 h$) es el volumen medido del hidrogel en el estado hidratado.

El grado de hinchamiento (Q_w) fue estimado con la ecuación 2:

$$Q_W = \frac{W_1}{W_2} \quad (2)^{20}$$

Todas las mediciones se tomaron 24 h después de la inmersión del hidrogel en agua a dos temperaturas (4 y 37 °C). El exceso de agua superficial se eliminó con un papel de filtro antes de cada medición.

3.2.4.3. Ensayos reológicos

Las medidas de las propiedades mecánicas de los hidrogeles se llevaron a cabo mediante ensayos reológicos en un reómetro de esfuerzo controlado (AR2000ex, TA Instruments) equipado con una placa Peltier de control de temperatura para medir el módulo de cizalla dinámico (una medida de la rigidez dinámica de la matriz).

Los hidrogeles químicamente entrecruzados e hidratados se midieron a dos temperaturas (4° C y 37° C) con una geometría de platos paralelos (12 mm de diámetro) y con una fuerza normal de 0,3 N para evitar el deslizamiento. Se realizó un barrido de amplitud para confirmar que las muestras se encontraban dentro de la región de

viscoelasticidad lineal. Las mediciones de G* (módulo complejo), G′ (módulo de almacenamiento) y G″ (módulo de pérdida o viscoso) se llevaron a cabo en función de la frecuencia (entre 0.1 y 10 Hz) en un modo de deformación constante (0.1%).

También se llevó a cabo el estudio de la conversión de la disolución a gel, llamado proceso sol-gel, que tiene lugar debido a la termogelificación reversible del $(E50I60)_2$ mediante su autoensamblado. Se utilizó una geometría de platos paralelos de 20 mm de diámetro y un volumen de muestra de 200µL en PBS. Los barridos en temperatura y las cinéticas de gelificación se llevaron a cabo a una deformación constante de 0.1% y una frecuencia de 1 Hz. Los experimentos de cinética se realizaron en el rango de concentraciones de 5.0-15.0% en peso calentando la muestra de 5 a 37°C. Para la determinación de la temperatura de gelificación y de la reversibilidad del proceso, se realizó un ensayo de calentamiento a una velocidad de 1.0° C/min desde 5 a 37° C y a continuación se realizó el proceso inverso de enfriamiento en las mismas condiciones.

3.2.4.4. Microscopía óptica y electrónica de barrido.

El análisis morfológico de la microestructura en superficie de los hidrogeles se ha visualizado con un microscopio óptico Nikon ECLIPSE 80i mediante contraste interdiferencial (DIC).

Además, la morfología superficial y tangencial de las muestras (fracturadas con nitrógeno líquido) fue evaluada en un microscopio electrónico de barrido SEM (JEOL, JSM-820). Los hidrogeles hidratados a 2 temperaturas (4 y 37 °C) se congelaron instantáneamente en nitrógeno líquido y se liofilizaron. Posteriormente se metalizaron con oro (Balzers-SCD 004) antes de su observación en el microscopio.

Se ha utilizado también microscopía electrónica de barrido ambiental (ESEM) en modo de bajo vacío para la observación de los hidrogeles hidratados y previamente estabilizados a 4 y 37° C. Los experimentos se llevaron a cabo en un equipo FEI Quanta 200FEG. La microestructura de la superficie de los geles autoensamblados se ha visualizado también con esta microscopía ya que no se requiere ningún tratamiento previo de la muestra.

El tamaño medio del poro y las dimensiones de las microestructuras se han calculado utilizando el software *Image J* tomando al menos 30 poros en tres áreas diferentes para muestras en triplicado.

3.2.4.5. Análisis estadístico.

Se realizaron tratamientos estadísticos sobre los datos que se han representado como media ± desviación estándar (SD), n = 3. Los ensayos estadísticos se llevaron a cabo en los resultados obtenidos con los hidrogeles porosos entrecruzados de REDV10 y más concretamente se realizaron mediante ANOVA de un factor con el software GraphPad Prism 4.0. Un valor de *p* menor de 0.05 fue considerado estadísticamente significativo (expresado con un asterisco [*]) y cuando *p* fue menor de 0.01 se indicó con dos asteriscos [**].

3.2.5. Preparación de muestras para la obtención de nano-objetos

Las disoluciones acuosas de los ELbcRs se prepararon a partir de los polímeros E50A40, E100A40 y E50A40E50 liofilizados en las concentraciones adecuadas a la técnica de medida (0.02-5 mg/mL) en agua ultrapura tipo I a temperatura ambiente y filtrándose con membranas de PVDF de 0.45 µm. El pH neutro se ajustó mediante la adición de pequeñas cantidades de HCl o NaOH. Para las mediciones de turbidez y dispersión de luz se añadió aceite mineral en la parte superior de las disoluciones

introducidas en las cubetas porta muestras para evitar la evaporación y así el error asociado a las posibles variaciones en la concentración de las disoluciones preparadas.

3.2.6. Técnicas experimentales para la caracterización de ELbsRs y de la formación de nano-objetos

3.2.6.1. Medida de la turbidez

Los experimentos de turbidez se realizaron utilizando un espectrofotómetro UV-Vis (Varian Cary 50) equipado con agitación magnética y una cámara de muestra termostatizada. La concentración de las muestras estudiadas fue de 25 µM. La densidad óptica (OD) se evaluó por el cambio de absorbancia a 350 nm en función de la temperatura mediante barridos en calentamiento y enfriamiento y entre 30 y 80° C. Las medidas se tomaron cada 5° C estabilizando las muestras a cada temperatura hasta un valor constante de turbidez, que se consideró como la densidad óptica de la muestra a esa temperatura.

3.2.6.2. Dispersión de luz dinámica y estática

Se utilizó dispersión de luz dinámica (DLS) y estática (SLS) para caracterizar la agregación de los ELbcRs.

El valor del índice de refracción (n_D), el cual es necesario para trabajar en SLS, se estudió experimentalmente para los tres ELbcRs en un amplio rango de concentraciones ((0.02-3.40) x 10^{-3} g/ml) y de temperaturas (20-50°C) usando un refractómetro digital (Mettler Toledo RE50) equipado con un termostato Peltier. El valor del incremento del índice de refracción específico (d*n*/ dc) se dedujo a partir de la pendiente de las curvas

del índice de refracción frente a la concentración para cada ELbcR en los valores obtenidos para las cuatro diferentes temperaturas estudiadas.

Los experimentos de dispersión de luz se realizaron con un goniómetro multiángulo BI-200SM (Brookhaven) con un laser verticalmente polarizado de 33 mW de He-Ne a una longitud de onda de 632.8 nm, un correlador digital (BI-9000AT) y un baño termostatizado de decalina.

Las mediciones DLS fueron monitorizadas en un ángulo de dispersión de 90°. Las disoluciones a una concentración de 25 mM se introdujeron en tubos portamuestras de vidrio y fueron estabilizadas durante 10 minutos a la temperatura deseada entre 30 y 80° C antes de las medidas. Las funciones de autocorrelación (medidas a 65° C) se utilizaron para calcular la distribución del tamaño de las nanopartículas (radio hidrdinámico R_h) y el índice de polidispersidad.

Las experimentos SLS se realizaron utilizando las disoluciones estabilizadas previamente a 65° C en un baño de agua externo y para un intervalo de concentraciones de entre 1.0 y 5.0 mg/ml y de ángulos de dispersión de luz entre 50 y 130°. Los datos resultantes fueron analizados para determinar el radio de giro (R_g) y el peso molecular de los agregados ($M_{w,\ agg}$).

3.3. CARACTERIZACIONES REALIZADAS EN SERVICIOS EXTERNOS

3.3.1. Análisis de aminoácidos

La composición de aminoácidos de los hidrogeles obtenidos con REDV10 y químicamente entrecruzados fue determinada por el Servicio Científico-Técnico de la Universidad de Barcelona (España). Para ello, los hidrogeles fueron liofilizados y se

hidrolizaron con HCl. Los aminoácidos se derivatizaron mediante el método de AccQ-Tag Waters y se analizaron por HPLC (WATERS600 HPLC) con detección UV (WATERS2487) acoplada para su cuantificación. Cada muestra fue analizada por triplicado.

3.3.2. Determinación del peso molecular

Los análisis para la determinación del peso molecular mediante MALDI TOF MS han sido realizados en la unidad de proteomica (CRG/UPF) de Barcelona utilizando un espectrómetro de masas (Applied Biosystems Voyager STR).

La determinación del peso molecular de $(E50I60)_2$ se realizó en CovalX (Suiza) y se utilizó un Bruker Reflex IV MALDI TOF equipado con HM2 que permite la detección de altos pesos moleculares (0 a 1500 kDa).

En ambos casos las muestras fueron analizadas por triplicado.

3.3.3. Calorimetría de titulación isotérmica

Para la determinación de la concentración de agregación crítica (CAC) se realizaron experimentos utilizando calorimetría de titulación isotérmica (ITC) en el Grupo de Física de Coloides y Polímeros de la Universidad de Santiago de Compostela con un microcalorímetro VP-ITC (Microcal). Se inyectaron alícuotas de 5 ó 10 ml delas disoluciones desgasificadas de E50A40, E100A40 y E50A40E50 de concentración 10 mg/mL con una jeringa Hamilton en la celda de muestra con agua y sometida a una agitación a 200 rpm a 65° C. El flujo de calor asociado al proceso de formación de los nano-objetos se midió a cada concentración de ELbcR inyectado y los datos se analizaron con el software *Origin* proporcionado por Microcal.

3.3.4. Dicroísmo circular

Los experimentos de dicroísmo circular (CD) se realizaron en los Servicios Técnicos de Investigación de la Universidad de Alicante. Los espectros de los ELbcRs se obtuvieron en un espectropolarímetro Jasco J-810 equipado con un sistema Peltier de control de temperatura. La velocidad de barrido fue de 50 nm/min, la longitud del recorrido óptico de la celda de la muestra de 0.1 mm y la velocidad de los ciclos de calentamiento fue de 5° C / min estabilizando la muestra 10 minutos a cada temperatura. Todas las curvas de CD se suavizaron utilizando un algoritmo de reducción de ruido mediante una transformada de Fourier.

3.3.5. Microscopía de transmisión electrónica

La visualización de los nano-objetos se realizó mediante microscopía electrónica de transmisión (TEM) en un microscopio JEOL JEM-1230 en la plataforma del CIC Biogune en el Parque Tecnólogico de Vizcaya. Las muestras se prepararon mediante la deposición de las disoluciones (25 μM) calentadas previamente a 65° C, en una rejilla de cobre recubierta con carbono, tratada con plasma previamente. A continuación se dejó evaporar el agua a la misma temperatura de 65° C. Algunas de las muestras se tiñeron con una disolución de acetato de uranilo (1.0% en peso) para mejorar el contraste de las nanopartículas.

En la Universidad de Barcelona (SCT-PCB) las muestras se prepararon a partir de la disoluciones por un proceso de criofractura con un micrótomo (“freeze-fracture”) y después las muestras fueron replicadas en rejillas metálicas y se observaron en un microscopio JEM-FS2200 HRP en el Parque Científico de la Universidad de Valladolid.

3.3.6. Microscopía de fuerza atómica.

Los experimentos de microscopía de fuerza atómica (AFM) para la caracterización de los nano-objetos se llevaron a cabo en la Universidad de Barcelona (CCiTUB). Las muestras se prepararon sobre mica siguiendo el mismo procedimiento usado para muestras TEM sin tinción. Las medidas de AFM se llevaron a cabo en aire a 25° C con un 8 MultiMode AFM acoplado a un Nanoscope V en el modo de no-contacto (tapping).

4. RESULTADOS Y DISCUSIÓN

4.1. Hidrogeles bioactivos y químicamente entrecruzados obtenidos a partir de recombinámeros de tipo elastina para ingeniería de tejidos

En este resumen se mostrarán solamente los resultados más representativos de los artículos publicados y presentados en los capítulos 2 (*3D microstructuring of smart bioactive hydrogels based on recombinant elastin-like polymers*[15]) y 3 (*Synthesis and characterization of macroporous thermosensitive hydrogels from recombinant elastin-like polymers*[16]*)* de esta tesis. Se han obtenido dos tipos de hidrogeles químicamente entrecruzados; microestructurados en superficie[15] y porosos[16] utilizando dos ELRs el HRGD6 y el REDV10. Estos ELRs, como ya se comentó, son multifuncionales e incorporan cada uno una secuencia bioactiva de adhesion celular, RGD (derivada de fibronectina) o REDV (específico para células endoteliales) respectivamente.

La reacción de entrecruzamiento químico tiene lugar entre los grupos ε-amino libres de las lisinas que contiene el recombinámero y un agente entrecruzante homodifuncional, HDI, que contiene dos grupos isocianato para formar enlaces urea. Con el fin de que dichos sustratos alcancen las propiedades óptimas se ha llevado a cabo el estudio de los diferentes parámetros de reacción que pueden influir en las

características, tanto físicas como químicas de estos hidrogeles. En este sentido, se ensayaron diferentes mezclas de disolventes orgánicos (0:100; 50:50; 80:20 y 100:0) de DMSO: DMF, proporciones de ELR: entrecruzante (1:1; 1:3; 1:4 y 1:7), concentraciones del polímero (50, 80 y 100 mg/mL) y temperatura (-20, 4 y 25º C) entre otros, con el fin de optimizar las propiedades de los geles. Estas propiedades se han medido teniendo en cuenta el carácter termosensible de estos polímeros a dos temperaturas, por debajo (4º C) y por encima (37º C) de la temperatura de transición que es específica para cada polímero y que se encuentra en todo caso entre ambas.

Una vez optimizada esta reacción ha sido posible la elaboración de dispositivos más complejos como pueden ser hidrogeles con superficies microstructuradas para el estudio del comportamiento celular en sistemas de guiado celular o confinamiento y sistemas 3D porosos para el desarrollo de implantes biomédicos y su aplicación como soporte bioactivo en terapias celulares. Con este objetivo se abrieron dos líneas de investigación que consistieron en la obtención de hidrogeles con superficies microestructuradas e hidrogeles porosos.

4.1.1. Hidrogeles con superficies microestructuradas

La aplicación de las microtecnologías en biomateriales basados en ELRs, es un paso importante hacia el desarrollo de sistemas biomédicos avanzados, basados en el efecto de la topografía sobre el comportamiento celular en ingeniería de tejidos. De esta manera, los hidrogeles podrían ser estudiados desde dos perspectivas: En primer lugar, sería importante estudiar el efecto intrínseco de la bioactividad del sustrato en el comportamiento celular y en segundo lugar el efecto que podría ejercer una superficie microestructurada. Así, hemos obtenido hidrogeles, microestructurados en su superficie,

químicamente entrecruzados con HDI sobre moldes de PDMS que presentan distintas morfologías del orden de micras tales como: pilares, surcos y hendiduras (Figura 7).[15]

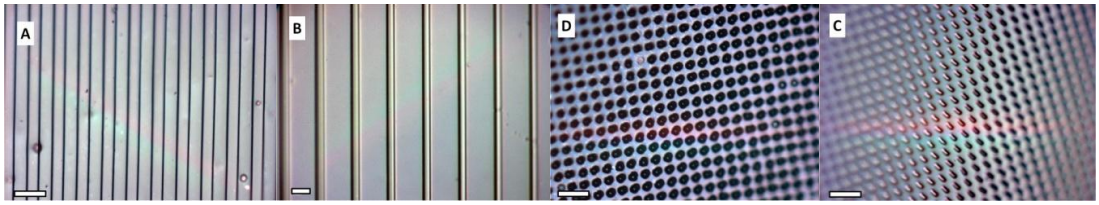

Figura 7. *Microscopías opticas de diferentes topografías de la superficie de los hidrogeles. Barra de escala: 50 µm.*

El grado de hinchamiento y las propiedades mecánicas de los hidrogeles fueron modificados variando la proporción de entrecruzante. Así, para hidrogeles obtenidos con relaciones molares ELR: HDI de 1: 4 y 1: 7 los módulos elásticos (G') obtenidos mediante medidas reológicas fueron 4311±131 y 9947 ± 230 Pa respectivamente.

Los hidrogeles presentaron una T_t de 20º C (obtenida mediante DSC), por lo que su estudio se realizó a bajas temperaturas (4º C) y a la temperatura fisiológica de 37º C. La topografía de la superficie de estos hidrogeles y el efecto en el grado de hinchamiento que causan los cambios de temperatura para los hidrogeles obtenidos con una relación molar ELR:HDI de 1:7 y sumergidos en agua fueron analizados mediante microscopía óptica (Tabla 3).

Tabla 3. *Influencia de la temperatura en las dimensiones de los hidrogeles.*

Dimensiones	Molde de PDMS	Hidrogel 4 °C	Hidrogel 37 °C
Diámetro (mm)	-	6.8 mm	4.0 mm
Anchura: Interdistancia (µm)	25: 25 20: 100	18.7 ± 0.3 : 22.2 ± 0.3 20.3± 1.0 : 71.8 ± 1.3	11.7 ± 0.5 : 13.9 ± 0.6 13.7 ± 1.0 : 50.4 ± 3.1

Los resultados mostraron una disminución del tamaño de la muestra al superar la T_t pasando de un diámetro de 6.8 a 4.0 mm. Las dimensiones de los patrones en los hidrogeles sumergidos en agua a 4º C fue de 18.7 ± 0.3: 22.2 ± 0.3 μm para las líneas de 25: 25 μm y de 20.3 ± 1.0: 71.8 ± 1.3μm para las de 20: 100μm como consecuencia del hinchamiento. El colapso causado por el cambio de temperatura tanto para los diámetros de las muestras como para las dimensiones de los patrones de las líneas fue de un 30-35% para ambas superficies, demostrando que el comportamiento termosensible se mantiene en los biomateriales entrecruzados. La posibilidad de cambiar las dimensiones de las microestructuras con la temperatura, ajustando la T_t en un intervalo de interés, por ejemplo modificando la composición de aminoácidos en el ELR, confiere a los geles un factor adicional que puede ser de gran interés en el estudio del comportamiento celular en sistemas dinámicos.

4.1.2. Hidrogeles porosos

En una segunda fase, se han obtenido hidrogeles porosos químicamente entrecruzados con porosidades y tamaño de poro controlado con el fin de poder realizar cultivos celulares tridimensionales (3D) y optimizar las condiciones más adecuadas para promover la adhesión y la colonización celular. Puesto que estas condiciones dependen del sustrato, del tipo de células y del entorno en el que se van a implantar, el objetivo de este trabajo era estudiar la microestructura interna de los hidrogeles y conseguir diversos entornos de porosidad y tamaño de poro controlado. La optimización de estos sustratos requiere conseguir una elevada porosidad e interconectividad, con una distribución controlada del tamaño del poro y adecuadas propiedades mecánicas y de esta forma promover su colonización celular. Estos hidrogeles se obtuvieron utilizando el recombinámero REDV10 e incorporando sales durante la reacción de

entrecruzamiento con HDI en disolvente orgánico. [16]Dichas sales fueron NaCl y/o $NaHCO_3$ y el proceso se ha descrito en el apartado 3.2.1.2. de Métodos.

Los hidrogeles entrecruzados sin sales mostraban una microporosidad intrínseca con tamaños de poro de 29.0 ± 11.1µm a 4º C y que además al colapso producido por su termosensibilidad reducían su tamaño a 1.3 ± 0.4µm a 37º C, lo cual no los hacía adecuados para cultivos celulares en 3D. Por ello, se realizó un primer ensayo con NaCl y se conseguía controlar la distribución del tamaño del poro mediante el tamizado previo de las sales, pero la ausencia de interconectividad impedía su utilización con éxito para el objetivo perseguido. Por este motivo, a continuación se utilizó como sal, $NaHCO_3$, que además de controlar el tamaño de poro, posibilita un proceso efervescente mediante la utilización de ácido cítrico. Con estos hidrogeles entrecruzados con NaHCO3 y seguidos del proceso efervescente se realizó el estudio de los tamaños de poro mediante microscopía electrónica. Dicha efervescencia permitió romper las paredes de los poros y la superficie de los hidrogeles mejorando así la interconectividad y la infiltración celular a través de la superficie (Figuras 8A y 8B).

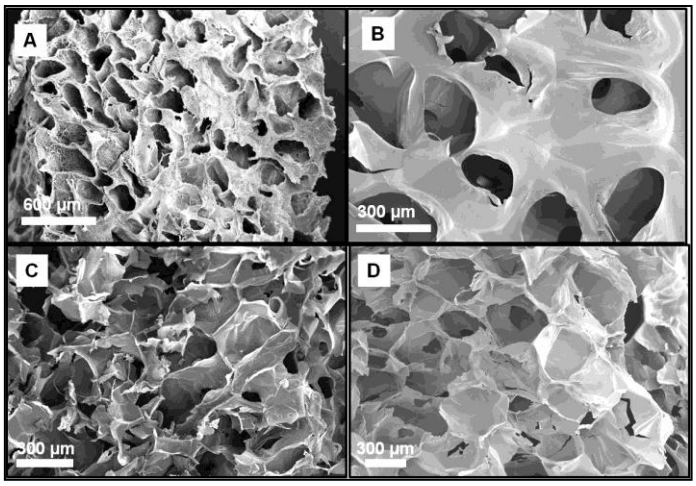

Figura 8. *Micrografías SEM de los hidrogeles obtenidos con NaHCO3/ ácido cítrico. Vistas de la superficie (A, B). Vistas de la sección transversal fracturada con diferentes tamaños de sal: (C) 180-250, (D) 250-425 µm.*

Los hidrogeles fracturados con una relación en masa de sal/ELR 10:1 mostraron una distribución media de tamaño de poro de 208.6 ± 33.5 µm para la sal tamizada entre 180-250 µm y 318.7 ± 60.3 µm para el rango 250-425 µm (Figuras 8C y 8D).

Mediante el análisis de aminoácidos de los hidrogeles se comprobó que la presencia de sales no afectó al grado de entrecruzamiento que fue del 78% en todos los casos. La caracterización física en términos de porosidad, grado de hinchamiento y propiedades mecánicas (G*) se llevó a cabo a dos temperaturas, por debajo (4º C) y por encima (37º C) de la T_t (20º C) en agua. Los resultados para los hidrogeles obtenidos con distintas proporciones de sal/ ELR están reflejados en la Tabla 4.

Tabla 4. *Influencia de la temperatura en las propiedades físicas.*

Sal/ ELR	**Porosidad (%)**		**Hinchamiento**		**G* (Pa)**	
	4ºC	**37 ºC**	**4ºC**	**37 ºC**	**4ºC**	**37 ºC**
0/1	50.38 ± 1.55	30.18 ± 1.65	3.37 ± 1.10	1.70 ± 0.30	4699 ± 109	6669 ± 205
10/1	65.65 ± 1.48	50.98 ± 2.09	28.43 ± 3.63	2.61 ± 0.16	3186 ± 120	4237 ± 50
20/1	74.63 ± 1.57	71.75 ± 3.99	36.28 ± 1.63	10.10 ± 0.49	2589 ± 84	2638 ± 209

En primer lugar estos resultados demuestran que los hidrogeles porosos también mantienen su comportamiento termosensible y que este colapso origina una disminución de la porosidad y del grado de hinchamiento dando lugar en todos los casos a geles con módulos mayores, es decir, más resistentes mecánicamente cuando se pasa a un estado colapsado, excepto en los hidrogeles obtenidos con una relación de peso de sal/ ELR 20:1 donde no hay diferencias significativas entre los valores de porosidad y propiedades mecánicas a 4º C y 37º C. En segundo lugar, los resultados mostraron claras diferencias en las propiedades físicas de los hidrogeles generados con distintas proporciones de peso de sal/ ELR. La porosidad y el grado de hinchamiento aumentan significativamente con la cantidad de sal. Sin embargo, la cantidad de sal tiene un efecto negativo sobre los módulos disminuyendo a medida que se incrementa la relación en peso sal/polímero y dando lugar a hidrogeles menos resistentes, como es razonable. Para concluir cabe destacar que el efecto más acusado del aumento de sales se produce en el grado de hinchamiento para todos los casos.

Para comprobar la viabilidad de los hidrogeles como soportes celulares o matrices extracelulares artificiales se llevaron a cabo ensayos *in vitro* de cultivos celulares con células endoteliales. Esta última serie de ensayos tenía dos objetivos principales; en primer lugar, testar la biocompatibilidad del hidrogel in vitro y, en segundo lugar, comprobar que la estructura porosa de los hidrogeles era adecuada para la infiltración de células endoteliales a través de su superficie. La transparencia de los hidrogeles facilitó la observación de las células infiltradas con microscopia de fluorescencia (Figura 9A). Las muestras se fracturaron para ser estudiadas mediante microscopia electrónica y esto permitió observar las células en el interior de los poros (Figuras 9B y 9C).

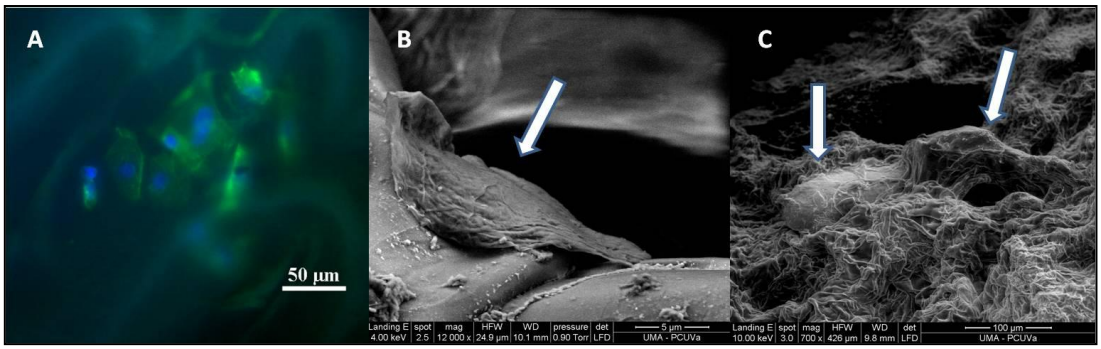

Figura 9. *Captura óptica de fluorescencia (A) y micrografías electrónicas de la sección transversal (B, C) de HUVECs sembradas en hidrogeles después de 48h de incubación.*

Los hidrogeles demostraron su viabilidad para promover la adhesión y la colonización celular dentro de la estructura tridimensional revelando no sólo su buena biocompatibilidad sino también su gran potencial para su utilización como una matriz extracelular artificial al conseguir un alto control de sus propiedades y termosensibilidad.

Así en la primera parte de este trabajo consistente en obtener sustratos entrecruzados adecuados para ingeniería de tejidos se ha estudiado la influencia de la temperatura a nivel macro- y microscópico en los sustratos obtenidos a partir de HRGD6 y REDV10. Se ha demostrado que este comportamiento termosensible se conserva en los hidrogeles entrecruzados, y esto amplía significativamente el potencial de estos sistemas como herramienta en ingeniería de tejidos porque, por ejemplo, su naturaleza termo-sensible se podría explotar combinando esta estrategia con procesos de liberación de fármacos. Con esta metodología se pueden modular tanto sus propiedades mecánicas como su morfología microestructural interna o en superficie en función del tipo de tejido final que se quiera imitar abriendo la utilización de estos sistemas para numerosas aplicaciones en medicina regenerativa.

4.2. Estudio de la formación de nano-objetos a partir de corecombinámeros de tipo elastina

En la segunda parte de la tesis se exploró la posibilidad de obtener diferentes nano-objetos autoensamblados reversibles con recombinámeros anfifílicos de bloque (ELbcRs).[23] En este resumen se mostrarán solamente los resultados más representativos del artículo publicado y presentado en el capítulo 4 (*Temperature-Triggered Self-Assembly of Elastin-Like Block Co-Recombinamers: the Controlled Formation of Micelles and Vesicles in an Aqueous Medium*[23]).

El estudio de la formación de nano-objetos en medio acuoso y a pH neutro se llevó a cabo con técnicas de dispersión de luz, turbidimetría, TEM y AFM entre otras. La preparación de las muestras se ha descrito en el apartado 3.2.5. Se seleccionó para el estudio de comparación de los ELbcRs una temperatura de trabajo de 65º C, puesto que los agregados se formaban a temperaturas superiores a 50º C y una vez formados eran estables en número y tamaño durante al menos 15 días. En la Tabla 5 se resumen los resultados obtenidos.

Tabla 5. *Propiedades de los nano-objetos.*

ELbcRs	$R_h=D_h/2$ (nm)	*P*	CAC (μM)	R_g (nm)	$\rho=R_g/R_h$	$M_{w,agg}$ (10^7g/ mol)	N_{agg}	Morfología
E50A40	74 (± 1)	0.05	5	58(±2)	0.78	1.2	312	Micela
E100A40	100 (± 3)	0.06	5	83(±3)	0.83	2.0	337	Vesícula
E50A40E50	96 (± 2)	0.04	3	87(±2)	0.91	1.1	185	Vesícula

R_h, Radio hidrodinámico; D_h, diámetro hidrodinámico; P, polidispersidad; CAC, concentración de agregación crítica; ρ, factor de forma; $M_{w,agg}$, peso molecular de los agregados; N_{agg}, número de agregación.

Los sistemas propuestos son capaces de autoensamblarse para formar nano-objetos monodispersos en solución acuosa a pH neutro por encima de la temperatura crítica a través de la desolvatación selectiva y el colapso de los bloques hidrófobos (A).

Los resultados del análisis mostraron distribuciones de tamaño, crecientes con el peso molecular, resultando valores de D_h de 140, 205 y 215 nm para E50A40, E100A40 and E50A40E50 respectivamente. La concentración de agregación crítica (CAC) fue determinada mediante calorimetría isotérmica de titulación reportando valores típicos de copolímeros de bloque anfifílicos. Mediante dispersión de luz estática se determinaron el radio de giro (R_g) que oscila entre 58 y 87 nm y el peso molecular de los agregados ($M_{w,\ agg}$) entre (1.1 y 2.0) x 10^7 g/ mol. Con estos resultados se puede estimar el parámetro ρ, el cual es sensible a la estructura y proporciona información sobre la distribución de la densidad de las partículas y por lo tanto de su morfología. Los valores de ρ cercanos a 1.0 se atribuyen a una morfología de vesículas, mientras que valores más bajos se encuentran generalmente en las micelas esféricas (teóricamente ρ = 0,77). Los valores de ρ de la Tabla 5 sugerían inicialmente que las nanopartículas autoensambladas eran micelas esféricas monodispersas para E50A40, mientras que E100A40 y E50A40E50 se autoensamblaban formando una mezcla de micelas y vesículas, siendo la formación de vesículas mayoritaria en el tribloque. Estos resultados, tanto sobre el tamaño como sobre la morfología, fueron constatados con TEM y AFM, donde se observa que la estructura de los nano-objetos formados a partir del E100A40 fue de vesícula. A modo de ejemplo, algunas de las imágenes se han representado en la Figura 10.

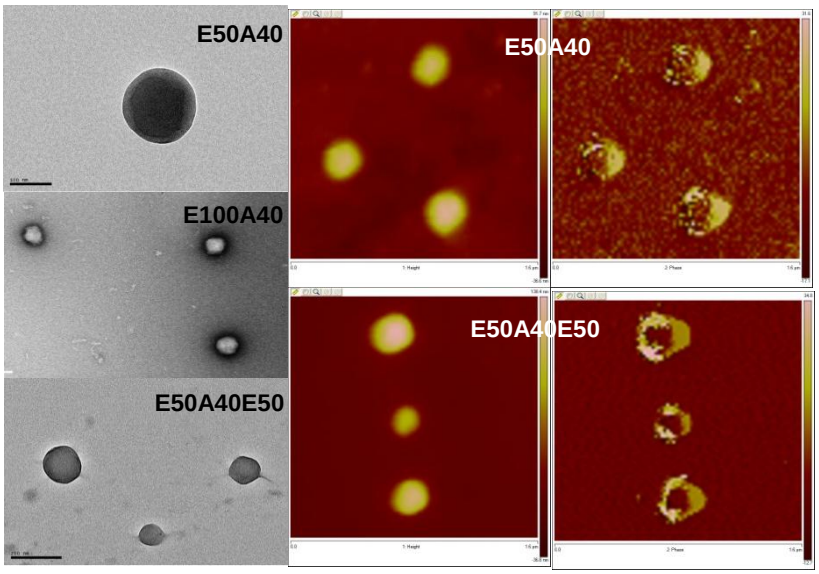

Figura 10. *Imágenes TEM (izquierda) y de altura y fase de AFM (derecha) de los nano-objetos.*

Los resultados de TEM (ver Figura 10 izquierda) revelaron nano-objetos esféricos y confirmaron la distribución de tamaños obtenida por DLS. El análisis de las muestras teñidas con acetato de uranilo al 1 % mostró la morfología característica de micelas para el E50A40 con un núcleo oscuro hidrófobo y una corona gris hidrófila indicativa de la menor densidad electrónica. Sin embargo, las imágenes de TEM correspondientes a E100A40 y E50A40E50 son completamente diferentes mostrando morfologías de vesículas convencionales. Por lo tanto, aunque los valores ρ encontrados en los experimentos de dispersión de luz no eran demasiado concluyentes, especialmente para E100A40, las imágenes de TEM muestran la ausencia de estructuras micelares y revelan el colapso de las vesículas debido a la exposición a alto vacío. Para completar estos resultados, se utilizó AFM y así observar en detalle las diferentes morfologías (ver Figura 10 derecha). Se observó un efecto similar al visto en TEM en la

deformación de las vesículas, probablemente como resultado de la fuerza inducida por la sonda de AFM.

De este modo, los resultados obtenidos muestran una evolución desde una estructura micelar (E50A40) a una vesícula hueca cambiando simplemente la longitud en el dibloque (E100A40) o el orden de los bloques hidrófilos en un tribloque (E50A40E50) incluso cuando otras propiedades moleculares, tales como el peso molecular o la polaridad media, permanecen sin cambios.

También es notable que el diámetro de las micelas es mayor que la encontrada en otros dibloques de polímero sintéticos más convencionales de peso molecular similar, lo cual puede ser explicado por el hecho de que la estructura plegada de los ELbcRs contiene una cantidad sustancial de agua (~ 50%).

Otra de las propiedades generales de estos sistemas de ElbcRs es su reversibilidad. Sin embargo, estos materiales se diseñaron específicamente para que presentaran histéresis, de manera que la redisolución de los nano-objetos no se produce llevando la muestra a la temperatura de formación, sino que sólo tiene lugar bajo un fuerte enfriamiento lo cual es característico y único de la composición del bloque A. De esta manera, los nano-objetos podrían tener aplicaciones biomédicas en condiciones fisiológicas, siempre que se formen a altas temperaturas.

Estos resultados han demostrado por tanto que estos materiales se pueden utilizar de forma eficaz, ya que la alta precisión conseguida con la producción genética de macromoléculas sintéticas permite controlar la morfología, la reversibilidad y el tamaño de los nano-objetos. Las micelas pueden actuar como vehículos de principios activos ya que pueden encapsular, por ejemplo, fármacos insolubles, vitaminas o aceites, lo cual las hace muy útiles en el campo médico, farmacéutico y cosmético

incrementando el tiempo de residencia del principio activo en el sitio de aplicación, con lo que se logra una mejora en la eficacia y en la biodisponibilidad del mismo. Además se ha conseguido con éxito la obtención de vesículas, las cuales son más versátiles para el desarrollo de vehículos de liberación en terapias combinadas, ya que pueden secuestrar moléculas hidrófobas en la membrana y encapsular especies hidrófilas en la cavidad acuosa interior (Figura 11). El siguiente paso en el desarrollo de estos nano-objetos será posibilitar simultáneamente diferentes funcionalidades en la superficie para la focalización de dianas terapéuticas en diversas aplicaciones.

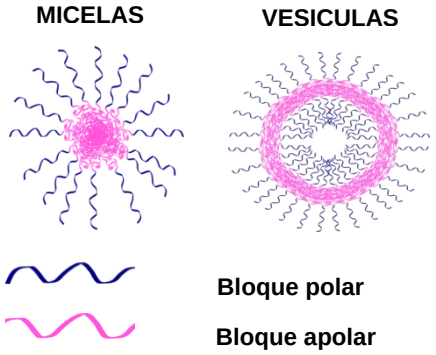

Figura 11. *Representación esquemática de micelas y vesículas.*

4.3. Hidrogeles autoensamblados o físicamente entrecruzados

El desarrollo de hidrogeles inyectables biocompatibles como soportes o vehículos tanto celulares como de diversos principios activos o agentes terapéuticos es de gran interés en la actualidad porque son sistemas mínimamente invasivos y especialmente indicados en terapias locales. En este sentido, los hidrogeles inyectables constituyen otra parte importante de esta tesis y serían de especial interés porque se podrían formar "in situ" adaptándose a la forma de la lesión sin difundir, y adherirse al tejido circundante durante la formación del gel. Con el fin de conseguir un sistema

inyectable se ha diseñado un tetrabloque $(E50I60)_2$ anfifílico de mayor orden que los sistemas anteriores que presenta termogelificación reversible con la temperatura en condiciones fisiológicas.[20] Se mostrarán solamente los resultados más representativos del artículo publicado y presentado en el capítulo 5 (*Rapid Micropatterning by Temperature-Triggered Reversible Gelation of a Recombinant Smart Elastin-Like Tetrablock-Copolymer*[20]*).*

Para conseguir que el sistema tuviera una T_t inferior a la temperatura corporal se modificó la secuencia apolar (bloque I). La formación de los hidrogeles autoensamblados tiene lugar al rebasar la T_t cuando los bloques apolares (I), en negro, forman "enlaces" físicos por agregación hidrófoba mientras que los bloques polares o hidrófilos (E), en azul, proporcionan las propiedades elásticas uniendo los diferentes agregados (Figura 12).

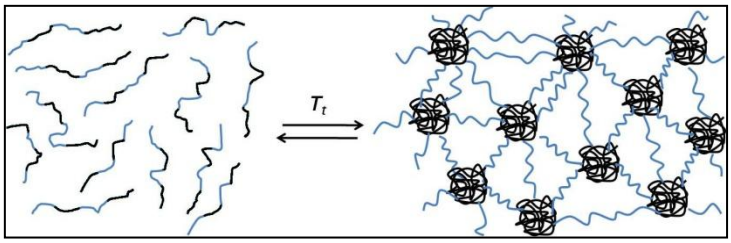

Figura 12. *Esquema de agregación hidrófoba en sistemas acuosos del tetrabloque* $(E50I60)_2$*.*

Se ha optimizado la concentración y las condiciones salinas en tampones fosfato (PBS) para su utilización como un sistema inyectable. Estos ELbcRs son solubles y fácilmente inyectables a 5 ºC y gelifican por encima de su T_t (8-15 ºC) dependiendo de su concentración. Las propiedades viscoelásticas se han estudiado mediante ensayos reológicos en función del tiempo y de la temperatura para distintas concentraciones del $(E50I60)_2$ (Tabla 6).

Tabla 6. *Resumen de los valores obtenidos mediante reología de los hidrogeles de* $(E50I60)_2$ *en función de la concentración*

Concentración (% peso)	Módulo elástico G'(Pa)	Tiempo de gelificación (minutos)
5	3.3×10^4	20
10	6.2×10^4	12
15	1.6×10^6	3

El calentamiento de 5 a 37º C en PBS mostró claramente una transición "sol-gel" (paso de una disolución a un estado sólido-gel) en un tiempo de gelificación menor de 5 minutos para un 15,0% en peso.[20] Además, combinando este proceso "sol-gel" con moldes microestructurados de PDMS hemos obtenido geles físicamente entrecruzados con distintas topografías que podrían utilizarse para cultivos celulares como en el caso de los geles químicamente entrecruzados, sin utilizar disolventes ni reactivos químicos que comprometan la viabilidad celular. También, la reversibilidad de este sistema podría ser explotada en estrategias combinadas en las que, una vez que las células hubieran crecido sobre el sustrato, podrían ser recogidas enfriando el sistema simplemente por debajo de la temperatura de gelificación. El control de la composición de los bloques y en particular la secuencia de aminoácidos del bloque apolar pueden utilizarse para modular la reversibilidad del sistema y la temperatura de gelificación. No obstante, ya para esta composición es posible modificar diferentes parámetros ya que por ejemplo el tiempo de gelificación varía de pocos segundos a varios minutos según sea la concentración de la muestra. De esta concentración depende también la temperatura de gelificación que varía entre 8 y 15º C. Para examinar la inyectabilidad y la formación del gel *in vivo*, se inyectaron subcutáneamente 100 µL de una disolución en PBS al 15% en peso a 4º C en ratones Balb-C (Figura 13). La gelificación tuvo lugar

instantáneamente dando lugar a un gel adherente y elástico en el sitio de inyección que pudo ser despegado fácilmente en su totalidad.

Figura 13. *Formación del gel in vivo. Las fotografías fueron tomadas 15 minutos después de la inyección subcutánea del* $(E50I60)_2$ *en el ratón.*

De estos resultados se puede concluir que los requerimientos de cada aplicación determinarán las condiciones de trabajo más adecuadas y que la gran versatilidad de estos sistemas autoensamblables ofrece nuevas perspectivas al diseño de hidrogeles biocompatibles.

De este diseño inicial del material inyectable, han surgido distintas estrategias en el grupo que engloban inclusiones de bloques adicionales con distintas propiedades como bioactividad, proteolisis programada o biomineralización. Como ejemplo, hemos incluido un bloque bioactivo basado en la secuencia general de adhesión celular RGD en el tetrabloque descrito para obtener un inyectable que induce adhesión y proliferación celular. Este sistema ha dado lugar a una patente (PCT/ ES2010/ 070084 (“*Biopolímero, implante que lo comprende y sus usos”*)) que se encuentra recogida en este trabajo. Además se han obtenido prometedores resultados en terapias avanzadas con células madre y como consecuencia ha llevado a cabo a un ensayo preclínico de regeneración osteocondral en el modelo de conejo (Figura 14).

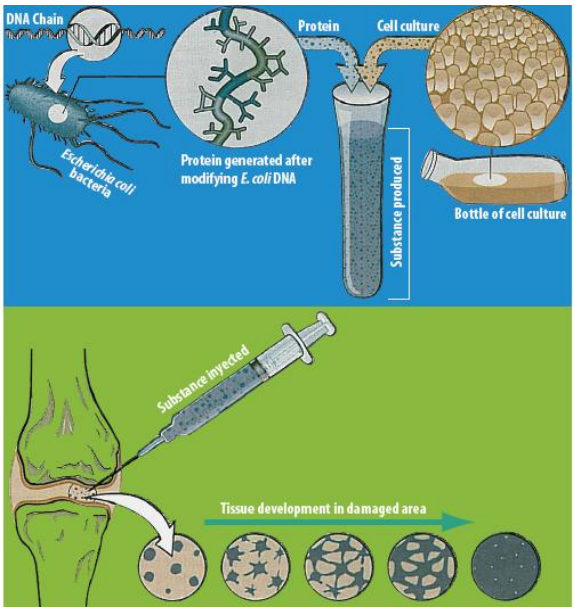

Figura 14. *Esquema general del proyecto para la regeneración de lesiones articulares.*

5. CONCLUSIONES

1.- Los recombinámeros (ELRs) y corecombinámeros (ELbcRs) de tipo elastina utilizados han demostrado poseer las propiedades para las que fueron diseñados originando sistemas biocompatibles y multifuncionales. Estos sistemas son sensibles a diferentes estímulos como la temperatura y el pH e incluyen diversas bioactividades en su cadena peptídica mostrando una extraordinaria versatilidad para aplicaciones biomédicas y nanobiotecnológicas.

2.- Los ELRs (HRGD6 y REDV10) que incorporan diversos dominios bioactivos, tales como péptidos de adhesión celular o de reconocimiento de elastasas, junto con dominios de entrecruzamiento han dado lugar mediante entrecruzamiento químico con HDI en disolventes orgánicos a hidrogeles bioactivos y termosensibles.

- El estudio de las propiedades mecánicas de los hidrogeles mediante reología ha demostrado que se pueden obtener hidrogeles con distintos módulos de elasticidad variando los parámetros de la reacción de entrecruzamiento. El

análisis de estas propiedades a temperaturas por debajo (4ºC) y por encima (37ºC) de su temperatura de transición ha confirmado que estos biomateriales entrecruzados mantienen la termosensibilidad de los ELRs de partida.

- Se han obtenido superficies microestructuradas con distintas topografías en los hidrogeles de HRGD6 utilizando moldes de PDMS con patrones. El estudio de los cambios en las dimensiones de la microestructura de los hidrogeles con la temperatura ha permitido confirmar el colapso estructural por encima de la temperatura de transición, y por consiguiente, el cambio en las dimensiones a nivel macro- y microscópico.
- También se han obtenido hidrogeles 3D porosos a partir de REDV10 con las mismas técnicas de entrecruzamiento químico en presencia de sales efervescentes combinando $NaHCO_3$ y ácido cítrico. Mediante la optimización de esta técnica se ha conseguido obtener hidrogeles con tamaño de poro controlado e interconectados, y que van desde 180 hasta 425 µm.
- Los hidrogeles porosos obtenidos han demostrado su viabilidad como sistemas multifuncionales y bioactivos con células endoteliales, observándose una colonización celular completa de toda la estructura del hidrogel y confirmando la interconectividad entre los poros conseguida mediante esta técnica.

3.- Se ha demostrado que es posible generar distintos nano-objetos a partir de los ELbcRs anfifílicos (E50A40, E100A40, y E50A40E50).

- Los nano-objetos formados en medio acuoso y a pH neutro como respuesta al incremento de la temperatura por encima de la correspondiente temperatura de transición han demostrado ser estables tanto en número como en tamaño durante al menos 15 días.

- Se ha confirmado que la redisolución de los nano-objetos no se produce llevando la muestra a la temperatura de formación, sino que sólo tiene lugar bajo un fuerte enfriamiento lo cual es característico y único de la composición del bloque hidrófobo introducido para que el fenómeno de histéresis esté presente
- El análisis del tamaño y la morfología de los nano-objetos autoensamblados muestra que se puede modular la formación de micelas y vesículas regulando el tamaño y la disposición del bloque polar. Los resultados obtenidos muestran una evolución desde una estructura micelar (E50A40) a una vesícula hueca cambiando simplemente la longitud en el dibloque (E100A40) o el orden de los bloques hidrófilos en un tribloque (E50A40E50).
- El conocimiento adquirido en la determinación de la arquitectura molecular más adecuada al tipo requerido de plataforma nanotecnológica abre el campo de aplicación a nuevos sistemas nanoterapéuticos.

4.- El diseño de un tetrabloque anfifílico de ELbcR como el (E50I60)2 ha demostrado su utilidad como hidrogel inyectable en condiciones fisiológicas.

- El sistema presenta termogelificación reversible en condiciones fisiológicas y en un amplio rango de concentraciones las cuales permiten modular la temperatura de trabajo y la cinética del proceso.
- La combinación de este proceso “sol-gel” con moldes microestructurados de PDMS ha permitido la obtención de geles físicamente entrecruzados con distintas topografías, y en condiciones fisiológicas.
- El examen de inyectabilidad subcutánea y la formación del gel in vivo han revelado su gran utilidad. La gelificación es instantánea, dando lugar a un gel

adherente y elástico en el sitio de inyección que puede ser extraído fácilmente y en su totalidad.

- Estos biomateriales inyectables han abierto el campo a una nueva familia de corecombinámeros y a una patente posibilitando su utilización en terapias mínimamente invasivas y avanzadas de ingeniería de tejidos que están demostrando resultados muy prometedores en ensayos "in vivo" y en regeneración de diversos tejidos en terapias combinadas con células madre.

REFERENCIAS

1. Langer, R.; Tirrell, D. A. *Designing materials for biology and medicine*. Nature 2004, **428**,487-492.
2. Sarikaya, M.; Tamerler, C.; Jen, A. K. Y.; Schulten, K.; Baneyx, F. *Molecular biomimetics: nanotechnology through biology*. Nature Mater. 2003, **2**, 577-585
3. Badylak, S. F.; Freytes, D. O.; Gilbert, T. W. *Extracellular matrix as a biological scaffold material: Structure and function.* Acta Biomater. 2009, **5**, 1-13.
4. Hynes, R. O. *Integrins: Bidirectional, allosteric signaling machines.* Cell 2002, **110**, 673-687.
5. Heilshorn, S. C.; DiZio, K. A.; Welsh, E. R.; Tirrell, D. A. *Endothelial cell adhesion to the fibronectin CS5 domain in artificial extracellular matrix proteins*. Biomaterials 2003, **24**,4245-4252.
6. Masuda, T.; Sakuma, C.; Kobayashi, K.; Kikuchi, K.; Soda, E.; Shiga, T.; Kobayashi, K.; Yagunima, H. *Laminin peptide YIGSR and its receptor regulate sensory axonal response to the chemoattractive guidance cue in the chick embryo.* J Neurosci Res. 2009, **87**, 353-359.
7. Lombard, C.; Bouchu, D.; Wallach, J.; Saulnier, J. *Proteinase3 hydrolysis of peptides derived from human elastin exon 24.* Amino Acids, 2005, **28**, 403-408.
8. Gilbert, M.; Shaw, W. J.; Long, J. R.; Nelson, K.; Drobny, G. P.; Giachelli, C. M.; Stayton, P. S. *Chimeric peptides of statherin and osteopontin that bind hydroxyapatite and mediate cell adhesion.* J. Biol. Chem. 2000, **275**,16213-16218.

9. Slaughter, B. V.; Khurshid, S. S.; Fisher, O. Z.; Khademhosseini, A.; Peppas, N. A. *Hydrogels in regenerative medicine.* Adv. Mater. 2009, **21**, 3307–3329.

10. Ma, P. X. *Biomimetic materials for tissue engineering*. Adv. Drug Delivery Rev. 2008, **60**, 184-198.

11. Nair, L. S.; Laurencin, C. T. *Biodegradable polymers as biomaterials.* Prog. Polym. Sci. 2007, **32**, 762-798.

12. Elisseeff, J.; McIntosh, W.; Anseth, K.; Riley, S.; Ragan, P.; Langer, R. *Photoencapsulation of chondrocytes in poly(ethylene oxide)-based semi- interpenetrating networks.* J. Biomed. Mater. Res. 2000, **51**, 164-171.

13. Mahapatro, A.; Singh, D. K. *Biodegradable nanoparticles are excellent vehicle for site directed in-vivo delivery of drugs and vaccines.* J. Nanobiotechnol. 2011, **9**, 55

14. Peer, D.; Karp, J.M.; Hong, S.; Farokhzad, O.C.; Margalit R.; Langer. R. *Nanocarriers as an emerging platform for cancer therapy.* Nature Nanotechnology 2007, **2**, 751–760.

15. Rodríguez-Cabello, J. C.; Martín, L.; Alonso, M.; Arias, F. J.; Testera, A. M. *"Recombinamers" as advanced materials for the post-oil age.* Polymer 2009, **50**, 5159-5169.

16. Rodríguez-Cabello J.C., Martín L., Girotti A., García-Arévalo C., Arias F.J., Alonso M. *Emerging Applications of Multifunctional Elastin-Like Recombinamers.* Nanomedicine 2011, **6**, 111-122.

17. Rabotyagova, O. S.; Cebe, P.; Kaplan, D. L. *Protein-based block copolymers.* Biomacromolecules, 2011, **12**, 269-289.

18. Ribeiro, A.; Arias, F. J.; Reguera, J.; Alonso, M.; Rodríguez-Cabello, J. C. *Influence of the amino-acid sequence on the inverse temperature transition of elastin-like polymers.* Biophys. J. 2009, **97**, 312-320.

19. Martín, L.; Alonso, M.; Moller, M.; Rodríguez-Cabello, J. C.; Mela, P. *3D microstructuring of smart bioactive hydrogels based on recombinant elastin-like polymers.* Soft Matter 2009, **5**, 1591-1593.

20. Martín, L.; Alonso, M.; Girotti, A.; Arias, F. J.; Rodríguez-Cabello, J. C. *Synthesis and characterization of macroporous thermosensitive hydrogels from recombinant elastin-like polymers.* Biomacromolecules 2009, **10**, 3015-3022.

21. García-Arévalo,C.; Pierna, M.; Girotti, A.; Arias, F. J.; Rodríguez-Cabello, J.C. *A Comparative Study of Cell Behavior on Energetic and Bioactive Different Polymeric Surfaces Made from Elastin-Like Recombinamers.*Soft Matter 2012, **8**, 3239 - 3249.

22. Tejeda-Montes, E.; Smith, K. H.; Poch, M.; López-Bosque, M. J.; Martín, L.; Alonso, M.; Engel, E.; Mata, A. *Engineering Membrane Scaffolds with Both Physical and Biomolecular Signaling.* Acta Biomater. 2012, **8**, 998-1009.

23. Srivastava, G.K.; Martín, L.; Singh, A.K.; Fernandez-Bueno, I.; Gayoso, M. J.; García-Gutierrez, M. T.; Girotti, A.; Alonso, M.; Rodríguez-Cabello, J. C.; Pastor, J. C. *Elastin-Like Recombinamers as Substrates for Retinal Pigment Epithelial (RPE) Cell Growth.* J.Biomed.Mater.Res. Part A 2011, **97A**, 243-250.

24. Martín, L.; Arias, F. J.; Alonso, M.; García-Arévalo, C.; Rodriguez-Cabello, J.C. *Rapid micropatterning by temperature-triggered reversible gelation of a recombinant smart elastin-like tetrablock-copolymer.* Soft Matter 2010, **6**, 1121-1124.

25. Oliveira, M. B.; Song, W.; Martín, L.; Oliveira, S. M.; Caridade, S. G.; Alonso, M.; Rodriguez-Cabello, J. C.; Mano, J.F. *Development of an Inyectable System Based on Elastin-Like Recombinamer Particles for Tissue Engineering Applications.*Soft Matter 2011,**7**,6426-6434.

26. Rincón A.C.; Molina-Martinez, I. T.; de las Heras, B.; Alonso, M.; Baílez, C.; Rodríguez-Cabello, J.C.; Herrero-Vanrell, R. *Biocompatibility of elastin-like polymer poly(VPAVG) microparticles: in vitro and in vivo studies.*J. Biomed. Mater. Res. Part A, 2006, **78A**, 343-351.

27. Martín, L.; Castro, E.; Ribeiro, A.; Alonso, M.; Rodríguez-Cabello, J. C.*Temperature-Triggered Self-Assembly of Elastin-Like Block Co-Recombinamers: The Controlled Formation of Micelles and Vesicles in Aqueous Medium.* Biomacromolecules 2012, **13**, 293-298.

28. Girotti, A.; Reguera, J.; Rodríguez-Cabello, J. C.; Arias, F. J.; Alonso. M.; Testera, A. M. *Design and bioproduction of a recombinant multi(bio)functional elastin-like protein polymer containing cell adhesion sequences for tissue engineering purposes.* J. Mater. Sci. Mater. Med. 2004, **15**, 479-484.

CHAPTER 1

General Introduction:

‘‘Recombinamers’’ as Advanced Materials for the Post-oil Age

The work presented in this chapter has been published in:

J. C. Rodríguez-Cabello, L. Martín, M. Alonso, F. J. Arias, A. M. Testera. 2009

“Recombinamers” as advanced materials for the post oil age.

Polymer 50 (22): 5159-5169

‘‘Recombinamers’’ as advanced materials for the post-oil age

J. Carlos Rodríguez-Cabello*, Laura Martín, Matilde Alonso, F. Javier Arias and Ana M. Testera

G.I.R. Bioforge, University of Valladolid, CIBER-BBN, Paseo de Belén 11, 47011 Valladolid, Spain

Keywords: Elastin-like Recombinamers; Self-assembly; Tissue Engineering; Recombinant Protein Polymers

*Correspondence to:

J. Carlos Rodríguez-Cabello

Tel.: +34 983 184 686

Fax: +34 983 184 698

E-mail: cabello@bioforge.uva.es

A b s t r a c t

Biotechnology offers powerful solutions to the challenges that arise during the design and development of new complex biomimetic materials to achieve specific biological responses. Recombinant DNA technologies, in particular, provide unique solutions in the biomaterials field, especially regarding the control of macromolecular architectures involving protein sequences with the aim of addressing the multiple functional requirements needed for biomaterials' applications. Here, elastin-like recombinamers are presented as an example of an extraordinary convergence of different properties that is not found in any other polymer system. These materials are highly biocompatible, stimuli-responsive, show unusual self-assembly properties and can include bioactive domains along the polypeptide chain. Applications of these engineered biomimetic polymers in nanotechnological systems, stimuli-responsive biosurfaces and tissue engineering will be discussed.

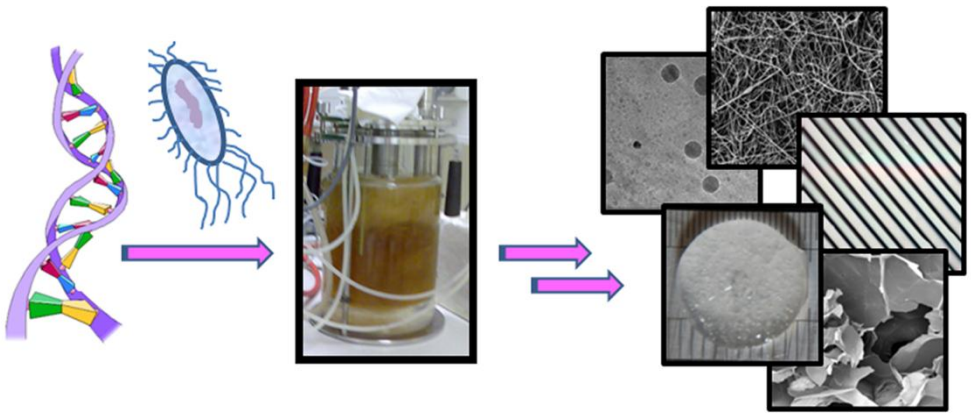

1. Introduction

Polymer science has clearly shown over several decades that macromolecules are excellent candidates for the creation of highly functional materials. As a result of the availability of thousands of different monomers and the multiple possibilities arising from their different combinations, polymer science has succeeded in producing a specific material for a particular application on many occasions, ranging from very simple materials for use as bulk commodities to highly sophisticated ones with special biomedical, engineering or nanotechnological uses. Very few other technical developments in history have shown the same rapid development and had the same deep impact on society as polymer science. The number of different technologies enabled by the existence of the appropriate polymer is amazing, and the crucial role of polymer science in the development of modern society and human wellbeing is unquestionable.

Most of the synthetic methodologies and the polymers we produce nowadays are, however, based exclusively on petroleum derived chemicals. Although there is no consensus regarding how many oil reserves remain, it is clear that this resource is finite and that its price will continue to increase if we maintain our increasing rate of demand. Additionally, we would be well advised not to wait until the imminent exhaustion of our planet's oil reserves to reduce its use as a source of energy and plastics. Growing evidence that the recent increase in atmospheric CO_2 levels is causing a measurable modification of the global climate could, in the mid- to long-term, lead us to abandon, or at least drastically reduce, oil as our main source of raw materials for plastics [1]. Polymer science will therefore soon face a similar reduction in its dependence on oil to that currently being experienced by the energy sector.

Our current state of technological development and well-being cannot be maintained by sacrificing the expectations of future generations-sustainability must

therefore also be a key objective in polymer science. However, we must be fully aware of the actual meaning of ‘‘sustainability’’. We are obliged to develop sustainable technologies that fulfill the needs of future generations. This does not mean that we must search for alternative and sustainable technological solutions, simply to maintain our current level of development. Therefore, with the degree of technical development that our grandparents enjoyed, our grandchildren will not be satisfied by a world in which polymers produced from renewable sources ‘‘only’’ match the performance of the ‘‘old’’ oil-derived plastics.

The challenge that polymer science is currently facing must therefore be tackled from all sides. We, as polymer scientists, must develop technologies to change our current oil-dependence and unsustainability. This challenge must also be considered an opportunity to create a new polymer science which, in addition to being sustainable, will launch a technological revolution that will lead to new concepts, materials and products which will be more efficient, functional and than those we have today. Part of the aim of the present manuscript is to present evidence that this purpose is not just a utopian yearning for a better world and that some signs that this is possible may already be present.

Our level of technological development has been supported by a progressive abandonment of natural products and the extensive use of ‘‘synthetic’’ elements which, in terms of composition and concept, are far from being natural substances. Paradoxically, one of the most promising strategies for solving current problems is to reconsider natural products, or rather to introduce concepts imported from nature in our future synthetic materials and systems, and not only for the sake of sustainability. Thus, taking polymer science as an example, biology discovered long ago that

macromolecules are the best option for obtaining highly functional materials. Relatively novel concepts in materials science such a hierarchical organization, mesoscale self-assembly or stimuli-responsiveness are common to many natural macromolecules such as proteins, nucleic acids or polysaccharides (or combinations of them). In fact, the slow but relentless process of natural selection has produced materials that show a level of functionality significantly more complex than that reached by synthetic materials. One of the best (and nicest) examples of this is the proteins. The proteins in living cells show an amazing set of capabilities in terms of functionality, ranging from the structural proteins, all of which show a significant ability to self-assemble, to the extraordinary enzymes, with their superior catalytic performance, and highly efficient molecular machines such as the flagellar rotary motor, etc. Natural proteins are usually large and very complex molecules which contain diverse specific functional groups that generate and promote self-assembly and function. Nature also makes use of different physical processes that allow directed and controlled organization from the molecular to the macroscopic level. In general, both local organization through functional chemical groups and the physical properties that give rise to order on larger scales provide the properties and functions that the biological systems require to function efficiently.

Nevertheless, the basis for all of this amazing functionality displayed by natural proteins seems to be based on one simple concept, namely a complex and completely defined primary structure. Protein biosynthesis in living cells occurs with an absolute control of the amino-acid sequence, from the first amino acid to the last, with a complete absence of randomness. Indeed, the need for such absolute control becomes dramatically apparent in some genetic disorders where the lack or substitution of just one amino acid in the protein leads to a complete loss of the original function, which can have dramatic consequences in patients with sickle cell anemia, phenylketonuria

and cystic fibrosis [2]. If we want to create truly functional materials, we must therefore find a way to synthesize complex and completely defined macromolecules. This task, which is currently too difficult for even our most sophisticated chemical methods, occurs routinely in all living cells. One further characteristic of protein biosynthesis should be highlighted at this point, namely that the machinery for protein biosynthesis is extraordinarily flexible. Ribosomes are able to process and produce practically any amino-acid sequence stored in the information elements known as genes, which means that the flexibility of this process is essentially absolute. From a practical point of view, if we can therefore somehow control the information that genes deliver into the machinery, we can also control the biosynthesis process itself.

This idea also has remarkable precedents. In the last few years, significant effort has been dedicated to replacing petrochemical-based chemical processes with biological methods using renewable resources. Thus, fermentation processes for the production of biological monomers have been improved by numerous studies involving the metabolic engineering of microorganisms and the directed development of enzymes. Such microorganisms have been widely exploited for medical, agricultural, food and industrial applications. In addition, they have been engineered to produce recombinant proteins, amino acids and chemicals for use as drugs and biofuels [3, 4]. For example, various monomers have been produced via different biological pathways, depending on the microorganism, from substrates such as succinic acid, lactic acid or some diols [5]. This process involves the whole metabolic and regulatory network together with fermentation, recuperation and subsequent purification processes.

The development of new technologies has made it possible to follow protein expression in cells and tissues through proteomics and it has allowed researchers to

engineer proteins with new functions that lead to extraordinary technical applications. Nature has designed proteins with specific functional properties, such as the ability to self-assemble, recognition specificity or monodispersity, and scientists are now starting to exploit and enhance these properties in protein-based materials. Genetic and protein engineering provide us with the tools to precisely produce numerous protein-based polymers far above the current capabilities of synthetic polymer chemistry. These techniques allow us to synthesize protein chains with absolute control over their molecular mass, composition, sequence and stereochemistry. This is a key drawback of conventional chemical synthesis, where any increase in the complexity of the final molecule unavoidably leads to an almost exponential increase in the time and cost of the synthesis.

The use of recombinant DNA technologies to obtain protein-based polymers with total control of the randomness of the polymer sequence permits us to design the required functionalities of the final biomaterial in a highly precise manner. The success of engineered protein polymers in material applications will, however, depend on being able to obtain materials with specified physical and chemical properties. As an example of these approaches, we show here how elastin-like polymers (ELPs) play an important role in the synthesis of advanced materials, with a particular emphasis on biomedical and nanotechnological uses.

1.1. Genetic Engineering of Protein-Based Macromolecules

In the last few years, the application of powerful molecular biological methods has allowed the design and synthesis of new advanced materials almost at will. The use of the 20 naturally occurring amino acids in the design and production of genetically engineered functional protein-based macromolecules with specific or multifunctional properties offers practically infinite possibilities and a significant number of advantages.

First, DNA technologies allow the introduction of tailored synthetic genes into the genetic make-up of a microorganism, plant or other organisms which induces the production of its encoded protein-based polymer as a recombinant protein [6, 7]. These macromolecules offer the possibility to obtain materials with some of the complex properties found in natural proteins in combination with functions of particular technological interest that are not displayed in living organisms. Secondly, the degree of control and complexity attained by genetic engineering is clearly superior to that achieved by conventional chemical synthesis. These polymers, for example, are strictly monodisperse and can be obtained with molecular weights ranging from a few hundred Daltons to more than 200 kDa [8]. This has enabled the study of the dependence of different material properties on molecular mass in a simple and highly precise manner [9]. Thirdly, the production cost of those materials is not related to their complexity as the most costly task in terms of both time and money is the gene construction. However, once the genetically modified (micro)organism is obtained, its fast and cheap production rapidly compensates for the costs associated with the molecular biology steps. This intrinsic advantage also has environmental benefits as recombinant protein-based materials are obtained by an easily scalable technology fermentation that uses only moderate amounts of energy and temperatures, with water as the only solvent. Finally, the genetic engineering of protein-based polymers is a relatively new methodology and only a limited number of research groups and companies have adopted this approach for their production. Despite the fact that interest in these materials has mainly concentrated on two major polymer families, namely spider-silk polymers [10, 11] and ELPs [12-16], and their combinations [17, 18], other interesting

protein polymers, such as those based on resilin [19], abductin [20] or gluten [21], among others, have also been studied.

1.1.1. Some Considerations Regarding Nomenclature

There is no consensus on how those materials should be named. The term most often used in the literature is ‘‘Recombinant Protein Polymers’’, although this term is unsuitable for many reasons. First of all is too long to be of practical use and, more importantly, it is confusing and does not describe what it tries to. ‘‘Protein polymer’’ can be understood as a polymer made of proteins, which of course is not the case. These materials are proteins only because they are produced as recombinant proteins, although their composition is the result of an engineered design step and the creation of a synthetic gene which is often totally unrelated to the composition of any natural protein. In addition, the term ‘‘polymer’’ is not adequate in most cases. The recombinant materials obtained from an artificial gene are normally macromolecules with a molecular mass comparable to that of conventional polymers. However, these recombinant materials are in many cases made from huge and complex monomers that are only repeated a few times (or do not repeat at all) in the final molecule so, despite their high molecular mass, they should strictly speaking be termed oligomers. In light of these considerations, we propose the use of a specific term that can be specifically associated with this new kind of macromolecules and which is sufficiently informative to clearly describe the main characteristics of this emerging class of materials. This term is ‘‘recombinamer’’, which clearly indicates the oligomeric nature of these compounds and their production as recombinant proteins. In addition, recombinamer strongly resembles the term polymer, thereby suggesting the macromolecular nature of these materials but without requiring that they involve a continual repetition of small and simple monomers. The term recombinamer also prevents the reader from automatically

identifying these molecules with natural proteins, or some modification thereof, but rather suggests a molecule whose composition is defined strictly by engineering design. This term will therefore be used throughout this manuscript.

1.1.2. The Example of Elastin-Like Recombinamers (ELRs)

ELRs are a promising model of biocompatible protein-based polymers. The basic structure of ELRs is a repeat sequence found in the mammalian elastic protein elastin, or a modification thereof [22]. Some of their main characteristics are derived from those of the natural protein. For example, the cross-linked matrices of these polymers retain most of the striking mechanical properties of elastin [23], which becomes important when this behavior is accompanied by other interesting properties, such as biocompatibility [24], stimuli-responsive behavior, and the ability to self-assemble. These properties are based on a molecular transition of the polymer chains called the inverse temperature transition (ITT). This transition is the key to the development of new peptide-based polymers as molecular devices and materials.

The expansion of molecular biology has allowed the design of complex bioengineered ELRs as well-defined polymers [9, 15, 25, 26]. The most well known members within the ELR family are based on the pentapeptide VPGVG (or its permutations), and a wide variety of polymers with the general formula (VPGXG), where X represents any natural amino acid except proline, have been (bio)synthesized [15, 27, 28]. All the polymers with this general formula found in the literature display functional properties such as acute stimuli-responsive behavior. The substitution of any of the other amino acids in the pentamer is not so simple. For example, the first glycine can only be substituted by *L*-alanine [27].

All functional ELRs exhibit a reversible phase transition in response to changes in temperature [29]. In aqueous solution, and below a certain transition temperature (T_t), the free polymer chains remain disordered, random coils [30] that are fully hydrated, mainly by hydrophobic hydration. This hydration is characterized by ordered clathrate-like water structures surrounding the apolar moieties of the polymer with a structure somewhat similar to that described for crystalline gas hydrates, although with a more heterogeneous structure that varies in terms of perfection and stability [31, 32]. Above T_t, however, the chain folds hydrophobically and assembles to form a phase-separated state containing 63% water and 37% polymer by weight in which the polymer chains adopt a dynamic, regular, non-random structure known as a β-spiral, which involves type II β-turns as the main secondary feature and is stabilized by intra-spiral, inter-turn, and inter-spiral hydrophobic contacts [27]. This is an effect of the ITT. In this folded and associated state, the chain loses essentially all of the ordered water structures arising from hydrophobic hydration. During the initial stages of polymer dehydration, hydrophobic association of the b-spirals means they take on a fibrillar form. This process starts with the formation of filaments composed of three-stranded dynamic polypeptide b-spirals which grow to form particles several hundred nanometers in diameter before settling into a visible phase-separated state. This folding is completely reversible on lowering the sample temperature below T_t [27].

However, coacervation can be a complex process that is strongly influenced by the composition of the ELP. This is evident, for example, by examining the molecular and microscopical phenomena taking place in the coacervation of tropoelastin. Recent studies suggests the presence of complex structures involved in the coacervation of the that natural protein. Circular dichroism has showed the importance of α-helices and subsequent helical side chain interactions that limit the conformation of tropoelastin

during coacervation [33]. Further, studies support a role for domain 26 [34], a junction between 10, 19, and 25 [35] and more recently for domain 30 [36].

2. Stimuli-Responsiveness and Self-Assembly Properties of ELRs

The responsive behavior of peptide-based materials has been defined as their ability to respond to external stimuli. This behavior is even more interesting when the materials show reversibility at either the structural or functional levels, thereby offering obvious advantages as stimuli-responsive materials. The T_t of the ITT can be measured by different techniques, the most widely used being turbidity measurements and calorimetric methods that measure the heat flow during the transition. The turbidity profile and heat flow from a differential scanning calorimetry (DSC) measurement are plotted against the temperature in **Fig. 1.**

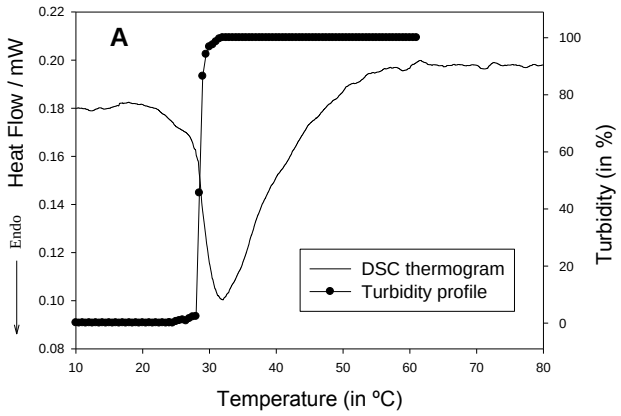

Fig. 1. *DSC thermogram of poly(VPGVG) (50 mg/ml) in water (heating rate: 5 °C/min) and turbidity profile as a function of temperature for a 5 mg/ml aqueous solution of the same polymer. The two photographs are taken below (4 °C) and above (40 °C) the T_t [16].*

The T_t values obtained by these methods often differ depending on the method, with several factors likely to be responsible for these differences [16]. In addition, T_t also depends on the molecular mass, the mean polarity of the polymer [9], and the

presence of other ions and molecules [37-39]. In conclusion, all these factors make the comparison of T_t values a very delicate matter.

As regards self-assembly, many synthetic strategies have been developed to obtain advanced devices in an attempt to mimic the behavior of biology in nature. These techniques have been based on the concept of self-organization and self-assembly in order to arrange hierarchically ordered complexes. Both of these mechanisms are widely used by nature and can be exploited in synthetic devices. Peptides and proteins are useful building blocks to obtain ordered nanostructures via self-assembly due to their well-stabilized folding, stability, and protein-protein interactions [40].

Natural elastin undergoes a self-aggregation process in its natural environment, leading to the formation of nanofibrils from a water-soluble precursor called tropoelastin [27, 41]. This ability resides in certain relatively short amino acid sequences, which are known to coacervate and form fibrillar aggregates with a high degree of β-turn structure [42]. The development of genetic engineering techniques has allowed tailored molecular designs of ELRs with wide-ranging possibilities of being able to form other topologies and nanostructures to be obtained. Thus, the pH-responsive ELR $[(VPGVG)_2(VPGEG)(VPGVG)_2]_{15}$ is able to form polymer sheets containing self-assembled nanopores (see **Fig. 2**) [43].

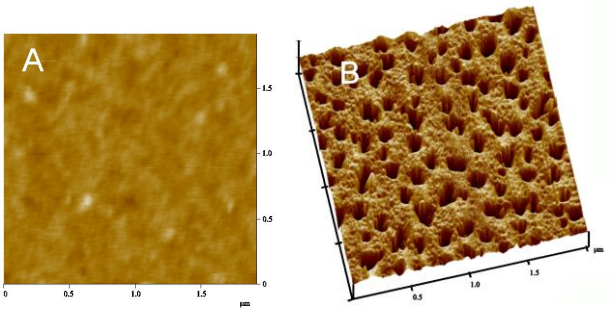

Fig. 2. *AFM image of* $[(VPGVG)_2(VPGEG)(VPGVG)_2]_{15}$ *deposited from a water solution onto a hydrophobic Si substrate. Sample conditions: (A) 10 mg/ml in aqueous*

0.02 M HCl solution (acid solution). (B) 10 mg/ml in aqueous 0.02 M NaOH solution (basic solution) [43].

An atomic force microscopy (AFM) study of the topology of polymer spin-coated films of the Glu-containing ELR, from acid and basic solutions, onto a hydrophobic Si substrate at temperatures below T_t has shown that, under acidic conditions, the polymer film shows only a flat surface with no outstanding topological features (**Fig. 2A**). When deposited from basic solution, however, the polymer film clearly shows an aperiodic pattern of nanopores (width of approximately 70 nm and separated by approximately 150 nm; **Fig. 2B**). This different behavior as a function of pH has been explained in terms of the different polarity shown by the γ-carboxyl group of the glutamic acid. In the carboxylate form, this moiety has a markedly higher polarity than the rest of the polymer domains and the substrate itself. The charged carboxylate groups therefore impede any hydrophobic contacts in their surroundings, which is the predominant assembly method for this kind of polymer. These charged domains, along with their hydration sphere, therefore become segregated from the hydrophobic surrounding, thus leading to nanopore formation.

3. ELRs as Advanced Materials for Biomedical Applications

ELRs show an additional property which is highly relevant for the use of these polymers as advanced materials for biomedical applications, namely their extraordinary biocompatibility [24]. In addition, their biodegradability is obvious as the secondary products of their bioabsorption are simply natural amino acids.

3.1. Nanotechnological Systems

The increasing need for drug-delivery systems that improve specificity and activity whilst at the same time reducing toxicity to ensure maximum treatment safety

has led to the development of a wide variety of new materials, many of which have been employed to control the release of drugs and other active agents. Polymeric systems are, however, often the system of choice because of their desirable physical properties [44].

Recombinant polymers, such as thermo-responsive ELRs, represent one of the possible next steps in the development of drug carriers beyond traditional, synthetic polymers. Elastin biopolymers respond to external stimuli by undergoing a reversible phase transition where, at temperatures above T_t, the ELR hydrophobically self-assembles into an insoluble aggregate, thus forming nano- and microparticles which could be loaded with a drug. The first ELR-based drug-delivery system was a simple device in which γ-radiated cross-linked poly(VPGVG) hydrogels of different shapes were loaded with a model water-soluble drug (Biebrich Scarlet), which was released by diffusion. Additionally, the inclusion of some glutamic acids along the polymer chains was used to control the hydrolyzable cross-linking. The cross-linking was of the carboxyamide type and the drug was released as these cross-links were hydrolyzed at a given rate [45]. Poly(VPAVG) nano- and microparticles have also been tested as carriers of the model drug dexamethasone phosphate in order to develop injectable systems for controlled drug release [46]. Nanoparticles with a diameter of around 300-400 nm have recently been obtained from ELRs by a novel application of the electrospray technique to encapsulate drugs. The morphology and size of these polymer nanoparticles can be controlled by varying the composition, molecular mass, and solvent, amongst others [47]. In other recently study, nanoscale protein particles with less than 100 nm in diameter were constructed using temperature-sensitive ELR and polyaspartic acid chain under physiological conditions. The critical temperature of formation of the particle can be adjusted by the lengths of the aspartic acid chain and the

ELR. Therefore if a lower critical temperature is required, it is only necessary to elongate the ELR [48].

ELRs are particularly attractive for the synthesis of block copolymers that self-assemble into polymer nanostructures such as micelles. The first work in this area involved an elastin-mimetic di-block copolymer containing VPGEG-$(IPGAG)_4$ and VPGFG- $(IPGVG)_4$ as the hydrophilic and hydrophobic blocks, respectively [49]. The resulting micelles were studied by dynamic light scattering (DLS) and DSC was used to measure the enthalpy of self-assembly. A tri-block copolymer was subsequently synthesized and the TEM images of this polymer showed that it formed spherical aggregates [50]. Other multivalent spherical micelles have been obtained from linear elastin-like AB di-block copolymers in the temperature range 37- 42 °C with the aim of targeting cancer cells [51]. Bidwell et al. have also exploited the ELRs for its ability to serve as macromolecular carriers for thermally targeted delivery of drugs. Attachment of doxorubicin to ELR-based system showed enhanced cytotoxicity in uterine sarcoma cells when aggregation was induced with hyperthermia [52].

We have also synthesized amphiphilic di- and tri-block copolymers to study the micelle self-assembly process. These block copolymers contain two different blocks: one with the monomer [$(VPGVG)_2$-(VPGEG)-$(VPGVG)_2$] (E-block) and the second with the monomer [$(VPGAVG)_m$] (A-block). Both these blocks are thermoresponsive and the E-block is also pH-responsive [53]. The spontaneous formation of nanostructures can therefore be controlled by changing both the pH and the temperature, and vesicles with different sizes have been obtained [54] (**Fig. 3**).

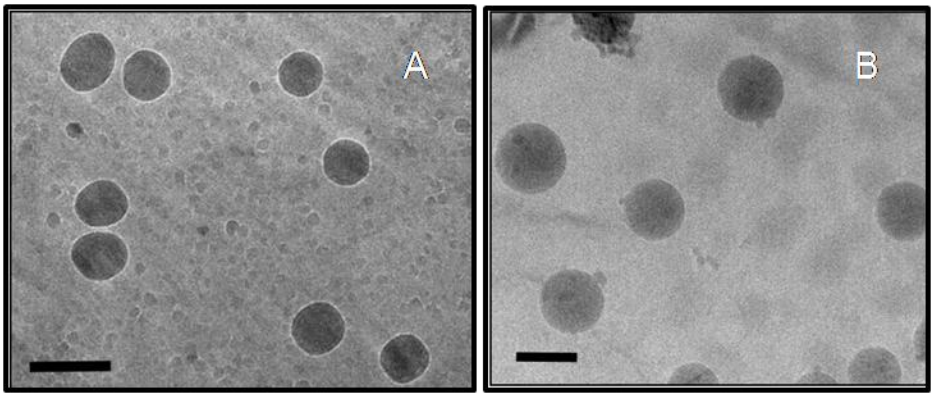

Fig. 3. *Cryo-TEM images in aqueous solution: (A) E50A60E50, (B) E50A60. Scale bars: 200 nm.*

3.2. Biosurface Engineering

Surface engineering is an important tool for understanding the molecular mechanisms involved in protein adsorption and cell-surface interactions. The design and control of these features is a key challenge for diverse specific biological applications [55, 56]. Multiple approaches involving physical and chemical modifications, such as coatings and grafts or the introduction of small biological ligands (peptides or proteins), have been developed in the surface engineering of biomaterials [55-59]. These approaches allow surfaces to be functionalized with fouling-anti fouling features, specific groups for cell-material interactions, responsive behavior (stimuli or environmentally sensitive), or with micro- and nano-patterns.

3.2.1. Functionalized Surfaces with ELRs

The modification of surfaces with stimuli-responsive polymers that vary their physical and chemical properties in response to changes in their environment or external stimuli makes these polymers excellent candidates for the development of stimuli-responsive surfaces [60-62]. In most cases, the surface is grafted with derivatives of poly(N-isopropylacrylamide), a well-known thermo-sensitive polymer. ELRs exhibit some additional advantages that make them excellent candidates for the development of responsive surfaces. Therefore, Ozturk et al. have prepared recently micropatterned

pNIPAM films as thermo-responsive cell carriers. They were chemically modified by ELR adsorption containing RGD amino acid sequence to promote cell adhesion. They have studied the thermal responsiveness to apply mechanical stress on cells under in vitro conditions to induce bone formation showing that ELR is crucial for maintaining the cells attached on the surface in dynamic culturing [63]. For instance, genetic engineering allows them to be designed with extraordinary control of the sequence and with desirable properties, which means that in addition to their thermo-responsive behavior they can also respond to other stimuli such as pH, light, or ionic strength, amongst others. On the other hand, biosynthesis enables precise control of the reactive sites on the polypeptide chain for use in surface grafting. For example, the nanometric control of their position leads to a tremendous potential for self-assembly and other functionalities displayed by these systems. Biosensing surfaces can take advantage of the reversible phase-transition behavior of ELRs to obtain an active surface whose properties such as hydrophobicity and functionality can be quickly modulated by a simple temperature change. However, in spite of the enormous potential of these biopolymers, there are only a few examples of surfaces functionalized with ELRs, one of which makes use of the above-described topologically modified self-assembly ability of the recombinant ELR $[(VPGVG)_2\text{-}(VPGEG)\text{-}(VPGVG)_2]_{15}$. Thus, by covalently micropatterning ELRs onto glass surfaces, Chilkoti's group has created what they have called ''thermodynamically reversible addressing of proteins'' (TRAP) [55,61]. This allows the reversible, spatio-temporal modulation of protein binding at a solid liquid interface and can be applied in different systems for bio-analytical devices.

Other techniques used for ELRs include layer-by-layer deposition of alternating ELR-polyelectrolytes, which is a simple technique to generate bioactive surfaces [64].

These ultra-thin nanoscale coatings promote cell adhesion and proliferation and the results show that the thickness and mechanical integrity of the multilayer assembly modulates the cell response. Costa *et al.*, for example, have developed thermo-responsive thin coatings using electrostatic self-assembly (ESA). A recombinant ELR containing the cell attachment sequence RGD has been deposited onto chitosan and has been found to show enhanced cell adhesion in comparison with the original chitosan monolayers or glass substrates [65]. These examples open up the field of polymeric coatings that include specific biofunctional responses.

3.2.2. Nano- and Microtopographical Surfaces

In the last few years the combination of surface chemistry with microfabrication techniques has provided new tools to study the interactions of cells with their environment. Using lithography and patterning techniques, peptides and proteins can be deposited with complete spatial control on specific regions of a surface [66, 67]. The ability to obtain nano- and micrometer-sized patterns of biological macromolecules is of great importance for several applications, including biological assays, miniaturized biosensors, and biomedical diagnostics.

ELRs have been employed in the design and development of regenerable biosensors and microfluidic bioanalytical devices, as reported by Chilkoti et al. [68]. Thus, nanostructured surfaces that are able to capture and release proteins using the self-assembly properties of ELRs have been obtained by combining ELRs and dippen nanolithography.

In our group, we have adapted the simple method of replica molding to obtain 3D microstructured thermo-responsive hydrogels [69]. Replica molding is a fast, flexible, and straightforward micropatterning technique that can be carried out routinely and consists of only a few steps: dispensing of the polymer on the mold, cross-linking, and

release of the replica ELR hydrogel. In this study, which aimed to test the thermally responsive behavior of macroscopic and micropatterned features, we obtained hydrogels with micropatterns such as lines or pillars with different dimensions and spacings (see **Fig. 4**).

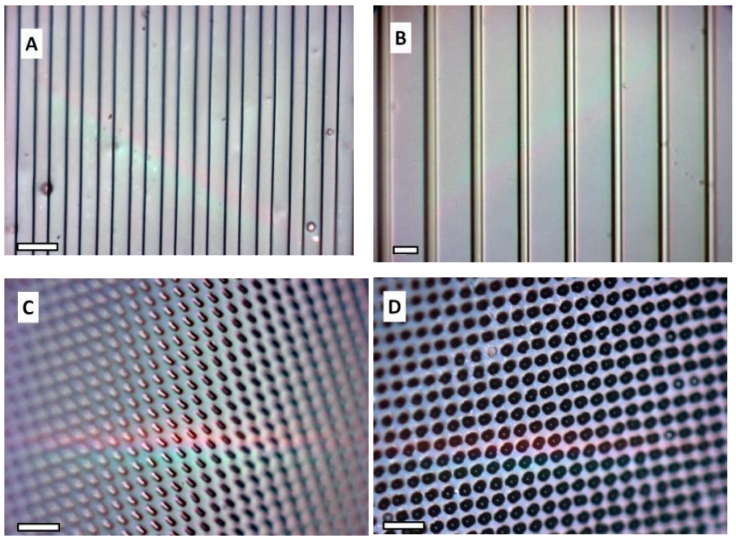

Fig. 4. Optical micrographs of different micropatterned hydrogels. Scale bars: 50 μm [69].

The dimensions of the microfeatures with micropatterned lines were tested with respect to the water temperature, with a 30- 35% decrease in dimensions being observed for both patterns at a temperature above the transition temperature of the hydrogels (20 °C). This thermo-responsive behavior does not modify the topography and can be used to change the dimensions of the micropatterned features during cell culture. Furthermore, these systems permit controlled topography to be added as a further factor for studying cell behavior and cell-surface interactions, thereby improving the extraordinary properties of ELR hydrogels, particularly their bioactivity, biocompatibility, and the "tenability" of their mechanical properties.

The ability to generate micro/nanoscale features with synthetic and natural polymers has been improved by using a simple fabrication technology known as

electrospinning [70, 71]. This process has been widely used in the textile industry and organic polymer science and has now reappeared as a novel tool for fabricating biopolymer scaffolds [72-74]. The electrospinning process involves applying a high voltage to create an electrically charged jet of polymer solution, which dries to leave a polymer nanofiber mesh. The fibers produced by this process usually have diameters on the order of a few micrometers down to less than a hundred nanometers. Their structural properties depend on processing parameters such as polymer concentration and viscosity, flow rate, and applied voltage, amongst others [75]. The ability to vary fiber size in the nanometer range opens up the possibility of mimicking the size scale of fibrous proteins found in the natural extracellular matrix. Indeed, fibers made from different proteins such as fibrinogen [76], gelatin [73], collagen-elastin mixtures [77], or silk-like proteins [78] have been obtained. The first elastin-mimetic protein fibers were produced from a genetically engineered ELR [79]. Different morphological patterns, such as beaded fibers, thin filaments, or broad with a ribbon-like appearance, were obtained by varying the solution concentration. To date, electrospun elastin analogs have only played a key role in modulating the viscoelastic properties of the resulting blended material the inclusion of bioactive domains in their structure has not been reported. We have also exploited this technique to obtain nanofibers from an aqueous solution of multifunctional recombinant ELRs containing cell-attachment sequences [80]. These fibers were chemically cross-linked after deposition and immersed in water to study their morphology. **Fig. 5** shows the SEM micrographs of our ELR nanofibers.

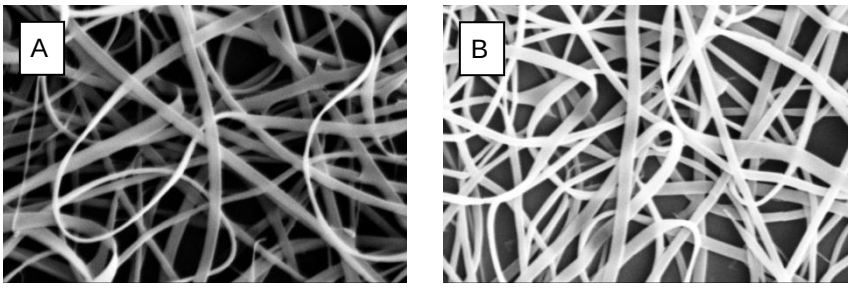

Fig. 5. SEM micrographs of ELR nanofibers: A) as-deposited fibers; B) cross-linked fibers. Scale bars: 5 μm.

The average size indicated a diameter increase of about 15-20% after the cross-linking reaction. These substrates were tested in different cell human lines and showed interesting properties in terms of cell adhesion. An ELR with a similar composition but lacking bioactive domains has shown non-fouling properties, thereby suggesting future applications where nonspecific adhesion could be desirable [80].

4. Tissue Engineering

The design of functional biomaterials that induce a specific cellular response is a major challenge in the field of materials science. Methods for fabricating stimuli-responsive biomaterials have allowed these materials to play a more interactive role in tissue engineering [81, 82]. However, there are several requirements that a biocompatible material should provide to promote cell attachment, differentiation, and proliferation. Thus, the scaffold must be biocompatible and biodegradable and it should show properties that support tissue morphogenesis. This generally requires an artificial extracellular matrix that can supply temporary mechanical support until the engineered tissue has sufficient mechanical integrity to support itself.

The extracellular matrix (ECM), which contains a complex composition of fibrous proteins and heteropolysaccharides, is an important model for biomaterials' design. Recombinant DNA technologies allow the design and expression of artificial genes to

prepare artificial analogues of ECM proteins with controlled mechanical properties that incorporate domains to modulate cellular behavior [83]. Future advances in tissue engineering will depend on the development of biomimetic materials that actively participate in the formation of functional tissue.

The first candidate ELRs for tissue engineering were poly-(VPGVG) and their cross-linked matrices [12]. These materials were tested for cell adhesion and it was found that cells did not adhere to them. This provided a starting point to obtain key biomaterials which maintain their biocompatibility and adequate mechanical properties but lack nonspecific bioactivity. The subsequent incorporation of active peptides as cell-adhesion ligands resulted in a high capacity to promote cell attachment. These bioactive (VPGVG) derivatives containing the general adhesion peptides RGD and REDV, the latter of which is specific for endothelial cells, showed similar cell attachment behaviors to human fibronectin [84]. Once genetic engineering was adopted as the production method of choice, the molecular designs started to increase in complexity. The addition of different functionalities as cross-linking domains facilitates the attainment of more uniform substrates, which are usually based on lysine residues incorporated in the elastin-based repeat unit (VPGXG) [23,26,85]. ELR hydrogels produced by photoinitiation [86], irradiation [87, 88], amine reactivity [13, 23, 26, 85, 89-93], and enzymatic cross-linking by tissue transglutaminase [94] show interesting properties as stimuli-responsive substrates. These hydrogels are a new class of soft materials which, in response to a small change in temperature, light, or other environmental stimulus, swell to several times their original volume or shrink to the same degree [81, 95]. These materials have proved extremely useful in biomedical and pharmaceutical applications due to their high water content and rubbery nature, which is similar to that of natural tissue.

Chemical cross-linking in organic solvents leads to the formation of more uniform hydrogels as the ELR molecules exhibit no inverse phase transition. McMillan et al., for example, have used a bis(sulfosuccinimidyl) suberate cross-linker to join ELRs containing lysine residues in phosphate buffer at pH 8.5 or in dimethyl sulfoxide. These authors studied the effect of the solvent on the cross-linking density and the gel structures [91, 92]. The physical properties of chemically cross-linked hydrogels can be modulated by varying the ELR's molecular mass, concentration, and lysine content. This ability to prepare "tunable" hydrogels allows these ELRs to be used in a wide range of applications [96]. Although there are many examples of ELR hydrogels cross-linked in organic solvents, the application of in situ cross-linking in an aqueous medium is limited by factors such as the toxicity of the reagents and byproducts and slow gelation kinetics. Lim et al. have reported that the chemical gelation of ELRs in physiological conditions provides a biocompatible and injectable biomaterial for support-tissue regeneration [93].

In our group, Girotti et al. have bioproduced the ELR polymer $[(VPGIG)_2$-VPGKG-$(VPGIG)_2$-(EEIQIGHIPREDVDYHLPY)-$(VPGIG)_2$-VPGKG-$(VPGIG)_2$ $(VGVAPG)_3]_n$ (n =10; MW= 80925 Da) [7]. The monomer unit contains four different functional domains in order to achieve an adequate balance between mechanical and bioactive responses. The $(VPGIG)_n$ sequence in this material confers its excellent mechanical properties, extreme biocompatibility, and stimuli-responsive nature. The second building block is a modification of the first, with a lysine instead of isoleucine, which means that the lysine ε-amino groups can be used for cross-linking and other chemical modifications whilst retaining the properties of ELRs. The third group contains the (REDV) peptide sequence found within the alternatively spliced CS5

fibronectin domain, which is specifically recognized by the integrin α1β4 [97]. This integrin is present in a few cell lines and its specificity for REDV tetrapeptide has been confirmed in endothelial cells, which selectively bind to REDV-coated surfaces [98]. Finally, the polymer possesses another functional block, in this case a recurring hexapeptide derived from the human elastin exon 24-encoded product $(VGVAPG)_3$ [99]. This sequence was introduced to drive enzymatic hydrolysis of the synthetic scaffold by the same physiological pathways as natural elastin during ECM remodeling as it is a target for certain proteolytic enzyme elastases [99].

REDV-ELR biopolymer biodegradation was tested with a specific protease, namely human leukocyte elastase I (**Fig. 6**).

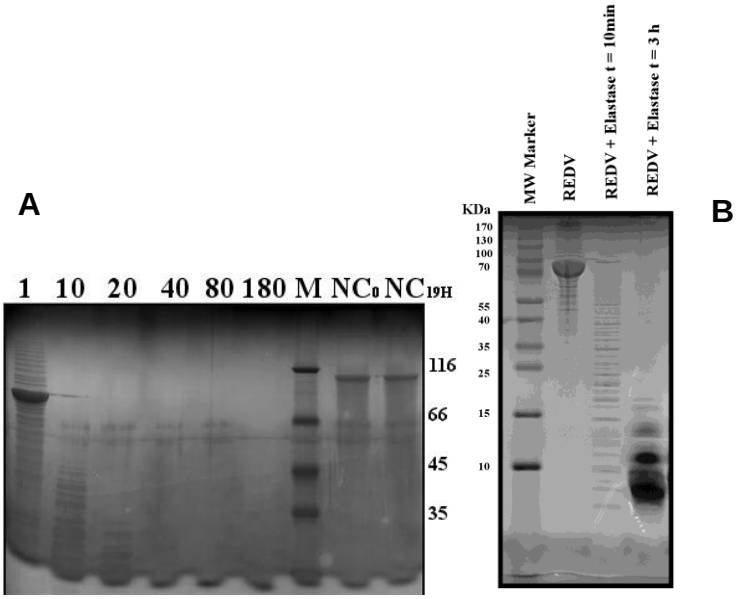

Fig. 6. *SDS-PAGE analysis of ELR proteolysis: A) digested fragments obtained at different incubation times; B) tricine SDS-PAGE is used to separate the resulting total digestion fragments. The numbers at the side of the images indicate the position and size of the molecular mass protein marker.*

When recombinant ELRs were incubated under optimal enzymatic conditions the elastase was found to quickly and completely digest the REDV biopolymer and no

significant degradation of the control biopolymer (lacking the target hexapeptide) was observed even when extending the experimental time (**Fig. 6A**).

The molecular mass of the bands produced in a complete digestion was analyzed in tricine SDS-PAGEs [100]. This electrophoresis method allows us to separate bands corresponding to proteins and/or peptides with a molecular mass of less than 9000 Da. The bands of the ELR proteolytic fragments resulting from complete enzymatic hydrolysis were found to possess a similar molecular mass to that of the theoretical fragments produced by specific elastase proteolysis (**Fig. 6B**).

We have also tested the adhesion of human umbilical vein endothelial cells (HUVECs) to chemically cross-linked ELR film scaffolds containing REDV adhesion sequences and to a negative control (lacking the bioactive sequences) [101]. On REDV-ELR scaffolds the cells showed a spread morphology with the cytoskeleton actin filaments (stained green) well organized into stress fibers, which is indicative of strong adhesion (**Fig. 7A**). The cell number and morphology of the HUVECs seeded on the ELR-negative control were completely different from those seeded on the REDV scaffold, with few smaller and rounded cells with minor lamelopodia extensions, thus indicating that passive adhesion was the main cell-scaffold interaction (**Fig. 7B**).

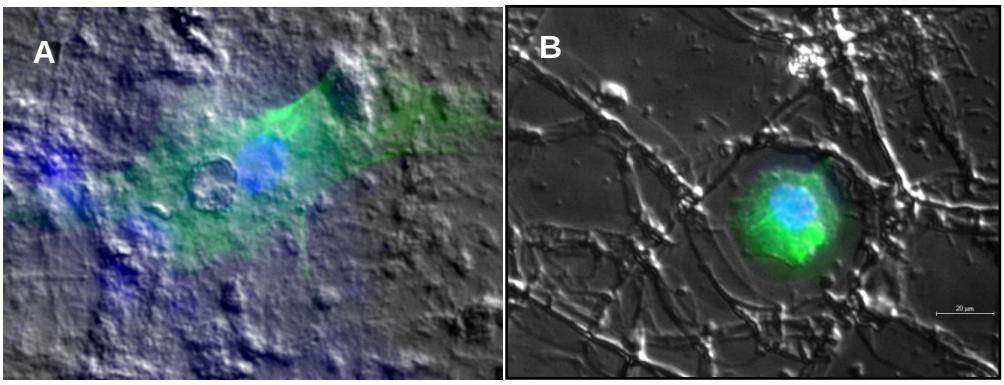

Fig. 7. *Microscopy images of HUVECs seeded on ELR films after 16 hours of incubation: A) REDV film; B) negative control.*

This ELR-containing REDV cell-adhesion sequence has also been used to prepare hybrid scaffolds [102] as the introduction of ELR as an elastic element in collagen-based scaffolds enhances their mechanical properties. In this study, enzymatic cross-linked ELR-collagen scaffolds were tested in vitro as substrates to study cell viability with different cell lines. An increasing ELR fraction in the scaffold was found to have an antifouling effect in fibroblasts, whereas endothelial cells displayed normal behavior and proliferation in the hybrid scaffolds. Varying the proportion of both materials should allow us to design the optimal requirements for future applications, such as vascular tissue or skin wound healing.

Highly porous hydrogels formed from recombinant elastin-like polymers chemically cross-linked with hexamethylene diisocyanate have been obtained by the salt leaching/gas foaming technique for use in 3D cell culture [103]. The pore size of these gels can be controlled by varying the size of the salt particle incorporated during the cross-linking reaction. Physical properties such as the porosity, swelling ratio, and mechanical properties are also influenced by the salt/polymer weight ratio. The thermal behavior of these gels was also studied in terms of the physical properties. Thus, the swollen hydrogels were heated to test the effect on the pore size (see **Fig. 8**). The collapse observed due to the phase transition above Tt decreased the mean pore size by about 30%. This technique should provide a simple approach to the fabrication of advanced scaffolds with “tunable” biological and physical properties in which the elasticity and thermo-responsive behaviour expand the range of potential applications of these materials.

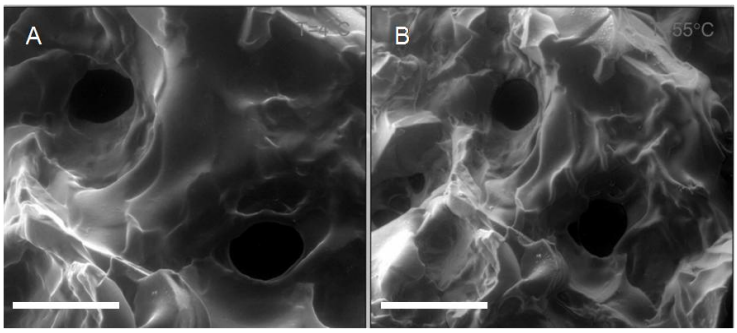

Fig. 8. *ESEM micrographs showing the change in pore-size with temperature in swollen hydrogels in water: A (4 °C); B (55 °C). Scale bars: 100 µm.*

Reverse thermosensitive polymers are very promising base materials for ‘‘in situ generated implants’’. The ability to produce low viscosity physiological solutions at room temperature which form a gel at higher temperature opens up numerous possibilities, although these are normally directed in two main directions: hydrophobic materials which acquire desired mechanical properties or water-based systems for the controlled release of hydrophilic macromolecules. The structural complexity of ELRs with specific mechanical, chemical, and biological properties allows us to design specific features that make it possible to acquire some or all of these properties. The self-assembly behavior of ELRs, for example, has been triggered by the addition of different main peptide blocks in the structure. Thus, hydrophilic blocks provide conformationally elastic properties whereas hydrophobic blocks form physical cross-links through hydrophobic aggregation (see **Fig. 9**).

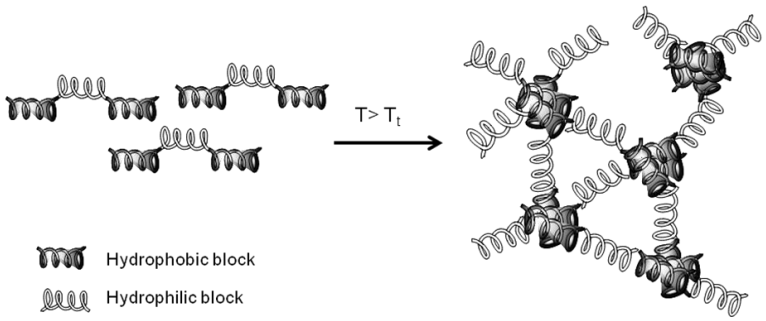

Fig. 9. *Hydrophobic aggregation scheme of ELR tri-block copolymers in aqueous systems.*

In a recent example, ELR tri-block copolymers with different hydrophobic architecture were found to form gels with a complex shear modulus ranging from 4.5 to 10.5 kPa and which can be increased by changing the hydrophilicity of the inner block [104]. This elastic modulus has been enhanced by including additional chemical cross-linking sites in the polymers' composition [105], thus making them excellent candidates for biomedical applications.

5. Conclusions

The goal of replacing current oil-based chemical processes with biological methods has resulted in the development of a method to produce complex recombinamers with a well-defined sequence and complete control of the molecular architecture. In this review we have summarized some examples that demonstrate the versatility of ELRs for a wide range of applications. The potential of ELRs to self-assemble in response to environmental changes makes them attractive for the construction of nano-devices for use as controlled delivery systems, stimuli-responsive biosurfaces, or advanced nanobiotechnological applications. The tailored introduction of cross-linking groups, cell-binding domains, and enzymatic biodegradation along the polypeptide chain makes these materials excellent substrates which can be used to mimic some of the most important characteristics of the ECM for tissue engineering.

Thus, ELR hydrogels are promising candidates in terms of microstructure, ‘‘tunable’’ mechanical properties, and topography for the study of cell behavior and cell-surface interactions, which is an important step towards the development of cell-based biomedical systems.

Acknowledgments

We are grateful for financial support from the MICINN (projects MAT 2007-66275-C02-01, NAN2004-08538, and PSE-300100-2006-1), the JCyL (projects VA087A06, VA016B08, and VA030A08), the CIBER-BBN (project CB06-01-0003), the JCyL and the Instituto de Salud Carlos III under the ‘‘Network Center of Regenerative Medicine and Cellular Therapy of Castilla and León’’, and the Marie Curie RTN Biopolysurf (MRTN-CN-2004-005516).

References

[1] United Nations Framework Convention on Climate Change<http://unfccc.int/2860.php>.

[2] Massimini K. *Genetic disorders sourcebook: basic consumer health information about hereditary diseases and disorders, including cystic fibrosis, down syndrome, hemophilia, Huntington's disease.* Detroit, MI: Omnigraphics Inc; 2001.

[3] Zhao, H. M.; Chen, W. Chemical biotechnology: Microbial solutions to global change. *Curr.Opin. Biotechnol.* 2008, **19**, 541-543.

[4] Park, J. H.; Lee, S. Y. Towards systems metabolic engineering of microorganisms for amino acid production. *Curr.Opin. Biotechnol.* 2008, **19**, 454-460.

[5] Lee, S. Y.; Hong, S. H.; Lee, S. H.; Park, S. J. Fermentative production of chemicals that can be used for polymer synthesis. *Macromol. Biosci.* 2004, **4**, 157-164.

[6] McGrath, K.; Kaplan, D. S. *Protein-based materials.* Boston: Birkhauser; 1997.

[7] Girotti, A.; Reguera, J.; Rodríguez-Cabello, J. C.; Arias, F. J.; Alonso, M.; Testera, A.M. Design and bioproduction of a recombinant multi(bio)functional elastin-like protein polymer containing cell adhesion sequences for tissue engineering purposes. *J. Mater. Sci. Mater. Med.* 2004, **15**, 479-484.

[8] Lee, J.; Macosko, C. W.; Urry, D. W. Elastomeric polypentapeptides cross-linked into matrixes and fibers. *Biomacromolecules* 2001, **2**, 170-179.

[9] Girotti, A.; Reguera, J.; Arias, F. J.; Alonso, M.; Testera, A. M.; Rodríguez-Cabello, J. C. Influence of the molecular weight on the inverse temperature transition of a model genetically engineered elastin-like pH-responsive polymer. *Macromolecules* 2004, **37**, 3396-3400.

[10] Shao, Z. Z.; Vollrath, F. Materials: Surprising strength of silkworm silk. *Nature* 2002, **418**, 741-741.

[11] Hardy, J. G.; Romer, L. M.; Scheibel, T. R. Polymeric materials based on silk proteins. *Polymer* 2008, **49**, 4309-4327.

[12] Urry, D. W.; Nicol, A.; Gowda, D. C.; Hoban, L. D.; McKee, A.; Williams, T.; Olsen, D. B.; Cox, B. A. *Medical applications of bioelastic materials.* In: Biotechnological polymers: medical, pharmaceutical and industrial applications. Editor: Gebelein, C. G. Atlanta: Technomic.1993, 82-103.

[13] Panitch, A.; Yamaoka, T.; Fournier, M. J.; Mason, T. L.; Tirrell, D. A. Design and biosynthesis of elastin-like artificial extracellular matrix proteins containing

periodically spaced fibronectin CS5 domains. *Macromolecules* 1999, **32**, 1701-1703.

[14] Chilkoti, A.; Dreher, M. R.; Meyer, D. E. Design of thermally responsive recombinant polypeptide carriers for targeted drug delivery. *Adv. Drug Deliv. Rev.* 2002, **54**, 1093-1111.

[15] Martino, M.; Perri, T.; Tamburro, A. M. Biopolymers and biomaterials based on elastomeric proteins. *Macromol. Biosci.* 2002, **2**, 319-328.

[16] Rodríguez-Cabello, J. C.; Reguera, J.; Girotti, A.; Alonso, M.; Testera, A. M. Developing functionality in elastin-like polymers by increasing their molecular complexity: the power of the genetic engineering approach. *Prog. Polym.Sci.* 2005, **30**, 1119-1145.

[17] Kumar, M.; Sanford, K. J.; Cuevas, W. P.; Du, M.; Collier, K. D.; Chow, N. Designer protein-based performance materials. *Biomacromolecules* 2006, **7**, 2543-2551.

[18] Cappello, J.; Crissman, J.; Dorman, M.; Mikolajczak, M.; Textor, G.; Marquet, M.; Ferrari, F. Genetic engineering of structural protein polymers. *Biotechnol. Prog.* 1990, **6**, 198-202.

[19] Elvin, C. M.; Carr, A. G.; Huson, M. G.; Maxwell, J. M.; Pearson, R. D.; Vuocolo, T.; Liyou, N. E.; Wong, D. C. C.; Merritt, D. J.; Dixon, N. E. Synthesis and properties of crosslinked recombinant pro-resilin. *Nature* 2005, **437**, 999-1002.

[20] Bochicchio, B.; Jimenez-Oronoz, F.; Pepe, A.; Blanco, M.; Sandberg, L. B.; Tamburro, A. M. Synthesis of and structural studies on repeating sequences of abductin. *Macromol. Biosci.* 2005, **5**, 502-511.

[21] Shewry, P. R.; Halford, N. G.; Belton, P. S.; Tatham, A. S. *Philosophical Transactions of the Royal Society of London Series B-Biological Sciences* 2002, **357**, 133-142.

[22] Miao, M.; Bellingham, C. M.; Stahl, R. J.; Sitarz, E. E.; Lane, C. J.; Keeley, F.W. Sequence and structure determinants for the self-aggregation of recombinant polypeptides modeled after human elastin. *J. Biol.Chem.* 2003, **278**, 48553-48562.

[23] Di Zio, K.; Tirrell, D. A. Mechanical properties of artificial protein matrices engineered for control of cell and tissue behavior. *Macromolecules* 2003, **36**, 1553-1558.

[24] Urry, D. W.; Parker, T. M.; Reid, M. C.; Gowda, D. C. Biocompatibility of the bioelastic materials, poly(GVGVP) and its γ-irradiation cross-linked matrix: Summary of generic biological test results. *J. Bioact. Compat.Polym.*1991, **6**, 263-282.

[25] Meyer, D. E.; Chilkoti, A. Genetically encoded synthesis of protein-based polymers with precisely specified molecular weight and sequence by recursive directional ligation: Examples from the elastin-like polypeptide system. *Biomacromolecules* 2002, **3**, 357-367.

[26] Welsh, E. R.; Tirrell, D. A. Engineering the extracellular matrix: a novel approach to polymeric biomaterials. I. Control of the physical properties of artificial protein matrices designed to support adhesion of vascular endothelial cells. *Biomacromolecules* 2000, **1**, 23-30.

[27] Urry, D. W. *What sustains life? consilient mechanisms for protein-based machines and materials.* New York: Springer-Verlag; 2005.

[28] Gowda, D. C.; Parker, T. M.; Harris, R. D.; Urry, D. W. *Synthesis, characterization and medical applications of bioelastic materials.* In: Peptides:

design, synthesis and biological activity. Editor:. Basava, C.; Anantharamaiah, G. M. Boston: Birkhäuser. 1994, 81-111.

[29] Urry, D. W. Molecular machines: How motion and other functions of living organisms can result from reversible chemical changes. *Angew. Chem. Int. Ed. Engl.*1993, **32**, 819-841.

[30] San Biagio, P. L.; Madonia, F.; Trapane, T. L.; Urry, D.W. The overlap of elastomeric polypeptide coils in solution required for single-phase initiation of elastogenesis. *Chemical Physics Letters* 1988, **145**, 571-574.

[31] Tanford, C. *The hydrophobic effect: formation of micelles and biological membranes.* New York: Wiley; 1973.

[32] Rodríguez-Cabello, J. C.; Alonso, M.; Perez, T.; Herguedas, M. M. Differential scanning calorimetry study of the hydrophobic hydration of the elastin-based polypentapeptide, poly(VPGVG), from deficiency to excess of water. *Biopolymers* 2000, **54**, 282-288.

[33] Muiznieks, L. D; Jensen, S. A.; Weiss, A. S. Structural changes and facilitated association of tropoelastin. *Arch. Biochem. Biophys.* 2003, **410**, 317-323.

[34] Jensen, S. A.; Vrhovski, B.; Weiss, A. S. Domain 26 of tropoelastin plays a dominant role in association by coacervation. *J. Biol. Chem.* 2000, **275**, 28449-28454.

[35] Brown-Augsburger, P.; Tisdale, C.; Broekelmann, T.; Sloan, C.; Mecham, R. P. Identification of an elastin cross-linking domain that joins three peptide chains. Possible role in nucleated assembly. *J. Biol. Chem.* 1995, **270**, 17778-17783.

[36] Kozel, B. A.; Wachi, H.; Davis, E. C.; Mecham, R. P. Domains in tropoelastin that mediate elastin deposition in vitro and in vivo. *J. Biol. Chem.* 2003, **278**, 18491-18498.

[37] Alonso, M.; Reboto, V.; Guiscardo, L.; Mate, V.; Rodríguez-Cabello, J. C. Novel photoresponsive *p*-phenylazobenzene derivative of an elastin-like polymer with enhanced control of azobenzene content and without pH sensitiveness. *Macromolecules* 2001, **34**, 8072-8077.

[38] Alonso, M.; Reboto, V.; Guiscardo, L.; San Martin, A.; Rodríguez-Cabello, J. C. Spiropyran derivative of an elastin-like bioelastic polymer: photoresponsive molecular machine to convert sunlight into mechanical work. *Macromolecules* 2000, **33**, 9480-9482.

[39] Rodríguez-Cabello, J. C.; Alonso, M.; Guiscardo, L.; Reboto, V.; Girotti, A. Amplified photoresponse of a *p*-phenylazobenzene derivate of elastin-like polymer by α-cyclodextrin: the amplified ΔT_t mechanism. *Adv. Mater.* 2002, **14**, 1151-1154.

[40] Rajagopal, K.; Schneider, J.P. Self-assembling peptides and proteins for nanotechnological applications. *Curr. Opin. Struct. Biol.* 2004, **14**, 480-486.

[41] Yang, G.C.; Woodhouse, K. A.; Yip, C. M. Substrate-facilitated assembly of elastin-like peptides: studies by variable-temperature in situ atomic force microscopy. *J. Am. Chem. Soc.* 2002, **124**, 10648-10649.

[42] Pepe, A.; Guerra, D.; Bochicchio, B.; Quaglino, D.; Gheduzzi, D.; Ronchetti, V. P.; Tamburro, A. M. Dissection of human tropoelastin: supramolecular organization of polypeptide sequences coded by particular exons. *Matrix Biology* 2005, **24**, 96-109.

[43] Reguera, J.; Fahmi, A.; Moriarty, P.; Girotti, A.; Rodríguez-Cabello, J. C. Nanopore formation by self-assembly of the model genetically engineered elastin-like polymer $[(VPGVG)_2(VPGEG)(VPGVG)_2]_{15}$. *J. Am. Chem. Soc.* 2004, **126**, 13212-13213.

[44] Goldberg, M.; Langer, R.; Jia, X. Q. Nanostructured materials for applications in drug delivery and tissue engineering. *J. Biomater. Sci. Polym. Ed.* 2007, **18**, 241-268.

[45] Urry, D. W. *Abst. Pap. Am. Chem. Soc.*1990, **200**, 74.

[46] Herrero-Vanrell, R.; Rincón, A. C.; Alonso, M.; Reboto, V.; Molina-Martínez, I. T.; Rodríguez-Cabello, J. C. Self-assembled particles of an elastin-like polymer as vehicles for controlled drug release. *J. Control. Release* 2005, **102**, 113-122.

[47] Wu, Y.Q.; MacKay, J. A.; McDaniel, J. R.; Chilkoti, A.; Clark, R. L. Fabrication of elastin-like polypeptide nanoparticles for drug delivery by electrospraying. *Biomacromolecules* 2009, **10**, 19-24.

[48] Fujita, Y.; Mie, M.; Kobatake, E. Construction of nanoscale protein particle using temperature-sensitive elastin-like peptide and polyaspartic acid chain. *Biomaterials* 2009, **30**, 3450-3457.

[49] Lee, T. A. T.; Cooper, A.; Apkarian, R. P.; Conticello, V. P. Thermo-reversible self-assembly of nanoparticles derived from elastin-mimetic polypeptides. *Adv. Mater.*2000, **12**, 1105-1110.

[50] Wright, E. R.; McMillan, R. A.; Cooper, A.; Apkarian, R. P.; Conticello, V. P. *Adv. Funct. Mater.* 2002, **12**, 149-154.

[51] Dreher, M. R.; Simnick, A. J.; Fischer, K.; Smith, R. J.; Patel, A.; Schmidt, M.; Chilkoti, A. Temperature triggered self-assembly of polypeptides into multivalent spherical micelles. *J. Am. Chem. Soc.* 2008, **130**, 687-694.

[52] Bidwell, G. L.; Fokt, I.; Priebe, W.; Raucher, D. Development of elastin-like polypeptide for thermally targeted delivery of doxorubicin. *Biochem. Pharmacol.* 2007, **73**, 620-631.

[53] Ribeiro, A.; Arias, F. J.; Reguera, J.; Alonso, M.; Rodríguez-Cabello, J.C. Influence of the amino-acid sequence on the inverse temperature transition of elastin-like polymers. *Biophys. J.* 2009; **97**, 312-320.

[54] Ribeiro, A.; Mateo, R. A.; Arias, F. J.; Castro, E.; Lecommandoux, S.; Rodríguez-Cabello, J. C. *J. Am. Chem. Soc.*, Submitted for publication.

[55] Nath, N.; Hyun, J.; Ma, H.; Chilkoti, A. Surface engineering strategies for control of protein and cell interactions. *Surf. Sci.*2004, **570**, 98-110.

[56] Castner, D. G.; Ratner, B. D. Biomedical surface science: foundations to frontiers. *Surf. Sci.*2002, **500**, 28-60.

[57] Kato, K.; Uchida, E.; Kang, E. T.; Uyama, Y.; Ikada, Y. Polymer surface with graft chains. *Prog. Polym.Sci.* 2003, **28**, 209-259.

[58] Luzinov, I.; Minko, S.; Tsukruk, V. V. Adaptive and responsive surfaces through controlled reorganization of interfacial polymer layers. *Prog. Polym.Sci.* 2004, **29**, 635-698.

[59] Hyun, J.; Lee, W. K.; Nath, N.; Chilkoti, A.; Zauscher, S. Capture and release of proteins on the nanoscale by stimuli-responsive elastin-like polypeptide "switches". *J. Am. Chem. Soc.* 2004, **126**, 7330-7335.

[60] Idota, N.; Tsukahara, T.; Sato, K.; Okano, T.; Kitamori, T. The use of electron beam lithographic graft-polymerization on thermoresponsive polymers for

regulating the directionality of cell attachment and detachment. *Biomaterials* 2009, **30**, 2095-2101.

[61] Nath, N.; Chilkoti, A. Creating 'smart' surfaces using stimuli responsive polymers. *Adv. Mater.*2002, **14**, 1243-1247.

[62] Shi, J.; Alves, N. M.; Mano, J. F. Thermally responsive biomineralization on biodegradable substrates. *Adv. Funct. Mater*.2007, **17**, 3312-3318.

[63] Ozturk, N.; Girotti, A.; Kose, G. T.; Rodríguez-Cabello, J. C.; Hasirci, V. Dynamic cell culturing and its application to micropatterned, elastin like protein-modified poly(N-isopropylacrylamide) scaffolds. *Biomaterials* 2009, **30**, 5417-5426.

[64] Swierczewska, M.; Hajicharalambous, C. S.; Janorkar, A. V.; Megeed, Z.; Yarmush, M. L.; Rajagopalan, P. Controlling cell interactions to polyelectrolyte multilayer assemblies based on elastin-like polymer conjugates. *Acta Biomater.* 2008, **4**, 827-837.

[65] Costa, R. R.; Custódio, C. A.; Testera, A. M.; Arias, F. J.; Rodríguez-Cabello, J. C.; Alves, N. M.; Mano, J. F. Stimuli-responsive thin coatings using elastin-like polymers for biomedical applications. *Adv. Funct. Mater.* 2009, **19**, 1-9.

[66] Offenhausser, A.; Bocker-Meffert, S.; Decker, T.; Helpenstein, R.; Gasteier, P.; Groll, J.; Moller, M.; Reska, A.; Schafer, S.; Schulte, P.; Eisele-Vogt, A. Microcontact printing of proteins for neuronal cell guidance. *Soft Matter* 2007, **3**, 290-298.

[67] Bernard, A.; Renault, J. P.; Michel, B.; Bosshard, H. R.; Delamarche, E. Microchannel networks for nanowire patterning. *Adv. Mater.* 2000, **12**, 1067-1070.

[68] Nath, N.; Chilkoti, A. Fabrication of reversible functional arrays of proteins directly from cells using a stimuli responsive polypeptide. *Anal. Chem.* 2003, **75**, 709-715.

[69] Martín, L.; Alonso, M.; Moller, M.; Rodríguez-Cabello, J. C.; Mela, P. 3D microstructuring of smart bioactive hydrogels based on recombinant elastin-like polymers. *Soft Matter* 2009, **5**, 1591-1593.

[70] Li, D.; Xia, Y. N. Electrospinning of nanofibers: reinventing the wheel?. *Adv. Mater.* 2004, **16**, 1151-1170.

[71] Huang, Z. M.; Zhang, Y. Z.; Kotaki, M.; Ramakrishna, S. A review on polymer nanofibers by electrospinning and their applications in nanocomposites. *Compos. Sci. Technol.* 2003, **63**, 2223-2253.

[72] Buchko, C. J.; Chen, L. C.; Shen, Y.; Martin, D. C. Processing and microstructural characterization of porous biocompatible protein polymer thin films. *Polymer* 1999, **40**, 7397-7407.

[73] Li, M. Y.; Mondrinos, M. J.; Gandhi, M. R.; Ko, F. K.; Weiss, A. S.; Lelkes, P. I. Electrospun protein fibers as matrices for tissue engineering. *Biomaterials* 2005, **26**, 5999-6008.

[74] Nair, L. S.; Bhattacharyya, S.; Laurencin, C. T. Development of novel tissue engineering scaffolds via electrospinning. *Expert Opin. Biol. Ther.* 2004, **4**, 659-668.

[75] Sill, T. J.; von Recum, H. A. Electrospinning: applications in drug delivery and tissue engineering. *Biomaterials* 2008, **29**, 1989-2006.

[76] Wnek, G. E.; Carr, M. E.; Simpson, D. G.; Bowlin, G. L. Electrospinning of nanofiber fibrinogen structures. *Nano Lett.* 2003, **3**, 213-216.

[77] Buttafoco, L.; Kolkman, N.G.; Engbers-Buijtenhuijs, P.; Poot, A. A.; Dijkstra, P. J.; Vermes, I.; Feijen, J. Electrospinning of collagen and elastin for tissue engineering applications. *Biomaterials* 2006, **27**, 724-734.

[78] Jin, H. J.; Chen JS; Karageorgiou V; Altman GH; Kaplan DL. Human bone marrow stromal cell responses on electrospun silk fibroin mats. *Biomaterials* 2004, **25**, 1039-1047.

[79] Huang, L.; McMillan, R. A.; Apkarian, R. P.; Pourdeyhimi, B.; Conticello, V. P.; Chaikof, E. L. Generation of synthetic elastin-mimetic small diameter fibers and fiber networks. *Macromolecules* 2000, **33**, 2989-2997.

[80] García-Arévalo, C.; Pierna, M.; Girotti, A.; Arias, F. J.; Rodríguez-Cabello, J. C. *Eur. Cell. Mater*. Submitted for publication.

[81] Furth, M. E.; Atala, A.; Van Dyke, M. E. Smart biomaterials design for tissue engineering and regenerative medicine. *Biomaterials* 2007, **28**, 5068-5073.

[82] Anderson, D. G.; Burdick, J. A.; Langer, R. Smart biomaterials. *Science* 2004, **305**, 1923-1924.

[83] Badylak, S. F.; Freytes, D. O.; Gilbert, T. W. Extracellular matrix as a biological scaffold material: Structure and function. *Acta Biomater*. 2009, **5**, 1-13.

[84] Nicol, A. G. D.; Parker, T. M.; Urry, D. W. In: Gebelein C, Carraher C, editors. *Biotechnology and bioactive polymers.* New York: Plenum Press; 1994.

[85] Nowatzki, P. J.; Tirrell, D. A. Physical properties of artificial extracellular matrix protein films prepared by isocyanate crosslinking. *Biomaterials* 2004, **25**, 1261-1267.

[86] Nagapudi, K.; Brinkman, W. T.; Leisen, J. E.; Huang, L.; McMillan, R. A.; Apkarian, R. P.; Conticello, V. P.; Chaikof, E. L. Photomediated solid-state cross-

linking of an elastin-mimetic recombinant protein polymer. *Macromolecules* 2002, **35**, 1730-1737.

[87] Lee, J.; Macosko, C. W.; Urry, D. W. Mechanical properties of cross-linked synthetic elastomeric polypentapeptides. *Macromolecules* 2001, **34**, 5968-5974.

[88] Lee, J.; Macosko, C. W.; Urry, D. W. Mechanical properties of cross-linked synthetic elastomeric polypentapeptides. *Macromolecules* 2001, **34**, 4114-4123.

[89] Heilshorn, S. C.; DiZio, K. A.; Welsh, E. R.; Tirrell, D. A. Endothelial cell adhesion to the fibronectin CS5 domain in artificial extracellular matrix proteins. *Biomaterials* 2003, **24**, 4245-4252.

[90] Liu, J. C.; Tirrell, D. A. Cell response to RGD density in crosslinked artificial. Extracellular matrix protein films. *Biomacromolecules* 2008, **9**, 2984-2988.

[91] McMillan, R. A.; Caran, K. L.; Apkarian, R. P.; Conticello, V. P. High resolution topographic imaging of environmentally responsive, elastin-mimetic hydrogels. *Macromolecules* 1999, **32**, 9067-9070.

[92] McMillan, R. A.; Conticello, V. P. Synthesis and characterization of elastin-mimetic protein gels derived from a well-defined polypeptide precursor. *Macromolecules* 2000, **33**, 4809-4821.

[93] Lim, D. W.; Nettles, D. L.; Setton, L. A.; Chilkoti, A. Rapid crosslinking of elastin-like polypeptides with hydroxymethylphosphine in aqueous solution. *Biomacromolecules* 2007, **8**, 1463-1470.

[94] McHale, M. K.; Setton, L. A.; Chilkoti, A. Synthesis and in vitro evaluation of enzymatically cross-linked elastin-like polypeptide gels for cartilaginous tissue repair. *Tissue Eng.* 2005, **11**, 1768-1779.

[95] Kopecek, J. Hydrogel biomaterials: a smart future? *Biomaterials* 2007, **28**, 5185-5192.

[96] Trabbic-Carlson, K.; Setton, L. A.; Chilkoti, A. Swelling and mechanical behaviors of chemically cross-linked hydrogels of elastin-like polypeptides. *Biomacromolecules* 2003, **4**, 572-580.

[97] Mould, A. P.; Wheldon, L. A.; Komoriya, A.;Wayner, E. A.; Yamada, K. M.; Humphries, M. J. Affinity chromatographic isolation of the melanoma adhesion receptor for the IIICS region of fibronectin and its identification as the integrin α4β1. *J. Biol. Chem.* 1990, **265**, 4020-4024.

[98] Plouffe, B. D.; Njoka, D. N.; Harris, J.; Liao, J.; Horick, N. K.; Radisic, M.; Murthy, S. K. Peptide-mediated selective adhesion of smooth muscle and endothelial cells in microfluidic shear flow. *Langmuir* 2007, **23**, 5050-5055.

[99] Lombard, C.; Bouchu, D.; Wallach, J.; Saulnier, J. Proteinase 3 hydrolysis of peptides derived from human elastin exon 24. *Amino Acids* 2005, **28**, 403-408.

[100] Schägger, H. *Nature* 2006, **1**, 16-22.

[101] Girotti, A.; Martín, L.; Pierna, M.; Arias, F. J.; Rodríguez-Cabello, J. C. *Biomacromolecules*. Submitted for publication.

[102] Garcia, Y.; Hemantkumar, N.; Collighan, R.; Griffin, M.; Rodríguez-Cabello, J. C.; Pandit, A. In vitro characterization of a collagen scaffold enzymatically cross-linked with a tailored elastin-like polymer. *Tissue Eng. Part A* 2009, **15**, 887-899.

[103] Martín, L.; Alonso, M.; Girotti, A.; Arias, F. J.; Rodríguez-Cabello, J. C. *Biomacromolecules*; in press.

[104] Nagapudi, K.; Brinkman, W. T.; Thomas, B. S.; Parkm, J. O.; Srinivasarao, M.; Wright, E.; Conticello, V. P., Chaikof, E. L. Viscoelastic and mechanical behavior of recombinant protein elastomers. Biomaterials 2005, **26**, 4695-4706.

[105] Sallach, R. E.; Cui, W.; Wen, J.; Martinez, A.; Conticello, V. P.; Chaikof, E. L. Elastin-mimetic protein polymers capable of physical and chemical crosslinking. *Biomaterials* 2009, **30**, 409-422.

CHAPTER 2

3D Microstructuring of Smart Bioactive Hydrogels based on Recombinant Elastin-like Polymers

The work presented in this chapter has been published in:

L. Martín [a]; M. Alonso [a]; M. Möller [b]; J.C. Rodríguez-Cabello [a]; P. Mela [b]. 2009

3D microstructuring of smart bioactive hydrogels based on recombinant elastin-like polymers

Soft Matter, 5: 1591–1593

3D Microstructuring of Smart Bioactive Hydrogels based on Recombinant Elastin-like Polymers

Laura Martín [1], Matilde Alonso [2], Martin Möller [2], J. Carlos Rodríguez-Cabello *[1] and Petra Mela *[2]

[1] G.I.R. Bioforge, University of Valladolid, Ciber-bbn, Paseo de Belén 11, 47011 Valladolid, Spain.

[2] Institute of Technical and Macromolecular Chemistry, RWTH Aachen and DWI e.V., Pauwelsstr. 8, D-52056 Aachen, Germany.

*Correspondence to:

J. Carlos Rodríguez-Cabello

Tel: +34 983 184 686

E-mail: cabello@bioforge.uva.es

Petra Mela

Tel: +49 241 8023351

E-mail: mela@dwi.rwth-aachen.de

Abstract

We describe a simple method of replica moulding to obtain novel 3D microstructured smart hydrogels based on protein polymers mimicking the structure and behaviour of the extracellular matrix (ECM).

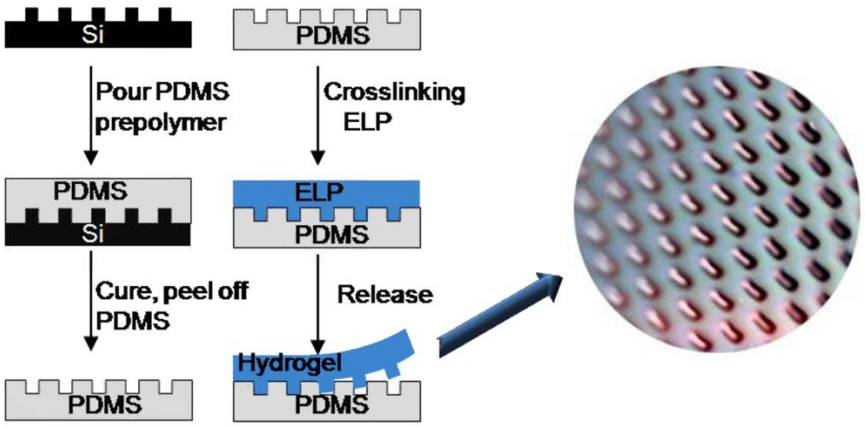

Future advances in areas of biosciences and biotechnology strongly rely on the development of appropriate systems mimicking *in vivo* cellular environments, enabling *in vitro* studies of cell–matrix interactions [1]. Numerous studies show the need for more sophisticated and biologically relevant substrates with well defined biological and chemical activity, tunable mechanical properties and controlled topography [2, 3, 4]. Therefore, considerable effort has been directed towards the development of new materials and fabrication techniques to generate novel substrates that exhibit some of the most important chemical, biological and physical characteristics of the extracellular matrix (ECM).

Recombinant DNA methods have been exploited to create protein polymers with programmable sequences of functional oligopeptide blocks and, therefore, desired properties. These methods allow the design of polymer compositions with unmatched degree of complexity and control that can incorporate structural and functional domains derived from ECM proteins.

Elastin-like polymers (ELPs) [5] have been attracting interest because of their excellent biocompatibility and bioactivity [6] and their intrinsic ‘‘smart’’ stimuli-responsive nature. These protein polymers undergo a phase transition in response to changes in the temperature. Below the so-called inverse transition temperature (ITT) the uncrosslinked polymer chains are soluble in water, however, above the transition temperature (T_t) the polymer chains form nano and micro aggregates which segregate from the solution. ELPs have been used in the form of electrospun fibers [7], hybrid hydrogels [8] and 2D films [9] showing their great potential as biomimetic materials for a variety of biomedical applications ranging from scaffolds for tissue engineering to cell-based microdevices. Interestingly, hydrogels based on ELPs retain the

thermoresponsiveness characteristics of the ELP family and a clear T_t can be studied in crosslinked hydrogels by calorimetric techniques [10].

Here we demonstrate, for the first time, the fabrication of 3D structures made of ELP-based hydrogels by means of replica moulding. In this way, we obtain novel substrates with well controlled micro-topography, tunable mechanical properties and a smart nature.

For this purpose we synthesized by genetic engineering techniques a recombinant elastin-like polymer (ELP) with peptidic sequences providing bioactivity and other functionalities. The monomer unit contains three different functional blocks in order to achieve an adequate balance of mechanical and bioactive response (**Fig. 1**).

{[$(VPGIG)_2$VPGKG$(VPGIG)_2$]$_2$ (AVTGRGDSPASS) [$(VPGIG)_2$VPGKG$(VPGIG)_2$]$_2$}$_6$

Fig. 1 *A scheme of the blocks and amino acid sequences of the designed polymer.*

The $(VPGIG)_n$ sequence confers the excellent mechanical properties, the extreme biocompatibility and the ‘‘smart’’ nature. The second building block is a modification of the first, containing lysine instead of isoleucine, so that the lysine ε-amino groups can be used for crosslinking purposes and other chemical modifications. The last block contains a peptide loop present in the human fibronectin protein with the well known RGD sequence for cell adhesion. Finally, a tag of histidines (His_6) was incorporated to the polymer sequence in the terminal amino position. The His_6 tag can be used as a tracking epitope of interest, allowing protein analysis and purification [11].

Replica moulding is a fast, flexible, straightforward micropatterning technique that can be carried out routinely on a bench top and consists of only a few steps:

dispensing of the polymer on the mould, crosslinking and release of the replica from the mould. Here the replica moulding was performed on polydimethylsiloxane (PDMS) micropatterned substrates as moulds.

The PDMS prepolymer and curing agent were thoroughly mixed at a 10:1 (wt/wt) ratio and degassed for 1 h. The mixture was then cast onto previously fluorosilanized patterned silicon masters and cured at 65 °C for 1 h. The PDMS replicas were carefully peeled off from the silicon wafer and used without any further surface treatment. We used four different silicon masters presenting grooves or pillars with different dimensions and interdistances. Specifically, grooves with 25 µm width and 25 µm interdistance, grooves with 20 µm width and 100 µm interdistance, pillars with 5 µm diameter and 15 µm interdistance, pillars with 10 µm diameter and 10 µm interdistance. The step height of the micro-features was 5 µm for the grooves 9 µm for the pillars.

The hydrogels were obtained by chemical crosslinking. A polymer solution was prepared by dissolving 4 mg of RGD containing-ELP (100 mg/ml) in N,N-dimethylformamide (DMF, Fluka) at 4 °C. A solution of hexamethylene diisocyanate (HDI, Sigma Aldrich) was prepared at -20 °C in DMF. The two solutions were mixed under vigorous stirring with desired polymer: HDI ratios, then poured into PDMS stamps and allowed to react overnight at room temperature. The hydrogels were taken off and immersed in ultra pure water. They were thoroughly washed in ultra pure water to remove remaining unreacted chemical reagents and solvent. Crosslinking reaction is very efficient. The amount of polymer finally incorporated in the hydrogel was always higher than the 85% in weight of the initial amount used, as determined by the weight of the lyophilized hydrogels (result not shown).

Fig. 2 shows macroscopic pictures of swollen hydrogels as prepared in this study.

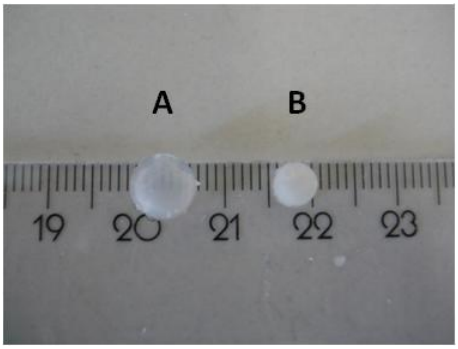

Fig. 2. *Macroscopic pictures of swollen crosslinked hydrogels with different polymer: crosslinker ratios after 24 h stabilization in water. (A) Molar ratio of polymer: crosslinker, 1: 4. (B) Molar ratio of polymer: crosslinker, 1: 7.*

We could modulate the swelling degree of the hydrated hydrogels and their mechanical properties by changing the polymer: crosslinker ratio. A lower crosslink density (**2A**) resulted in gels of larger dimensions and more transparent appearance. With a decrease in the ratio of polymer: crosslinker, the size of the hydrogels decreased and their transparency became poor (**2B**). Rheological measurements confirmed that the polymer: crosslinker ratio also strongly affects the mechanical properties of the swollen gels. The measurements were performed with an AR-2000ex rheometer (TA Instruments) at room temperature in a constant strain mode. Swollen gels were placed between parallel plates (12 mm diameter) and the gap was adjusted starting from the sample to reach a normal force about 10 mN in order to prevent slippage. An amplitude sweep (storage modulus G′ measured as a function of strain) was performed to confirm that the measurements were obtained within the linear region of viscoelasticity. Measurements were then realized in a constant strain (0.5%) mode as a function of frequency (from 0.1 to 10Hz). Gels formed with molar ratio polymer: crosslinker of 1: 7 have higher elastic modulus (9947 ± 230 Pa) than the ones formed with a 1 : 4 ratio with elastic modulus (4311 ± 131 Pa).

The thermally responsive behaviour of the crosslinked gels with a polymer: crosslinker ratio of 1: 7 is shown in **Fig. 3.**

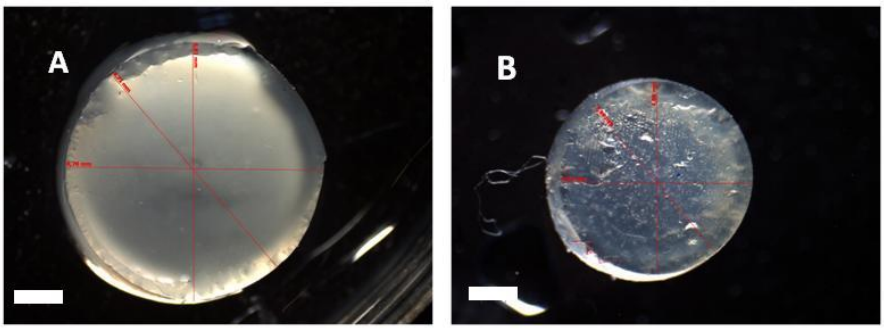

Fig. 3. *Optical stereomicroscope images of hydrogels under (A) and above (B) the transition temperature, after 24 h water immersion. (A) 4 °C, diameter =6.8mm (B) 37 °C, diameter = 4.0 mm. Scale bars, 2.0 mm.*

The hydrogels retained the ‘‘smart nature’’ of the elastin-like polymers, with a transition temperature (T_t) of 20 °C [10]. A clear difference in the dimensions of the gels after immersion in water at temperatures below and above the T_t is observed. It demonstrates that genetically engineered ELP polymers may be chemically crosslinked to yield thermally responsive hydrogels with ‘‘tunable’’ physical properties. In addition the transition temperature (T_t) can be modified with the polymer amino acid composition among others [12].

The surface topography of these micropatterned RGD hydrogels was analysed using a Zeiss AxioPlan Imaging light microscope. The four different patterns are presented in **Fig. 4.**

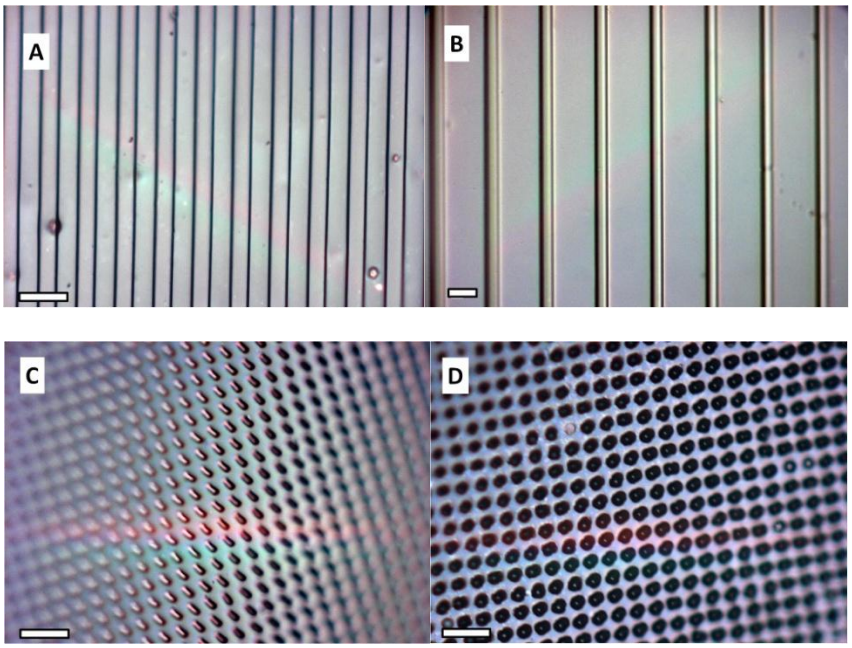

Fig. 4. *Optical micrographs of different micropatterned hydrogels swollen in DMF. Scale bars, 50 µm.*

These hydrogels were crosslinked with a polymer: crosslinker ratio of 1: 7. The optical micrographs were obtained after the crosslinking reaction, with swollen gels in DMF at room temperature. **Fig. 5** shows one of the patterns after 24 h equilibration in water at temperatures below Tt (4 °C, **Fig. 5A**) and above Tt (37 °C, **Fig. 5B**).

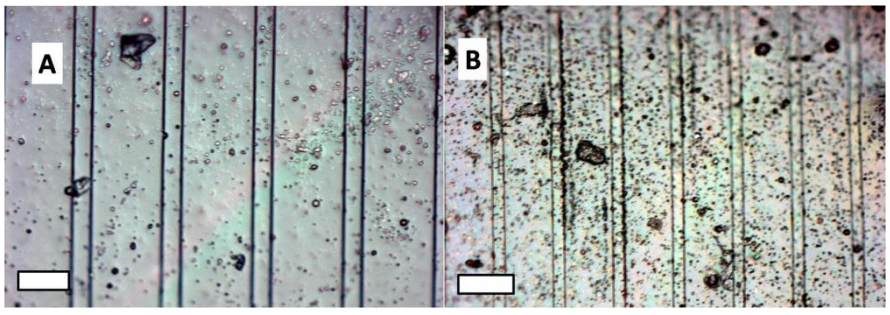

Fig. 5. *Optical micrographs of micropatterned hydrogels previously immersed in water at (A) 4 °C; and (B) 37 °C. Scale bars, 50 µm.*

This equilibration is related with the swelling ratio and both depend on the crosslinking ratio. To estimate the dimensions of the microfeatures with respect to the water temperature, two different locations were analysed for each pattern and a total of

30 measurements were performed. The results obtained for the two patterns of grooves are presented in Table 1. About a 30–35% decrease in dimensions was observed for both patterns at a temperature above the transition temperature of the hydrogels. Therefore, the ‘‘smart’’ behaviour does not modify the nature of the topography. However, some changes in the optical properties and roughness can be observed in **Fig. 5A** and **5B**. In addition, there exists certain hysteresis behaviour during a swelling–deswelling cycle. The topographical features of the surfaces do not fully recover the original dimensions after the completion of one cycle, although the observed differences are small and always below 10% (result not shown).

Table 1. Influence of water temperature on the dimensions of the micropatterns.

Width: interdistance PDMS stamp/ µm	Width: interdistance at 4 °C/ µm	Width: interdistance at 37 °C/ µm
25: 25	18.7 ± 0.3 : 22.2 ± 0.3	11.7 ± 0.5 : 13.9 ± 0.6
20: 100	20.3± 1.0 : 71.8 ± 1.3	13.7 ± 1.0 : 50.4 ± 3.1

In conclusion, we have demonstrated the processability of ELP polymers by replica moulding to obtain patterned hydrogels with tunable mechanical properties and smart behaviour in aqueous media.

Bioactive ELPs containing the RGDdomain show a high capacity for promoting cell attachment [9, 13]. We can now add controlled topography as a factor to study and eventually control cell behaviour. Furthermore, the smart nature of the gels makes the substrates active, with the possibility of changing the dimensions of the microstructures during cell culture, provided that the Tt is adjusted in the right range. This can be obtained, for example, by tuning the amino acid composition of the polymer [12].

The application of microfabrication techniques to ELPs is an important step towards the development of cell-based biomedical systems.

References

[1] Nelson, C.M.; Tien, J. Microstructured extracellular matrices in tissue engineering and development. *Curr. Opin. Biotechnol.*2006, **17**, 518–523.

[2] Falconet, D.; Csucs, G.; Grandin, H. M.; Textor, M. Surface engineering approaches to micropattern surfaces for cell-based assays. *Biomaterials*, 2006, **27**, 3044–3063.

[3] Zhang, Y.; Lo, C.W.; Taylor, J. A.; Yang, S. Replica molding of high-aspect-ratio polymeric nanopillar arrays with high fidelity. *Langmuir*, 2006, **22**, 8595–8601.

[4] Bettinger, C. J.; Orrick, B.; Misra, A.; Langer, R.; Borenstein, J. T. Microfabrication of poly(glycerol-sebacate) for contact guidance applications. *Biomaterials*, 2006, **27**, 2558–2565.

[5] Rodríguez-Cabello, J. C.; Prieto, S.; Arias, F. J.; Reguera, J.; Ribeiro, A. Tailored recombinant elastin-like polymers for advanced biomedical and nano(bio)technological applications. *Nanomedicine*, 2006, **1**, 267–280.

[6] Urry, D. W.; Parker, T. M.; Reid, M. C.; Gowda, D. C. Biocompatibility of the bioelastic materials, poly(GVGVP) and its gamma-irradiation cross-linked matrix - summary of generic biological test-results. *Journal of Bioactive and Compatible Polymers*, 1991, **6**, 263–282.

[7] Huang, L.; McMillan, R. A.; Apkarian, R. P.; Pourdeyhimi, B.; Conticello, V. P.; Chaikof, E. L. Generation of synthetic elastin-mimetic small diameter fibers and fiber networks. *Macromolecules*, 2000, **33**, 2989–2997.

[8] Garcia, Y.; Hemantkumar, N.; Collighan, R.; Griffin, M.; Rodríguez-Cabello, J. C.; Pandit, A. In vitro characterization of a collagen scaffold enzymatically cross-

linked with a tailored elastin-like polymer. *Tissue Engineering: Part A*, 2008, **14**, 887-899.

[9] Liu, J. C.; Tirrell, D. A. Cell response to RGD density in crosslinked artificial extracellular matrix protein films. *Biomacromolecules*, 2008, **9**, 2984–2988.

[10] Prieto, S.; Santo, V. E.; Testera, A. M.; Arias, F. J.; Alonso, M.; Mano, J. F.; Rodríguez-Cabello, J. C. *Acta Biomater.* Submitted.

[11] Ong, S. R.; Trabbic-Carlson, K. A.; Nettles, D. L.; Lim, D. W.; Chilkoti, A.; Setton, L. A. Epitope tagging for tracking elastin-like polypeptides. *Biomaterials*, 2006, **27**, 1930–1935.

[12] Urry, D. W.; Gowda, D. C.; Parker, T. M.; Luan, C. H.; Reid, M. C.; Harris, C. M. Hydrophobicity scale for proteins based on inverse temperature transitions. *Biopolymers*, 1992, **32**, 1243–1250.

[13] Dunehoo, A. L.; Anderson, M.; Majumdar, S.; Kobayashi, N.; Berkland, C.; Siahaaan, T. J. Cell adhesion molecules for targeted drug delivery. *J. Pharm. Sci.* 2006, **95**, 1856-1872.

CHAPTER 3

Synthesis and Characterization of Macroporous Thermosensitive Hydrogels from Recombinant Elastin-Like Polymers

The work presented in this chapter has been published in:

L. Martín; M. Alonso; A. Girotti: F. J. Arias; J. C. Rodríguez-Cabello. 2009

Synthesis and Characterization of Macroporous Thermosensitive Hydrogels from Recombinant Elastin-Like Polymers

Biomacromolecules, 10: 3015-3022

Synthesis and Characterization of Macroporous Thermosensitive Hydrogels from Recombinant Elastin-Like Polymers

Laura Martín, Matilde Alonso, Alessandra Girotti, F. Javier Arias and J. Carlos Rodríguez-Cabello*

G.I.R. Bioforge, University of Valladolid, Ciber-bbn, Paseo de Belén 11, 47011 Valladolid, Spain.

Keywords: Elastin-like polymers, Porous Hydrogels, Thermal responsiveness, Tissue Engineering

*Correspondence to:

J. Carlos Rodríguez-Cabello

Tel: +34 983 184 686

E-mail: cabello@bioforge.uva.es

Abstract

Multifunctional bioactive chemically cross-linked elastin-like polymers (ELPs) have been prepared as three-dimensional scaffolds for tissue engineering. The salt-leaching/gas-foaming technique was found suitable to prepare highly porous biodegradable hydrogels based on this novel material type. The porosity can be controlled by the amount of sodium hydrogen carbonate incorporated during the cross-linking reaction, whereas the mean pore size is determined by the salt particle size. The gas-foaming process, which involves immersion in a citric acid solution after the cross-linking, facilitates pore interconnectivity and allows a grooved surface essential for cell colonization. Due to the thermoresponsive nature of the ELPs, their physical properties are strongly influenced by the temperature of the aqueous medium. The feasibility to obtain tridimensional scaffolds for tissue engineering has been studied by testing the adhesion and spreading of endothelial cells into the porous ELP hydrogels. The methods and structures described herein provide a starting point for the design and synthesis of macroporous multifunctional elastin-like hydrogels with potential broad applicability.

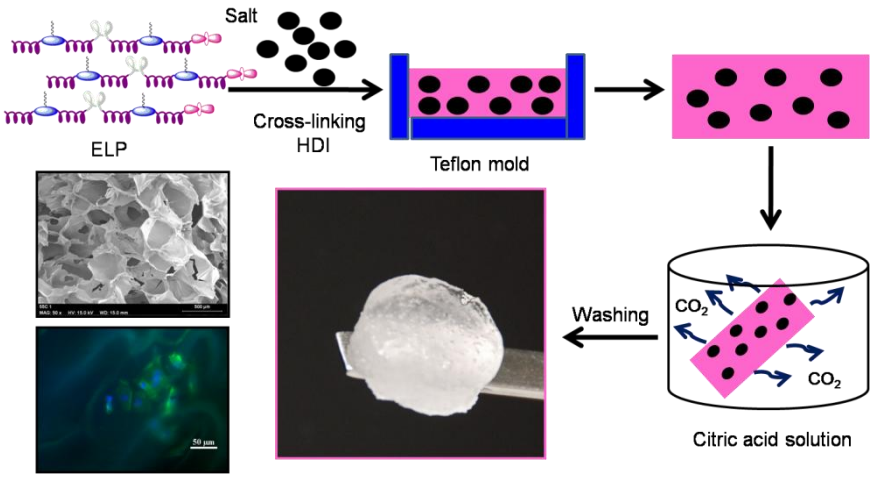

1. Introduction

Researchers in the field of tissue engineering are continually searching for materials with additional tissue-specific properties or which could be tailored to several tissue systems. The scaffold composition may include desirable properties such as specific interactions with extracellular matrix components, growth factors or cell-surface receptors. A great deal of interest is currently being focused on new classes of biodegradable polymers with specific or controllable bioactivity. The extracellular matrix (ECM) is a composite material which contains a complex mixture of fibrous proteins and heteropolysaccharides and provides an important model for the design of biomaterials [1, 2].

Modern genetic engineering techniques allow the design and expression of artificial genes to prepare proteinaceous analogues of ECM proteins with controlled mechanical properties, and which incorporate domains that modulate cellular behavior [3-6]. The goal of mimicking the ECM's structure and biological functions requires the design of artificial scaffolds that reproduce one or, preferably, more of the properties and functionalities of the natural tissue.

One of the most important examples of this new generation of ECM-mimicking materials is the family of recombinant elastin-like polymers (ELPs). They are inspired by the amino acid sequence of native elastin, one of the most abundant ECM proteins. In its natural state, elastin is an insoluble protein due to the presence of cross-links. However, its soluble forms, such as tropoelastin [7] or R-elastin [8], are frequently used as biomaterials. In both cases, although more evident for ELPs, biotechnological techniques have been exploited to create tailored protein polymers with programmable sequences. This allows highly complex ELPs containing structural and functional domains derived from different ECM proteins to be obtained with total control of the

molecular architecture. These biomimicking biopolymers can include cell-binding peptides such as RGD, REDV, and so on, which are sequences that promote specific cellular responses by mediating cell adhesion via integrins [9-11]. The ELP family of polymers shows a wide range of interesting properties that are rarely found together in any other polymeric material, namely, biocompatibility, mechanical properties (similar to those of natural ECM), a stimuli-responsive nature, and self-assembly behavior, and the obvious possibility of incorporating any function derived from peptidic domains into their composition. The most peculiar property of these polymers, however, is probably their stimuli-responsive behavior. ELPs undergo a phase transition in response to temperature changes. Below a critical temperature, known as the transition temperature (T_t), the un-cross-linked polymer chains are soluble in water, whereas above T_t the polymer chains form nano- and microaggregates, which separate from solution [3, 12]. An understanding of the molecular basis of this stimuli-responsive behavior has opened up the opportunity to create ELPs that respond, under isothermal conditions, to a number of external stimuli, including light, redox changes, pH, concentration of diverse analytes, and pressure, by exploiting the so-called ΔT_t and amplified ΔT_t mechanisms [13-15].

The enormous potential of this kind of protein polymer as a truly advanced material for a variety of biomedical applications, ranging from scaffolds for tissue engineering and regenerative medicine to cell-based microdevices, has boosted the exploration of the different ways that these peculiar polymers can be processed to achieve practical scaffolds and systems for use in different contexts, thereby showing the potential to improve the currently existing alternatives. In this regard, ELP scaffolds have been produced in the form of electrospun fibers [16], hybrid hydrogels [17] and

2D films [18], and ELP hydrogels have been produced by photoinitiation [19], irradiation [20, 21] amine reactivity [22- 26], and enzymatic cross-linking by tissue transglutaminase [27]. However, due to the short history of this family and the fact that these materials are not commercially available, a great deal of fundamental knowledge regarding their properties is still lacking. For example, although ELP hydrogels with different compositions have been tested in terms of bioactivity, swelling ratio, or mechanical properties, their microstructure, which is very important for tissue engineering applications, has not been studied in-depth. One of the most obvious knowledge gaps for ELP hydrogels is that few studies concerning the possibility of obtaining suitable macroporous scaffold structures for subsequent use in 3D cell culture procedures have been performed.

Three-dimensional polymer scaffolds provide a suitable space in which transplanted cells can grow and generate their own extracellular matrix. This artificial scaffold should ideally degrade into nontoxic components that can be eliminated or reabsorbed from the implant site. A high porosity is required to offer sufficient space for tissue ingrowth and to improve the invasion of surrounding tissues. A well-defined pore size and interconnecting pore network are also essential for vascularization and nutrient diffusion. It is also desirable that these scaffolds are biocompatible, biodegradable, and exhibit appropriate mechanical properties if required for the application and manufacturing technique to be used [28, 29]. Several methods have been used to obtain these kinds of porous scaffolds from biodegradable materials, including solvent casting/porogen leaching [30, 31], gas foaming with pressurized carbon dioxide [8, 32], electrospinning [33, 34], emulsion freeze-drying [35, 36], 3D printing [37, 38], salt leaching/gas foaming [39, 40], and, more recently, combinations of these methods. These techniques have been used with both natural (gelatin, chitosan or alginate) and

synthetic biodegradable polymers such as polyesters, poly(vinyl alcohol), or poly(urethane)s, although their use with ELPs has not been reported [1, 41].

Due to the water solubility of most ELPs, many of the existing methods to create macroporous structures cannot be used. Among those methods that could be used, however, salt leaching is one of the most attractive. We have therefore evaluated the possibility of adapting current technology for this purpose. In this work, we adapt the standard salt-leaching/gas-foaming method to obtain appropriate bioactive scaffolds for 3D tissue engineering from ELPs. In general, the salt-leaching technique has shown, with other polymer systems, that porosity and pore size can be controlled by varying the amount of salt present and its particle size, respectively. The salt (usually NaCl) is incorporated during the cross-linking reaction with materials such as gelatin, poly-*L*-lactic acid (PLLA) or poly-*DL*-lactic-*co*-glycolic acid (PLGA), among others [36, 42], although it is difficult to obtain interconnected structures with this technique and the scaffolds often present a surface skin layer. It is possible to minimize these disadvantages of the salt-leaching technique by using the salt-leaching/gas-foaming method [40], which is based on the idea that sieved particles of bicarbonate salts, dispersed within a polymer-solvent mixture, generate carbon dioxide gas in the matrix upon contact with hot water or acid solution, thereby producing highly porous scaffolds.

The pore size required depends on the type of cell to be grown on that scaffold and on the material. For example, a pore diameter of 100 μm and above is required to ensure a rich blood supply, nutrient delivery and gas exchange to promote the colonization of bone cells [43, 44]. Pore-size control is therefore critical for controlling cellular colonization rates, angiogenesis, and organization within an engineered tissue. The pore morphology can also affect the scaffold degradation kinetics and the

mechanical properties of the tissue significantly. In tissue engineering, scaffolds should supply mechanical support for the cellular microenvironment as well as transmit mechanical stimuli. Hydrogels are not simply elastic materials, but behave viscoelastically [45- 47]. The viscoelastic properties correlate strongly with the microstructure and could provide useful information for tailoring their performance characteristics to suit given applications.

In this study, we present a simple method for preparing ELP-based macroporous hydrogels with tunable pore sizes and mechanical properties with the aim of gaining a fundamental understanding of how the introduction of salt particles affects the physical properties of thermally responsive ELP hydrogels. The reviewed literature suggests that there is no "ideal" scaffold for all tissue types, and we demonstrate herein that the physical properties of these materials can be tailored to future applications in tissue engineering and regenerative medicine by varying the size of the salt particles [48, 49]. Furthermore, we have studied the influence of temperature on scaffolds made from stimuli-responsive ELPs. If this thermoresponsive behavior is found to remain in the cross-linked hydrogels, this could significantly broaden the potential of these biological systems for tissue engineering purposes because, for example, their thermoresponsive nature could be exploited in combined drug-delivery and tissue-engineering strategies.

2. Experimental Section

Materials. The elastin-like polymer was biosynthesized and its biochemical and physical properties characterized by previously reported methods [11]. N,N-Dimethylformamide (DMF), dimethyl sulfoxide (DMSO), hexamethylene diisocyanate (HDI), sodium chloride (NaCl), sodium hydrogen carbonate (NaHCO3), and anhydrous citric acid were purchased from Fluka Sigma-Aldrich (Madrid, Spain).

Salt particles were sieved in two different ranges [250-425 μm (A) and 180-250 μm (B)] before use.

Human umbilical vein endothelial cells (HUVECs; cat. no. cc-2517), endothelial growth medium (EGM; Clonetic, cat. no. cc-3124), serum-free culture medium (EBM Clonetics cat. no. cc-3121), accutase (cat. no. A6964 Sigma Aldric), DAPI (cat. no. PA-3013), Phalloidin-Alexa Fluor488 Conjugate (cat. no. PA-3010), and all other tissue culture reagents were purchased from Lonza. The remaining consumables for cell culture were obtained from Corning Inc. Costar.

Preparation of Porous ELP Hydrogels. The hydrogels were obtained by mixing a solution of the ELP (80 mg/mL) in DMSO/DMF (80:20) with an appropriate solution (25 mg/mL) of the homobifunctional cross-linker hexamethylene diisocyanate (HDI) in DMF in a polymer/cross-linker molar ratio of 1:3 at 4 °C. The mixture was stirred and poured into customized Teflon molds (Ø = 13.5 mm; *h* = 2 mm). Previously sieved NaCl or $NaHCO_3$ was added in a salt/polymer weight ratio of 10:1 or 20:1 and stirred to homogenize the sample. The reaction mixture was kept at room temperature for 3 h, then the salt-hydrogel samples incorporating $NaHCO_3$ were extracted from the mold and immersed in a 3 M citric acid solution for 45 min in an ultrasound bath. Finally, all the matrices were thoroughly washed with Milli-Q water to eliminate unreacted reagents and salts. Hydrogels prepared without porogen salts were used for reference.

Differential Scanning Calorimetry (DSC). The experiments were performed on a Mettler Toledo 822^e DSC with a liquid-nitrogen cooler, calibrated with a standard sample of indium. For analysis of the ELP, 20 μL of a 50 mg/ mL polymer solution in Milli-Q water were placed in a 40 μL aluminum pan hermetically sealed. An equal

volume of water was placed in the reference pan. For ELP-hydrogel analysis, 20 mg of the hydrated hydrogel was placed on the sample pan. To account for the exact amount of polymer in the assayed hydrogel, the sample was lyophilized and weighted after the DSC run. The heating program for both kinds of samples includes an initial isothermal stage (5 min at 0 °C) followed by heating at a constant rate of 5 °C/ min from 0 to 50 °C.

Amino Acid Analysis. The amino acid composition was determined by the Technical-Scientific Service at the University of Barcelona (Spain) by HCl hydrolysis, derivatization by the AccQ-Tag Waters method and subsequent analysis by HPLC with UV detection for quantification. Each sample has been analyzed by triplicate.

Physical Properties of ELP Hydrogels. The porosity of the hydrogels was determined in the swollen state in water using eq 1 [50]

$$porosity\ \% = \frac{W_1 - W_2}{d_{water}} \times \frac{100}{V} \quad (1)$$

The swelling ratio (Q_w) of the hydrogels was estimated using eq 2

$$Q_W = \frac{W_1}{W_2} \quad (2)$$

where W_1 and W_2 are the weight of the swollen and lyophilized gel, respectively, d_{water} is the density of pure water, and V ($\Pi r^2 h$) is the measured volume of the hydrogel in the swollen state. All measurements were taken 24 h after soaking the hydrogel in water at the appropriate temperature. Excess surface water was removed with a filter paper before each measurement.

Lyophilization or freeze-drying (FreeZone 1, LABCONCO) was performed from frozen hydrogels in liquid nitrogen previously swollen in water at the corresponding testing temperature.

Mechanical tests were performed on a strain-controlled rheometer (AR2000ex, TA Instruments) to measure the dynamic shear modulus (a measure of dynamic matrix

stiffness). Swollen gels were placed between parallel plates (12 mm in diameter) and the gap adjusted starting from the sample to reach a normal force of about 0.3 N to prevent slippage. An amplitude sweep (storage modulus G′ measured as a function of strain) was performed to confirm that the measurements were within the linear region of viscoelasticity. Measurements were then carried out in constant-strain mode (0.1%) as a function of frequency (from 0.1 to 10 Hz).

All physical properties mentioned above were measured at two testing temperatures: below (4 °C) and above (37 °C) T_t.

Microstructural Morphology. Freeze-dried ELP hydrogels were fractured after immersion in liquid nitrogen. The samples were coated with Au (Balzers-SCD 004) prior to SEM (JEOL, JSM-820) observation at 15.0 kV.

In addition, swollen hydrogels were heated from 4 to 37 °C and observed without sample preparation using environmental scanning electron microscopy (ESEM) (FEI Quanta 200FEG). The mean pore size was estimated using *Image J* software with at least 30 pores in three different spots for triplicate samples.

Statistical Analysis. Data are represented as the mean ± standard deviation (SD), n = 3. Statistical comparisons were performed by one-way ANOVA using Bonferroni corrected t-test with Graphpad Prism 4.0 software. A p-value of less than 0.05 was considered to be statistically significant (expressed in the figure with asterisks [*]: *P <0.05; **P < 0.01; when present).

Cell Culture Assays. HUVECs were grown in EGM, which was replaced every two days, and were incubated at 37 °C in a 5% CO_2 humidified environmental chamber. Hydrogels for these cell culture assays were made with sodium hydrogen carbonate: polymer weight ratio of 20/1 using particles in the 180-250 μm size range. They were

sterilized for cell culture by UV exposure overnight and stored in 70% ethanol. Before use, they were washed with sterile Milli-Q water, lyophilized, and placed in a 24-well plate. Near confluence HUVECs (passages 3-5) were harvested by accutase treatment and then washed and resuspended in EBM, seeded at 10000 cells/ cm2 on dried ELP hydrogels, and incubated at 37 °C. EBM minimal medium was used to promote specific cell-scaffold interaction. A total of 48 h after cell seeding, the hydrogels were washed with PBS to remove nonadhered cells and then fixed.

Samples for phase-contrast and epifluorescence were fixed in 4% paraformaldehyde for 10 min, permeabilized with 0.2% Triton X-100, and stained with the fluorescent dyes Phalloidin-Alexa Fluor488R and DAPI, as indicated in the text. The samples were observed by phase-contrast and fluorescence microscopy using a Nikon Eclipse Ti inverted microscope (Nikon Instruments/Europe) at a magnification of 10-20-40×.

Hydrogels seeded with cells for SEM analysis were fixed in Palay fixative [37] (1% gluteraldehyde and paraformaldehyde in 0.1 N calcium chloride solution) at pH 7.4 for 2 h at room temperature. Samples were progressively dehydrated in ethanol solutions (15, 30, 50, 70, 90, and, three times, 100%).

3. Results and Discussion

Cross-Linked Hydrogels and Thermal Behavior.

The bioactive protein polymer used in this work was designed to be employed in tissue engineering with peptide sequences that provide an appropriate balance of bioactivity (cell adhesion sequence and specific biodegradability) and other functionalities (cross-linking domains and mechanical properties) [11]. The monomer unit contains four different functional blocks (**Fig. 1**).

((VPGIG)$_2$ VPGKG (VPGIG)$_2$EEIQIGHIPREDVDYHLYP(VPGIG)$_2$VPGKG(VPGIG)$_2$(VGVAPG)$_3$)$_{10}$

Fig. 1. *Scheme of the peptide domains and amino acid sequence of the designed polymer.*

Thus, the $(VPGIG)_n$ sequence confers elasticity, biocompatibility, and thermoresponsive nature [12]. Some of the elastic domains have been modified to include lysines for cross-linking purposes and other potential chemical modifications while retaining the ELP properties. The next block contains periodically spaced fibronectin CS5 domains enclosing the cell attachment sequence REDV, which has been found to be specific for endothelial cells [9]. Finally, a target hexapeptide sequence for elastase-proteolitic action with bioactive properties (modulation of proliferation and migration among others) has been introduced.

Polymer cross-linking was performed by forming covalent links between the homobifunctional cross-linker HDI and the ε-amine groups of the polymer lysines in the organic solvent mixture described above. The cross-linking ratio (polymer/crosslinker 1:3) was selected to obtain hydrogels with optimal consistency and transparency (data not shown). To decrease the solution freezing point, a mixture of DMSO and DMF was chosen. Both solutions were stored at low temperature (4 °C) before mixing to decrease the cross-linker reactivity during the initial mixing and molding stages.

The inverse temperature transition (ITT) can be characterized by T_t and the enthalpy involved in the phase transition. Crosslinked ELP hydrogels prepared in the absence of salt particles retain the thermoresponsiveness characteristics of the ELPs displaying T_t (**Fig. 2**).

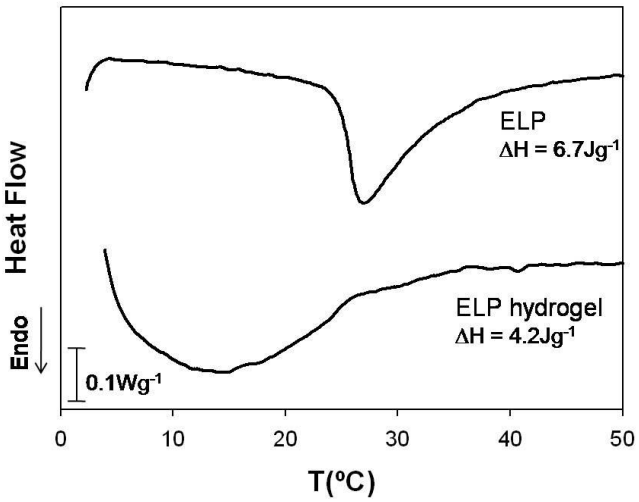

Fig. 2. *DSC thermograms of the ELP and the ELP-hydrogel at heating rate of 5 °C/ min. The enthalpy of the phase transition is shown on the plot.*

T_t is lower for the ELP hydrogel than for the free ELP. This was expected as the reaction of the ε-amine groups for cross-linkings causes a decrease in the mean polarity, which according to the literature is always accompanied by a decrease in T_t [12]. The enthalpy of the transition found in the hydrogel is slightly lower than the one found for the uncrosslinked polymer. Although, in principle, the decrease in T_t should be accompanied by an increase in the enthalpy [12], the dense cross-linked network leads to a decrease in chain mobility and partial loss of the conformational freedom. That would hinder the chain folding that takes place as an ELP is heated above its T_t, which could explain the relatively low value found for the enthalpy. Furthermore, there is a substantial broadening in the endotherm, caused also by the hindered chain mobility, which plays an additional kinetic effect.

Cross-linked ELP hydrogels were first prepared in the absence of salt particles. Those samples exhibited certain intrinsic microporosity, as can be seen from the SEM micrographs in **Fig. 3**.

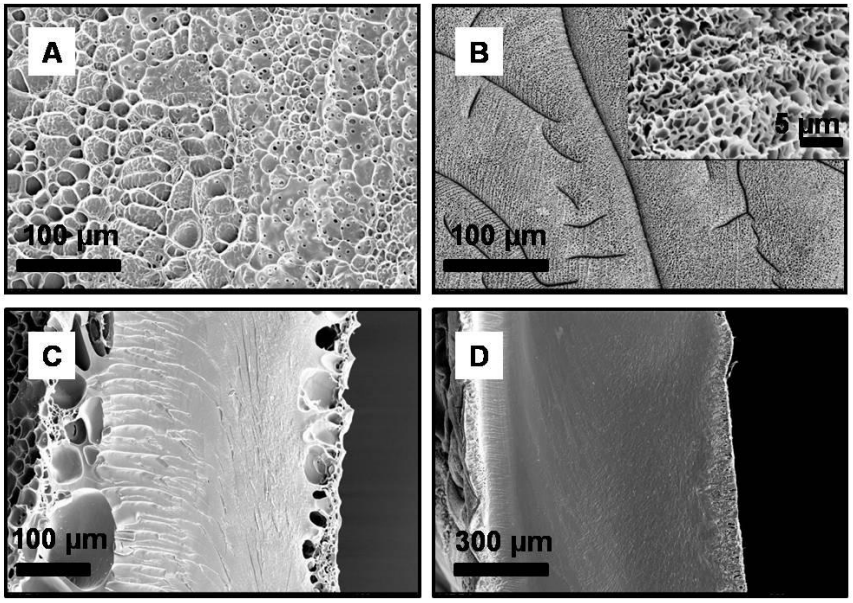

Fig. 3. *Swelling behavior and SEM micrographs of elastin-like hydrogels cross-linked in the absence of salt particles. Surface views: (A) 4 °C, (B) 37 °C; and cross sections: (C) 4 °C and (D) 37 °C.*

However, this intrinsic porosity proved to be of no use for creating 3D scaffolds for tissue engineering. Inspection of these images reveals that the surface shows a closed-pore structure. The mean pore size at 4 °C is 29.0 ± 11.1 µm (**Fig. 3A**) as the structure is completely expanded, whereas at 37 °C, above T_t, the hydrogel collapses, which results in a substantial decrease in the mean pore size (1.3 ± 0.4 µm; **Fig. 3B**). In addition, there is no porous organization inside the lyophilized hydrogel obtained in the absence of porogen salts at both tested temperatures (**Fig. 3C, D**). These results show that the matrix retains the thermoresponsive nature of the original ELP but that the pore size and internal structure in ELP hydrogels crosslinked without porogen salts would not be suitable for cell colonization.

These results clearly indicate the need to use suitable methodologies to enhance the porosity and mean pore size in order to obtain adequate macroporous hydrogels for 3D cell culture. A first option in this direction is the simple method of salt leaching

(with sodium chloride). As an example on the possibilities of this approach, ELP hydrogels were prepared with sieved sodium chloride particles at the following conditions: polymer weight ratio of 10/1 and particle size in the range 180-250 μm. The porous structure obtained is shown in **Fig. 4**.

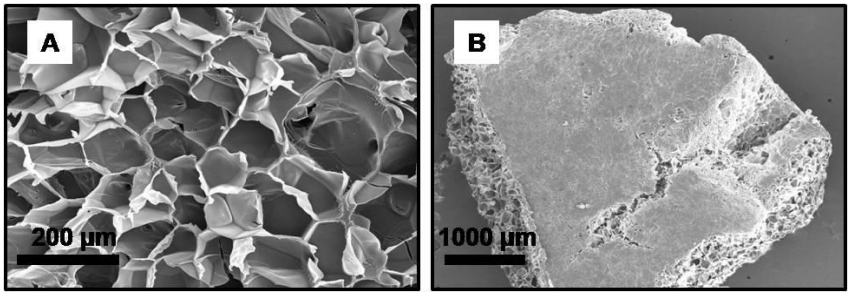

Fig. 4. *SEM micrographs of ELP hydrogels obtained by salt leaching: cross-sectional (A) and surface view (B).*

SEM micrograph in **Fig. 4A** demonstrates that it is possible to adapt this standard technique to ELPs to obtain homogeneous porous structures with a controlled pore size. However, this material contains no interconnected structures and the surface also exhibits a skin layer (**Fig. 4B**). These results clearly show that this technique is suitable for obtaining macroporous scaffolds but that the interconnectivity still needs to be enhanced and the surface characteristics improved to allow cell colonization. The salt-leaching/gas-foaming method was therefore utilized to improve the properties of the hydrogels obtained using the salt-leaching method alone.

Morphological Characterization of Porous ELP Hydrogels Obtained by the Salt-Leaching/Gas-Foaming Method.

Fig. 5. *Macroscopic pictures of swollen hydrogels in water at 4 °C with different salt/polymer weight ratios: (A) 0/1, (B) 10/1, and (C) 20/1.*

Fig. 5 shows macroscopic pictures of the swollen hydrogels. The hydrogel in **Fig. 5A** was prepared in the absence of porogen salts, whereas the porous hydrogels shown in **Fig. 5B and C** were prepared by the salt-leaching/gas-foaming method using increasing amounts of sodium hydrogen carbonate particles. As expected, the presence of pores clearly results in decreased gel transparency.

Amino acid analysis was used to study the degree of crosslinking; the results are summarized in Table 1.

Table 1. Amino Acid Analysis Comparing Theoretical and Experimental Results for Un-Cross-Linked ELP and Cross-Linked Hydrogels[a]

Amino acid type	Theoretical number of amino acids	Experimental number for uncross-linked ELP [12]	Experimental number for hydrogels weight ratio salt/ polymer		
			0/1	10/1	20/1
Lys (K)	20	20.05	5.04±0.03	4.04±0.02	4.11±0.04
Arg (R)	10	11.20	10.58±0.01	10.84±0.06	10.95±0.04
Glx (E+Q)	41	42.13	39.67±0.08	40.55±0.20	40.87±0.17
Asp (D)	20	20.41	21.34±0.13	21.73±0.06	21.81±0.08
Val (V)	171	172.17	169.82±0.27	170.98±0.43	171.06±0.73

[a] Date reported as mean ± SD (*n*= 3).

The degree of cross-linking can be determined from the content of free amino groups in the cross-linked hydrogels. This analysis clearly demonstrates the specific

reactivity of HDI toward lysines in organic solvents as the content of other amino acids was not affected by the cross-linking reaction. The good specificity of HDI is of particular interest as undesirable specific reactions with possible reactive amino acids such as arginine (R), glutamic acid (E), or aspartic acid (D) involved in cell-adhesion induction could inhibit the bioactivity of the CS5 domain [24]. The presence of salt particles during the cross-linking reaction did not affect the degree of cross-linking significantly, with highly cross-linked hydrogels being obtained in all cases.

Scaffolds were prepared from sieved salt particles in two different size ranges: 180-250 and 250-425 µm. The scaffold pore morphology obtained with these two different size ranges was found to be retained in the hydrogel microstructures. The hydrogels show a uniform pore morphology with evenly distributed pores, as evidenced by the cross-sectional SEM micrographs (**Fig. 6**), as was the case for the ELP hydrogels obtained using the salt-leaching method alone (**Fig. 4**), thus, indicating that the salt type does not influence the pore organization inside the structure.

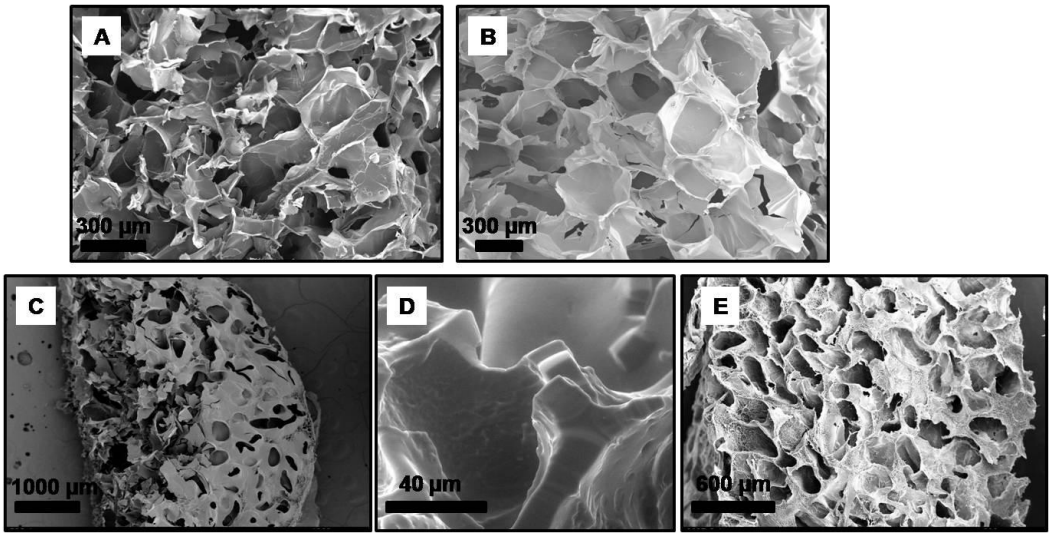

Fig. 6. *SEM micrographs of hydrogels obtained with different salt particle size ranges: (A) 180-250, (B) 250-425 µm. Surface views (C, D) and cross-sectional micrograph (E) of the 180-250 µm ELP hydrogels.*

The average pore size in the scaffolds was 208.6 ± 33.5 μm for materials obtained using salt particles in the range 180-250 μm (**Fig. 6A**) and 318.7 ± 60.3 μm for materials obtained using particles in the 250-425 μm size range (**Fig. 6B**). The pore-size distribution in the hydrogels is therefore in full agreement with the initial salt particle size-ranges. The interconnectivity between pores was found to be improved by the effervescent-ultrasound process, and macropores connected to adjacent pores via openings in the pore walls can be observed in the cross-sectional SEM micrographs shown in **Fig. 6A, B**. The surface of these samples was found to be highly grooved and did not show any substantial formation of a skin layer, as can clearly be seen in **Fig. 6C.** This feature differentiates our materials from many of the other hydrogels reported in the literature, including the ELP hydrogels mentioned above, where the existence of such a skin is quite a common feature. A magnified view of a surface pore in the hydrogel is shown in **Fig. 6D**. This micrograph shows a pore wall thickness of a swollen hydrogel, which is about 15 μm. In addition to the macroporous structure induced by the salt particles, an intrinsic microporosity can still be observed in hydrogels at 37 °C, a temperature above T_t, which contributes to the enhanced structure roughness (**Fig. 6E**) and could be important for promoting cell attachment.

Changes in the pore size of hydrogels immersed in water, due to the thermoresponsive behavior of ELPs, were observed by ESEM (**Fig. 7**).

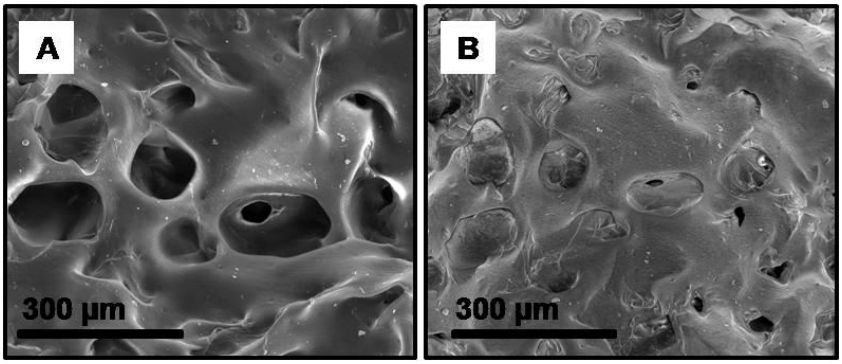

Fig. 7. *ESEM micrograph showing the change in pore size with temperature in swollen hydrogels: (A) 4 °C, (B) 37 °C.*

A decrease in pore size of about 30% was observed for the same pores as the temperature was increased to above T_t. This responsive nature offers the possibility of changing the dimensions of the pore during the cell culture to study possible modifications in cell behavior. In any case, and for the pore sizes used in this work, the decrease in pore dimensions is not enough to compromise the possibility of cell infiltration as it will be later demonstrated in the cellular studies.

Effect of Salt Particle Size on Porosity.

Porous hydrogels were prepared with two different salt particle ranges of sodium hydrogen carbonate to evaluate the dependence of porosity on the salt particle size. All hydrogels were synthesized by triplicate with a sodium hydrogen carbonate: polymer weight ratio of 10/1 and quantified using eq 1. In addition, the porosity of the swollen hydrogels was studied in water at two temperatures, one below (4 °C) and the other above (37 °C) Tt, to observe the influence of the temperature on the porosity.

The salt particles were sieved in the same ranges as above (180-250 and 250-425 µm). The results are plotted in **Fig. 8**.

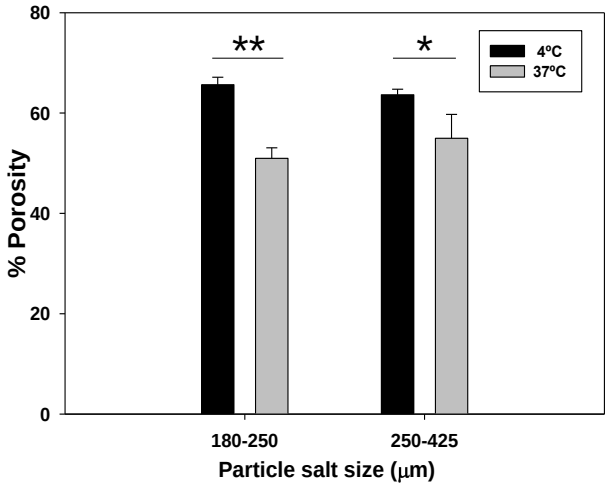

Fig. 8. *Effect of salt particle size and T_t on the porosity of hydrogels with a salt/polymer weight ratio of 10:1. Data are reported as mean ± SD (n = 3). Asterisk denotes significantly different p-values (*P <0.05; **P < 0.01).*

The most obvious result is that porosity is influenced by temperature. The ELP hydrogels showed a porosity in the range 51-65% for the salt amount tested. The collapse above T_t due to the phase transition decreases the porosity significantly. Statistical analysis confirmed that there were no significant differences between the hydrogels obtained with different particle sizes at the same temperatures ($p > 0.05$) for similar amounts of salts. Hydrogels with similar porosity can therefore be prepared with different pore diameters simply by utilizing microsieved salt particles of different sizes.

Effect of the Salt/Polymer Weight Ratio on Porosity.

Because porosity is not dependent on the salt particle size for equal salt amounts, hydrogels were prepared in triplicate with a salt particle size range of 180-250 μm, to study the influence of different salt amounts on the porosity. The hydrogels produced in the absence of salt porogens were used as reference; the porosity was calculated using

eq 1. **Fig. 9** shows the influence of the salt fraction on the porosity below (4 °C) and above T_t (37 °C).

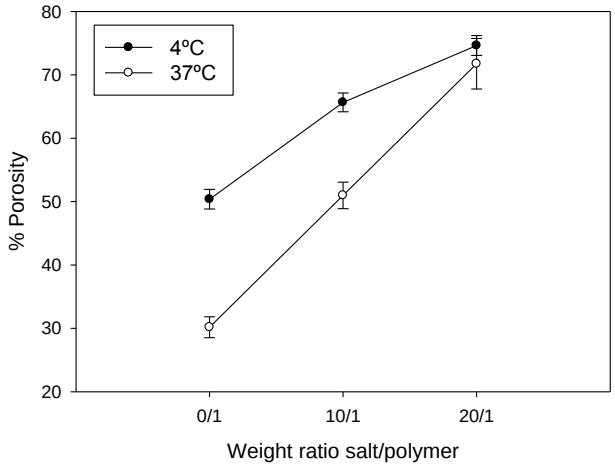

Fig. 9. *Influence of salt/polymer weight ratio on the porosity. SD indicated, n = 3.*

An increase in the salt/polymer ratio results in a high porosity of the cross-linked hydrogels under identical conditions, reaching as high as 75% at the highest salt amount tested in this work. Raising the temperature from 4 to 37 °C results in a decrease in the porosity, in agreement with the collapse previously observed in ELP hydrogels. Significant differences were found between samples with different salt/polymer ratios at the two testing temperatures except for hydrogels with high salt concentrations (20/1), which showed no significant differences in porosity with temperature.

Effect of Salt/Polymer Weight Ratio on Swelling.

The swelling ratio was determined from eq 2 by soaking the hydrogels in Milli-Q water for 24 h. The results of this analysis are summarized in Table 2.

Table 2. Swelling Ratio of Hydrogels Prepared with Sodium Hydrogen Carbonate (Size Range: 180-250 μm) in Water[a]

Salt/polymer weight ratio	Q_w (4 °C)	Q_w (37 °C)
0/1	3.37±1.10	1.70±0.30
10/1	28.43±3.63	2.61±0.16
20/1	36.28±1.63	10.10±0.49

[a] Data are reported as mean ± SD (n = 3)

The swelling ratio was found to increase significantly with an increase in the salt/polymer weight ratio. Thus, an increase in the salt/polymer weight ratio from 0/1 to 20/1 resulted in an increase in the swelling ratio (Q_w) from 3.37 ±1.10 to 36.28 ±1.63 at 4 °C. These results are in agreement with the increase in porosity. The swelling ratio decreases above T_t (37 °C) due to hydrogel collapse.

The phase transition of the ELP hydrogels can also be observed in the degree of swelling and contraction in aqueous solution and its dependence on temperature.

Effect of the Salt/Polymer Weight Ratio on the Rheological Properties.

In general, hydrogels are viscoelastic materials. Their mechanical properties can be determined by rheological measurements in the linear viscoelastic range. Knowledge of the linear viscoelastic properties is of great importance since it allows to obtain information of the material in conditions close to unperturbed state. Therefore, in compliance with the principle of small deformation rheology [46, 47], the hydrogels must be tested within their respective linear viscoelastic ranges to ensure their stability. Samples were tested in their equilibrium swollen state completely immersed in a thermally regulated water bath during the analysis, and a dynamic strain sweep was

performed to determine the range of strain amplitudes for which ELP hydrogels exhibit that linear stress-strain behavior. Results confirmed that linear behavior was observed up to 0.3% strain, so that all subsequent tests were performed for a 0.1% strain. Thus, the dynamic shear modulus (a measure of dynamic matrix stiffness) was measured by frequency sweep tests between 0.1 and 10.0 Hz, showing a lineal behavior. The magnitudes of the dynamic shear modulus (G*) are reported from data of a single frequency, 1.0 Hz, to compare among ELP hydrogels of varying salt amounts. Shear modulus (G*) confirms that there is an inverse dependence between the mechanical properties and the porosity (**Fig. 10**).

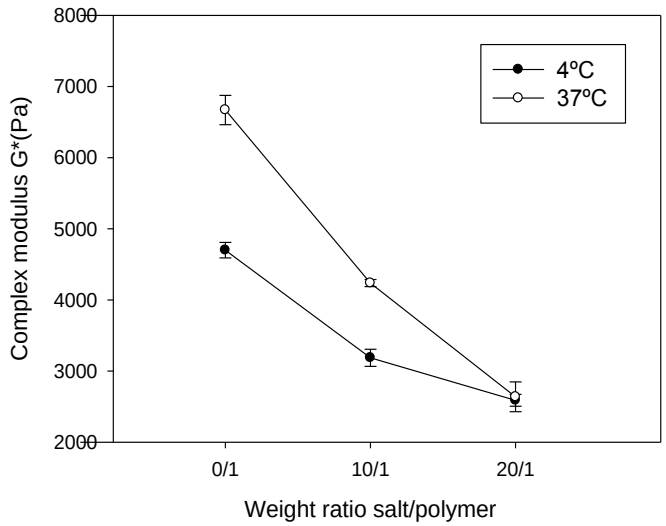

Fig. 10. *Influence of the salt/polymer weight ratio on the complex shear modulus. SD indicated, n = 3.*

The behavior below T_t confirms that the gel networks maintain contractile sensitivity to temperature changes. Raising the temperature from 4 to 37 °C, however, results in an increase in the elastic modulus with the salt/polymer weight ratio, thereby suggesting stiffer hydrogels at higher temperatures. Significant differences were found between samples with different salt/polymer ratios at both temperatures, except for those hydrogels with a high salt content (20/1). The thermal behavior of these hydrogels

confirmed the results obtained on porosity (**Fig. 9**) upon measuring the rheological properties.

The comparison with characterized cross-linked ELP hydrogels previously published in the literature allows to obtain a combined conclusion about their physical properties (Table 3).

Table 3. Review of Physical Properties of Different Chemically Cross-Linkable ELP Hydrogels

Cross-linker[a]	Q_w (H_2O)	Mechanical evaluation	Reference
HDI	3-36[b] 1.7-10[c]	G*=2.5-6.5 kPa	present study
HDI	0.37[b]	G= 0.13-0.31 MPa	25
TSAT	~2-3.5[b] ~0.2-0.6[c]	G*= 1.6-15 kPa	26
THPP	12.3[b] 3.7[c]	G*=5.8-45.8 kPa	4

[a]*Abbreviations: HDI, hexamethylene diisocyanate; TSAT, tris-succinimidyl aminotriacetate; THPP, tris(hydroxymethyl)phosphino-propionic acid.* [b]*Swelling temperature: 4ºC.* [c] *Swelling temperature: 37ºC.*

The swelling capacity of the ELP hydrogels fabricated in this study is considerable higher than other elastin-based hydrogels, because the addition of different salt amounts has substantial effect in the swelling behavior. The study of the dynamic shear modulus indicates that the type of cross-linker has an important effect, in addition to the cross-linking degree, which allows to tune the mechanical properties. The

reviewed literature confirms that there is not a study about the microstructure in hydrogels from ELPs.

Cell Viability and Morphology in Macroporous ELP Hydrogels.

HUVECs have been shown selective binding and retention in REDV-coated surfaces [51] or REDV-ELP-coated surfaces [22]. Cell culture assays were performed to assess the suitability of 3D REDV-containing scaffolds toward endothelial cells, in vitro. This last set of assays has two main goals. First, to test the biocompatibility of the scaffold in vitro and, second, that the open pore structure is suitable for cell infiltration. With the aim of promoting cell infiltration in the scaffold, the cells were seeded on lyophilized hydrogels to achieve quicker diffusion inside of matrices during the rehydration process. HUVECs viability and colonization of 3D ELP hydrogel were evaluated by microscopy. Due to the transparency of the hydrogels, we were able to visualize by fluorescence microscopy the HUVECs integration in the scaffolds. As shown in **Fig. 11** numerous cells can be observed both in surface and inner layers of hydrogels situated in different focal planes testing that the cells were present in almost the totality of the hydrogel.

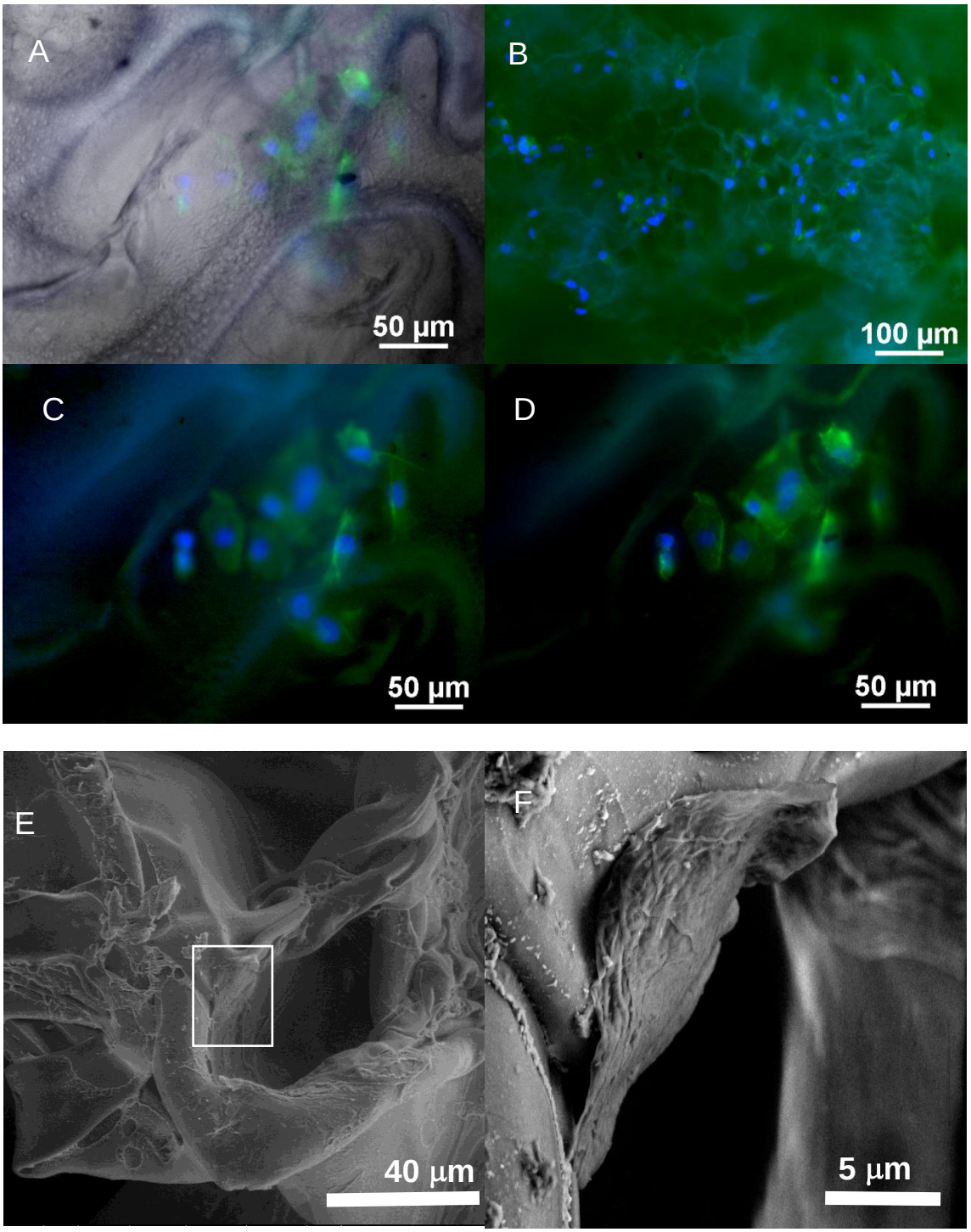

Fig. 11. *Microscopic captures and SEM micrographs of HUVECs seeded in macroporous ELP hydrogels after 48 h of incubation. Phase-contrast and fluorescence microscopy (A), fluorescence microscopy with Phalloidin Alexa Fluor488 and DAPI staining (B, C D). Cross-sectional SEM micrographs (E) and magnified view (F).*

This is specially evident in **Fig. 11C and D**, where the same spot in the sample has been photographed at different depths. The macroporous structure of ELP hydrogels seems to offer a suitable environment for HUVECs that showed a well-spread morphology with large extensions, and their cytoskeleton actin filaments (green stained) were well organized in stress fibers (**Fig. 11C and D**).

A cross-section of the cell-seeded ELP hydrogels was also analyzed by low vacuum SEM assays of cryo-fractured samples. **Fig. 11E, F** shows the presence of cells within the internal pores.

4. Conclusions

A simple method for obtaining macroporous ELP hydrogels is reported in this work. Pore size can be controlled by varying the size of the salt particles incorporated during the cross-linking reaction. The results of this study demonstrate that the salt-leaching/ gas-foaming technique can be used to synthesize chemically cross-linked highly porous ELP hydrogels with tunable physical properties. The use of gas-forming salts allows the formation of a highly interconnected porous structure, which is difficult to obtain in ELP hydrogels using more conventional salt-leaching techniques. The porosity, swelling ratio, and mechanical properties have been shown to depend on the salt/ polymer weight ratio and temperature. The thermal behaviour of these materials has also been tested with respect to pore size and internal morphology. In addition to the macroporous structures resulting from the salt particles, these ELP hydrogels have also been shown to exhibit microporosity, which is intrinsic of these biomimetic materials.

In addition, we have demonstrated the feasibility of these ELP hydrogels to promote HUVECs adhesion and infiltration inside the porous structure of those matrices. This technique is therefore a straightforward approach to obtain advanced scaffolds with tunable biological and physical properties necessary for 3D cell culture.

Bioactive, multifunctional ELP hydrogels have great potential for use as an artificial extracellular matrix in which the elasticity and thermoresponsive behavior of these materials could expand their range of potential applications.

Acknowledgments

We acknowledge financial support from the MICINN (Projects MAT 2007-66275-C02-01, NAN2004-08538, and PSE-300100-2006-1), the JCyL (Projects VA034A09, VA016B08, and VA030A08), the CIBER-BBN (Project CB06-01-0003), and the JCyL and the Instituto de Salud Carlos III under the "Network Center of Regenerative Medicine and Cellular Therapy of Castilla and León".

References

[1] Ma, P. X. Biomimetic materials for tissue engineering. *Adv. Drug Delivery Rev.* 2008, **60**, 184-198.

[2] Badylak, S. F.; Freytes, D. O.; Gilbert, T. W. Extracellular matrix as a biological scaffold material: Structure and function. *Acta Biomater.* 2009, **5**, 1-13.

[3] Rodríguez-Cabello, J. C.; Reguera, J.; Girotti, A.; Arias, F. J.; Alonso, M. Genetic engineering of protein-based polymers: The example of elastin-like polymers. *Adv. Polym. Sci.* 2006, **200**, 119-167.

[4] Lim, D. W.; Nettles, D. L.; Setton, L. A.; Chilkoti, A. In situ cross-linking of elastin-like polypeptide block copolymers for tissue repair. *Biomacromolecules* 2008, **9**, 222-230.

[5] Huang, J.; Wong, C.; George, A.; Kaplan, D. L. The effect of genetically engineered spider silk-dentin matrix protein 1 chimeric protein on hydroxyapatite nucleation. *Biomaterials* 2007, **28**, 2358-2367.

[6] Urry, D. W.; Pattanaik, A.; Xu, J.; Woods, T. C.; McPherson, D. T.; Parker, T. M. Elastic protein-based polymers in soft tissue augmentation and generation. *J. Biomater. Sci., Polym. Ed.* 1998, **9**, 1015-1048.

[7] Mithieux, S. M.; Rasko, J. E. J.; Weiss, A. S. Synthetic elastin hydrogels derived from massive elastic assemblies of self-organized human protein monomers. *Biomaterials* 2004, **25**, 4921-4927.

[8] Annabi, N.; Mithieux, S. M.; Weiss, A. S.; Dehghani, F. The fabrication of elastin-based hydrogels using high pressure CO_2. *Biomaterials* 2009, **30**, 1-7.

[9] Mould, A. P.; Wheldon, L. A.; Komoriya, A.; Wayner, E. A.; Yamada, K. M.; Humphries, M. J. Affinity chromatographic isolation of the melanoma adhesion receptor for the IIICS region of fibronectin and its identification as the integrin $\alpha_4\beta_1$. *J. Biol. Chem.* 1990, **265**, 4020-4024.

[10] Hubbell, J. A.; Massia, S. P.; Desai, N. P.; Drumheller, P. D. Endothelial cell-selective materials for tissue engineering in the vascular graft via a new receptor. *Nat. Biotechnol.*1991, **9**, 568-572.

[11] Girotti, A.; Reguera, J.; Rodríguez-Cabello, J. C.; Arias, F. J.; Alonso, M.; Testera, A. M. Design and bioproduction of a recombinant multi(bio)functional elastin-like protein polymer containing cell adhesion sequences for tissue engineering purposes. *J. Mater. Sci.: Mater. Med.* 2004, **15**, 479-484.

[12] Urry, D. W. *What sustains life? Consilient mechanisms for protein based machines and materials*; Springer-Verlag: New York, 2006.

[13] Kostal, J.; Mulchandani, A.; Chen, W. Tunable biopolymers for heavy metal removal. *Macromolecules* 2001, **34**, 2257-2261.

[14] Meyer, D. E.; Kong, G. A.; Dewhirst, M. W.; Zalutsky, M. R.; Chilkoti, A. Targeting a genetically engineered elastin-like polypeptide to solid tumors by local hyperthermia. *Cancer Res*. 2001, **61**, 1548-1554.

[15] Rodríguez-Cabello, J. C.; Alonso, M.; Guiscardo, L.; Reboto, V.; Girotti, A. Amplified photoresponse of a p-phenylazobenzene derivate of elastin-like polymer by α-cyclodextrin: The amplified Δt_t mechanism. *Adv. Mater*. 2002, **14**, 1151-1154.

[16] Huang, L.; McMillan, R. A.; Apkarian, R. P.; Pourdeyhimi, B.; Conticello, V. P.; Chaikof, E. L. Generation of synthetic elastin-mimetic small diameter fibers and fiber networks. *Macromolecules* 2000, **33**, 2989-2997.

[17] García, Y.; Hemantkumar, N.; Collighan, R.; Griffin, M.; Rodríguez- Cabello, J. C.; Pandit, A. In vitro characterization of a collagen scaffold enzymatically cross-linked with a tailored elastin-like polymer. *Tissue Eng., Part A* 2009, **15**, 887-899.

[18] Liu, J. C.; Tirrell, D. A. Cell response to RGD density in cross-linked artificial extracellular matrix protein films. *Biomacromolecules* 2008, **9**, 2984-2988.

[19] Nagapudi, K.; Brinkman, W. T.; Leisen, J. E.; Huang, L.; McMillan, R. A.; Apkarian, R. P.; Conticello, V. P.; Chaikof, E. L. Photomediated solid-state cross-linking of an elastin-mimetic recombinant protein polymer. *Macromolecules* 2002, **35**, 1730-1737.

[20] Lee, J.; Macosko, C. W.; Urry, D. W. Mechanical properties of cross-linked synthetic elastomeric polypentapeptides. *Macromolecules* 2001, **34**, 5968- 5974.

[21] Lee, J.; Macosko, C. W.; Urry, D. W. Swelling behavior of γ irradiation cross-linked elastomeric polypentapeptide-based hydrogels. *Macromolecules* 2001, **34**, 4114- 4123.

[22] Heilshorn, S. C.; DiZio, K. A.; Welsh, E. R.; Tirrell, D. A. Endothelial cell adhesion to the fibronectin CS5 domain in artificial extracellular matrix proteins.. *Biomaterials* 2003, **24**, 4245-4252.

[23] Lim, D. W.; Nettles, D. L.; Setton, L. A.; Chilkoti, A. Rapid cross-linking of elastin-like polypeptides with (hydroxymethyl)phosphines in aqueous solution. *Biomacromolecules* 2007, **8**, 1463-1470.

[24] Nowatzki, P. J.; Tirrell, D. A. Physical properties of artificial extracellular matrix protein films prepared by isocyanate crosslinking. *Biomaterials* 2004, **25**, 1261-1267.

[25] Di Zio, K.; Tirrell, D. A. Mechanical properties of artificial protein matrices engineered for control of cell and tissue behavior. *Macromolecules* 2003, **36**, 1553-1558.

[26] Trabbic-Carlson, K.; Setton, L. A.; Chilkoti, A. Swelling and mechanical behaviours of chemically cross-linked hydrogels of elastin-like polypeptides. *Biomacromolecules* 2003, **4**, 572-580.

[27] McHale, M. K.; Setton, L. A.; Chilkoti, A. Synthesis and in vitro evaluation of enzymatically cross-linked elastin-like polypeptide gels for cartilaginous tissue repair. *Tissue Eng.* 2005, **11**, 1768-1779.

[28] Chen, G. P.; Ushida, T.; Tateishi, T. Scaffold design for tissue engineering. *Macromol. Biosci*. 2002, **2**, 67-77.

[29] Weigel, T.; Schinkel, G.; Lendlein, A. Design and preparation of polymeric scaffolds for tissue engineering. *Expert Rev. Med. Dev.* 2006, **3**, 835-851.

[30] Mikos, A. G.; Thorsen, A. J.; Czerwonka, L. A.; Bao, Y.; Langer, R.; Winslow, D. N.; Vacanti, J. P. Preparation and characterization of poly(L-lactic acid) foams. *Polymer* 1994, **35**, 1068-1077.

[31] Barbanti, S. H.; Zavaglia, C. A. C.; Duek, E. A. D. Effect of salt leaching on PCL and PLGA(50/50) resorbable scaffolds. *Mater. Res.* 2008, **11**, 75-80.

[32] Sheridan, M. H.; Shea, L. D.; Peters, M. C.; Mooney, D. J. *Bioadsorbable polymer scaffolds for tissue engineering capable of sustained growth factor delivery.* 5th Symposium on Controlled Drug Delivery, Noordwijk Aan Zee, Netherlands, Apr 01-03, 1998, 91-102.

[33] Zhao, L.; He, C. G.; Gao, Y. J.; Cen, L.; Cui, L.; Cao, Y. L. Preparation and cytocompatibility of PLGA scaffolds with controllable fiber morphology and diameter using electrospinning method. *J. Biomed. Mater. Res.* 2008, **87B**, 26-34.

[34] Kim, T. G.; Chung, H. J.; Park, T. G. Macroporous and nanofibrous hyaluronic acid/collagen hybrid scaffold fabricated by concurrent electrospinning and deposition/leaching of salt particles. *Acta Biomater*. 2008, **4**, 1611-1619.

[35] Sultana, N.; Wang, M. Fabrication of HA/PHBV composite scaffolds through the emulsion freezing/freeze-drying process and characterisation of the scaffolds. *J. Mater. Sci.: Mater. Med.* 2008, **19**, 2555-2561.

[36] Kang, H. W.; Tabata, Y.; Ikada, Y. Fabrication of porous gelatin scaffolds for tissue engineering. *Biomaterials* 1999, **20**, 1339- 1344.

[37] Liu, C. Z.; Xia, Z. D.; Han, Z. W.; Hulley, P. A.; Triffitt, J. T.; Czernuszka, J. T. Novel 3D collagen scaffolds fabricated by indirect printing technique for tissue engineering. *J. Biomed. Mater. Res.* 2008, **85B**, 519-528.

[38] Lee, K. W.; Wang, S. F.; Lu, L. C.; Jabbari, E.; Currier, B. L.; Yaszemski, M. J. Fabrication and characterization of poly(propylene fumarate) scaffolds with controlled pore structures using 3-dimensional printing and injection molding, *Tissue Eng.* 2006, **12**, 2801-2811.

[39] Nam, Y. S.; Yoon, J. J.; Park, T. G. A novel fabrication method of macroporous biodegradable polymer scaffolds using gas foaming salt as a porogen additive. *J. Biomed. Mater. Res.* 2000, **53**, 1-7.

[40] Wachiralarpphaithoon, C.; Iwasaki, Y.; Akiyoshi, K. Enzyme-degradable phosphorylcholine porous hydrogels cross-linked with polyphosphoesters for cell matrices. *Biomaterials* 2007, **28**, 984-993.

[41] Nair, L. S.; Laurencin, C. T. Biodegradable polymers as biomaterials. *Prog. Polym. Sci.* 2007, **32**, 762-798.

[42] Tsioptsias, C.; Tsivintzelis, I.; Papadopoulou, L.; Pallayiotou, C. A novel method for producing tissue engineering scaffolds from chitin, chitin–hydroxyapatite, and cellulose. *Mater. Sci. Eng., C* 2009, **29**, 159-164.

[43] Roach, P.; Eglin, D.; Rohde, K.; Perry, C. C. Modern biomaterials: a review-bulk properties and implications of surface modifications. *J. Mater. Sci.: Mater. Med.* 2007, **18**, 1263-1277.

[44] Freyman, T. M.; Yannas, I. V.; Gibson, L. Cellular materials as porous scaffolds for tissue engineering. *J. Prog. Mater. Sci.* 2001, **46**, 273-282.

[45] Anseth, K. S.; Bowman, C. N.; BrannonPeppas, L. Mechanical properties of hydrogels and their experimental determination. *Biomaterials* 1996, **17**, 1647-1657.

[46] Meyvis, T. K. L.; Stubbe, B. G.; Van Steenbergen, M. J.; Hennink, W. E.; De Smedt, S. C.; Demeester, J. A comparison between the use of dynamic mechanical analysis and oscillatory shear rheometry for the characterisation of hydrogels. *Int. J. Pharm.* 2002, **244**, 163-168.

[47] Kavanagh, G. M.; Ross-Murphy, S. B. Rheological characterisation of polymer gels. *Prog. Polym. Sci.* 1998, **23**, 533-562.

[48] Rehfeldt, F.; Engler, A. J.; Eckhardt, A.; Ahmed, F.; Discher, D. E. Cell responses to the mechanochemical microenvironment–implications for regenerative medicine and drug delivery. *Adv. Drug Delivery Rev.* 2007, **59**, 1329-1339.

[49] Discher, D. E.; Janmey, P.; Wang, Y. L. Tissue cells feel and respond to the stiffness of their substrate. *Science* 2005, **310**, 1139-1143.

[50] Zeng, X. F.; Ruckenstein, E. Control of pore sizes in macroporous chitosan and chitin membranes. *Ind. Eng. Chem. Res.* 1996, **35**, 4169-4175.

[51] Plouffe, B. D.; Njoka, D. N.; Harris, J.; Liao, J.; Horick, N. K.; Radisic, M.; Murthy, S. K. Peptide-mediated selective adhesion of smooth muscle and endothelial cells in microfluidic shear flow. *Langmuir* 2007, **23**, 5050-5055

CHAPTER 4

Temperature-Triggered Self-Assembly of Elastin-Like Block Co-Recombinamers: the Controlled Formation of Micelles and Vesicles in an Aqueous Medium

The work presented in this chapter has been published in:

L. Martín [a]; E. Castro [b]; A. Ribeiro [a], M. Alonso [a], and J. C.Rodríguez-Cabello [a].

2012

Temperature-Triggered Self-Assembly of Elastin-Like Block Co-Recombinamers: the Controlled Formation of Micelles and Vesicles in an Aqueous Medium

Biomacromolecules, 13: 293-298.

Temperature-Triggered Self-Assembly of Elastin-Like Block Co-Recombinamers: the Controlled Formation of Micelles and Vesicles in an Aqueous Medium

Laura Martín [1], Emilio Castro [2], Artur Ribeiro [a], Matilde Alonso [1] and José Carlos Rodríguez-Cabello* [1]

[1] Bioforge group, University of Valladolid, CIBER-BBN, Paseo de Belén 11, 47011 Valladolid, Spain

[2] Grupo de Física de Coloides y Polímeros. University of Santiago de Compostela, 15782 Santiago de Compostela, Spain

Keywords: Amino acids, block copolymers, nanoparticles, self-assembly, elastin-like polymers.

*Correspondence to:

J. Carlos Rodríguez-Cabello

Tel: +34 983 184 686

E-mail: cabello@bioforge.uva.es

Abstract

The possibility of obtaining different self-assembled nano-structures in reversible systems based on elastin-like block co-recombinamers is explored in this work. The results obtained show how an evolution from a more common micellar structure to a hollow vesicle can be attained simply by changing the block arrangements and lengths, even when other molecular properties, such as molecular weight or mean polarity, remain essentially unchanged. This work sheds light on the possibility of obtaining hollow nano-objects, based on elastin-like recombinamers, which can assemble and disassemble in response to a change in their surroundings. This kind of system can be an example of how high precision in the genetic production of synthetic macro-molecules can be used, on an exclusive basis, to control the shape and size of their derived nano-objects.

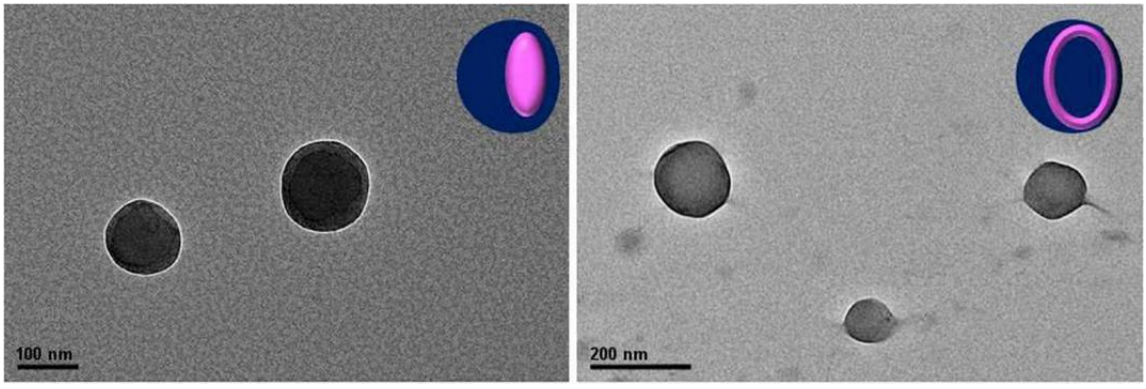

1. Introduction

The self-assembly of nano-objects with different shapes is a highly interesting topic due to its implications and significance in both basic and applied science. Generally speaking, the most versatile self-assembled nano-objects are obtained from macromolecules. However, although micelles are most easily obtained by way of many different molecular interactions, other more complex shapes often require the existence of precise molecular interactions that drive the self-assembled objects to adopt hollow vesicular or tubular structures [1-3]. Typically, such interactions are of the hydrogen-bonding or ion-pair type and give rise to strong and stable cores in which the molecular segments involved show characteristics such as crystallinity, swelling, directionality and rigidity, amongst others [4]. However, although such relatively strong interactions can be tuned to model the shape of the self-assembled object, they tend to lead to practically irreversible self-assembly.

Many of the applications envisaged for advanced nanocarriers, such as targeted and/or intracellular gene or drug delivery, require fast delivery of the cargo when the carrier reaches its target. In most cases, this action requires the disruption of the nano-object [5, 6], thus meaning that smart behavior of the macromolecule is an excellent option to create nanocarriers that can load and deliver their cargo in response to a change in their surroundings. In aqueous environments, for example, the most efficient smart macromolecules follow lower critical solution temperature (LCST) behavior [7, 8], thus implying that the main intermolecular interactions are weak hydrophobic interactions, which are more prone to be reversible. Many different materials based in stimuli-responsive polymers with different molecular architectures have been reported as the basis of self-assembled nano-objects [9-19]. However, in almost all previous

cases, the self-assembly driven by LCST behavior leads to the formation of micelles. Other shapes, such as hollow vesicles, can simultaneously incorporate functionality at their surface, which makes them excellent candidates as more versatile delivery vehicles for combinatorial drug therapies [20-23].

The main target of this work is to explore the feasibility of tuning and controlling the shape and topology of self-assembled nano-objects in recombinant LCST-based macromolecules, avoiding the use of rigid segments with stronger interaction that could hamper the reversibility of the self-aggregation. The materials chosen to test this concept are elastin-like recombinamers (ELRs). The expansion of molecular biology has allowed the design of complex bioengineered ELRs as well-defined polymers [24-26]. Different ELR derivatives have been reported being sensitive to stimulus such as temperature, pH, light and other in aqueous solution. They can also easily include diverse functionalities such as targeting ligands, cell-adhesion sequences and fluorescent or contrast agents, amongst others, which, together with their good expected biocompatibility and favorable degradation rate and products, make them promising materials for (bio)nanotechnological applications [27-29]. All functional ELRs exhibit a reversible phase transition in response to changes in temperature. In aqueous solution and below a certain transition temperature (T_t), the free ELR chains are disordered, consisting in fully hydrated random coils, mainly by hydrophobic hydration. This kind of hydration is characterized by ordered clathrate-like water structures surrounding the apolar moieties of the polymer. When the temperature is increased above T_t, the structure loses the water molecules to form a phase-separated state consisting of 63% water and 37% polymer by weight and the chains fold and assemble in a dynamic, regular, nonrandom structure known as a β-spiral. This structure contains type II β-turns

as the main secondary feature, which is formed by intrachain hydrogen bonding around the *L*-proline residue, and is stabilized by interturn. In this arrangement, the apolar side chains of the constituting amino acids point to the outer shell of the β-spiral, facilitating the existence of extensive intramolecular hydrophobic contacts and, finally, phase segregation. This folding is completely reversible if the temperature of the sample decreases again below T_t [24].

Recently, recombinant DNA techniques have enabled the formation of block copolymers with programmed sequences from simple amino acid building blocks with an absolute degree of control and complexity clearly superior to that achieved by synthetic copolymers [30]. Amphiphilic elastin-like block co-recombinamers (ELbcRs) may also boost the formation of stable self-assembled nanoparticles as protein-like micellar systems [9-12]. However, other nano-objects have not been explored, which opens up the possibility of using molecular weight and molecular design, in a high precision approach, as a way of tuning the shape of self-assembled nano-objects using the acquired knowledge from synthetic block copolymers. For these reasons, the working hypothesis is the possibility of tuning the self-assembled morphology simply by varying the block arrangements and lengths in the ELbcRs. Therefore, in the reductionist approach used in this work, the designed ELbcRs show a relatively simple composition in order to isolate the aforementioned factors.

2. Experimental Section

Materials. All reagents were purchased from commercial supplies and used as received. Standard molecular biology techniques were used to construct the ELbcRs genes. The production was carried out using cellular systems for genetically engineered protein biosynthesis in *Escherichia coli* and the purification was performed with several cycles of temperature-dependant reversible precipitation. The purity and molecular

weight of the recombinamers were verified by sodium dodecyl sufate-polyacrylamide gel electrophoresis (SDS-PAGE) and mass spectrometry (MALDI-TOF/ MS). Detailed procedures are also found in the Supporting Information.

Sample Preparation. Aqueous solutions of amphiphilic ELbcRs were prepared from lyophilized purified specimens dissolved at the appropriate concentration in Millipore ultrapure water at room temperature and filtered using a 0.45 μm PVDF syringe filter. A neutral pH was achieved by adding small amounts of HCl or NaOH. Mineral oil was added to the top of solution cells to prevent evaporation in turbidity and light scattering measurements.

Turbidity and Isothermal Titration Calorimetry (ITC). Turbidity experiments were conducted using a Varian Cary 50 UV-Vis spectrophotometer (Varian, Cary, NC) with a thermostated sample chamber. Optical density (OD) was assessed by the change in absorbance at 350 nm of a stabilized 25 μM ELbcR solution as a function of temperature in the range 30.0 to 80.0 °C (ramp 2.0 °C/ min). Samples were stabilized at each given temperature until a constant turbidity value was reached, which was considered the optical density for the sample at that temperature.

Microcalorimetry was performed using a VP-ITC microcalorimeter (Microcal, Northampton, MA). We injected 5 or 10 μL aliquots of degassed solutions of ELbcRs from a Hamilton syringe into a sample cell containing water at 65 °C, with stirring at 200 rpm. The heat flow associated with the process was measured at each titrant concentration and the data were analyzed with the Origin software provided by Microcal to determine the critical aggregation concentration (CAC).

Dynamic (DLS) and Static (SLS) Light Scattering. The refractive index value (n_D) was studied experimentally for the three ELbcRs in a wide range of concentrations

((0.02-3.40) × 10^{-3} g/ mL) and temperatures (20.00- 50.00 °C) using a digital refractometer (Mettler Toledo RE50, Mettler-Toledo, Greifensee, Switzerland) with a Peltier thermostat. The value of the specific refractive index increment (d*n*/dc) was deduced from the slope of plots of the refractive index versus concentration for each ELbcR at the four different temperatures studied.

Light scattering measurements were performed using a BI-200SM multiangle goniometer (Brookhaven Instrument, Holtsville, NY) with a 33-mW He-Ne vertically polarized laser at a wavelength of 632.8 nm and a digital correlator (BI-9000AT).

For the DLS measurements monitored at a scattering angle of 90°, recombinamer solutions at a concentration of 25 µM were introduced into glass cells and stabilized for 10 min at the desired temperature (30-80 °C) in a thermostated decalin bath to compare the thermally driven aggregation with turbidity experiments. DLS autocorrelation functions (measured at 65 °C) were also used to calculate the size distribution and polydispersity index.

SLS measurements were performed using filtered ELbcR solutions equilibrated at 65 °C at concentrations from 1.0 to 5.0 mg/ mL and for scattering angles between 50° and 130°. The resulting data were fit and used to determine the gyration radius (R_g) and molecular weight of the aggregates ($M_{w,\ agg}$).

Transmission Electron Microscopy (TEM) and Atomic Force Microscopy (AFM). TEM measurements were conducted on a JEOL JEM-1230 electron microscope operating at 120 kV. The specimens were prepared by placing a drop of the stabilized heated solution (25 µM) at 65 °C on a preheated plasma-treated carbon-coated copper grid followed by water evaporation at the same temperature. Further samples were stained with uranyl acetate solution (1.0 wt %) to enhance the contrast of the

nanoparticles. Samples were also prepared by a freeze-fracture process and observed with a JEM-FS2200 HRP working at 200 keV.

All samples for AFM were prepared on mica following the same procedure as used for TEM samples without staining. AFM was performed in air at 25 °C using a MultiMode 8 AFM attached to a Nanoscope V electronics (Veeco Instruments, Santa Barbara, CA) in tapping-mode. Both topography and phase signals images were recorded with 512 × 512 data points.

3. Results and Discussion

Three ELbcRs (E50A40, E100A40 and E50A40E50), which undergo thermal and pH-responsiveness were used [31]. Translation of the genes in *E. coli* expression strains yields monodisperse ELbcRs of totally controlled composition (see **Fig. S1** of the Supporting Information). These compounds are formed by combination of two different blocks; a *L*-glutamic acid-containing block (E–block) and a fixed size of the block that contains the *L*-alanine residue (A–block). The E block is based on the monomer $[(VPGVG)_2\text{-}(VPGEG)\text{-}(VPGVG)_2]$, whereas the A block is based on [VPAVG]. The notation used to name the different blocks includes the letter (E or A) and a number to indicate the amount of pentamers in the block, which is directly related to their length. In general, the blocks that form part of the different corecombinamers structures were found to be in the soluble-extended state when cooled below their transition temperature (T_t), and in a collapsed-aggregated state above T_t. In addition, even though the E-block did not show an LCST behavior at pH values above the pK_a, of the γ-carboxyl group of the glutamic acid, the T_t associated with the A-block was modified by the presence and arrangement of the E-block [31].

The solution behavior of these thermally driven amphiphilic ELbcRs was investigated in water at neutral pH, where they were found to undergo selective segregation by hydrophobic interactions. Turbidity and dynamic light scattering (DLS) measurements were performed as a function of the temperature of aqueous 25 μM ELbcR solutions in order to investigate the aggregation temperature and the stability of the aggregates (see **Fig. 1**).

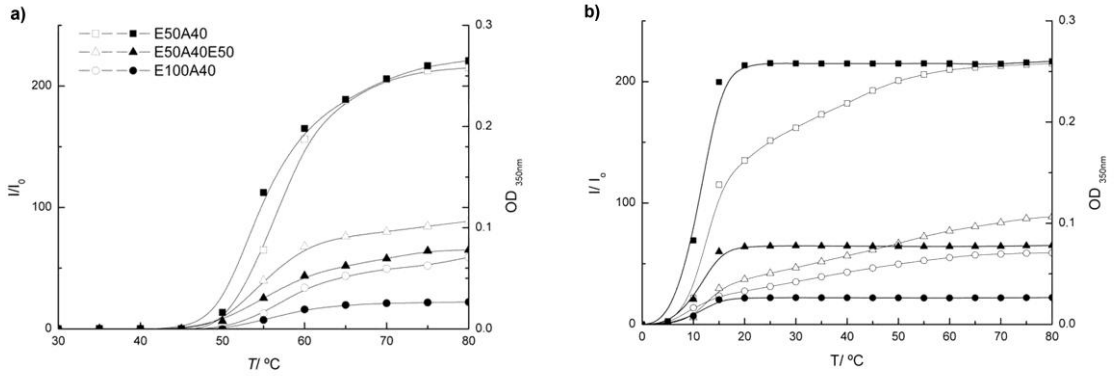

Fig. 1. *Plots of normalized scattered light intensity (open symbols) and turbidity (filled symbols) versus temperature. (a) Heating and (b) Cooling.*

The thermally driven aggregation (see **Fig. 1a**), as monitored by DLS, showed that aggregates were formed at temperatures above 50 ºC, with a significant increase in the scattered light intensity due to the conformational change and self-organization of the ELbcRs. The normalized scattered light intensity (I/I_0) showed an aggregation temperature in agreement with turbidity results. We therefore selected 65 ºC as the working temperature to compare the three ELbcRs in subsequent experiments, since their intensity was not dependent on heating. Furthermore, the ELbcRs were found to display two different particle aggregation behaviors, with E50A40 exhibiting a higher scattering intensity, thus suggesting the formation of different, or more, aggregates. The known special self-assembling characteristics of the A-block [32, 33], which, as a

particularity among others ELRs, were tested in cooling experiments. (See **Fig. 1b.**) The reverse dissolution of the aggregates took place only after the temperature was undercooled down to 15 ºC. This degree of large undercooling has been found to be strongly dominated by kinetics, and the acute hysteresis behavior seems to govern the hydration process [32].

The autocorrelation functions obtained from DLS at a scattering angle of 90º (**Fig. S3** of the Supporting Information) were analyzed using the CONTIN algorithm [34]. The results of this analysis (**Fig. 2**) showed the size distributions for each system and a set of hydrodynamic diameters, D_h, of approximately 140, 205 and 215 nm, respectively, for E50A40, E100A40 and E50A40E50. E50A40 therefore forms smaller nanoparticles than the others, which is in agreement with the decreasing in molecular weight.

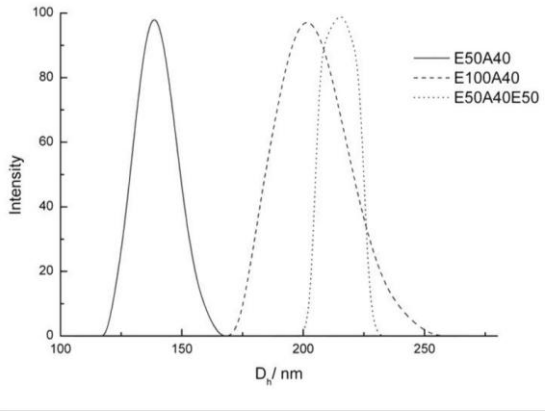

Fig. 2. *Size distributions, as measured by DLS at 65 ºC.*

The D_h values obtained are higher than those of other reported ELbcRs with similar molecular weights but different composition, thus indicating that their nanoscale features can be modulated by the amino acid composition, and particularly for the presence of *L*-alanine residues in the ELbcRs [9-11]. For the nanoaggregates obtained here, an increase in temperature did not affect their size distribution (**Fig. S4** of the

Supporting Information). The stability of the formed aggregates was tested after 3 weeks of storage at 65 ºC showing no changes in their geometrical parameters (result not shown). Polydispersities were determined to be 0.05, 0.06 and 0.04, respectively, for E50A40, E100A40 and E50A40E50.

Isothermal titration calorimetry (ITC) was used to determine the CAC of the ELbcRs. The CACs calculated at 65ºC were ~ 3 µM for E50A40E50, and 5 µM for E50A40 and E100A40, which is consistent with results reported for other amphiphilic copolymers [19, 11]. To characterize these aggregates further, we performed static light scattering (SLS) measurements at 65°C over a concentration range of 1.0- 5.0 mg /mL (where D_h remains almost constant) and for scattering angles of between 50 and 130°. The specific refractive index increment, d*n*/dc, of the three ELbcR solutions showed a minimal dependence on temperature and molecular weight (Table S1 and **Fig. S2** of the Supporting Information). In light of this, we used a dn/dc value of 0.170 mL /g for all three ELbcRs. Since a conventional Zimm plot showed a curvature of the angular dependence in our self-assembled nanoparticles, a Berry plot was deemed more pertinent (**Fig. S5** of the Supporting Information) for determination of the gyration radius (R_g) and the molecular weight of the aggregates ($M_{w,\ agg}$) [35-38]. The aggregation numbers (N_{agg}) of the nanoparticles (i.e., number of ELbcR chains per nanoparticle) were calculated by dividing $M_{w,agg}$ by the corecombinamer's M_w, and the structure of the self-assembled nanoparticles was further characterized by combining the DLS and SLS data to calculate the ρ ratio ($\rho = R_g / R_h$), where R_h is the hydrodynamic radius. A summary of the properties of the ELbcR self-assembled nanoparticles, including R_h, R_g, $M_{w,agg}$, ρ ratio and N_{agg}, is provided in Table 1.

Table 1. Summary of ELbcR nanoparticles' properties.

ELbcRs	$R_h=D_h/2$ (nm)	R_g (nm)	$\rho=R_g/R_h$	$M_{w,agg}$ (10^7g/ mol)	N_{agg}
E50A40	74 (± 1)	58(±2)	0.78	1.2	312
E100A40	100 (± 3)	83(±3)	0.83	2.0	337
E50A40E50	96 (± 2)	87(±2)	0.91	1.1	185

R_g can be seen to range between 58 and 87 nm, and $M_{w,agg}$ between (1.1 and 2.0) × 10^7 g /mol. ρ is a structure-sensitive parameter that provides information regarding the density distribution of the particles and thereby on particle morphology [39]. Thus, ρ values close to 1.0 are attributed to a vesicle-type morphology, whereas smaller values are generally encountered with spherical micelles (theoretically ρ= 0.77) [39]. The ρ values in Table 1 therefore apparently suggest the self-assembled nanoparticles to be relatively monodisperse spherical micelles for E50A40, whereas E100A40 and E50A40E50 self-assemble into a mixture of micelles and vesicles, with the formation of vesicles being majority in the triblock ELbcR. It is also noticeable that the micelle diameter is higher than the one found in other more conventional polymer diblocks of similar M_w. This is likely due to the fact that the folded structure of the ELRs still contains a substantial amount of water (~ 50%) [24]. Relatively few amphiphilic ELbcRs have been synthesized and the size comparison with reported micelles [9, 11] of similar M_w is not so straightforward because the particular composition in the hydrophobic block, as mentioned above, leads to a more stable folding state [32] and the hydrophilic block, which is negatively charged at neutral pH and remains hydrated and molecularly mobile, does not exhibit a transition in the examined temperature range, persisting as a random coil above the T_t of the hydrophobic block [11] (**Fig. S7** of the Supporting Information). In addition, E50A40E50 displayed similar nanoparticle

size but differs of reported ELbcRs triblocks [12], which contained similar both central hydrophilic block and two hydrophobic end blocks, in having lower M_w and different secondary structure, demonstrating that block orientation plays a significant role in the morphology of the nanoparticles in ELbcRs, specially for protein-based copolymers [30]. The N_{agg} of ELbcRs nanoparticles has not been thoroughly reported in the literature, even vesicles. Kim et al. [11] suggested that at high density of glutamic acid units, charge repulsion would limit the association of the hydrophilic blocks decreasing the ELbcR chains per vesicle and this effect would be more pronounced in the triblock.

These arguments were further supported by TEM (**Fig. 3**). Samples observed without staining (**Fig. 3, top**) revealed nano-objects with spherical shape and confirmed the data provided by DLS experiments regarding the nanoparticle size. Image analysis of the stained samples (**Fig. 3, middle**) clearly showed characteristic core-shell micelles for E50A40, with dark cores and gray-colored shells. However, the stained TEM images corresponding to E100A40 and E50A40E50 are completely different. TEM observations for those two show exclusively nano-objects with morphology of conventional vesicles (**Fig. S9** of the Supporting Information). Therefore, although the ρ values found in light scattering experiments were not too conclusive, especially for E100A40, TEM images indicate the absence of micelle structures. In addition, for a polymeric vesicle or a hollow sphere, ρ may be less or larger than 1.0, depending on the thickness and density of the wall [40] and we speculate that the structure of the nanoparticles becomes more compact than for the triblock, affecting in this way the ρ value by making it not too directly comparable to the one found in other vesicles formed from block copolymers of different chemical nature. Vesicle formation was also corroborated by the collapse of these structures following exposure to the high vacuum of TEM (**Fig. 3e**), whereas the micelles found for E50A40 preserved a more compact

structure. The remnants of these freeze-fractured samples were further analyzed by TEM to support these arguments (**Fig. 3, bottom**).

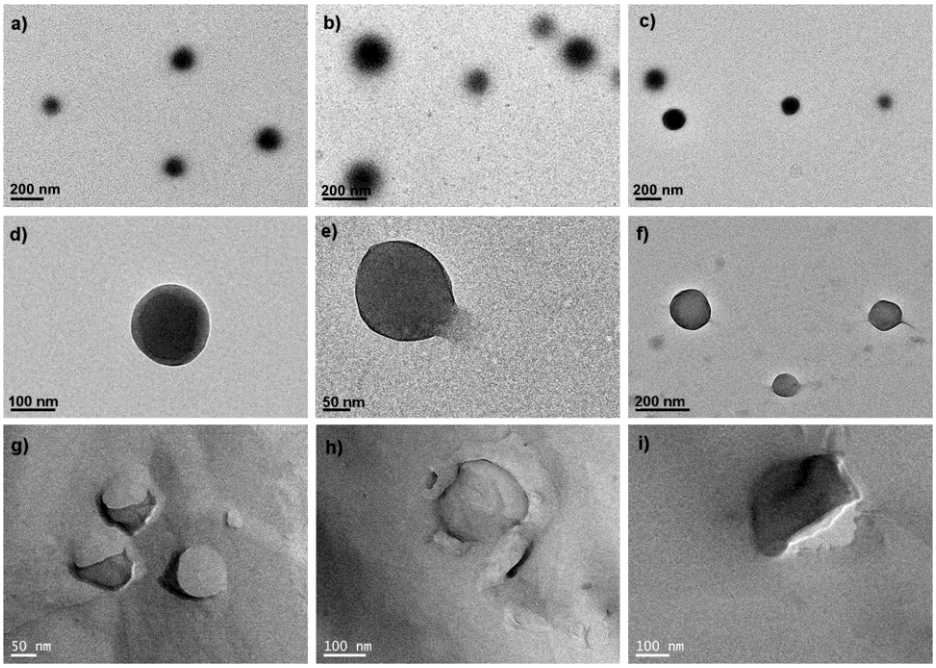

Fig. 3. *TEM images of self-assembled nanoparticles without staining (top), stained (middle) with 1% uranyl acetate and freeze-fractured (bottom): a, d, g) E50A40; b, e, h) E100A40; and c, f, i) E50A40E50.*

A schematic representation of the thermally driven self-assembled structures obtained in water is represented in **Fig. 4**.

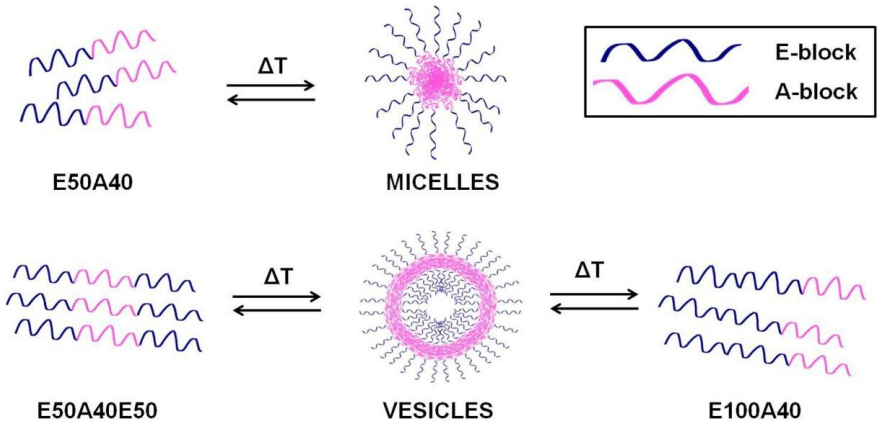

Fig. 4. *Schematic representation of micelles and vesicles obtained from the self-assembly of the ELbcRs in water.*

In light of these results, AFM was used to observe further those different morphologies (see **Fig. 5**). A similar effect as in the TEM images was observed, probably as a result of the force induced by the AFM probe resulting in deformation of the vesicles. Additionally, the 3D representations of the AFM study clearly show a plateau in the nanostructures corresponding to E50A40E50 (**Fig. 5f**), while a pointed shape is observed for the representative E50A40 structure, giving additional support to the identification of hollow vesicles in the case of E50A40E50, and micelles for E50A40.

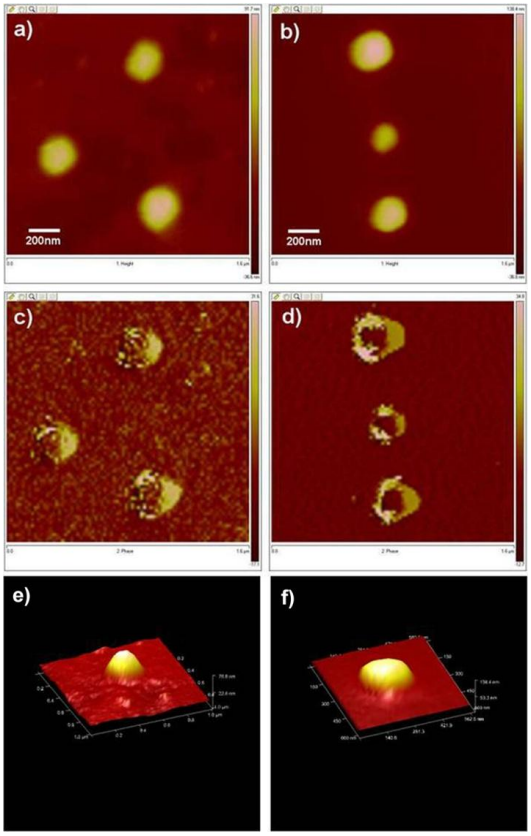

Fig. 5. *Tapping-mode AFM height (top), phase (middle) and 3D images (bottom) of self-assembled nanoparticles deposited on mica surfaces: (a, c, e) E50A40; and (b, d, f) E50A40E50.*

4. Conclusions

It can be concluded that the ability of these ELbcRs to self-assemble into micelles or vesicles upon varying their architecture could be used to construct a new type of drug- and gene-delivery systems. The ability of some of the recombinamers studied to form vesicles is noteworthy as this structure is much more elusive than that of a micelle. This work also highlights the possibility of forming hollow vesicles in a molecular system in which the intermolecular interactions are weak hydrophobic contacts, with no assistance from stronger and conditioning domains of rigid segments interacting by, for example, hydrogen bonding. Further studies are needed to get a better insight, especially on the theory relating each structure to its corresponding aggregate morphology.

Finally, an appropriate balance of the amino acid composition will allow the aggregation temperature to be tuned in order to adapt the stimuli-responsive behavior of such systems to the operating conditions of the desired applications.

Acknowledgment

This work was supported by the ERDF from the EU, from the MICINN (MAT 2009 14195-C03 03, ACI2009-0890, MAT2010-15310 and MAT2010-15982), the JCyL (VA034A09 and VA030A08) and CIBER-BBN. E.C. acknowledges the Angeles Alvariño (Xunta de Galicia, Spain, and FSE, EU) program.

Supporting Information

Details about the gene construction, bioproduction, MALDI-TOF spectra, light scattering, circular dichroism, TEM and ITC.

References

[1] Li, Y.; Lokitz, B. S.; McCormick, C. L. Thermally responsive vesicles and their structural "locking" through polyelectrolyte complex formation. *Angew. Chem. Int. Ed.* 2006, **45**, 5792-5795.

[2] Zhang, S. G. Fabrication of novel biomaterials through molecular self-assembly. *Nat. Biotechnol.* 2003, **21**, 1171-1178.

[3] Discher, B. M.; Won, Y. Y.; Ege, D. S.; Lee, J. C. M.; Bates, F. S.; Discher, D. E.; Hammer D. A. Polymersomes: tough vesicles made from diblock copolymers. *Science*, 1999, **284**, 1143-1146.

[4] Discher, D. E.; Ahmed. F. Polymersomes. *Annu. Rev. Biomed. Eng.* 2006, **8**, 323-341.

[5] Kataoka, K.; Harada, A.; Nagasaki, Y. Block copolymer micelles for drug delivery: design, characterization and biological significance. *Adv. Drug Deliv. Rev.* 2001, **47**, 113-131.

[6] Soussan, E.; Cassel, S.; Blanzat, M.; Rico-Lattes, I. Drug delivery by soft matter: matrix and vesicular carriers. *Angew. Chem. Int. Ed.* 2009, **48**, 274-288.

[7] Akimoto, J.; Nakayama, M.; Sakai, K.; Okano, T. Temperature-induced intracellular uptake of thermoresponsive polymeric micelles. *Biomacromolecules,* 2009, **10**, 1331-1336.

[8] Chilkoti, A.; Dreher, M. R.; Meyer, D. E.; Raucher, D. Targeted drug delivery by heat sensitive polymers. *Adv. Drug Deliv. Rev.* 2002, **54**, 613-630.

[9] Dreher, M. R.; Simnick, A. J.; Fischer, K.; Smith, R. J.; Patel, A.; Schmidt, M.; Chilkoti, A. Temperature triggered self-assembly of polypeptides into multivalent spherical micelles. *J. Am. Chem. Soc.* 2008, **130**, 687-694.

[10] MacKay, J. A.; Chen, M. N.; McDaniel, J. R.; Liu, W. G.; Simnick, A. J.; Chilkoti, A. Self-assembling chimeric polypeptide–doxorubicin conjugate nanoparticles that abolish tumours after a single injection. *Nat. Mater.* 2009, **8**, 993-999.

[11] Kim, W.; Thevenot, J.; Ibarboure, E.; Lecommandoux, S.; Chaikof, E. L. *Angew. Chem. Int. Ed.* 2010, **49**, 4257-4260.

[12] Sallach, R. E.; Wei, M.; Biswas, N.; Conticello, V. P.; Lecommandoux, S.; Dluhy, R. A.; Chaikof, E. L. Self-assembly of thermally responsive amphiphilic diblock copolypeptides into spherical micellar nanoparticles. *J. Am. Chem. Soc.* 2006, **128**, 12014-12019.

[13] York, A. W.; Kirkland, S. E.; McCormick, C. L. Advances in the synthesis of amphiphilic block copolymers via RAFT polymerization: Stimuli-responsive drug and gene delivery. *Adv. Drug. Deliv.Rev*. 2008, **60**, 1018-1036.

[14] Sundararaman A.; Stephan T.; Grubbs, R. B. Reversible restructuring of aqueous block copolymer assemblies through stimulus-induced changes in amphiphilicity. *J. Am. Chem. Soc.* 2008, **130**, 12264-12265.

[15] Du, J.; O'Reilly, R. K. Advances and challenges in smart and functional polymer vesicles. *Soft Matter*, 2009, **5**, 3544-3561

[16] Wan S.; Jiang, M.; Zhang, G. Dual temperature- and pH-dependent self-assembly of cellulose-based copolymer with a pair of complementary grafts. *Macromolecules*, 2007, **40**, 5552-5558.

[17] Jiang, X.; Luo, S.; Armes, S. P.; Shi, W.; Liu, S. UV irradiation-induced shell cross-linked micelles with pH-responsive cores using ABC triblock copolymers. *Macromolecules*, 2006, **39**, 5987-5994.

[18] Betthausen, E.; Drechsler, M.; Förtsch, M.; Schacher, F. H.; Müller, A. H. E. Dual stimuli-responsive multicompartment micelles from triblock terpolymers with tunable hydrophilicity. *Soft Matter*, 2011, **7**, 8880-8891.

[19] Ku, T. H.; Chien, M. P.; Thompson, M. P.; Sinkovits, R.S.; Olson, N. H.; Baker, T. S.; Gianneschi, N. C. Controlling and switching the morphology of micellar nanoparticles with enzymes. *J. Am. Chem. Soc.* 2011, **133**, 8392-8395.

[20] Pangu, G. D.; Davis, K. P.; Bates, F. S.; Hammer. D. A. Ultrasonically induced release from nanosized polymer vesicles. *Macromol. Biosci.* 2010, **10**, 546-554.

[21] Won, Y. Y.; Brannan, A. K.; Davis, H. T.; Bates. F. S. Cryogenic transmission electron microscopy (Cryo-TEM) of micelles and vesicles formed in water by

poly(ethylene oxide)-based block copolymers. *J. Phys. Chem. B.* 2002, **106**, 3354-3364.

[22] Christian, D.A.; Cai, S.; Bowen, D.M.; Kim, Y.; Pajerowski, J.D.; Discher, D.E. Polymersome carriers: From self-assembly to siRNA and protein therapeutics. *Eur. J. Pharm. Biopharm.* 2009, **71**, 463-474.

[23] Disher, D.E.; Ortiz, V.; Srinivas, G.; Klein, M.L.; Kim, Y.; Christian, D.; Cai, S.; Photos P.; Ahmed, F. Emerging applications of polymersomes in delivery: from molecular dynamics to shrinkage of tumors. *Prog. Polym. Sci.* 2007, **32**, 838-857.

[24] Urry, D. W. *What sustains life? Consilient mechanisms for protein-based machines and materials*, Springer-Verlag, New York, 2006.

[25] Rodríguez-Cabello, J. C.; Martín, L.; Girotti, A.; García-Arévalo, C.; Arias, F. J.; Alonso, M. Emerging applications of multifunctional elastin-like recombinamers. *Nanomedicine*, 2011, **6**, 111-122.

[26] Maskarinec, S. A.; Tirrell, D. A. Protein engineering approaches to biomaterials design. *Curr. Opin. Biotechnol*.2005, **16**, 422-426.

[27] Martín, L.; Alonso, M.; Girotti, A.; Arias, F. J.; Rodríguez-Cabello, J. C. Synthesis and characterization of macroporous thermo sensitive hydrogels from recombinant elastin-like polymers. *Biomacromolecules*, 2009, **10**, 3015-3022.

[28] Rodríguez-Cabello, J. C.; Alonso, M.; Guiscardo, L.; Reboto, V.; Girotti, A. Amplified photoresponse of a p-phenylazobenzene derivate of elastin-like polymer by α-cyclodextrin: The amplified ΔT_t mechanism. *Adv. Mater.* 2002, **14**, 1151-1154.

[29] Prieto, S.; Shkilnyy, A.; Rumplasch, C.; Ribeiro, A.; Arias, F. J.; Rodríguez-Cabello, J. C.; Taubert, A. Biomimetic calcium phosphate mineralization with

multifunctional elastin-like recombinamers. *Biomacromolecules*, 2011, **12**, 1480-1486.

[30] Rabotyagova, O. S.; Cebe, P.; Kaplan, D. L. Protein based block copolymers. *Biomacromolecules*, 2011, **12**, 269-289.

[31] Ribeiro, A.; Arias, F. J.; Reguera, J.; Alonso, M.; Rodríguez-Cabello, J. C. Influence of the amino-acid sequence on the inverse temperature transition of elastin-like polymers. *Biophys. J.* 2009, **97**, 312-320.

[32] Reguera, J.; Lagarón, J. M.; Alonso, M.; Reboto, V.; Calvo, B.; Rodríguez-Cabello, J.C. thermal behavior and kinetic analysis of the chain unfolding and refolding and of the concomitant nonpolar solvation and desolvation of two elastin-like polymers. *Macromolecules*, 2003, **36**, 8470-8476.

[33] Herrero-Vanrell, R.; Rincón, A. C.; Alonso, M.; Reboto, V.; Molina-Martínez, I. T.; Rodríguez-Cabello, J. C. Self-assembled particles of an elastin-like polymer as vehicles for controlled drug release. *J. Control. Release*, 2005, **102**, 113-122.

[34] Stepanek, P.; Lodge, T. P. *Light Scattering: Principles and Development*, W. Brown, Ed. Oxford University Press, New York, 1995.

[35] D'Souza, A. J. M.; Hart, D. S.; Middaugh, C. R.; Gehrke, S. H. Characterization of the changes in secondary structure and architecture of elastin-mimetic triblock polypeptides during thermal gelation. *Macromolecules*, 2006, **39**, 7084-7091.

[36] Sanson, C.; Schazt, C.; Le Meins J-F.; Brulet, A.; Soum, A.; Lecommandeux, S. Biocompatible and biodegradable poly(trimethylene carbonate)-b-poly (l-glutamic acid) polymersomes: size control and stability. *Langmuir*, 2010, **26**, 2751-2760.

[37] Iatrou, H.; Frielinghaus, H.; Hanski, S.; Ferderigos, N.; Ruokolainen, J.; Ikkala, O.; Richter, D.; Mays, J.; Hadjichristidis. N. Architecturally induced

multiresponsive vesicles from well-defined polypeptides. Formation of gene vehicles. *Biomacromolecules,* 2007, **8**, 2173-2181.

[38] Nardin, C.; Hirt, T.; Leukel J.; Meier, W. ABA triblock copolymer vesicles. *Langmuir,* 2000, **16**, 1035-1041.

[39] Burchard, W. Static and dynamic light scattering from branched polymers and biopolymers. *Adv. Polym. Sci.* 1983, **48**, 1-124.

[40] Li, J.; Ping, Y. Self-assembly of ibuprofen and bovine serum albumin-dextran conjugates leading to effective loading of the drug. *Langmuir,* 2009, **25**, 6385-6391.

Supporting Information

Temperature-Triggered Self-Assembly of Elastin-Like Block Co-Recombinamers: the Controlled Formation of Micelles and Vesicles in an Aqueous Medium.

Experimental details

Materials. *Escherichia coli* strain XL1-Blue and *Taq* DNA polymerase were obtained from Stratagene (La Jolla, CA). *E. coli* strain BLR (DE3) and pET-25(+) were obtained from Novagen (Madison, WI). T4 DNA ligase and all restriction enzymes were obtained from Fermentas (Burlington, Ontario, Canada). Synthetic oligonucleotides were purchased from IBA GmbH (Goettingen, Germany). Aqueous solutions of amphiphilic elastin-like block co-recombinamers (ELbcRs) E50A40, E100A40 and E50A40E50 were prepared from lyophilized specimens of the purified polymers dissolved at the appropriate concentration in Millipore ultrapure water at room temperature. A neutral pH was achieved by adding small amounts of HCl or NaOH. Mineral oil was added to the top of solution cells to prevent evaporation in turbidity and light scattering measurements.

Synthetic Gene Construction and Bioproduction. Standard molecular biology techniques were used to construct the genes, and their sequences were verified by automated DNA sequencing. Polymer production was carried out using cellular systems for genetic-engineering protein biosynthesis in E. coli. Expression conditions and purification protocols were as described previously [1]. Production yields for all polymers were around 150 $mg \cdot L^{-1}$ of bacterial culture. The final products were characterized by sodium dodecyl sulfate polyacrylamide gel electrophoresis (SDS-PAGE), amino-acid analysis and matrix-assisted laser desorption/ionization-time of flight (MALDI-TOF) mass spectrometry. High-mass MALDI-TOF MS analyses (**Fig. S1**) were performed using an Applied Biosystems Voyager STR mass spectrometer (Bruker, Bremen, Germany) at the CRG/UPF proteomics unit (Barcelona, Spain). The theoretical and experimental molecular weights (M_w) are listed in Table S1.

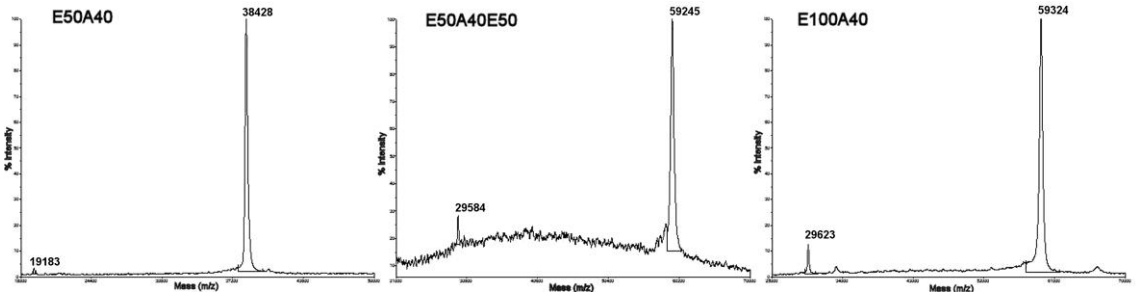

Fig. S1. *MALDI-TOF mass spectra of purified E50A40, E100A40 and E50A40E50.*

Table S1. Theoretical and experimental molecular weights (M_w) for the amphiphilic ELbcRs:

ELbcRs	Theoretical M_w (g/mol)	Experimental M_w (g/mol)
E50A40	38513	38428
E100A40	59290	59324
E50A40E50	59288	59245

Determination of the Refractive Index *(n_D)* and the Specific Refractive Index Increment *(*d*n*/dc). Measurements of the refractive index value (n_D) at 589.3 nm (Sodium D-line) were carried out using a digital refractometer (Mettler Toledo RE50, Mettler-Toledo GmbH, Schwerzenbach, Switzerland) with a Peltier thermostat that kept the samples at the working temperature to an accuracy of 0.02 °C. The apparatus was calibrated by measuring the refractive index of Millipore quality water. A minimum of three independent readings were taken for each composition. Standard uncertainties of measurements were established to be less than 5.0×10^{-5}. The n_D was studied experimentally for the three amphiphilic ELbcRs in a wide range of concentrations ($0.02–3.40 \times 10^{-3}$ g/ mL) and temperatures (20.00–50.00 °C). **Fig. S2** shows the linear dependence of n_D with concentration for E50A40 solutions at different temperatures. The plots for the other two ELbcRs are similar (figures not shown). In the temperature range considered, the refractive index varied linearly with concentration and temperature, decreasing at higher temperatures.

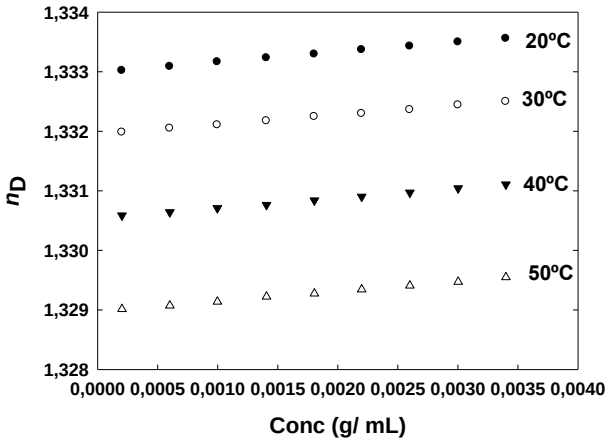

Fig. S2. *Temperature dependence of n_D for E50A40 in aqueous solution.*

The value of the specific refractive index increment (d*n*/dc) was deduced from the slope of plots of the refractive index versus concentration for each ELbcR at the four different temperatures studied. The results are listed in Table S2. The values obtained for the three ELbcRs showed that the dependence of d*n*/dc on temperature and molecular weight is minimal. In light of this, we used a d*n*/dc value of 0.17 mL/ g for the three ELbcRs in subsequent static light scattering experiments

Table S2. Specific refractive index increments, d*n*/dc, for E50A40, E100A40 and E50A40E50 in aqueous solution at different temperatures.

ELbcRs	d*n*/dc (mL/g)			
	T (°C) = 20.00	*T* (°C) = 30.00	*T* (°C) = 40.00	*T* (°C) = 50.00
E50A40	0.170	0.162	0.166	0.167
E100A40	0.176	0.174	0.175	0.171
E50A40E50	0.162	0.164	0.168	0.166

Dynamic (DLS) and Static (SLS) Light Scattering. Light scattering measurements were performed using a BI-200SM multiangle goniometer (Brookhaven Instrument Corp., NY, USA) with a 33-mW He-Ne vertically polarized laser at a wavelength of 632.8 nm and a digital correlator (BI-9000AT).

The temperature-dependent self-assembly of the ELbcRs was monitored by DLS at a scattering angle of 90° to confirm the results obtained by turbidity. Aqueous ELbcR solutions at a concentration of 25 μM were filtered at room temperature using a 0.45-μm PVDF syringe filter, then introduced into glass cells (diameter: 3 mm) stabilized for 10 min at the desired temperature (30–80 °C) in a thermostated decalin bath. The scattering light intensity (*I*) as a function of temperature showed an aggregation temperature in agreement with turbidity results, therefore a temperature of 65 °C was selected to compare the three ELbcRs in subsequent experiments. The intensity measurements were normalized against toluene (I_0).

The autocorrelation functions were measured in 25 µM water solutions at 65 °C (**Fig. S3**). The measured time correlation function C(τ), where τ is the delay time, was used to obtain the size distribution and polydispersity index by the cumulant method and CONTIN analysis.

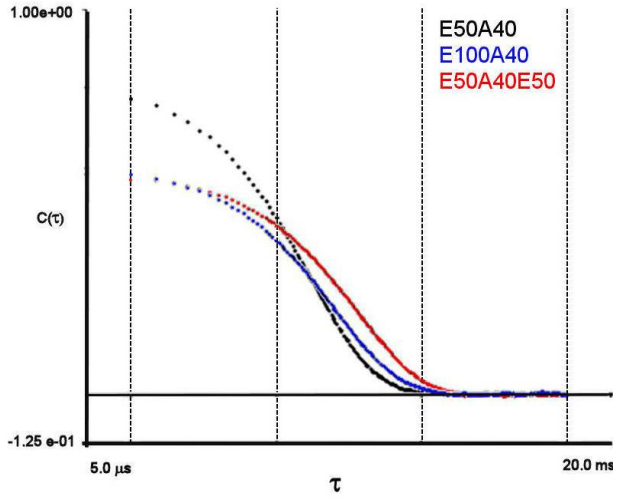

Fig. S3. *Autocorrelation functions for aqueous 25 µM E50A40, E100A40 and E50A40E50 solutions at 65 °C.*

For dilute systems where the decay or relaxation rate (Γ) is entirely due to translational, diffusive motion of the center of mass of the scattered nanoparticle, it can be shown that $\Gamma = D_{app} \cdot q^2$, where D_{app} is the apparent diffusion coefficient at a given concentration and q is the magnitude of the scattering wave vector. This magnitude is given by,

$q = \frac{4\pi n}{\lambda} \sin\left(\frac{\theta}{2}\right)$ where λ is the wavelength of the incident laser beam, n is the refractive index of the solution and θ is the scattering angle. The effective

hydrodynamic radius (R_h) was calculated from the diffusion coefficient by the Stokes-Einstein relation:

$$R_h = \frac{k_B T}{6\pi\eta D_{app}}$$ where k_B is the Boltzmann constant, T is the temperature, and η is the viscosity of the solution.

As can be seen in **Fig. S4**, an increase in temperature above the transition temperature did not affect the size of the formed nanoaggregates.

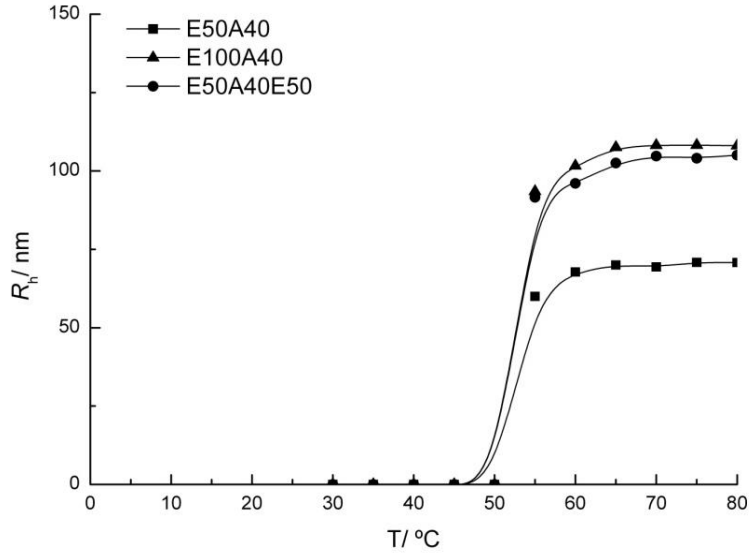

Fig. S4. *Temperature-dependence of the hydrodynamic radius (R_h) for aqueous 25 μM E50A40, E100A40 and E50A40E50 solutions.*

Static light scattering (SLS) measurements were performed using filtered amphiphilic ELbcR solutions equilibrated at 65 °C for at least 15 minutes in the scattering cell, but at concentrations ranging from 1.0 to 5.0 mg/ mL and for scattering angles of between 50° and 130°. The elastic (static) intensity was measured using toluene as the standard with a known absolute scattering intensity. A curvature of the

angular dependence in a Zimm plot is often observed in our self-assembled nanoparticles, which present hydrodynamic radius of about 100 nm. This curvature was best considered using the Berry equation [2]:

The optical constant, *K*, is defined as $K = (2\pi^2 n_0^2/\lambda^4 N_A)(dn/dc)^2$, where n_0 is the refractive index of the solvent, d*n*/dc is the specific refractive index increment, N_A is Avogadro's number, θ is the scattering angle, λ is the wavelength, and *c* is the nanoparticle concentration.

$(Kc/\Delta R_\theta)^{1/2}$ was plotted against $(\sin^2(\theta/2) + kc)$, where *k* is an adjustable constant (**Fig. S5**). Extrapolation of the experimental data to zero concentration and zero angle yields the molecular weight of the aggregates ($M_{w,agg}$), the gyration radius (R_g), and the second virial coefficient (A_2). Only the calculated R_g and $M_{w,app}$ values were considered in this work. The aggregation number (N_{agg}) was calculated by dividing the $M_{w,agg}$ value obtained from SLS experiments by the monomers' M_w. The ratio ρ [3] was calculated as $\rho = R_g/ R_h$.

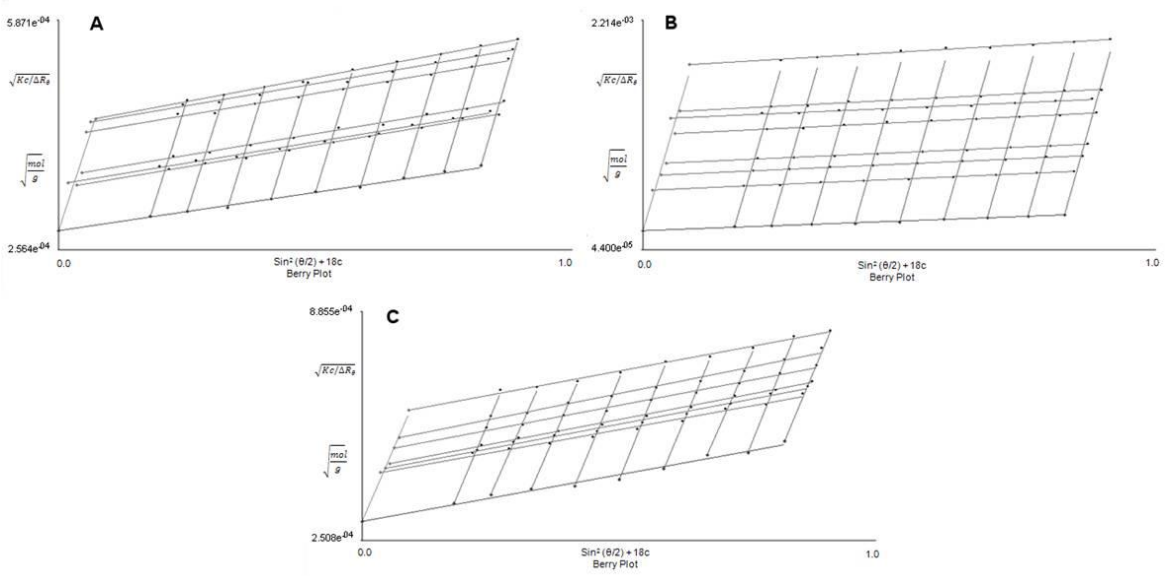

Fig. S5. *Berry plots of E50A40 (A), E100A40 (B) and E50A40E50 (C) obtained by SLS in water at 65 °C.*

Isothermal Titration Calorimetry (ITC)

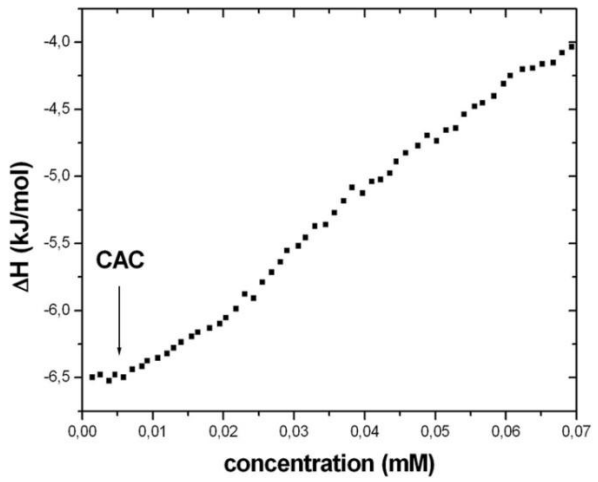

Fig. S6. *Enthalpy change as a function of E50A40 concentration. Arrow shows the critical aggregation concentration (CAC).*

Circular Dichroism (CD)

CD spectra were obtained on a Jasco J-810 spectropolarimeter (Jasco Inc., Easton, MD) at a scan rate of 50 nm/ min. The cell path length was 0.1 mm and heating cycles were performed at 5 ºC/ min with 10 min equilibration at each temperature. All CD curves were smoothed using a Fourier transform noise reduction algorithm.

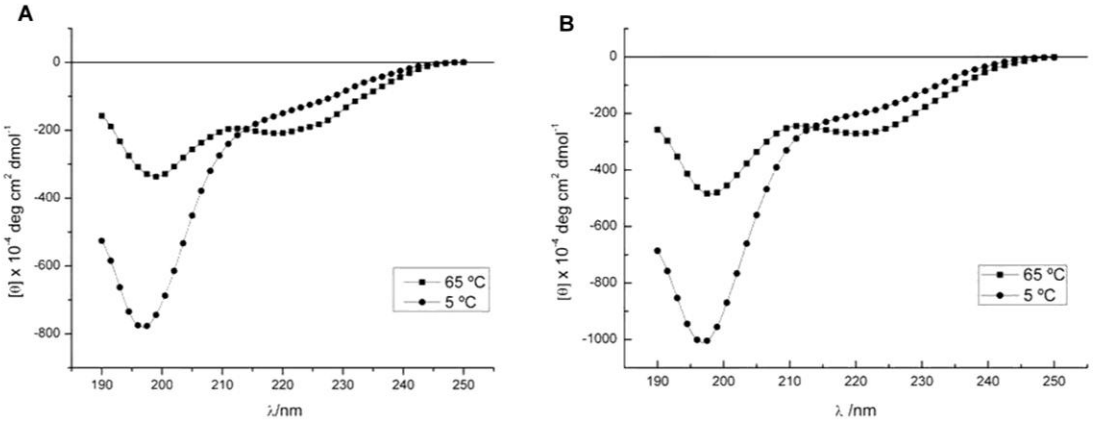

Fig. S7. *Circular dichroism spectra for aqueous 25µM E50A40 (A) and E50A40E50 (B) solutions at 5 and 65 ºC upon heating.*

Transmission electron microscopy (TEM)

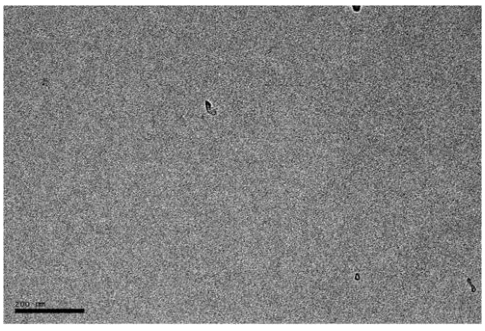

Fig. S8. *TEM image of E50A40 stained with 1% uranyl acetate prepared from the solution at 25 ºC.*

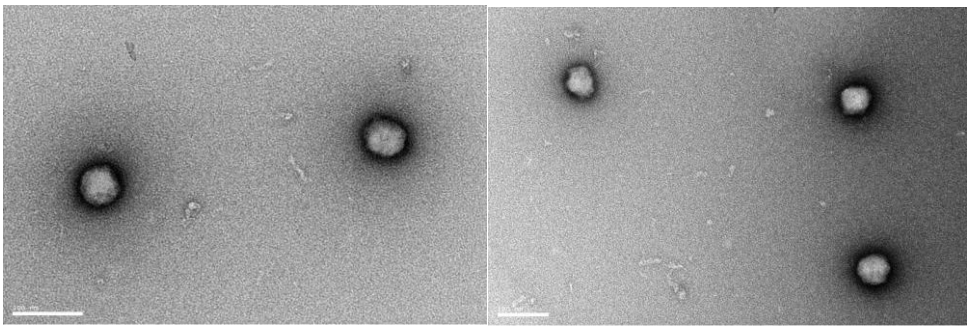

Fig. S9. *TEM images of self-assembled nanoparticles stained with 1% uranyl acetate for E100A40.*

References

[1] Girotti, A.; Reguera, J.; Rodríguez-Cabello, J.C.; Arias, F. J.; Alonso, M.; Testera, A. M. Design and biopoduction of a recombinant multi(bio)funtional elastin-like protein polymer containing cell adhesión sequences for tissue engineering purposes. *J. Mater. Sci. Mater. Med.* 2004, **15**, 479-484.

[2] Tanner, D. W.; Berry, G. C. Properties of Cellulose Acetate in Solution. I. Light Scattering, Osmometry and Viscometry on Dilute Solutions. *J. Polym. Sci., Polym. Phys.* Ed. 1974, **12**, 941-975.

[3] Burchard, W. Static and dynamic light scattering from branched polymers and biopolymers. *Adv. Polym. Sci.* 1983, **48**, 1-124.

CHAPTER 5

Rapid Micropatterning by Temperature-Triggered Reversible Gelation of a Recombinant Smart Elastin-Like Tetrablock-Copolymer

The work presented in this chapter has been published in:

L. Martín, F. J. Arias, M. Alonso, C. García-Arévalo and J. C.Rodríguez-Cabello.

2010

Rapid Micropatterning by Temperature-Triggered Reversible Gelation of a Recombinant Smart Elastin-Like Tetrablock-Copolymer

Soft Matter, 6: 1121-1124

Rapid Micropatterning by Temperature-Triggered Reversible Gelation of a Recombinant Smart Elastin-Like Tetrablock-Copolymer

Laura Martín, Francisco Javier Arias, Matilde Alonso, Carmen García-Arévalo and José Carlos Rodríguez-Cabello*

G.I.R. Bioforge, University of Valladolid, Ciber-bbn, Paseo de Belén 11, 47011 Valladolid, Spain.

*Correspondence to:

J. Carlos Rodríguez-Cabello

Tel: +34 983 184 686

E-mail: cabello@bioforge.uva.es

Abstract

We report a simple, fast, water-based method to obtain micropatterned biocompatible gels from a recently described family of elastin-like amphiphilic multiblock copolymers that combines reversible thermogelling properties under mild, physiological conditions with a means of replica molding.

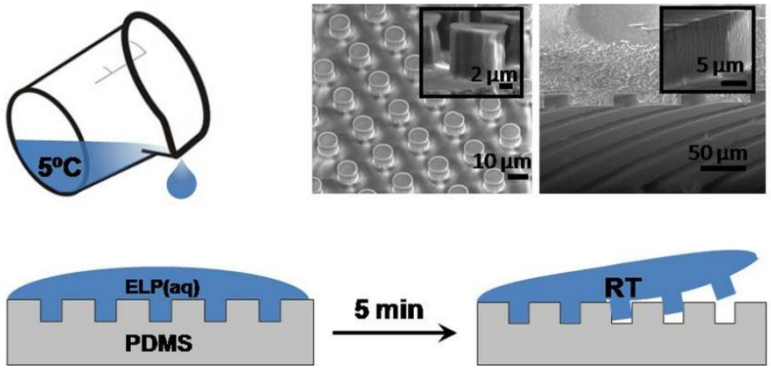

The design and development of systems with a well-defined topography, biochemical activity and controlled mechanical properties is a hot research topic due to their potential biomedical applications [1, 2]. However, whereas the versatility of thermosensitive synthetic copolymers has been widely exploited, the intrinsic toxicity or biodegradability of these systems is a major limitation. This tetrablock-copolymer system enables the highly reproducible fabrication of different microstructured surfaces and can be used as both an "*in situ*" implantable platform or as a substrate with a well-controlled microtopography to study spatially controlled cell behavior. The reversibility of this approach can also be exploited in combined strategies involving, for example, cell-harvesting procedures. The development of functional materials often involves the generation of well-defined micro- and nanopatterned surfaces. The huge interest in emulating natural systems shows the need for more sophisticated superhydrophobic or superhydrophilic surfaces, such as in biomimetic approaches to the surface properties of lotus leaves or gecko finger tips [3]. Another field of enormous interest concerns cell–material interactions, where cell behavior can be conditioned by a given well-defined topography of the material surface, either alone or in combination with specific bioactivity, which leads to a promising strategy for controlling cellular organization and function in tissue engineering [4, 5]. The major drawback of replica molding, a simple and straightforward method for fabricating topographically micropatterned structures with different features, is the choice of material. This implies the use of "*in situ*" thermal, photopolymerization, solvent-casting, or cross-linking reactions [6- 8], which are not reversible and usually result in traces of different chemicals and solvents on the micropatterned surfaces that can cause cell death. Herein we report a simple, fast, water-based method for obtaining micropatterned biocompatible gels under mild,

physiological conditions by exploiting the thermoresponsive nature of a recently described family of amphiphilic elastin-like multiblock-copolymers.

Elastin-like polymers (ELPs) are a new and attractive family of recombinant polypeptides that have found many applications as biomaterials due to their excellent biocompatibility, bioactivity, self-assembly, and "smart" stimuli-responsive nature [9-11]. Recombinant DNA technologies provide the tools for preparing block-copolymers with individual blocks with different tailored biological, physical, and mechanical properties. These blocks include complex well-defined sequences that are beyond the reach of any other macromolecular synthetic method [12, 13]. ELPs are strictly monodisperse and can be obtained with molecular weights ranging from a few hundred Daltons to more than 200 kDa [10]. The production cost is not related to the complexity and once the genetically modified (micro)organism is obtained, fermentation is a simple and cheap scalable technology that also shows evident environmental benefits. Although other options are available, the most basic composition for ELPs involves a repetition of the pentapeptide (VPGXG), where X represents any natural amino acid except proline [10]; the physicochemical properties of these polymers can be tuned simply by varying the amino acid X. Amphiphilic block copolymers based on the general (VPGXG) formula with a self-assembly behavior coupled to their smart nature have shown temperature-triggered micellar and other submicrometer structural self-assembly from aqueous solution. Triblock-copolymers with an apolar-polar-apolar structure have also recently been reported to form elastomeric hydrogels in which the hydrophilic blocks provide conformational elastic properties and the hydrophobic blocks form physical cross-links by hydrophobic aggregation [14].

The hypothesis of this work is that optimized amphiphilic ELP tetrablock copolymers could be used to obtain highly resolved micropatterns by biocompatible replica molding. This process would involve a one-step process in which the aqueous ELP solution is simply heated slightly above its gelation temperature (T_{gel}). The use of ELPs involves several advantages, not only restricted to thermal response, which cannot be found in other conventional biopolymers as proteins or polysaccharides. ELPs are designed at the gen level, so their properties can be tuned as desired with the adequate amino-acid composition, which are not easily achievable by more conventional biopolymers. This means that it is relatively simple obtain multibioactive versions of these self-gelating polymers with different functionalities, such as the interaction with cells or others, in addition to their physical gelation. However, in this work, a basic structural composition was used as the sole function in order to better isolate this temperature-triggered gelation effect and the proof of concept of obtaining replicas from this physical function. We therefore biosynthesized a recombinant amphiphilic ELP tetrablock-copolymer, with the amino acid sequence MESLLP{[$(VPGVG)_2$-(VPGEG)-$(VPGVG)_2$]$_{10}$-[VGIPG]$_{60}$}$_2$V (abbreviated $(E50I60)_2$), containing two different blocks (see bioproduction and characterization in the Supporting Information **Fig. S1, S2 and S3**). The first block (E-block) is pH-responsive whereas the I-block is a thermoresponsive polymer with no pH response. The sequences of the respective blocks were chosen such that only one of the two different blocks in the polymer undergoes a phase transition in response to temperature changes, exploiting its LCST behavior [13]. This reversible process was monitored by DSC showing a transition temperature (T_t) of 8.11°C (see Supporting Information **Fig. S4**). Both the I- and E-blocks are water-soluble at temperatures below T_t at neutral pH, whereas above T_t the I-blocks lose solubility and start to behave as a hydrophobic polymer, which means that they segregate from

solution and come into contact *via* hydrophobic interactions. The final result is a physical gel.

We investigated the thermogelling characteristics as a function of time and temperature using a controlled stress rheometer (AR-2000ex, TA Instruments) in a constant strain of 0.1% and a frequency of 1 Hz. The heating/cooling rate was 1.0 °C·min^{-1}. Thus, heating $(E50I60)_2$ from 5 to 37 °C in phosphate-buffered saline (PBS) resulted in a clear sol–gel transition over a wide concentration range (5.0–15.0 wt %), thereby confirming the hypothesis of temperature-triggered gelation. The change in modulus of the thus-formed gel as a function of time was followed by rheological measurements.

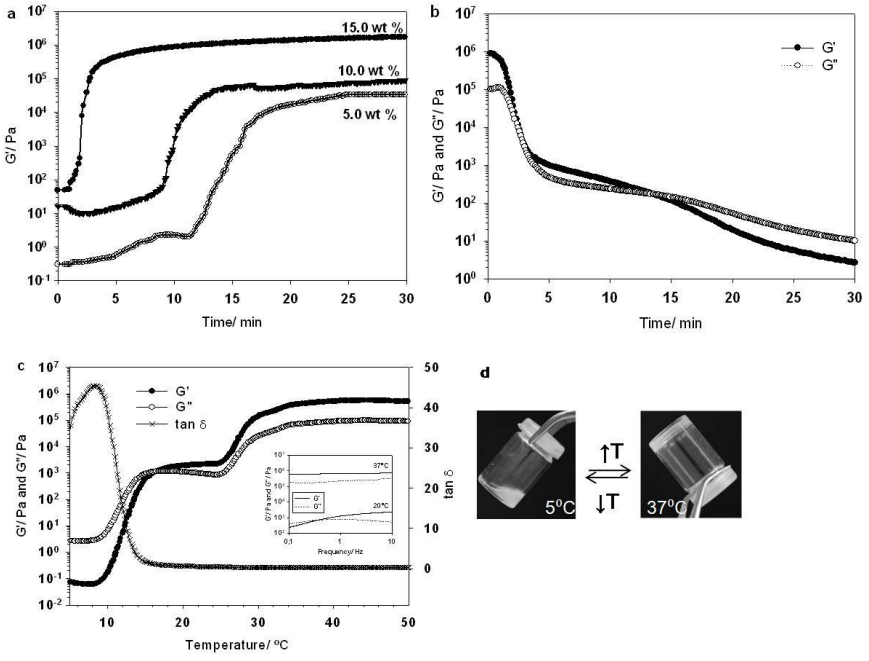

Fig. 1. *Thermogelling properties of the elastin-like tetrablock-copolymer in PBS solution. (a) Comparison of the evolution of the storage modulus at 37 °C for the ELP at different polymer concentrations with time. (b) Storage modulus (G') and loss*

modulus (G'') as a function of time upon cooling the 15.0 wt % gel from 37 to 5 °C. (c) Evolution of the viscoelastic properties of the ELP (15.0 wt %) as a function of temperature. G′, G″ and tan δ are the storage, loss moduli and loss tangent, respectively. The inset within the figure depicts the frequency sweeps for this solution at 20ºC and 37ºC at strain amplitude of 0.1%. (d) Pictures showing the sol (5 °C) and gel (37 °C) formed by the 15.0 wt % ELP.

Fig. 1a shows the change in storage modulus (G') at 37 °C for different concentrations. The polymer concentration plays an important role in controlling the gelation kinetic and viscoelastic properties of the gels. The gelation time was taken to be the time at which a stable G' is obtained in the gel state. This time varies from 5 to 20 minutes for concentrations in the range from 15.0 to 5.0 wt %, respectively. Likewise, the storage modulus changes from 3.3×10^4 to 1.6×10^6 Pa as the ELP concentration increases within this range. This is an indication of the extent of gel network formation. A working concentration of 15.0 wt % was chosen due to its short gelation time. Furthermore, due to the rapid sol-gel transition, the sample likely begins to form a gel some seconds before the system reaches the set temperature of 37ºC, showing in the initial point certain contribution of the gel state. The reversibility of this copolymer system was also monitored by cooling the gel to 5 °C (**Fig. 1b**). The polymer gel dissolves upon decreasing the temperature below T_t due to a gel–sol transition. Both moduli decrease rapidly even though the cooling device (Peltier) does not cool the sample so rapidly, and the polymer reaches its initial state in less than 30 minutes at the working concentration of 15.0 wt %.

The gel point is usually determined by using the G'-G'' crossover method where the gelation temperature (T_{gel}) is the temperature at which G' is equal to G'' (viscous modulus), but this only occurs in certain cases [15], in which this system cannot be

included. According to the rheological data, the gel formation takes place in the range 9-14ºC, which is evident for both the tan δ and the *G*'/*G*" plots for the 15.0 wt % PBS solution (**Fig. 1c**). The inflexion point for the three curves in that range fall on roughly 13ºC for the three plots. This is the value adopted as representative of the sol-gel transition determined by rheological methods. We have determined the T_{gel} from the inflexion point in the curve about 12 °C for the 15.0 wt % PBS solution (**Fig. 1c**).This value is in agreement with the T_t value observed by DSC when taking into account the thermal lag due to the different masses used in both experiments. When discussing rheological results, the experimental curves are usually divided into three main regions: sol, soft gel and hard gel. The first region is found below 15 °C, where *G*' is lower than *G*", thus indicating that the viscous component dominates the system in the sol state and shows the expected liquid-type behaviour. The sharp increase in *G*' is considered to be a result of the partial formation of aggregates by hydrophobic interactions and the onset of gelation reaching a plateau in G', which is characteristic of a gel state [16]. The next regions contain some soft gel (*G*' > *G*", low *G*' ≈ 2000 Pa; 15–27 °C) and an extensive region of hard gel (*G*' > *G*", high *G*' ≈ 5.0 × 10^5 Pa) resulting from gel toughening, which finally leads to the formation of stable gels. The second region is referred to as the soft gel, since its *G*' is more than 2 orders of magnitude smaller than that of the high-temperature gel, named hard gel [17]. The different viscoelastic properties of these gels at different temperatures were measured as a function of the frequency from 0.1 to 10 Hz in a constant strain of 0.1% showing that the rheological behavior at 20ºC is typical of a "soft gel", which has frequency dependence. In contrast, *G*' shows almost no dependence with frequency at higher temperatures, displaying characteristic features of a "hard gel". Pictures of the sol (5 °C) and gel (37 °C) are shown in **Fig. 1d**.

This type of thermally triggered gel is an excellent candidate as a new microstructured substrate for the study of cell adhesion and proliferation that emulates the microscale structure of tissues "*in vivo*". More importantly, ELPs are of particular interest, due to their peptidic nature and the way they are produced (recombinant technology), which means that it is relatively simple to obtain multibioactive versions of these self-gelating polymers that show different abilities to interact with cells (promoting cell adhesion, including growth factor, etc.) in addition to their physical gelation [18, 19]. The mild physiological conditions under which these polymers form gels, the exclusive use of water as solvent, and the absence of any chemical reagents in the process also make them excellent candidates for the development of new, rapid, flexible, multifunctional, and clean methods for achieving micropatterning using a replica molding approach for the fabrication of microscale geometries from microfabricated elastomeric templates. Replica molding was therefore carried out on micropatterned PDMS substrates as replicas. The PDMS prepolymer and curing agent were thoroughly mixed at a 10/1 (w/w) ratio and degassed for 1 h. The mixture was then cast onto different patterned silicon masters with different features (hexagonal pits: width (w) = 100 μm, spacing (s) = 100 μm; circular and square pits: w = s = 40 μm; grooves: w = 20 μm, s = 50 μm or w = 15 μm, s = 25 μm; cylindrical pillars: w = s = 10 μm). The step height of the micro-features was 15 μm for the pits and grooves and 9 μm for the pillars. The mixture was cured at 65% for 1 h. The PDMS was carefully peeled off from the silicon wafer and used as a mold. The hydrogels were obtained by pouring the 15.0 wt % polymer solution in PBS onto the PDMS replicas at 5 °C and then simply heating the system from 5 to 37 °C. The hydrogels were then peeled off and their surface topography observed, without any treatment or manipulation, by differential interference contrast (DIC) microscopy with a Nikon ECLIPSE 80i light microscope

and by ESEM in low vacuum mode (FEI Quanta 200 FEG). The six different patterns thus obtained are shown in **Fig. 2a**. The cross-sectional view, as observed by ESEM (**Fig. 2b**), clearly shows that the gel's micropatterns have the same height as the original silicon masters (15 and 9 μm for the grooves and cylindrical pillars, respectively).

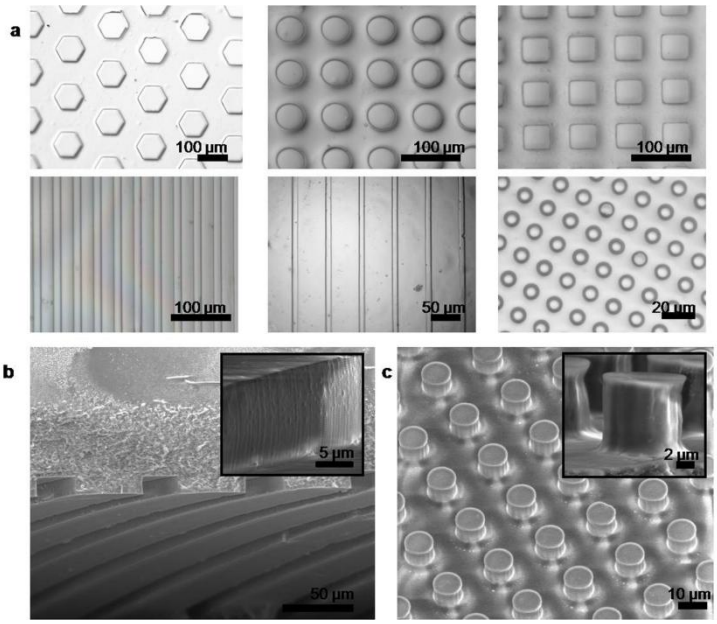

Fig. 2. *Micropatterned gels with different features obtained by replica molding.* ***(****a) Optical micrographs of swollen gels in PBS by DIC microscopy. (b-c), ESEM micrographs. (b), Cross-section of grooves (h = 15 μm, w = 20 μm, s = 50 μm). (c), Magnified surface and cross-section views of pillars (h = 9 μm, w = s= 10 μm).*

These images demonstrate the applicability of replica molding for obtaining microstructured surfaces with a controlled and well-defined topography. Interestingly, the micropatterned ELP gels maintain the dimensions of the original stamp with high fidelity. No significant swelling, shrinkage, or deformation of the microstructures was observed.

We have therefore demonstrated that the reversible sol–gel transition in amphiphilic tetrablock-ELP-copolymers under physiological conditions affords biocompatible elastic gels. This approach could be used to study cell behavior on microstructured surfaces created by replica molding with the possibility of tuning the mechanical properties during cell culture by varying the temperature. The gelation is fully reversible, thereby providing an interesting opportunity to use these systems in cell-harvesting procedures. For example, a given type of cell can be manipulated and compelled to grow under a desired morphology and cell film structure by the appropriate combination of microstructure and bioactivity of the micropatterned substrate. This cell film can then be harvested from the substrate simply by cooling the cell culture below T_t in a rapid and mild process that does not compromise cell viability or biofilm structure. These possibilities make this family of biocompatible tetrablock-copolymers excellent substrates for the development of cell-based biomedical devices. Other materials, such as certain polysaccharides, show also thermally-driven gelation properties. Therefore, the concept of micropatterning by replica molding in this kind of thermally-sensitive gels could be of use in many other materials, which could expand the range of applications to many different areas.

Acknowledgments

We acknowledge financial support from the MICINN (projects MAT 2007-66275-C02-01, NAN2004-08538, and PSE-300100-2006-1), the JCyL (projects VA034A09, VA016B08, and VA030A08), the CIBER-BBN (project CB06-01-0003), the JCyL, and the Instituto de Salud Carlos III under the "Network Center of Regenerative medicine and Cellular Therapy of Castilla and León".

Additional information

Supporting Information accompanies this paper.

References

[1] Mitragotri, S.; Lahann, J. Physical approaches to biomaterial design. *Nature Mater*. 2009, **8**, 15-23.

[2] Raghavan, S.; Chen, C. S. Micropatterned environments in cell biology. *Adv. Mater*. 2004, **16**, 1303-1313.

[3] Hassel, A. W.; Milenkovic, S.; Schurmann, U.; Greve, H.; Zaporojtchenko, V.; Adelung, R.; Faupel, F. Model systems with extreme aspect ratio, tunable geometry, and surface functionality for a quantitative investigation of the lotus effect. *Langmuir*, 2007, **23**, 2091-2094.

[4] Curtis, A.; Wilkinson, C. Topographical control of cells. *Biomaterials*, 1997, **18**, 1573-1583.

[5] Falconnet, D.; Csucs, G.; Grandin, M. H.; Textor, M. Surface engineering approaches to micropattern surfaces for cell-based assays. *Biomaterials*, 2006, **27**, 3044-3063.

[6] Yu, T. Y.; Ober, C. K. Methods for the topographical patterning and patterned surface modification of hydrogels based on hydroxyethyl methacrylate. *Biomacromolecules*, 2003, **4**, 1126-1131.

[7] Martín, L.; Alonso, M.; Moller, M.; Rodríguez-Cabello, J. C.; Mela, P. 3D microstructuring of smart bioactive hydrogels based on recombinant elastin-like polymers. *Soft Matter*, 2009, **5**, 1591-1593.

[8] Ber, S.; Kose, G. T.; Hasirci, V. Bone tissue engineering on patterned collagen films: An in vitro study. *Biomaterials*, 2005, **26**, 1977-1986.

[9] Rodríguez-Cabello, J. C.; Reguera, J.; Girotti, A.; Arias, F. J.; Alonso, M. Genetic engineering of protein-based polymers: The example of elastin-like polymers. *Adv. Polym. Sci.*, 2006, **200**, 119-167.

[10] Urry, D. W. *What sustains life? Consilient mechanisms for protein-based machines and materials*, Springer-Verlag, New York, 2006.

[11] Chow, D.; Nunalee, M. L.; Lim, D. W.; Simnick, A. J.; Chilkoti, A. Peptide-based biopolymers in biomedicine and biotechnology *Mater. Sci. Eng. R Rep.* 2008, **62**, 125-155.

[12] Chilkoti, A.; Christensen, T.; MacKay, J. A. Stimulus responsive elastin biopolymers: Applications in medicine and biotechnology. *Curr. Opin. Chem. Biol.* 2006, **10**, 652-657.

[13] Ribeiro, A.; Arias, F. J.; Reguera, J.; Alonso M.; Rodríguez-Cabello, J. C. Influence of the amino-acid sequence on the inverse temperature transition of elastin-like polymers. *Biophys. J.* 2009, **97**, 312-320.

[14] Sallach, R. E.; Cui, W.; Wen, J.; Martinez, A.; Conticello, V. P.; Chaikof, E. L. Elastin-mimetic protein polymers capable of physical and chemical crosslinking. *Biomaterials*, 2009, **30**, 409-422.

[15] Winter, H. H.; Chambon, F. Analysis of linear viscoelasticity of a crosslinking polymer at the gel point. *J. Rheol.* 1986, **30**, 367-382.

[16] Almdal, K.; Dyre, J.; Hvidt, S.; Kramer, O. Towards a phenomenological definition of the term "gel". *Polym. Gels Networks*, 1993, **1**, 5-17.

[17] Hvidt, S.; Jørgensen, E. B.; Schillén, K.; Brown,W. Micellization and gelation of aqueous solutions of a triblock copolymer studied by rheological techniques and scanning calorimetry. *J. Phys. Chem.*, 1994, **98,** 12320-12328.

[18] Liu, J. C.; Heilshorn, S. C.; Tirrell, D. A. Comparative cell response to artificial extracellular matrix proteins containing the RGD and CS5 cell-binding domains. *Biomacromolecules*, 2004, **5**, 497-504.

[19] Sarikaya, M.; Tamerler, C.; Jen, A. K. Y.; Schulten, K.; Baneyx, F. Molecular biomimetics: nanotechnology through biology. *Nature Mater.* 2003, **2**, 577-585.

Supporting Information

Rapid Micropatterning by Temperature-Triggered Reversible Gelation of a Recombinant Smart Elastin-Like Tetrablock-Copolymer

Bioproduction and Characterization of $(E50I60)_2$

Standard molecular biology techniques were used to construct the ELP gene and its sequence was verified by automated DNA sequencing. Polymer production was carried out using cellular systems for genetic-engineering protein biosynthesis in *Escherichia coli*. The $(E50I60)_2$ biopolymer was purified by three cycles of temperature-driven precipitation and the final bioproduction yield was around 520 mg/L of bacterial culture. A purified sample of the biopolymer was analyzed by polyacrylamide gel electrophoresis in the presence of sodium dodecyl sulfate with copper staining, which indicated a polypeptide purity of 95% (**Fig. S1**).

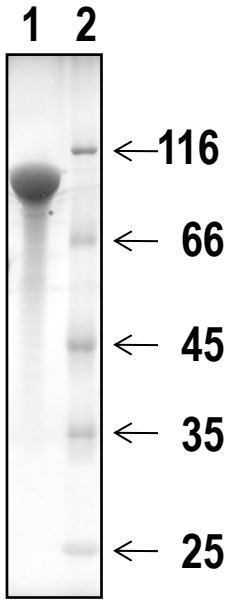

Fig. S1. *Analysis of $(E50I60)_2$ biopolymer purity by SDS-PAGE after staining with copper chloride. Lane 1: 20 μg of the purified biopolymer. Lane 2: protein markers. The numbers on the right indicate the corresponding apparent molecular weight values of the standards (in kDa).*

High-mass MALDI TOF MS analyses were performed using a Reflex IV MALDI TOF mass spectrometer (Bruker, Bremen, Germany) equipped with CovalX's HM2 high-mass detector system and focusing on different mass ranges from 0 to 1500 kDa. An external calibration with clusters of Insulin, BSA and IgG was applied to calibrate the instrument. Three spots were analyzed for the sample (300 laser shots per spot). The MS data were analyzed using the Complex Tracker analysis software.

The main protein detected in the three different spots for the $(E50I60)_2$ biopolymer corresponds to a protein with a molecular weight of 92,892±19 Da. The predicted molecular weight for this polymer is 93,176 Da. This is a variation of 0.3%, which is perfectly reasonable for this technique (**Fig. S2**).

The following results were obtained for the three spots:

$(E50I60)_2$	Concentration	Observed Molecular Weight (Da)
Spot 1	1 mg/ml	92,897
Spot 2	1 mg/ml	92,871
Spot 3	1 mg/ml	92,908

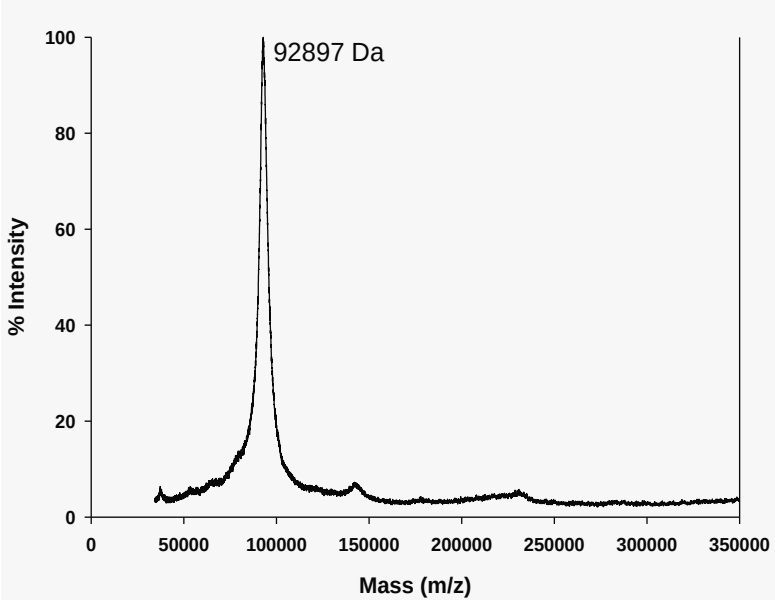

Fig. S2. *MALDI-TOF spectra of one of the spots analyzed for the* $(E50I60)_2$ *biopolymer.*

The polymer's amino acid composition was determined by the AccQ-Tag Waters method. The derivatized amino acids were analyzed by high performance liquid chromatography (HPLC) with UV detection, using a WATERS600 HPLC gradient system with a WATERS2487 detector. Quantification of the most represented amino acids was performed using the 1/10 dissolution.

The results of the amino acid composition analysis match the predicted amino acid composition very well taking into account the endogenous error inherent to this technique and the peculiar composition of this sample (**Fig. S3**).

	Predicted	Experimental
Asp	**0**	**0.47**
Ser	**1**	**1.09**
Glu	**21**	**22.01**
Gly	**440**	**432.83**
Thr	**0**	**0.22**
Ala	**0**	**0.37**
Pro	**221**	**224.02**
Tyr	**0**	**0.22**
Val	**301**	**304.8**
Lys	**0**	**0.22**
Ile	**120**	**119.34**
Leu	**2**	**1.91**

Fig. S3. *Predicted and measured amino acid compositions for the* $(E50I60)_2$ *biopolymer.*

The reversible process undergone by $(E50I60)_2$ was monitored by DSC, which showed a transition temperature (T_t) of 8.11 °C on heating and 7.35 °C on cooling (**Fig. S4**). Experiments were performed with a Mettler Toledo 822e with a liquid-nitrogen cooler. The solution was prepared at 15.0 wt % in sodium phosphate buffer (PBS) solution. For analysis, 25 µL of the solution was placed in a standard 40 µL aluminum pan and sealed hermetically. The same volume of PBS was placed in the reference pan. The following thermal procedure was used for heating-cooling cycle measurements:

isotherm at –10 °C for 5 min, ramp 1.0 °C·min^{-1} from –10 to 20 °C, isotherm at 20 °C for 1 min, and ramp 1.0 °C·min^{-1} from 20 to –10 °C.

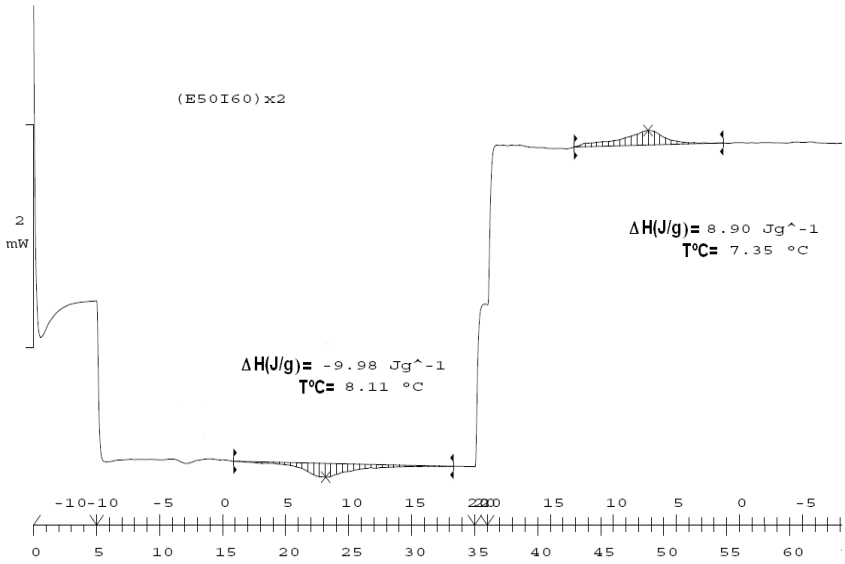

Fig. S4. *DSC thermo grams for a heating–cooling cycle (1.0 °C·min^{-1}) for (E50I60)$_2$ at 15.0 wt % in sodium phosphate buffer (PBS) solution.*

CHAPTER 6

Final Conclusions and Future Perspectives: Emerging Applications of Multifunctional Elastin-like Recombinamers

The work presented in this chapter has been published in:

J. C. Rodríguez-Cabello; L. Martín; A. Girotti, C. García-Arévalo, F. J. Arias;

M. Alonso. 2011

Emerging Applications of Multifunctional Elastin-Like Recombinamers

Nanomedicine 6 (1): 111-122.

Emerging Applications of Multifunctional Elastin-like Recombinamers

J. Carlos Rodríguez-Cabello*, Laura Martín, Alessandra Girotti, Carmen García-Arévalo, F. Javier Arias and Matilde Alonso.

G.I.R. Bioforge, University of Valladolid, CIBER-BBN, Paseo de Belén 11, 47011 Valladolid, Spain

Keywords: Drug delivery, Elastin-like recombinamers, nano-devices, protein purification, surface engineering, tissue engineering.

*Correspondence to:

J. Carlos Rodríguez-Cabello

Tel: Tel.: +34 983 184 686

Fax: +34 983 184 698

E-mail: cabello@bioforge.uva.es

Abstract

Elastin-like recombinamers (ELRs) have grown in popularity in the field of protein-inspired biomimetic materials and have found widespread use in biomedical applications. Modern genetic-engineering techniques have allowed the design of multifunctional materials with an extraordinary control over their architecture and physicochemical properties, such as stimuli-responsiveness, monodispersity, biocompatibility or self-assembly, amongst others. Indeed, these materials are playing an increasingly important role in a diverse range of applications, such as drug delivery, tissue engineering and "smart" systems. Herein, we review some of the most interesting examples of recent advances and progressive applications of ELRs in the biomaterial and nano-engineering sciences in the last years.

1. Introduction

As a result of their unique and specific interactions with other macromolecules and inorganic compounds, proteins are an indispensable part of biological structures and systems, especially as regards control of tissue formation, biological functions or physical performance [1]. Nano-biotechnological approaches focused on genetically engineered, protein-based biopolymers have been considered to show great promise for the development of advanced biomaterials with applications in medicine-related fields and nanotechnology owing to their valuable properties, such as their propensity to form hydrophilic networks, their expected good biocompatibility, favorable degradation rate and products, very low cytotoxicity and immunogenicity, and the ability to design structurally complex constructs with tunable mechanical, physical or biological properties [2,3]. Indeed, considerable progress has been made with regards to the use of these protein-based biomaterials in recent years, with elastin-like polypeptides being one of the most studied protein-like structures [4-6].

Elastin is an insoluble elastic protein that dominates flexible tissues where elasticity is of major importance (e.g., skin, ligament, arteries, lungs, and specialized cartilages). The increasing availability of recombinant forms of elastin that are virtually invisible to the immune system has allowed the formation of a wide range of biomaterial constructs and composites that benefit from elastin's inherent properties of innate assembly and elasticity [4]. The term elastin-like recombinamers (ELRs) highlights the fact that these constructs are oligomeric macromolecules whose composition is strictly defined by engineering design, that they are produced as recombinant proteins that exhibit monodispersity and a high control over amino-acid sequence, and that they mimic the basic properties of elastin [7]. ELRs, which are made of repeating amino acid sequences from the five-member unit (VPGX_{aa}G), where X_{aa} is

any natural amino-acid except proline, or its permutations, can be tailor-made to form self-assembled systems with controlled structures and functions [8]. The hydrophobic, clathrate-like, hydrated chains of ELRs break above a characteristic transition temperature (T_t), thereby allowing ELRs to fold hydrophobically to form a separated state in which the polymer chains adopt a dynamic, regular, nonrandom structure known as a β-spiral. This structure contains type II β-turns as the main secondary feature and is stabilized by intraspiral, interturn, and interspiral hydrophobic contacts. This process starts with the formation of filaments composed of three-stranded dynamic polypeptide β-spirals, which grow to form particles several hundred nanometers in diameter before settling into a visibly separate state, and is completely reversible upon lowering the sample temperature below T_t [9]. Although this β-spiral model is the structure that appears to best account for the available experimental data, there is still some controversy regarding its actual significance. Indeed, some studies have shown that other conformations are present in elastin (crosslinking and plastic domains) [10]. These observations include X-ray crystallography, solution and solid-state nuclear magnetic resonance (NMR) [11] spectroscopic studies and molecular dynamics simulations [12, 13]. However, in this kind of elastomeric ELR, where large amounts of water play an active role in increasing the dynamics of the polymer chain, it is not surprising that different methodological techniques, which observe the ELR chain on different time scales, give rise to apparently contradictory results.

The characteristic and reversible coacervation exhibited by ELRs in response to temperature changes in an aqueous environment can be a complex process that is strongly influenced by the composition of the ELRs but also depends on the molecular

mass, the degree of ionization of any functional side chains, the mean polarity of the polymer, salt concentration and the presence of other ions and molecules [7].

The control of nanostructures and the ordered 2D and 3D assembly of materials into useful functional structures and devices is one of the main challenges in the development of novel engineered biomaterials. The ability of ELR-based systems to display stimuli-driven variations in their nanostructures as a consequence of their self-assembling behavior in aqueous solution has been exploited in the development of complex "smart" biomaterials in which the combination of specific building blocks has led to a wide range of sizes, morphologies and functional possibilities. In addition, the recombinant route allows such polymers to be designed with a view to their intended use by taking advantage of the superior and easy sequence-control possibilities offered by this method, hence their physicochemical and mechanical properties can be fine-tuned to meet the desired applications (**Figure 1**).

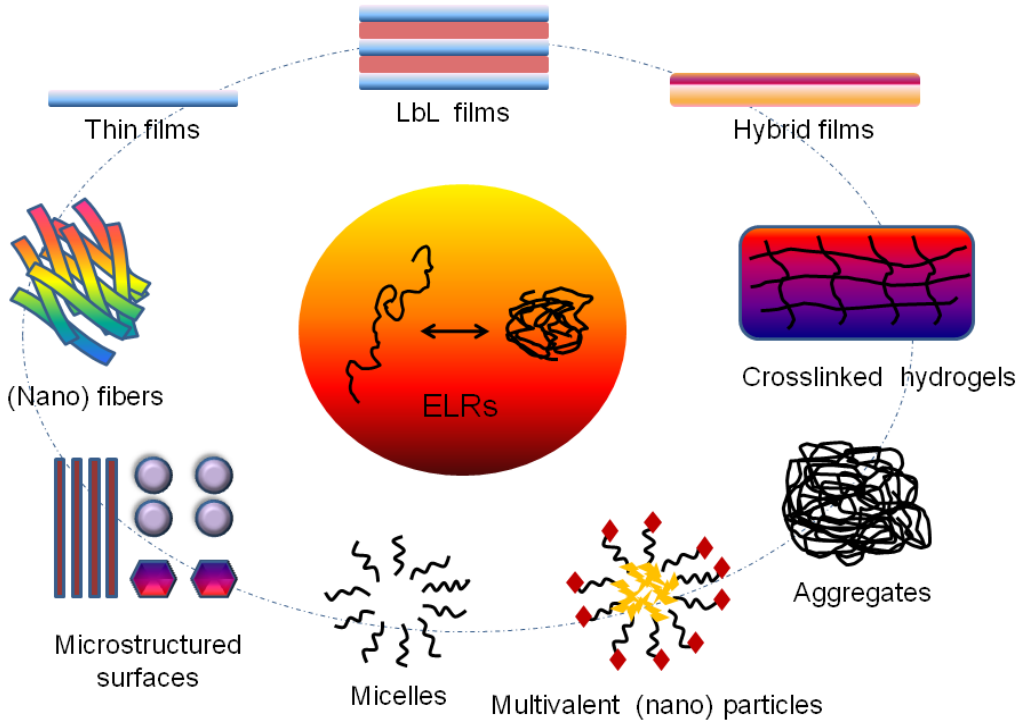

Figure 1. Summary of some applications of elastin-like recombinamers. *Different ELR-based devices, including aggregates, films (thin films or membranes of polymer networks, self-assembled LbL films or hybrid systems combining different polymers and particles), physically or chemically crosslinked hydrogels and nanofibers, and nanoparticles, such as micelles or multivalent nanoparticles, that assemble in solution have been developed for use in various applications (e.g., drug delivery, tissue engineering, cell harvesting, smart and bioactive surfaces and protein purification).*
ELR: Elastin-like recombinamer; LbL: Layer-by-layer.

2. Applications

2.1. Tissue Engineering

Owing to the fact that they are biomedical polymers, ELRs have found widespread use due to their ability to remain essentially invisible to the host immune system in a large spectrum of applications, mainly in the fields of tissue engineering and drug delivery. Indeed, the immune system appears to ignore these polymers and their degradation products (amino acids) as it is unable to distinguish them from natural elastin [14]. Scaffolds for either *in vitro* cultivation and subsequent transplantation or *in vivo* implantation directly into the body to support or replace specific biological or physiological functions (e.g., tissue repair or tissue engineering) should be colonized by cells that proliferate and secrete extracellular matrix and growth factors and must be suitable for the diffusion of nutrients, oxygen and waste from these cells until the cells themselves are able to support the defective organ, thus replacing the implanted scaffold and maintaining healthy cell development and functionality [15]. Thus, aspects related to both the topology and structure of the scaffolds and their bioactivity are crucial for the subsequent fate of these cell-supporting systems. However, finding the ideal

combination of a biomaterial and cells that provide suitable environmental conditions to form a functional biological system resembling the physiological one is a key challenge when designing such constructs. In this regard, ELRs are biocompatible starting materials that can be provided with the appropriate mechanical properties and lack non-specific bioactivities that could promote non-specific cell adhesion [16]. The anti-fouling properties and biocompatibility of simple ELRs and their cross-linked matrices have been reported [17, 18]. Likewise, recombinant human elastin polypeptide fragments in polymers have been shown to be an efficient coating on synthetic materials, demonstrating reduced platelet activation and adhesion in platelet-rich plasma *in vitro* and therefore great potential as a nonthrombogenic biomaterial [19]. These simple molecules were subsequently enriched with short peptides to provide specific bioactivities. To increase the complexity of ELRs, a simple substitution of the amino acid X in the elastin-based repeat unit (VPGXG) can result in the formation of cross-linking domains and thus more uniform and stable substrates. Thus, 2D and 3D cross-linked scaffolds with a lysine in the X position, which can be used in both enzymatic and chemical reactions for conjugation or cross-linking purposes, have been reported [20-22]. Likewise, ELR hydrogels have been produced by photoinitiation [23] or irradiation [24].

ELRs are able to form stable viscoelastic hydrogels with controlled mechanical and physico-structural features that maintain their interesting properties as stimuli-responsive substrates. Tirrell and coworkers have demonstrated that chemically cross-linked hydrogels formed in organic solvents from ELRs containing fibronectin cell-binding domains can successfully be used to support the growth and spread of endothelial cells [23, 26]. ELR hydrogels have also demonstrated the ability to induce the differentiation of adult human adipose stem cells into the chondrocytic phenotype

and the accumulation of cartilage-specific ECM in the absence of exogenous chondrogenic supplements *in vitro*, thereby potentially simplifying and reducing the cost of the differentiation process [27]. The chemical gelation of ELRs has also been performed in aqueous solution. Thus, Lim *et al.* have reported the formation of hydrogels with controlled mechanical properties in a biocompatible and injectable biomaterial for supporting tissue regeneration under physiological conditions [28]. Likewise, we have reported the production of 3D-ELR structured hydrogels with controlled microtopography (lines or pillars, squares, hexagons and so on) and different sizes and depths by replica molding. The resulting scaffolds showed a controlled microtopography with modulated mechanical properties and stimuli-responsive behaviour in aqueous media. These hydrogels may find a use in the study and control of cell behaviour by controlling their topography. Furthermore, the smart nature of these gels makes the substrates active, with the possibility of changing the dimensions of the microstructures during cell culture, provided the T_t is adjusted in the correct range [21].

Another alternative and very attractive approach, whereby some ELRs are able to form stable matrices under mild, physiological conditions based on their innate temperature responsiveness, has been shown to be effective for the formation of ELRs hydrogels in aqueous solution. Temperature-responsive polymers are very promising base materials for "*in situ*-generated implants" owing to their ability to form low viscosity physiological solutions at room temperature, which form gels at higher temperatures [29]. The modular structure of ELRs allows the design and incorporation of specific features to enhance the self-assembly behaviour, thereby resulting in physically cross-linked ELR hydrogels that are suitable for replacing soft tissue but lack the strength required for some other tissue-engineering applications [18]. Sallach *et al.*

have also developed a recombinant elastin-mimetic triblock-copolymer in the absence of either chemical or ionic crosslinking that shows a minimal inflammatory response and robust *in vivo* stability for periods exceeding 1 year, thus further highlighting the high and extraordinary biocompatibility of ELRs. These triblock-copolymers could also be used as structural components of artificial organs and engineered living tissues, as carriers for controlled drug release, or as biocompatible surface coatings [30]. Likewise, Martín *et al*. have demonstrated a simple, fast, water-based method to obtain highly resolved micropatterns by biocompatible replica molding involving a more complex optimized ELR amphiphilic elastin-like tetrablock-copolymer (**Figure 2**).

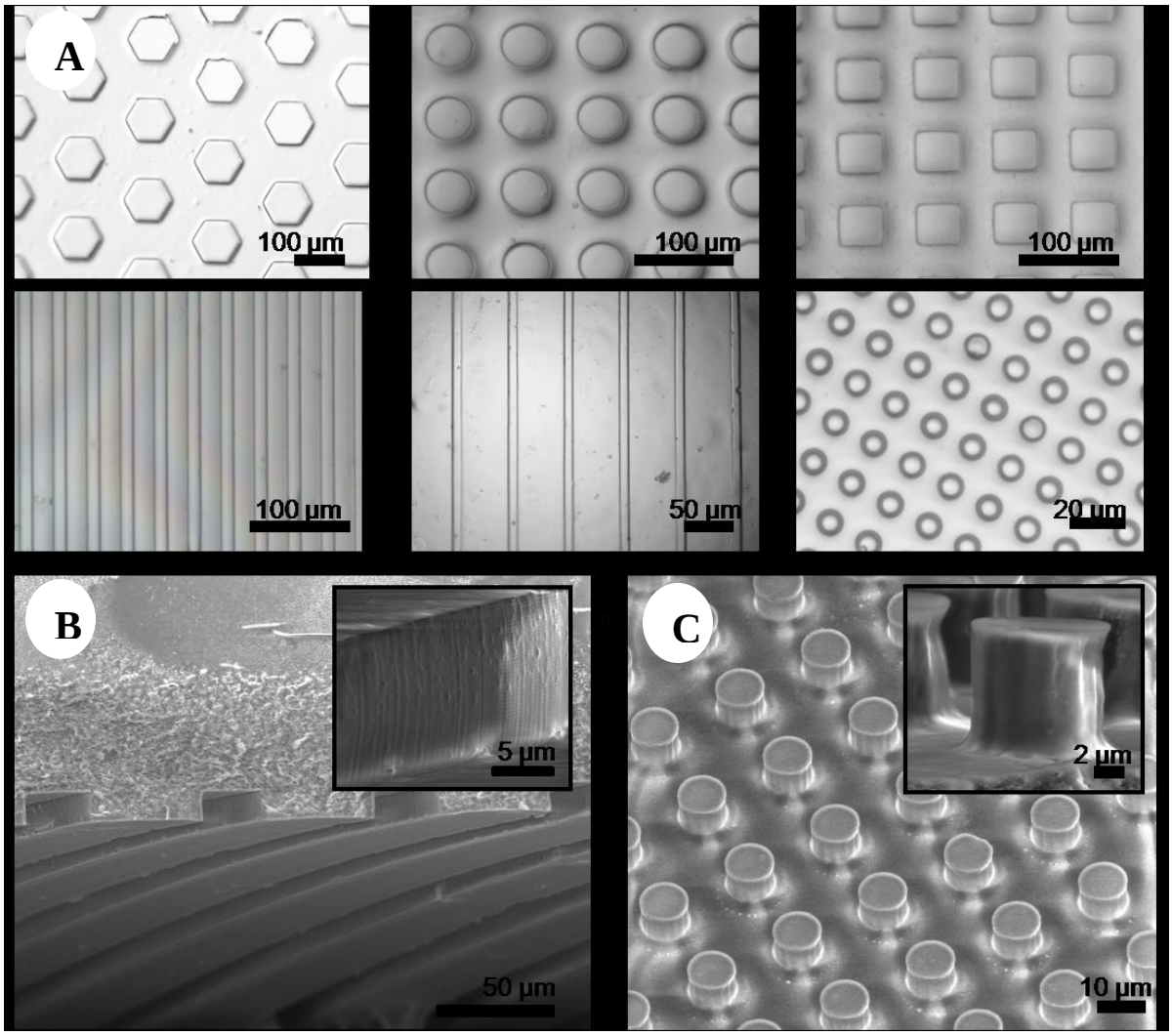

Figure 2. Micropatterned gels with different features obtained by replica molding. **(A)** *Optical differential interference contrast micrographs of swollen gels in phosphate buffered saline.* **(B & C)** *Environmental scanning electron microscope micrographs [29]*.

This process involves a one-step process in which the aqueous ELP solution is simply heated slightly above its gelation temperature (T_{gel}) to obtain micropatterned biocompatible gels [29]. The aim of this work was to demonstrate the processability of ELRs by replica molding to obtain different systems that mimic *in vivo* cellular environments, thereby enabling future *in vitro* studies of cell matrix interactions. There are currently no generally accepted trends in terms of cell behaviour control owing to differences in the numerous parameters involved, especially cell type, substrate stiffness and length scale features, amongst others [31]. A wide range of different geometries and topographies, with topographical features ranging from 10-100 μm in width, have been prepared. The step height of the micro-features was 15 μm for the pits and grooves and 9 μm for the pillars. In addition to the possibility to obtain multibioactive versions of these self-gelating polymers with different functionalities, such as interactions with cells or others, this physical gelation approach makes these polymers excellent substrates to emulate different tissues and as a proving ground for many studies dealing with cell-material interactions.

Diverse synthetic materials functionalized by the integration of extracellular adhesion ligands and growth factors have demonstrated their effectiveness in directing cell-material signaling [32]. Selected amino acid domains can also be incorporated into ELR monomer sequences with the aim of recreating the mechanical and physiological

features of ECM proteins. This strategy allows the synthetic biomaterial to be customized with selected bioactivity to acquire certain desired properties that can regulate cell-material interactions [33].

Several modular ELRs produced as biomaterials have been designed to mimic the ECM properties of elasticity, cell adhesion, cell signaling (cell-responsive) and biodegradability. The first bioactive peptides inserted into the polymer chain were the well-known, general purpose cell-adhesion peptides Arg-Gly-Asp (RGD) [34], which is found in several ECM proteins[35-38], and Arg-Glu-Asp-Val (REDV) [39,40], which is included in the CS5 domain of fibronectin and is specific for endothelial cell binding [41]. Both these bioactive peptides showed similar cell-adhesion properties to human fibronectin.

A further property, namely degradation responsiveness, which results in replacement of the initial artificial support upon reabsorption, thereby allowing the renovation and replacement of natural ECM by living tissue, has been introduced into the more advanced ELRs, and their derived tissue engineering scaffolds, for tissue repair [40, 42]. This process requires that specific cells are able to lead normal enzymatic processes, as occurs in natural ECM remodeling, principally through matrix metalloproteinases (MMPs). These enzymes, which are only expressed and secreted into the ECM when it needs to be renewed, act on specific sequences that are only present in ECM proteins. It is also known that, once released, some fragments of these hydrolyzed ECM proteins, known as “matrikines”, show strong bioactivity, including the promotion of cell differentiation, spreading and regeneration [43].

A sophisticated ELR has been biosynthesized to generate temporary scaffolds that support neural regeneration, thereby helping to repair injuries to the CNS. This ELR

was engineered to contain different bioactive domains for cell adhesion and cell-induced degradation of the artificial scaffold, namely RGD cell-adhesion sequences to enable neural attachment and sequences sensitive to cleavage by urokinase plasminogen activator (uPA), a protease secreted locally at the tips of growing neurites to enable highly localized and tuneable degradation. These ELRs were chemically crosslinked into highly swollen hydrogels with controllable mechanical properties. In addition, it was found that increasing the density of RGD peptides present in the protein substrates led to increased cell adhesion and more extensive neurite growth [42].

One of the ELRs bioproduced by our group is an 877 amino acid complex polymer (REDV-ELP biopolymer) whose monomer unit contains four different functional domains in order to achieve a suitable balance between mechanical and bioactive responses. The polymer framework contains two elastomeric pentapeptides (VPGIG and VPGKG), which provide the desired mechanical properties, stimuli-responsive nature, biocompatibility and crosslinking domains, the CS5 domain from fibronectin, which contains the cell-selective adhesion REDV motif [40], and the human elastin hexapeptide VGVAPG, which is targeted by the elastases that rearrange and renew the ECM. 3D matrices with controlled pore sizes formed from chemically cross-linked REDV-ELR have been obtained for use in cell culture, and salt-leaching and gas-foaming techniques have been used to improve the homogeneity of the pore size, the mechanical properties and their interconnectivity. The 3D culture of HUVEC endothelial cells has shown the suitability of these scaffolds, with infiltration of these cells inside the porous network being essentially complete [44]. A study of the physical changes which occurred as a result of their temperature responsiveness showed that the collapse due to the phase transition above T_t decreased the mean pore size by

approximately 30%. This technique is therefore a straightforward approach for the synthesis of advanced scaffolds with tunable biological and physical properties suitable for 3D cell culture (**Figure 3**).

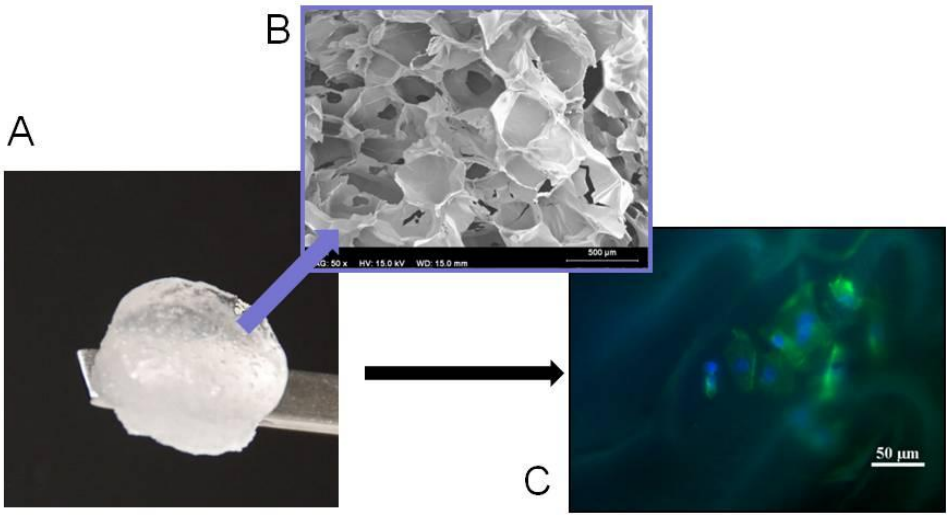

Figure 3. Macroporous thermosensitive hydrogels. (A) *Macroscopic picture of swollen hydrogel.* **(B)** *Cross-sectional scanning electron micrograph.* **(C)** *Fluorescence microscopy with Phalloidin Alexa Fluor® 488 and 4',6-diamidino-2-phenylindole staining [44].*

This REDV-ELR has also been used as a substrate to culture cells from the ocular surface. Corneal wound healing requires cell adhesion and proliferation, both of which are mediated by the binding of epithelial membrane-bound integrins to substrate ligands such as fibronectin. The corneal epithelial cell-ECM mimicking ELR interaction was investigated, and a significant improvement in the adhesion and proliferation of the conjunctival epithelial cell line on the REDV-ELR-coated surfaces was observed. This enhancement could be due to the epithelial integrins and REDV peptides binding to the ELR substrate. The REDV-ELR-coated surfaces also supported the normal phenotype and functions of epithelial cells *in vitro*, thus confirming that this recombinant polymer resembling the ocular surface ECM is a suitable substrate for sustaining epithelial cell

attachment and growth. This type of polymer may therefore be suitable for tissue engineering to restore vision by reconstructing the ocular surface. One of the potential applications we envision for this kind of protein-based polymer is the preparation of scaffolds to be used for ocular surface tissue engineering [45].

Hybrid scaffolds composed of collagen and increasing proportions of the REDV-ELR described above have been produced to mimic the natural collagen and elastin networks that contribute to a highly specialized biomechanical response in numerous tissues [22]. These hybrid hydrogels were obtained by enzymatic transglutaminase crosslinking, thus mimicking the natural crosslinking of structural proteins in the generation of functional tissue *in vivo*. REDV-ELR provides elastic elements in the collagen-based scaffolds and also increases their functionality, thus contributing to enhanced proteolytic sensitivity and endothelial cell adhesion. Crosslinking was found to affect the physicochemical properties of the ELR-collagen scaffolds, especially their porosity, temperature responsiveness and mechanical strength. The viability of different cell lines on these enzymatic crosslinked ELR collagen hydrogels was tested *in vitro*. The results of this study showed that increasing the proportion of ELR in the hybrid scaffold resulted in fibroblast antifouling, whereas endothelial cells displayed normal behavior and proliferation in the hybrid hydrogels. This specific colonization of the scaffolds by a specific cell type makes these scaffolds an attractive platform for biomedical applications, as varying the proportion of both materials should allow the optimal requirements for future applications, such as vascular-tissue or skin-wound healing, to be designed.

In recent times, complex hybrid scaffolds containing an ELR and collagen have been produced with the aim of creating an innovative acellular arterial substitute. Thus,

Caves *et al*. described the creation of artificial multilamellar vessel-like scaffolds consisting of several layers of an ELR matrix with the monomeric sequence $[(VPGAG)_2VPGEG(VPGAG)_2]_n$, which supplies appropriate mechanical properties, biocompatibility and cross-linking domains, reinforced with synthetic collagen microfibers [46]. The artificial vessels themselves were produced by embedding sheets of collagen microfibers in ELR solution, then crosslinking and rolling the resulting material. The authors analyzed the orientation and density of the two components to obtain the desired mechanical properties, including burst pressure, compliance, and suture retention strength.

Another type of hybrid scaffold has been synthesized for use as a provisional bone tissue scaffold. Thus, ELRs were amalgamated with chitosan to develop hydrogels with applications in bone tissue engineering, which requires temporary scaffolds to regenerate bone and improve its healing rate. These hydrogels can be implanted using a minimally invasive procedure by injection of a liquid that gels *in situ*. Chemically crosslinked chitosan hydrogels were prepared with an ELR coating containing an osteoconductive sequence on the preformed hydrogel. Incorporation of the ELR into the chitosan scaffold drastically improved the mechanical properties of this gel under physiological conditions and induced precipitation of calcium phosphate when the materials were soaked in simulated body fluid for 7days [47].

Ozturk *et al*. have demonstrated recently that RGD-ELR adsorbed on micropatterned poly(N-isopropylacrylamide) films is crucial to maintain the cell attachment in dynamic cell culturing. Thus, cell behaviour was studied upon application of mechanical stress generated by changing the temperature from 37 to 29 ºC to shrink and stretch poly(N-isopropylacrylamide) films under *in vitro* conditions. This is a promising strategy to obtain smart cell carriers for bone formation [48].

2.2. Fusion Protein Purification

One useful application of the thermal phase transition of ELRs in the last few years has resulted in an improvement in the recovery and purification efficiency of fusion proteins as an alternative to conventional chromatography methods. Although chromatography-based protein-purification methods yield proteins of high purity, they also have several drawbacks that limit their industrial scale-up, including their high cost, the need to remove the affinity tags, when present, from the purified protein, which can adversely affect the structure or activity of the protein and may pollute the final protein recovery with unwanted residues, the fact that the sample volume is limited by the physical size of the column, and the need to perform several concentration steps after protein elution [49]. The temperature-dependent, reversible aggregation of ELRs provides a novel means to avoid this cost-intensive affinity chromatography by one of several strategies, including direct ELR tagging by simple ELR-based protein purification or ELR coaggregation and purification by ELR-mediated affinity capture. In the first case, cleavage of the ELR moiety from the fusion protein by treatment with specific proteases could raise cost issues for large-scale protein production and could also result in some of the problems mentioned above inherent to protein recovery using conventional chromatographic procedures. However, a combination of ELR and intein technology, which is designed to induce self-cleavage, eliminates the need for post-purification enzymatic or chemical cleavage of the ELRs. In the second case, namely ELR-mediated affinity capture, the ELR can bind the fusion protein specifically and reversibly, thereby eliminating the need for post-purification enzymatic or chemical cleavage and possibly allowing re-use of the ELR-capture molecule [4]. In this regard, Araújo *et al*. have reported the microbial production of a functionalized high molecular

weight subtilisin for controlled enzymatic hydrolysis of wool surface whose activity was successfully restricted to the cuticle of wool, thereby allowing a significant reduction in pilling, weight loss and loss of tensile strength of the wool fibers [50].

2.3. *Functionalized Surfaces*

Recent progress made in the fields of nanoscience and nanotechnology has opened up novel frontiers in surface functionalization and characterization, which is often essential for endowing advanced materials and devices with desirable features. ELRs are excellent candidates for the development of smart surfaces as their sequence, length and stereochemistry can be closely controlled using recombinant technologies. This allows, amongst others, a precise nanometric-scale control of the position where functionality is located along the polypeptide chain and leads to an extensive potential for the self-assembly and other advanced functionalities displayed by these systems [7].

Surfaces modified with stimuli-responsive ELRs have been produced by Chilkoti's group, who refer to this technique, where an ELR is covalently micropatterned onto a glass surface against an inert background, as the "thermodynamically reversible addressing of proteins" (TRAP) [51, 52]. This TRAP technology enables the reversible, spatio-temporal modulation of ligand-binding triggered by the phase transition of an ELR at the solid-liquid interface and can be applied in different systems for bioanalytical applications, such as protein-based microsensors for detecting single biomolecules. The adhesion of other binding proteins coupled to designed polypeptides onto solid surfaces by hydrophobic interactions has also been reported [53]. Another fusion protein combining the RGD sequence, EGF and a hydrophobic sequence into one molecule has been shown to have both cell-adhesive and growth-factor activity, whilst its hydrophobic sequence contributed to assembly of

the RGD and retention of its activity on a solid-phase surface. This fusion protein could therefore prove to be of use for wound healing and tissue regeneration [54].

Another simple technique commonly used in the field of ELRs is the layer-by-layer deposition of ELR polyelectrolytes to generate bioactive surfaces to modulate cell response. Costa el al., for example, have developed thermoresponsive thin coatings by electrostatic self-assembly (ESA) [55], which involves simple deposition of an ELR containing the cell-attachment sequence RGD dissolved in aqueous solution onto chitosan surfaces. The thermoresponsive behavior of these coatings has shown that these systems can be exploited for tunable cell adhesion and controlled protein adsorption by nanoscale surface tailoring.

Aqueous ELR solutions are able to form interesting nano-architectures, thus providing highly reproducible nano- and micro-structured surfaces as both "*in situ*" implantable platforms or as substrates with well-controlled micro-topography, in a simple, one-step process by heating to slightly above the T_t. Selection of the appropriate sequence for the biomimetic modification of surfaces with ELRs has resulted, for example, in the production of biometallic implants with osteostimulative properties by polymeric deposition with an optimal combination of random surface topography and bioactivity [56]. A significant aspect of the biological control over material formation in these biomineralization processes involves protein/inorganic interactions [1].

2.4. Fibers

The use of polymer nanofibers for biomedical and nanotechnological applications has many advantages. Recent uses of these materials include tissue engineering, medical implants, biosensors and drug release, amongst others [57]. The most popular and

widely used technique is known as electrospinning, whereby a high voltage is applied to generate an electrically charged jet of polymer solution, which dries to leave a polymer nanofiber network containing fibers with diameters ranging from a few micrometers to less than a hundred nanometers. The first elastin-mimetic protein fibers were produced from a genetically engineered ELR [58]. Different morphological patterns, such as beaded fibers, thin filaments, or broad with a ribbon-like appearance, were subsequently obtained by varying the solution concentration. And as in other ELR constructions, the inclusion of specific biofunctionalities may provide a wide range of possibilities (**Figure 4**).

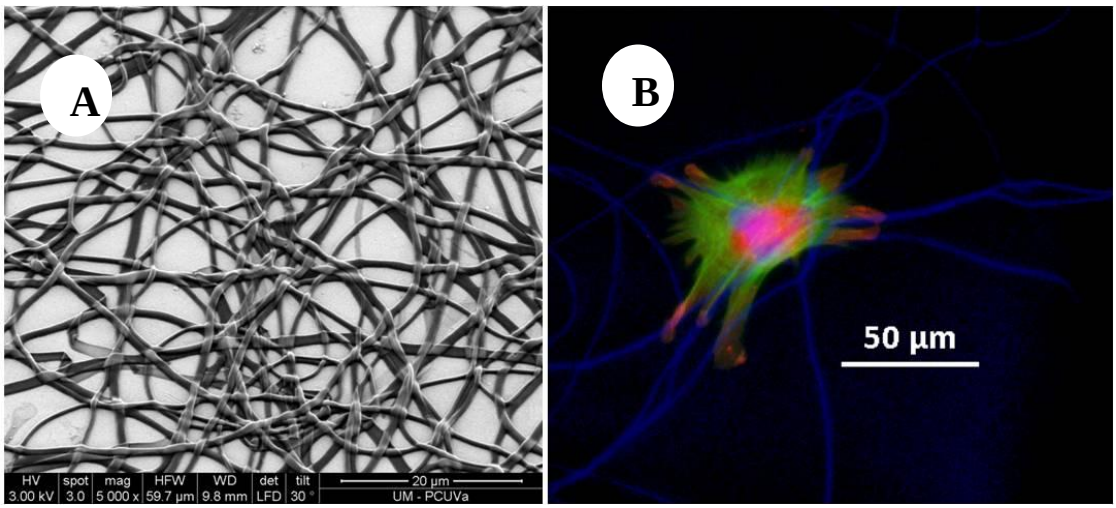

Figure 4. Elastin-like recombinamer nanofibers. (A) *Environmental scanning electron microscope micrograph of chemically crosslinked nanofibers obtained after random deposition of an elastin-like recombinamer (ELR)–Arg-Gly-Asp (RGD) aqueous solution using the electrospinning technique.* **(B)** *Fluorescence microscopy image of a primary human foreskin fibroblast cell (HFF1) specifically adhered to ELR–RGD nanofibers. Vinculin staining of the focal adhesions shows a strong integrin-mediated cell–material interaction. Nucleus and fibers (blue), F-actin (green) and vinculin (red).*

Recently, core-shell nanostructured cadium selenide (CdSe) nanoparticles with a shell of ELRs have been used as building blocks to fabricate functional 1D nanostructures. The ELR stabilizes the CdSe nanoparticles in an aqueous medium and controls their nucleation, growth, and spatial distribution, thus leading to the self-assembly of core-shell building blocks into fibril architectures. The use of non-toxic nanofibrous materials has shown that the combination of different materials with ELRs is a promising strategy to find new applications in fields such as medical nanotechnology and the diagnosis and treatment of various diseases [59].

2.5. Drug Delivery

The combination of genetic engineering techniques as ELRs has permitted the incorporation of targeting peptides, such as cell-penetrating domains [60, 61] or receptor ligands, and the introduction of reactive sites for chemical conjugation drugs [62] or fluorescent probes [63] into the ELR sequences. The polymer self-assembly process of ELRs may also boost the formation of stable micro- and nanospheres that are able to trap active substances and can be used for subsequent drug-delivery applications [64, 65]. The combined release of bone morphogenetic protein-2 and -14 by exploiting the inverse temperature transition of poly(VPAVG) in a sustained way over a period of 14 days has been reported to show significant potential for future bone tissue engineering applications [65]. More recent studies showed a hysteresis behavior in this polymer, with thermal absorption/release of components depending on the salt concentration of the polymer solution [66]. Electrospraying, which is a versatile, efficient and flexible technique, has also been used to generate nanoscale, bioresponsive, peptide-based particles with defined morphology that can encapsulate drugs, such as the chemotherapy agent doxorubicin [67, 68].

This ordered nanoscale assembly is sometimes driven by the incompatibility of the constituents of amphiphilic di- or tri-block polymers, which can give rise to the formation of monodisperse micelles in a narrow size range or fluid-filled sacs or vesicles [69]. ELR-based block copolymers can be tailor-made to form smart, self-assembling, protein-like micellar systems with controlled structure and function. For instance, MacEwan *et al*. have focused on potential therapeutic applications by increasing the affinity of the ELR-targeting vehicle of heat-triggered reversible ELR-containing micelles [6, 70]. Similarly, Dreher *et al.* have utilized diblock-ELRs with an N-terminal peptide ligand to form multivalent spherical micelles when heated slightly above body temperature. The critical micelle temperature is controlled by the length of the hydrophobic block, and the size of the micelle is controlled by both the total ELR length and hydrophilic-to-hydrophobic ratio. This study also identified a subset of elastin-like block co-recombinamers that could be useful for drug targeting by thermally triggered multivalency [71]. Recently, Kim *et al*. have developed stabilized nanoparticles through the use of disulfide cross-linking between two amphiphilic diblock polypeptides modified with cysteine residues incorporated at the core-shell interface that could be stable under complex, physiological conditions [72]. Most of these studies involve diblocks, although there are also some examples based on triblocks, including one where a reversible change in micelle compacticity was triggered by a helix-to-sheet protein folding transition upon raising the temperature above T_t [73].

2.6. Hybrid Nanomaterials

Other biomedical applications for which the use of ELRs has been proposed are based on functional inorganic-ELR hybrid nanostructured biomaterials for advanced diagnostic and therapeutic applications. These hybrid materials may help to overcome issues related to the poor solubility of the inorganic component in aqueous

environments, stability and toxicity, but have also been contemplated for the manufacture of specific biosensors and detectors and more efficient nanoprobes with multiple response properties and sensitivities, such as pH, temperature, light, concentration of ionic species and others, for drug- and gene-delivery applications in targeted therapy [74, 75].

The "one-pot" ELR-mediated synthesis of smart gold clusters has been reported recently by our group (**Figure 5**).

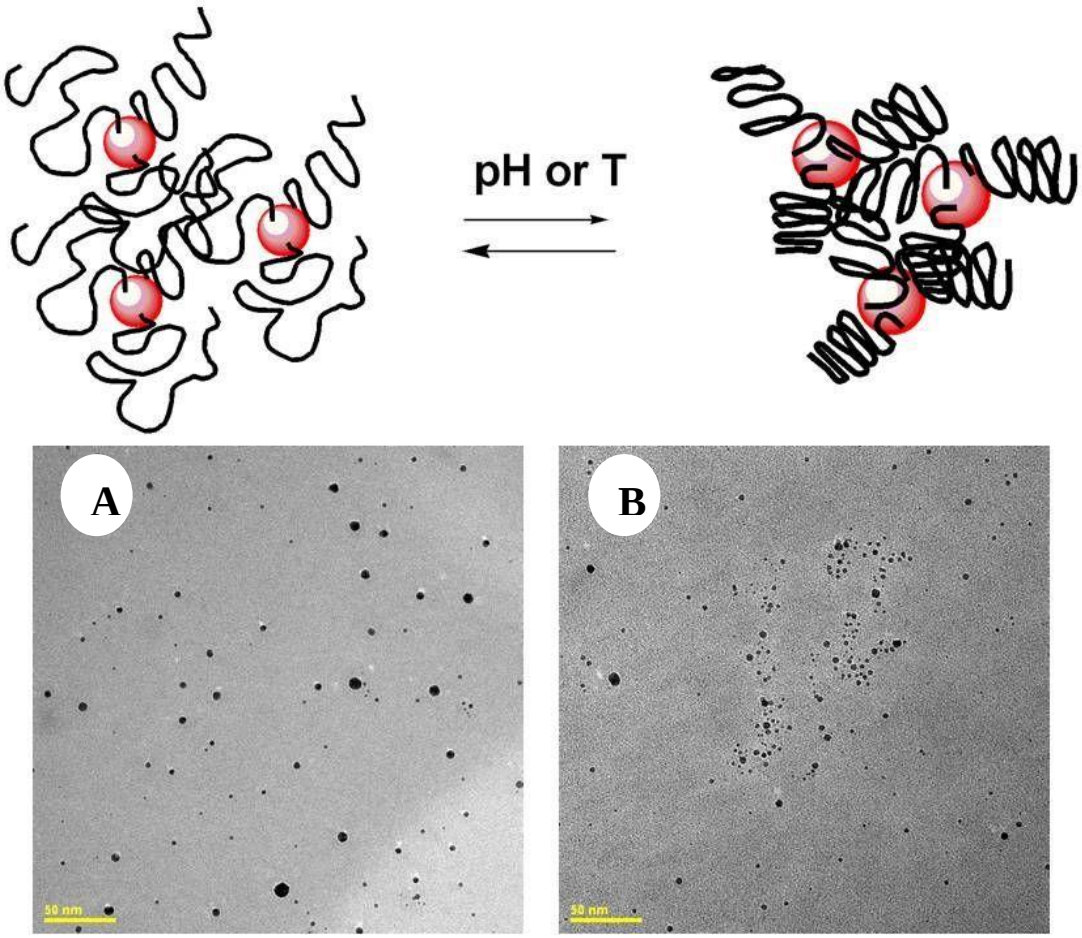

Figure 5. Self assembly exhibited by a gold–elastin-like recombinamer hybrid as a function of pH and temperature. *Cryotransmission electron micrographs obtained at pH 4, at* **(A)** *15ºC and* **(B)** *35ºC [74].*

This ELR promoted the formation of 2D linear arrangements of gold clusters with interparticle distances ranging from 10 to 40 nm. Furthermore, the gold-biopolymer hybrid displayed spectroscopic properties (UV-Vis absorption) that could be modulated by varying the pH and temperature of the environment as a result of the reversible aggregation-expansion of gold particles [76].

In a subsequent step, Álvarez-Rodríguez *et al*. have explored the use of cyclodextrins and the formation of alkanethiol mixed-monolayers over the previously described hybrid ELR in order to decouple the photoisomerization of azobenzene from the bulk phase absorption [77]. If they can be tuned to work under physiological conditions, these smart gold-ELR hybrids could be interesting for the development of multi-stimuli biosensors and drug-delivery applications.

3. Conclusion and Future Perspective

Sequence selection during the construction of ELR-based supports with specific physicochemical and mechanical properties will always depend on their intended applications. The wide spectrum of biomedical and biotechnological applications in tissue engineering, protein purification, drug delivery and surface engineering are only some examples of the enormous potential of these versatile materials. In tissue engineering, the tailored inclusion of bioactive domains along with the possibility of tuning the physical properties by changes in the amino acid composition, inclusion of crosslinking or self-assembling domains amongst others to induce specific cell colonization makes these scaffolds an attractive platform for future applications, such as vascular-tissue or skin-wound healing.

The potential of ELRs to self-assemble in response to environmental changes makes them hugely attractive for the fabrication of promising nanodevices for numerous

reasons, including the ability to load them with drugs during hydrophobic self-assembly above T_t under mild conditions of pH or in the absence of organic solvents, the possibility to target drug delivery to specific organs and tissues, and the ability to modulate subsequent drug release and optimize scaffold degradation by choosing an appropriate amino acid sequence for the polymer.

Executive summary

- **Elastin-like recombinamers (ELRs), obtained by repeating sequences found in natural elastin, are produced by genetic-engineering techniques with an extraordinary degree of complexity and control over their architecture and physicochemical properties.**

- **They are monodisperse, highly biocompatible, stimuli-responsive and can include diverse functionalities along the polypeptide chain.**

- **Their wide spectrum of biomedical and nanotechnological applications in tissue engineering, protein purification, drug delivery and surface engineering are only some examples of their enormous versatility.**

- **The tailored incorporation of bioactive domains, such as cell-binding peptides, together with the possibility of tuning the physical properties, which are retained in the ELR-derived substrates, makes them potentially useful materials for tissue engineering.**

- **Their self-assembly and stimuli-responsiveness properties are reversible at either a structural or a functional level. Furthermore, the increasing need for**

new systems with multiple response properties and sensitivities (pH and light sensitivity, drug and gene delivery, amongst others) that improve specificity and activity suggests the potential advantages of these materials in the field of nanodevices for targeted applications.

Acknowledgements

We acknowledge financial support through the European Regional Development Fund (ERDF) from EU, from the Ministerio de Ciencia e Innovación-Inoicio (MICINN ; projects MAT 2007-66275-C02-01, MAT 2007-61604, MAT 2009-14195-C03-03 and PSE-300100-2006-1), the Junta de Castilla y León (JCyL; projects VA034A09 and VA030A08), the El Centro de Investigación Biomédica en Red en Bioingeniería, Biomaterials y Nanomedicina (project CB06-01-0003), the JCyL and the Instituto de Salud Carlos III under the "Network Center of Regenerative Medicine and Cellular Therapy of Castilla and León".

References

Papers of special note have been highlighted as:

* of interest

** of considerable interest

[1] Sarikaya, M.; Tamerler, C.; Jen, A. K. Y.; Schulten, K.; Baneyx, F. Molecular biomimetics: nanotechnology through biology. Nature Mater. 2003, **2**, 577-585

[2] Rodríguez-Cabello, J. C.; Prieto, S.; Arias, F. J.; Reguera, J.; Ribeiro, A. Nanobiotechnological approach to engineered biomaterial design: the example of elastin-like polymers. *Nanomedicine* 2006, **1**, 267-280.

[3] Langer, R.; Tirrell, D. A. Designing materials for biology and medicine. *Nature* 2004, **428**, 487-492.

[4] Almine, J. F.; Bax, D. V.; Mithieux, S. M.; Nivison-Smith, L.; Rnjak, J.; Waterhouse, A.; Wise, S. G.; Weiss, A.S. Elastin-based materials. *Chem. Soc. Rev.* 2010, **39**, 3371 - 3379.

[5] Floss, D. M.; Schallau, K.; Rose-John, S. Conrad, U.; Scheller, J. Elastin-like polypeptides revolutionize recombinant protein expression and their biomedical application. *Trends Biotechnol.* 2010, **28**, 37-45.

* **Comprehensive review of recombinant protein-production and -purification tools in different heterologous host systems by using elastin-like tags.**

[6] MacEwan, S. R.; Callahan, D. J.; Chilkoti, A. Stimulus-responsive macromolecules and nanoparticles for cancer drug delivery. *Nanomedicine* 2010, **5**, 793-806.

[7] Rodríguez-Cabello, J. C.; Martín, L.; Alonso, M.; Arias, F. J.; Testera, A. M. "Recombinamers" as advanced materials for the post-oil age. *Polymer* 2009, **50**, 5159-5169.

* **Example of elastin-like recombinamer (ELR) biosynthesis as advanced materials obtained by a clean, oil-free and sustainable technology.**

[8] Ribeiro, A.; Arias, F. J.; Reguera, J.; Alonso, M.; Rodríguez-Cabello, J. C. Influence of the amino-acid sequence on the inverse temperature transition of elastin-like polymers. *Biophys. J.* 2009, **97**, 312-320.

[9] Urry, D. W. *What sustains life? Consilient mechanisms for protein-based machines and materials.* Springer-Verlag, New York, 2006.

** **Complete ELR "*encyclopedia*" containing most of the studies and applications. In addition, this book is a comprehensive compendium of concepts and technologies involving functional protein-based polymers and a seminal work on the application of the knowledge gained when studying ELRs to the physicochemical basis of natural protein function in living cells and organisms.**

[10] Muiznieks, L. D.; Weiss, A. S.; Keeley, F. W. Structural disorder and dynamics of elastin. *Biochem. Cell Biol.* 2010, **88**, 239–250.

[11] Pometun, M. S.; Chekmeven, E. Y.; Witterbort, R. J. Quantitative observation of backbone disorder in native elastin. *J. Biol. Chem.* 2004, **279**, 7982-7987.

[12] Li, B.; Alonso, D. O. V.; Daggett, V. Hydrophobic hydration is an important source of elasticity in elastin-based biopolymers. *J. Mol. Biol.* 2001, **305**, 581-592.

[13] Floquet N.; Héry-Huynh S.; Dauchez M.; Derreumaux, P.; Tamburro, A. M.; Alix, A. J. P. Structural characterization of VGVAPG, an elastin-derived peptide. *Biopolymers* 2004, **76**, 266-280.

[14] Shokouhi, B.; Coban, C.; Hasirci, V.; Aydin, E.; Dhanasingh, A.; Shi, N.; Koyama, S.; Akira, S.; Zenke, M.; Sechi, A. S. The role of multiple toll-like receptor signalling cascades on interactions between biomedical polymers and dendritic cells. *Biomaterials* 2010, **31**, 5759-5771.

[15] Annabi, N.; Mithieux, S. M.; Weiss, A. S.; Dehghani F. The fabrication of elastin-based hydrogels using high pressure CO_2. *Biomaterials* 2009, **30**, 1-7.

[16] Urry, D. W.; Parker, T. M.; Reid, M. C. Gowda, D. C. Biocompatibility of the bioeleastic material poly(GVGVP) and its γ- irradiation crosslinked matrix. *J. Bioact. Compat.* 1991, **6**, 263-282.

[17] Nicol, A.; Gowda, D. C.; Parker, T. M.; Urry, D. W. *J.* Elastomeric polytetrapeptide matrices: hydrophobicity dependence of cell attachment from adhesive $(GGIP)_n$ to nonadhesive (GGAP)n even in serum. *Biomed. Mater. Res.* 1993, **27**, 801-810.

[18] Sallach, R. E.; Cui, W.; Wen, J.; Martinez, A.; Conticello, V. P.; Chaikof, E. L. Elastin-mimetic protein polymers capable of physical and chemical crosslinking. *Biomaterials* 2009, **30**, 409-422.

[19] Woodhouse, K. A.; Klement, P.; Chen, V.; Gorbet, M. B.; Keeley, F. W.; Stahl, R.; Fromstein, J. D.; Bellingham, C. M. Investigation of recombinant human elastin polypeptides as non-thrombogenic coatings. *Biomaterials* 2004, **25**, 4543-4553.

[20] Nowatzki, P. J.; Tirrell, D. A. Physical properties of artificial extracellular matrix protein films prepared by isocyanate crosslinking. *Biomaterials* 2004, **25**, 1261-1267.

[21] Martín, L.; Alonso, M.; Moller, M.; Rodríguez-Cabello, J. C.; Mela, P. 3D microstructuring of smart bioactive hydrogels based on recombinant elastin-like polymers. *Soft Matter* 2009, **5**, 1591-1593.

[22] García, Y.; Hemantkumar, N.; Collighan, R.; Griffin, M.; Pandit, A. In vitro characterization of a collagen scaffold enzymatically cross-linked with a tailored elastin-like polymer. *Tissue Eng. Part. A* 2009, **15**, 887-899.

*** Investigates the modulation of the mechanical properties and specific cell-material interactions in ELR-collagen hybrid scaffolds.**

[23] Nagapudi, K.; Brinkman, W. T.; Leisen, J. E.; Huang, L.; McMillan, R. A.;

Apkarian, R. P.; Conticello, V. P.; Chaikof, E. L. Photomediated solid-state cross-linking of an elastin-mimetic recombinant protein polymer. *Macromolecules* 2002, **35**, 1730-1737.

[24] Lee, J.; Macosko, C. W.; Urry, D. W. Swelling behavior of gamma-irradiation cross-linked elastomeric polypentapeptide-based hydrogels. *Macromolecules* 2001, **34**, 4114-4123.

[25] Liu, J. C.; Tirrell, D. A. Cell response to RGD density in cross-linked artificial extracellular matrix protein films. *Biomacromolecules* 2008, **9**, 2984-2988.

[26] Di Zio, K.; Tirrell, D. A. Mechanical properties of artificial protein matrices engineered for control of cell and tissue behavior. *Macromolecules* 2003, **36**, 1553-1558.

[27] Betre, H.; Ong, S. R.; Guilak, F.; Chilkoti, A.; Fermor, B.; Setton, L. A. Chondrocytic differentiation of human adipose-derived adult stem cells in elastin-like polypeptide. *Biomaterials* 2006, **27**, 91-99.

[28] Lim, D. W.; Nettles, D. L.; Setton, L. A.; Chilkoti, A. In situ cross-linking of elastin-like polypeptide block copolymers for tissue repair. *Biomacromolecules* 2008, **9**, 222-230.

[29] Martín, L.; Arias, F. J.; Alonso, M.; García-Arévalo, C.; Rodriguez-Cabello, J.C. Rapid micropatterning by temperature-triggered reversible gelation of a recombinant smart elastin-like tetrablock-copolymer. *Soft Matter* 2010, **6**, 1121-1124.

[30] Sallach, RE.; Cui, W.; Balderrama, F.; Martinez, A. W.; Wen, J.; Haller, C. A.; Taylor, J. V.; Wright, E. R.; Long, R. C.; Chaikof, E. L. Long-term biostability of self-assembling protein polymers in the absence of covalent crosslinking. *Biomaterials* 2010, **31**, 779-791.

** **Describes a simple method for ELR endotoxin removal and highlight the stealth properties of ELR implantation *in vivo*. This practical point is of great relevance to achieve efficient applications of ELRs in biomedicine.**

[31] Martínez, E.; Engel, E.; Planell, J. A.; Samitier, J. Effects of artificial micro- and nano-structured surfaces on cell behaviour. *Ann. Anat.* 2009, **191**, 126-35.

[32] Hirano, Y.; Mooney, D. J. Peptide and protein presenting materials for tissue engineering. *Adv. Mater.* 2004, **16**, 17-25.

[33] Rodríguez-Cabello, J. C.; Reguera, J.; Girotti, A.; Testera, A. M. Developing functionality in elastin-like polymers by increasing their molecular complexity: the power of the genetic engineering approach. *Prog. Polym. Sci.* 2005, **30**, 1119-1145.

[34] Hersel, U.; Dahmen, C.; Kessler, H. RGD modified polymers: biomaterials for stimulated cell adhesion and beyond. *Biomaterials* 2003, **24**, 4385-4415.

[35] Straley, K. S.; Heilshorn, S. C. Design and adsorption of modular engineered proteins to prepare customized, neuron-compatible coatings. *Front. Neuroengineering* 2009, **2**, 1-10.

[36] Nicol, A.; Gowda, D. C.; Urry, D. W. Cell-adhesion and growth on synthetic elastomeric matrices containing Arg-Gly-Asp-Ser. *J. Biomed. Mater. Res.* 1992, **26**, 393-413.

[37] Panitch, A.; Yamaoka, T.; Fournier, M. J.; Mason, T. L.; Tirrell, D. A. Design and biosynthesis of elastin-like artificial extracellular matrix proteins containing periodically spaced fibronectin CS5 domains. *Macromolecules* 1999, **32**, 1701-1703.

[38] Liu, J. C.; Heilshorn, S. C.; Tirrell, D. A. Comparative cell response to artificial extracellular matrix proteins containing the RGD and CS5 cell-binding domains. *Biomacromolecules* 2004, **5**, 497-504.

[39] Heilshorn, S. C.; DiZio, K. A.; Welsh, E. R.; Tirrell, D. A. Endothelial cell adhesion to the fibronectin CS5 domain in artificial extracellular matrix proteins. *Biomaterials* 2003, **24**, 4245-4252.

[40] Girotti, A.; Reguera, J.; Rodríguez-Cabello, J. C.; Arias, F. J.; Alonso. M.; Testera, A. M. Design and bioproduction of a recombinant multi(bio)functional elastin-like protein polymer containing cell adhesion sequences for tissue engineering purposes. *J. Mater. Sci. Mater. Med.* 2004, **15**, 479-484.

[41] Plouffe, B. D.; Njoka, D. N.; Harris, J.; Liao, J.; Horick, N. K.; Radisic, M.; Murthy, S. K. Peptide-mediated selective adhesion of smooth muscle and endothelial cells in microfluidic shear flow. *Langmuir* 2007, **23**, 5050-5055.

[42] Straley, K. S.; Heilshorn, S. C. Independent tuning of multiple biomaterial properties using protein engineering. *Soft Matter* 2009, **5**, 114-124.

*** First example of a scaffold that combines both cell and degradation responsiveness, thereby illustrating the degree of multifunctionality that can be achieved with the use of ELRs.**

[43] Maquart, F. X.; Pasco, S.; Ramont, L.; Hornebeck, W.; Monboisse, J. C. An introduction to matrikines: extracellular matrix-derived peptides which regulate

cell activity. Implication in tumor invasion. *Crit. Rev. Oncol. Hematol.* 2004, **49**, 199-202.

[44] Martín, L.; Alonso, M.; Girotti, A.; Arias, F. J.; Rodríguez-Cabello, J. C. Synthesis and characterization of macroporous thermosensitive hydrogels from recombinant elastin-like polymers. *Biomacromolecules* 2009, **10**, 3015-3022.

[45] Martínez-Osorio, H.; Juarez-Campo, M.; Diebold, Y.; Girotti, A.; Alonso, M.; Arias, F. J., Rodríguez-Cabello, J. C.; García-Vázquez, C.; Calonge, M. Genetically engineered elastin-like polymer as a substratum to culture cells from the ocular surface. *Curr. Eye Res.* 2009, **34**, 48-56.

[46] Caves, J. M.; Kumar, V. A.; Martínez, A. W.; Kim, J.; Ripberger, C. M.; Haller, C. A.; Chaikof, E. L. The use of microfiber composites of elastin-like protein matrix reinforced with synthetic collagen in the design of vascular grafts. *Biomaterials* 2010, **31**, 7175-7182.

[47] Barbosa, J. S.; Ribeiro, A.; Testera, A. M.; Alonso, M.; Arias, F. J.; Rodríguez-Cabello, J. C.; Mano, J. F. Development of biomimetic chitosan-based hydrogels using an elastin-like polymer. *Adv. Eng. Mater.* 2010, **12**, B37-B44.

[48] Ozturk, N.; Girotti, A.; Kose, G. T.; Rodríguez-Cabello, J. C.; Hasirci, V. Dynamic cell culturing and its application to micropatterned, elastin-like protein-modified poly(N-isopropylacrylamide) scaffolds. *Biomaterials* 2009, **30**, 5417-5426.

[49] Chow, D.; Nunalee, M. L.; Lim, D. W.; Simnick, A. J.; Chilkoti, A. Peptide-based biopolymers in biomedicine and biotechnology. *Mater. Sci. Eng. R Rep.* 2008, **62**, 125-155.

[50] Araújo, R.; Silva, C.; Machado, R.; Casal, M.; Cunha, A. M.; Rodríguez-Cabello, J. C.; Cavaco-Paulo, A. Proteolytic enzyme engineering: A tool for wool. *Biomacromolecules* 2009, **10**, 1655-1661.

[51] Nath, N.; Chilkoti, A. Creating "smart" surfaces using stimuli responsive polymers. *Adv. Mater.* 2002, **14**, 1243-1247.

[52] Nath, N.; Hyun, J.; Ma, H.; Chilkoti, A. Surface engineering strategies for control of protein and cell interactions. *Surf. Sci.* 2004, **570**, 98-110.

[53] Wada, A.; Mie, M.; Aizawa M.; Lahoud, P.; Cass, A. E.; Kobatake, E. Design and construction of glutamine binding proteins with a self-adhering capability to unmodified hydrophobic surfaces as reagentless fluorescence sensing devices. *J. Am. Chem. Soc.* 2003, **125**, 16228-16234.

[54] Elloumi, I.; Kobayashi, R.; Funabashi, H.; Mie, M.; Kobatake, E. Construction of epidermal growth factor fusion protein with cell adhesive activity. *Biomaterials* 2006, **27**, 3451-3458.

[55] Costa, R. R.; Custodio, C. A.; Testera, A. M.; Arias, F. J.; Rodríguez-Cabello, J. C.; Alves, N. M.; Mano, J. F. Stimuli-responsive thin coatings using elastin-like polymers for biomedical applications. *Adv. Funct. Mater.* 2009, **19**, 3210-3218.

[56] Aparicio, C.; Salvagni, E.; Werner, M.; Engel, E.; Pegueroles, M.; Rodriguez-Cabello, C.; Munoz, F.; Planell, J. A.; Gil, J. Biomimetic treatments on dental implants for immediate loading applications. *J. Med. Device.* 2009, **3**, 027555.

[57] Li, D.; Xia, Y. N. Electrospinning of nanofibers: Reinventing the wheel? *Adv. Mater.* 2004, **16**, 1151-1170.

[58] Huang, L.; McMillan, R. A.; Apkarian, R. P.; Pourdeyhimi, R. P.; Conticello, V. P.; Chaikof, E.L. Generation of synthetic elastin-mimetic small diameter fibers and fiber networks. *Macromolecules* 2000, **33**, 2989-2997.

[59] Fahmi, A.; Pietsch, T.; Bryszewska, M.; Rodrıguez-Cabello, J. C.; Koceva-Chyla, A.; Arias, F. J.; Alonso, M.; Gindy, N. Fabrication of CdSe nanofibers with potential for biomedical applications. *Adv. Funct. Mater.* 2010, **20**, 1011-1018.

[60] Massodi, I.; Bidwell, G. L.; Raucher, D. Evaluation of cell penetrating peptides fused to elastin-like polypeptide for drug delivery. *J. Control. Release* 2005, **108**, 396-408.

[61] Bidwell, G. L.; Davis, A. N.; Raucher, D. Targeting a c-Myc inhibitory polypeptide to specific intracellular compartments using cell penetrating peptides. *J. Control. Release* 2009, **135**, 2-10.

[62] Furgeson, D. Y.; Dreher, M. R.; Chilkoti, A. Structural optimization of a "smart" doxorubicin-polypeptide conjugate for thermally targeted delivery to solid tumors. *J. Control. Release* 2006, **110**, 362-369.

[63] Dreher, M. R.; Liu, W. G.; Michelich, C. R.; Dewhirst, M. W.; Chilkoti, A. Thermal cycling enhances the accumulation of a temperature-sensitive biopolymer in solid tumors. *Cancer Res.* 2007, **67**, 4418-4424.

[64] Herrero-Vanrell, R.; Rincón, A. C.; Alonso, M.; Reboto, V.; Molina-Martinez, I. T.; Rodríguez-Cabello, J. C. Self-assembled particles of an elastin-like polymer as vehicles for controlled drug release. *J. Control. Release* 2005, **102**, 113-122.

[65] Bessa, P. C.; Machado, R.; Nurnberger, S.; Dopler, D.; Meinl, A.; Banerjee, A.; Cunha, A. M.; Rodríguez-Cabello, J. C.; Redl, H.; van Griensven, M.; Reis, R. L.; Casal, M. Thermoresponsive self-assembled elastin-based nanoparticles for delivery of BMPs. *J. Control. Release* 2010, **142**, 312-318.

[66] Machado, R.; Ribeiro, A. J.; Padrão, J.; Silva, D.; Nobre, A.; Teixeira, J. A.; Cunha, A. M.; Rodríguez-Cabello, J. C.; Casal, M. Exploiting the sequence of

naturally occurring elastin: construction, production and characterization of a recombinant thermoplastic protein based polymer. *J. Nano Res*. 2009, **6**, 133-145.

[67] Wu, Y. Q.; MacKay, J. A.; McDaniel, J. R.; Chilkoti, A.; Clark, R. L. Fabrication of elastin-like polypeptide nanoparticles for drug delivery by electrospraying. *Biomacromolecules* 2009, **10**, 19-24.

[68] Dreher, M. R.; Raucher, D.; Balu, N.; Colvin, O. M.; Ludeman, S. M.; Chilkoti, A. Evaluation of an elastin-like polypeptide-doxorubicin conjugate for cancer therapy. *J. Control. Release* 2003, **91**, 31-43.

[69] Carlsen, A.; Lecommandoux, S. Self-assembly of polypeptide-based block copolymer amphiphiles. *Curr. Opin. Colloid Interface Sci.* 2009, **14**, 329-339.

[70] MacKay, J. A.; Chen, M. N.; McDaniel, J. R.; Liu, W. G.; Simnick, A. J.; Chilkoti, A. Self-assembling chimeric polypeptide-doxorubicin conjugate nanoparticles that abolish tumours after a single injection. *Nature Mater.* 2009, **8**, 993-999.

*** *In vivo* demonstration of ELRs as promising nanovehicles for efficient cancer therapy.**

[71] Dreher, M. R.; Simnick, A. J.; Fischer, K.; Smith, R. J.; Patel, A.; Schmidt, M.; Chilkoti, A. Temperature triggered self-assembly of polypeptides into multivalent spherical micelles. *J. Am. Chem. Soc.* 2008, **130**, 687-694.

[72] Kim, W.; Thevenot, J.; Ibarboure, E.; Lecommandoux, S.; Chaikof, E. L. Self-Assembly of thermally responsive amphiphilic diblock copolypeptides into spherical micellar nanoparticles. *Angew. Chem. Int. Ed. Engl.* 2010, **49**, 4257-4260.

[73] Sallach, R. E,; Wei, M., Biswas, N.; Conticello, V. P.; Lecommandoux, S.; Dluhy, R. A.; Chaikof, E. L. Micelle density regulated by a reversible switch of protein secondary structure. *J. Am. Chem. Soc.* 2006, **128**, 12014-12019.

[74] Rodríguez-Cabello, J. C.; Reguera, J.; Girotti, A.; Arias, F. J.; Alonso, M. Genetic engineering of protein-based polymers: the example of elastin-like polymers. *Adv. Polym. Sci.* 2006, **200**, 119-167.

[75] Alonso, M.; Reboto, V.; Guiscardo, L.; Mate, V.; Rodríguez-Cabello, J. C. Novel photoresponsive p-phenylazobenzene derivative of an elastin-like polymer with enhanced control of azobenzene content and without pH sensitiveness. *Macromolecules* 2001, **34**, 8072-8077.

[76] Álvarez-Rodríguez, R.; Alonso, M.; Girotti, A.; Reboto, V.; Rodríguez-Cabello, J. C. One-pot synthesis of pH and temperature sensitive gold clusters mediated by a recombinant elastin-like polymer. *Eur. Polym. J.* 2010, **46**, 643-650.

[77] Álvarez-Rodríguez, R.; Arias, F. J.; Santos, M.; Testera, A. M.; Rodríguez-Cabello, J. C. Gold tailored photosensitive elastin-like polymer: synthesis of temperature, pH and UV-vis sensitive probes. *Macromol. Rapid Commun.* 2010, **31**, 568-573.

CONCLUSIONS

1.- The elastin-like recombinamers (ELRs) and elastin-like block corecombinamers (ELbcRs) used here have demonstrated properties that were designed for obtaining biocompatible and multifunctional systems, sensitive to different stimuli such as temperature and pH and including different bioactivities in the peptide chain to afford extraordinarily versatile substrates in biomedical and nanobiotechnological applications.

2.- The ELRs (HRGD6 and REDV10) incorporating various bioactive peptidic domains such as cell adhesion or sensitivity to proteolitic cleavage (elastases), together with domains of crosslinking have led to thermo-responsive bioactive hydrogels by chemical crosslinking with HDI in organic solvents.

The study of the mechanical properties of the hydrogels by rheology has shown that the hydrogels can be obtained with different moduli of elasticity by varying the parameters of the crosslinking reaction. The study of these properties at temperatures below (4° C) and above (37° C) T_t has confirmed that these crosslinked biomaterials maintain the characteristic thermo-responsiveness of the starting ELRs.

Different microstructured HRGD6 hydrogels have been obtained showing topographies by using patterned PDMS molds. The study of their dimensional changes of the microstructure with temperature has confirmed the collapse above T_t, and therefore, the change in dimensions both at macro- and microscopical level.

3D porous hydrogels of REDV10 have been obtained by using the same chemical crosslinking in the presence of NaHCO3 combining effervescent salts and citric acid.

With this technique, hydrogels have been obtained with controlled pore size between 180 and 425 μm.

The porous hydrogels obtained showed its viability as multifunctional and bioactive systems with endothelial cells, showing a complete cell colonization of the whole structure of the hydrogel and confirming the interconnectivity between the pores obtained with this technique.

3.- The amphiphilic ELbcRs (E50A40, E100A40 and E50A40E50) have shown its ability to self-assemble into different nano-objects as a consequence of an increase in temperature.

The formation of the nano-objects takes place in aqueous medium at neutral pH in response to increasing temperature above the corresponding T_t and once formed they are stable in number and size for at least 15 days.

We have confirmed that the redissolution of the nano-objects do not occurs at the temperature of formation. Redissolution takes place under a strong undercooling, caused by the hysteresis behaviour, which is characteristic of the composition of the hydrophobic block used.

The analysis of the size and morphology of the self-assebled nano-objects shows that the formation of micelles or vesicles can be modulated by the size and disposition of the polar block. The results show an evolution from a micellar structure (E50A40) to a hollow vesicle simply by changing the length of the polar block in the diblock (E100A40) or the arrangment of the hydrophilic blocks to form a triblock (E50A40E50).

The knowledge gained in the determination of the relationship between amino acid sequence and nanostructure opens the field of application to new nanotherapeutical systems and their adequacy and tailoring to the required type of nanotechnological platform.

4.- The design of the amphiphilic tetrablock ELbcR $(E50I60)_2$ has proven its ability injectable system under physiological conditions.

The system showed reversible thermogelling under physiological conditions in a wide range of concentrations which can be modulated to adjust the working temperature and the kinetic of the process.

The ocurrence of the "sol-gel" process over microstructured PDMS molds have led to the formation of physically crosslinked gels displaying different topographies on their surface. This takes place under physiological conditions.

Subcutaneous injectability and *in vivo* gel formation have proven successfully. Gelation takes place instantaneously, giving rise to an elastic gel at the site of injection that can be easily detached in the explants without breaking or deforming.

These injectable biomaterials have opened the field to a new family of corecombinamers that are showing very promising results *in vivo* for the regeneration of several tissues in combined cell therapies allowing their use in advance minimally invasive therapies.

APPENDIX

Patents

- "BIOPOLÍMERO, IMPLANTE QUE LO COMPRENDE Y SUS USOS"

Positive report on patentability of Pons Patentes y Marcas

Application of EPO patent no. P200900438. Report of the State of the art: only four found references classified with type A. The invention meets the requirements of novelty, inventive step and industrial application. Request Date: 16/02/09. Inventors: José Carlos Rodríguez Cabello, Matilde Alonso Rodrigo, Fco. Javier Arias Vallejo, Alessandra Girotti, Laura Martín Maroto, Ana M. Testera Gorgojo.

Request PCT: PCT/ES2010/070084. Request Date: 16/02/10. Date of publication: 21/12/2011 "BIOPOLYMER, IMPLANT COMPRISING IT AND USES THEREOF". International publication number: WO 2010/092224 (19.08.2010 Gazette 2010/33)

Other publications

- Oliveira, M. B., Song, W.; Martín, L.; Oliveira, S. M.; Caridade, S. G.; Alonso, M.; Rodríguez-Cabello, J. C.; Mano, J.F. Development of an inyectable system based on elastin-like recombinamer particles for tissue engineering applications. *Soft Matter* 2011, **7**, 6426-6434.
- Srivastava, G. K.; Martín, L.; Singh, A. K.; Fernandez-Bueno, I.; Gayoso, M. J.; García-Gutierrez, M. T.; Girotti, A.; Alonso, M.; Rodríguez-Cabello, J. C.; Pastor, J. C. Elastin-like recombinamers as substrates for retinal pigment epithelial (RPE) cell growth. *Journal of Biomedical Materials Research: Part A* 2011, **97A**, 243-250.

- Tejeda-Montes, E.; Smith, K. H.; Poch, M.; López-Bosque, M. J.; Martín, L.; Alonso, M.; Engel, E.; Mata, A. Engineering membrane scaffolds with both physical and biomolecular signaling. *Acta Biomateralia* 2012, **8**, 998-1009.

- García-Arévalo, C.; Bermejo-Martín, J. F.; Ricob, L.; Iglesias, V.; Martín, L.; Rodríguez-Cabello J. C.; Arias, F. J. Immunomodulatory nanoparticles from elastin-like recombinamers: single-molecules for tuberculosis vaccine development. *Molecular Pharmaceutics* 2012, submitted.

- Singh, A. K.; Srivastava, G. K.; Martín, L; Alonso, M.; Pastor, J. C. Bioactive substrates human retinal pigment epithelial cell growth from elastin-like recombinamers. *Journal of Biomedical Materials Research: Part A* 2012, submitted.

Chapter books

- Recombinant Antimicrobial Peptides. Rodríguez-Cabello, J. C.; García-Arévalo, C.; Girotti, A.; Martín, L.; Santos, M. Book: Antimicrobial Polymers (2011), Wiley (Edit: Lagaron, J. M.; Ocio, M. J.; Lopez-Rubio, A.). ISBN: 978-0-470-59822-1.

- Developments in recombinant silk and other elastic protein fibers for textile and other applications. Rodríguez-Cabello, J. C.; García-Arévalo, C.; Martín L.; Santos, M.; Reboto, V. Book: Advances in Textile Biotechnology (2010),

Woodhead Publishing Series in Textiles (Edit: Nierstrasz, V.; Cavaco-Paulo, A.) ISBN-13: 978-1845696252.

- Elastin like macromolecules. Costa, R. R.; Martín, L.; Mano, J. F.; Rodríguez-Cabello, J. C. Book: Biomimetic Approaches for Biomaterials Development (2012), Wiley-VCH Verlag GmbH & Co. lGaA (Edit: J. F. Mano). In press.